The regulation of Iroquois factors *Irx3* and *Irx5* in the developing ovary and in the impact of *Irx3* overexpression during gonad development

By
Megan L. Koth

A dissertation submitted in partial fulfillment of
the requirements for the degree of

Doctor of Philosophy
(Molecular and Cellular Pharmacology)

at the
UNIVERSITY OF WISCONSIN-MADISON
2019

Date of final oral examination: 08/05/2019
The dissertation is approved by the following members of the Final Oral Committee:

Joan S. Jorgensen, Associate Professor, Comparative Biosciences
Linda Schuler, Professor, Department of Comparative Biosciences
John P. Svaren, Professor, Department of Comparative Biosciences
Jyoti J. Watters, Professor, Department of Comparative Biosciences
Deane F. Mosher, Professor, Department of Biomolecular Chemistry

Acknowledgements

I am thoroughly indebted to my thesis advisor, Dr. Joan S Jorgensen, for the continuous support, advice, and mentorship throughout my graduate career. Dr. Jorgensen sees her students as a top priority in her life, and I couldn't imagine being in a more encouraging learning environment. I truly consider this lab my family, and I am so thankful that I had the opportunity to thrive here. Any future student would be lucky to work with Dr. Jorgensen and the talented scientists under her supervision. Dr. Jorgensen consistently encouraged me to become an independent thinker, to be critical of my own work, and to get out of my comfort zone. These are some of the reasons why my development as a young scientist have been successful, and I look forward to carrying these attributes into future endeavors.

I would also like to thank my graduate program, Molecular and Cellular Pharmacology, Dr. Anjon Audhya, and Kristin Cooper, for their endless support and encouragement. They gave me the opportunity to TA a new graduate class for Pharmacology students, which proved to be a challenge, albeit extremely rewarding.

My committee members Dr. Linda Schuler, Dr. John Svaren, Dr. Jyoti Watters, and Dr. Deane Mosher have also provided helpful insight and advice throughout my scientific progression, which has been an integral part of my personal and career development. Thank you for the tough discussions, critical questions, and guidance.

I was also lucky to have an amazing community of labs surrounding me with help around every corner. I would like to personally thank Debra Rugowski from the Schuler lab for technical support and many discussions, both science and non-science related. To the members of the Arendt lab, thank you for sharing reagents and plenty of food in

the hallway! And a big thank you to Mike Huelsmeyer, who never said no to equipment use, and who never failed to make me laugh.

To the thousands of mice who have sacrificed their lives for the betterment of mankind and our scientific understanding of gonad development and human disease, thank you.

Finally, I would like to thank my family. My husband Brian has been my rock over the past 6 years, allowing this rollercoaster called graduate school to take over my life. Thank you for being there for me when I needed you the most, and I'm looking forward to bringing a child into this world with you and Stella by my side. To my parents, who were always interested in hearing how my research was going, thank you for humoring me when I explained my experiments to you. I am incredibly fortunate to have you all in my life, cheering me on from the sidelines.

Dedication

This dissertation is dedicated to my wonderful husband, Brian, and our soon-to-be daughter, Emma. I wish for you to grow up into a strong, independent, and kind individual.

Table of Contents

Thesis Abstract

Irx3 and *Irx5* are critical transcription factors necessary for ovarian follicle development in the mouse. The knockout of *Irx3* and *Irx5* results in marked oocyte death, which is a feature common to Wnt/β-catenin knockout ovaries. Canonical Wnt/β-catenin are crucial factors involved in ovarian development and this similar phenotype suggests a link between *Irx3* and *Irx5* and this pathway. *Irx3* has been used as a marker for canonical Wnt signaling in several tissues, including the developing ovary; however, the mechanism by which regulation occurs is unclear. I hypothesized that β-catenin binds Wnt-responsive enhancer elements via TCF/LEF family members to stimulate *Irx3* and *Irx5* in the developing ovary. DNaseI-seq and ATAC-seq data helped identify potential regulatory elements in the somatic cell population of developing gonads, and I discovered two regions within the *IrxB* locus that may function as β-catenin responsive enhancers that stimulate *Irx3* and *Irx5* in ovarian development. Repressive histone marker H3K27me3 may also play a role in the repression of these enhancers in the testis, suggesting that histone modifications and β-catenin/TCF/LEF are regulating *Irx3* and *Irx5* expression in developing gonads at both the epigenetic and transcriptional levels.

We also have evidence to support that *Irx3* plays a critical role in the germ cell of the ovary. While I showed *Irx3* and *Irx5* are regulated by canonical Wnt/β-catenin signaling in the somatic cells, I hypothesized whether their regulatory mechanism is consistent in the oocyte. With the use of a newly developed germ-cell specific cre *Figla*Cre-EGFP, I was able to eliminate β-catenin in the oocyte of the ovary at an early

postnatal stage. IRX3 expression in the oocyte is not affected by the loss of β-catenin, indicating the regulation of *Irx3* in the oocyte differs from that in the somatic cells. Loss of β-catenin in the oocyte, additionally, does not affect ovarian development or follicle maturation, suggesting loss of β-catenin is not critical for ovarian health.

Irx3 has a dynamic expression profile in the ovary, where it is expressed in both somatic and germ cells at different points during development. Prior to primordial follicle formation, *Irx3* is confined to the somatic (pre-granulosa) cells of germline nests. After germline nest breakdown and primordial follicle formation, however, *Irx3* is expressed in the oocyte and remains in the oocyte into adulthood. My goal was to stabilize *Irx3* in the somatic cells in the ovary after expression would normally migrate to the germ cell, or to overexpress *Irx3* in the oocyte to explore if *Irx3* overexpression would affect ovarian health or female fertility. I can conclude that overexpression of *Irx3* in either the somatic or germ cells of the ovary does not affect ovarian morphology during development and adulthood and that these females are viable and fertile.

In addition, I also introduced *Irx3* in the testis in both somatic and germ cells where it is normally absent at all stages of development. While somatic cell *Irx3* overexpression did not affect testis histology or male fertility, germ cell *Irx3* overexpression revealed these males were sub-fertile and displayed a sperm agglutination phenotype. *Irx3* overexpression has yet to be connected to male infertility and warrants further investigation into the pathogenesis of this phenotype.

Altogether, I was able to elucidate the regulatory mechanism for *Irx3* and *Irx5* in the somatic cells of the ovary while I also discovered that this mechanism does not translate to the neighboring oocyte. Next, I showed that *Irx3* overexpression in the ovary

does not affect ovarian function, while germ cell overexpression of *Irx3* produces as unique phenotype in male mice. This work expands our understanding and opens new avenues of research for the study of *Irx3* and *Irx5* in gonad development and how the regulation of these factors may contribute to fertility defects in humans.

List of Acronyms

ATAC-seq: Assay for Transposase-Accessible Chromatin using sequencing

ChIP: Chromatin Immunoprecipitation

Ctnnb1: β-catenin

DNAseI-seq: DNase I hypersensitive sites sequencing

H3K27ac: Histone 3 Lysine 27 acetylation

H3K27me3: Histone 3 Lysine 27 trimethylation

Irx3: Iroquois homeobox protein 3

Irx5: Iroquois homeobox protein 5

POI: Premature Ovarian Insufficiency

Rspo1: Rspondin-1

Sry: Sex determining region Y

TCF/LEF: T-Cell Factor/Lymphoid Enhancer Binding Factor

Wnt4: Wingless-Type MMTV Integration Site Family member 4

Chapter 1

Literature Review

Dysregulation of genes involved in development could have a major impact on overall health later in life. Our lab focuses on two Iroquois genes, *Irx3* and *Irx5*, which are active during ovarian development and have an impact on both fetal and adult ovarian and follicle health. My thesis project outlines one of the pathways involved in their regulation, and how overexpression of *Irx3* affects both ovarian and testis development. This literature review will summarize the primary ovarian disease that we believe could be caused by deficient *Irx3* and/or *Irx5* expression, followed by a brief section on early gonad formation. Next, pathways involved in both testis and ovarian differentiation will be outlined, along with a summary of known epigenetic regulation in the gonad. This is then followed by the critical role of β-catenin in the ovary, and why we believe this protein is central to Iroquois factor regulation in the somatic cells of the developing gonad.

Premature Ovarian Insufficiency

Human infertility is a disorder classified by the failure to become pregnant after at least one year of timed, unprotected intercourse. The number of couples experiencing infertility is on the rise, currently estimated at 50 million couples worldwide (Datta et al., 2016; Mascarenhas, Flaxman, Boerma, Vanderpoel, & Stevens, 2012). Female factors leading to infertility, which account for about one-third of causes, include ovulation disorders, tubal disease, and endometrial pathology (Smith, Pfeifer, & Collins, 2003). In the female, each step leading to healthy and competent oocyte maturation and ovulation is crucial to ensure reproductive success in females. Dysfunction in any stage of this process could lead to premature ovarian insufficiency (POI), previously called

premature ovarian failure. POI is a complex and poorly understood disease and is defined by the loss of ovarian function before the age of 40 and is a common condition that occurs in roughly 1.5% of women worldwide (Luborsky, Meyer, Sowers, Gold, & Santoro, 2003). Abnormal follicle formation or premature depletion of oocytes are recognized as potential causes of POI (Persani, Rossetti, Cacciatore, & Fabre, 2011). Infertility is a primary symptom of the disease, but POI has far-reaching consequences for a woman in later life. Early menopause comes with increased risk of mortality (Cooper & Sandler, 1998; van der Schouw, van der Graaf, Steyerberg, Eijkemans, & Banga, 1996), cancer (Cramer, 1990), cardiovascular disease (Gold et al., 2001; Joakimsen, Bønaa, Stensland-Bugge, & Jacobsen, 2000; Senöz, Direm, Gülekli, & Gökmen, 1996; van der Schouw et al., 1996), and osteoporosis (Cooper & Sandler, 1997; Gökmen, Seçkin, Sener, Ozakşit, & Ekmekçi, 1995; Harlow & Signorello, 2000; Kritz-Silverstein & Barrett-Connor, 1993; Ohta et al., 1996).

POI is generally considered an idiopathic disease because the cause in the majority of cases is unknown (Coulam, Adamson, & Annegers, 1986; Nelson, Covington, & Rebar, 2005). Some underlying reasons for POI, however, have been established and can be grouped as follows: genetic abnormalities, autoimmunity, metabolism disorders, infections, and environmental factors. The most critical causes of POI to this thesis are genetic abnormalities; therefore, this section will expand on this topic.

Genetic abnormalities cause about 10.8% of POI cases (Lakhal et al., 2010). The most common chromosomal abnormality is Turner syndrome, which occurs when one or part of one X chromosome is missing in the female. Women with Turner syndrome

have dysgenic gonads that consist of fibrous tissue and primary amenorrhea, which illustrates the importance of two functional X chromosomes in ovarian health (Cordts, Christofolini, Dos Santos, Bianco, & Barbosa, 2011; Hjerrild, Mortensen, & Gravholt, 2008; Lakhal et al., 2010). The next most common genetic abnormality is the mutation of *Fmr1* on the X chromosome, which could lead to Fragile X syndrome. The severity of the disease depends on the number of CGG repetitions in the untranslated region of the X chromosome: 55-199 repetitions result in females with an increased risk of developing POI (Conway, 2010; Wittenberger et al., 2007). A full mutation, which results in greater than 200 repetitions, completely inactivate *Fmr1* by methylation, resulting in Fragile X syndrome (Monaghan, Lyon, Spector, & Genomics, 2013). Other commonly mutated genes that could lead to POI include *Bmp15* and *Gdf9*. Both are essential signaling factors that originate in the oocyte and impact folliculogenesis (Otsuka, McTavish, & Shimasaki, 2011; Spicer et al., 2008). Less common genes associated with POI include *Xist, Foxo4, Fshr, Foxl2, Cyp17A1, Cyp19A1,* and *Star* (not a complete list) (Goswami & Conway, 2005; Lakhal et al., 2010). Most of these genes can be related to the reproductive hormone axis.

POI is a severe medical problem, and it can significantly affect a woman's life. Because this disease has no common cause and prevention/treatment is nonexistent, it is imperative that all aspects of this disease are studied. We believe that two transcription factors, *Irx3* and *Irx5*, are associated with POI and we aim to show that these genes have a significant impact on ovarian development and follicular health.

The Bipotential Gonad

The mammalian gonad is an extraordinary organ that can change its fate depending on the signaling cascades activated early in gestation. Unlike any other organ during development, the cells within the early gonad can differentiate into either a testis or an ovary – two completely distinct systems. While both of these organs have the same functional outcome of reproduction, the male and female reproductive structures are quite different. Therefore, it is imperative that these systems are appropriately established during a critical window early in gonad development to ensure the reproductive strength of the organism.

During embryonic development, the bipotential gonad emerges at about embryonic day (E)10.5 in the mouse on the surface of the mesonephros within the urogenital ridge. Human gonads appear as a pair of longitudinal gonadal ridges in the 4-5th week after conception, and the primitive gonad is formed by proliferation of both the epithelium and the compression of the underlying mesenchyme (TW, 2000, 2012). Until E11.5-12.5 in the mouse and the 7th week of development in humans, there are no morphological differences in the mesonephros or gonad between XX and XY embryos (Jost, 1972; McLaren, 2000; Swain & Lovell-Badge, 1999).

There are several genes required for the gonad to form during the bipotential state that are not sex-dependent including *Emx2, Lhx9, Cbx2, Nr5a1* (*Sf1*), and *Wt1*. Based on mouse knockout models, mutations or deletions of these genes can result in a gonad that fails to develop beyond the bipotential state. Mice lacking *Emx2* completely lack gonads, kidneys, and genital tracts (Miyamoto, Yoshida, Kuratani, Matsuo, & Aizawa, 1997). While *Lhx9*-null mice also do not form gonads, *Lhx9*$^{-/-}$ XY mice develop as XX phenotypically

due to the downstream effects of the *Lhx9* deletion (Birk et al., 2000). *Lhx9* regulates expression of *Nr5a1* or *Sf1*, which is a critical transcription factor required for early gonad development (Hatano et al., 1994; Luo, Ikeda, & Parker, 1994; Wilhelm & Englert, 2002).

Nr5a1 or *Sf1* encodes a transcription factor that is present in both sexes in all somatic cells in the gonad and throughout the adrenal cortex (Ikeda, Shen, Ingraham, & Parker, 1994; Luo et al., 1994; Val, Lefrançois-Martinez, Veyssière, & Martinez, 2003). *Sf1* null mice have a severe phenotype, where both gonads and adrenal glands form, but dissolve into streak gonads by E12.5 (Luo et al., 1994). It is also important to note that *Sf1* plays a critical role in upregulating an important testis-determining factor *Sox9*, the master driver of Sertoli cell differentiation, (Sekido & Lovell-Badge, 2008), which is expanded upon in the male sex determination section.

Wt1 is vital for gonad formation and subsequently for testis differentiation. One isoform of *Wt1* in cooperation with *Sf1* is responsible for the transcriptional control of *Amh*, an early hormone produced by the testis and is essential for the regression of the female Müllerian ducts (Wilhelm & Englert, 2002). Mice lacking *Wt1* fail to develop both gonads and kidneys, which supports the idea that *Wt1* plays a vital role in early gonad formation (Kreidberg et al., 1993).

The final known gene required for the formation of the bipotential gonad is *Cbx2*. This gene encodes a component of the polycomb complex, which is necessary to maintain the repression of genes throughout development by way of chromatin remodeling or modification of histones (reviewed in (Golbabapour et al., 2013)). *Cbx2*$^{-/-}$ mice had delayed gonad development and eventual male-to-female sex reversal (Katoh-Fukui et al., 1998). A different study revealed *Cbx2* is required to upregulate

multiple testis-determination genes, including *Sf1*, *Wt1*, and *Sry* itself, which explains the male-to-female sex reversal phenotype (Katoh-Fukui et al., 2012). More recently, *Cbx2* was shown to actually stabilize the testis pathway by repressing female genes, specifically Wnt target gene *Lef1* (Garcia-Moreno, Lin, et al., 2019).

Male Sex Determination

Sox (*Sry*-related HMG box) genes are critical factors for testis differentiation. The first *Sox* gene identified in the early 1990s was *Sry*, which encodes the sex-determining region of the Y chromosome (Berta et al., 1990; Koopman, Gubbay, Vivian, Goodfellow, & Lovell-Badge, 1991; Koopman, Münsterberg, Capel, Vivian, & Lovell-Badge, 1990; Sinclair et al., 1990). This single gene is responsible for a waterfall cascade of other male-specific factors in the somatic cell lineage. *Sry* null male mice develop ovaries (Lovell-Badge & Robertson, 1990), and conversely, forced Sry expression in XX mice results in testis differentiation and morphogenesis (Koopman et al., 1991). *Sry* is essential for the initiation of testis development in addition to its indispensable role to upregulate its downstream target *Sox9* (Sekido, Bar, Narváez, Penny, & Lovell-Badge, 2004), which is then continuously expressed.

Sox9 is expressed in both XX and XY genital ridges until *Sry* expression initiates at E11.5 in XY gonads, causing the expression of *Sox9* to become male-specific (Hacker, Capel, Goodfellow, & Lovell-Badge, 1995; Kent, Wheatley, Andrews, Sinclair, & Koopman, 1996). *Sox9* positive cells then differentiate into Sertoli cells (Morais da Silva et al., 1996; Sekido et al., 2004); conditional knockout of *Sox9* in Sertoli cells results in a male-to-female sex reversal in mice (Barrionuevo et al., 2006; Chaboissier

et al., 2004). Conversely, ectopic overexpression of *Sox9* in ovaries resulted in the development of testes (Bishop et al., 2000; Vidal, Chaboissier, de Rooij, & Schedl, 2001). These phenotypes are similar to those of *Sry* deletion or exogenous overexpression, suggesting that *Sry* establishment of *Sox9* expression is the most crucial step to initiate differentiation of Sertoli cells and the morphological development of the testis.

Several pathways downstream of *Sox9* are involved in testis organogenesis. Some of these include: *Fgf9* (Colvin, Green, Schmahl, Capel, & Ornitz, 2001; Schmahl, Kim, Colvin, Ornitz, & Capel, 2004), *Dhh* (H. H. Yao, Whoriskey, & Capel, 2002)*, Pdgfr-alpha (Brennan, Tilmann, & Capel, 2003)*, insulin receptors (Nef et al., 2003), and prostaglandins (Malki et al., 2005; Wilhelm et al., 2005). Of these pathways, the best studied is *Fgf9*, and it is the only case where the deletion of this molecule results in Sertoli cell differentiation failure and sex reversal (Colvin et al., 2001; Y. Kim et al., 2006; Schmahl et al., 2004). Conclusions from these studies revealed that *Fgf9* arranges a regulatory network in conjunction with *Sry* and *Sox9* during early Sertoli cell differentiation. Without *Fgf9*, *Sox9* expression is depleted despite the natural expression of *Sry* and the initial drive of *Sox9*. Without appropriate levels of SOX9 achieved at the right time, the testis fails to differentiate and fails to form testis cords, suggesting that *Sry* requires *Fgf9* to successfully promote the male pathway. The Sertoli cells in these mice, however, do not die, but transdifferentiate into female-like somatic cells that express *Wnt4* and its downstream markers (DiNapoli, Batchvarov, & Capel, 2006; Y. Kim et al., 2006). **Figure 1.1** outlines these important genes for testis development and

their relationship to one another, as well as how they interact with the female pathway, which is discussed in the next section.

Female Sex Determination

Granulosa cells, the supporting cell lineage in the ovary, are the male equivalent Sertoli cells. Granulosa cells enclose female germ cells (oocytes) and secrete factors critical for oocyte growth and maturation within the follicle, the functional unit of the ovary. Each follicle, composed of a single oocyte surrounded by granulosa and theca cells, grows and matures throughout each cycle, ultimately resulting in ovulation of the oocyte for fertilization. During mouse ovary development, primordial germ cells are first organized into structures called germ cell nests, or germline cysts, where the germ cells will mature into oocytes. These nests are composed of clusters of oocytes surrounded by a layer of pre-granulosa cells, which are later broken down into individual follicles in early postnatal life (Hirshfield, 1991). Formation of the ovary was once considered the "default" gonad development pathway for many years, which only occurred in the absence of *Sry*. Studies show that this is not the case – several female-specific ovarian factors, such as WNT4, β-catenin, RSPO1, and FOXL2 were identified, and ovarian development cannot take place in their absence (C. F. Liu, Liu, & Yao, 2010).

One vital gene involved in ovarian development is *Foxl2*. In contrast to *Wnt4/Rspo1*, this protein is solely expressed in the ovarian somatic cells and is never expressed in the testis. FOXL2 expression arises at E12.5 and continues into adulthood; however, inactivation of *Foxl2* does not disrupt granulosa cell differentiation or the assembly of follicles. (Loffler, Zarkower, & Koopman, 2003; Ottolenghi et al.,

2005). In female mice lacking *Foxl2*, follicle development is not impaired, but the follicles fail to mature past the primary stage and subsequently degenerate (Schmidt et al., 2004; Uda et al., 2004). After birth, granulosa cells begin to express male markers (such as *Sox9* and *Dhh*) and transdifferentiate into Sertoli-like cells (Ottolenghi et al., 2005; Uhlenhaut et al., 2009). *Foxl2*$^{-/-}$ ovaries also develop Leydig-like cells, which are the cells responsible for steroid synthesis in the male. These mutant female ovaries were capable of secreting testosterone comparable to wild-type male controls (Uhlenhaut et al., 2009). There is also evidence to support a relationship between FOXL2 and ERα showing they synergistically repress *Sox9* in vitro. This relationship suggests that both proteins work together to prevent Sertoli cell differentiation and maintain the granulosa cell fate (Uhlenhaut et al., 2009). FOXL2 and the *Wnt/Rspo1* pathway appear to work independently of each other, which is demonstrated by the finding that *Foxl2* alteration does not affect *Rspo1* and *Wnt4* expression, or vice versa (Ottolenghi et al., 2007; Tomizuka et al., 2008).

The canonical Wnt signaling pathway has been extensively studied in development and is known to control progenitor cell differentiation and morphogenesis (reviewed in (Logan & Nusse, 2004)). The pathway is activated by the interaction of a WNT ligand, predominantly WNT4 in the ovary, with the Frizzled/LRP5/6 receptor complex at the membrane of the somatic cell surface. Without the binding of this ligand, a “destruction complex” is formed in the cytoplasm of the cell which targets β-catenin for degradation by the proteasome. When Wnt is bound, this “destruction complex” is disrupted, causing stabilization of β-catenin, which allows it to translocate to the nucleus and regulate target gene expression via TCF/LEF (T-cell factor/lymphoid enhancer-

binding factor) transcription factor binding. **Figure 1.2** shows a schematic outlining basic canonical Wnt signaling.

Canonical Wnt signaling is expressed in both XX and XY gonads prior to sex determination but becomes specific to XX gonads after E11.5, where it upregulates in the developing ovary and downregulates in the testis (Vainio, Heikkilä, Kispert, Chin, & McMahon, 1999). Female mice lacking *Wnt4* develop partially sex-reversed gonads that contain XY gonad features including testis vasculature and the production of androgens. The ovaries of these mice contain oocytes, but the number is significantly reduced compared to a control ovary (Heikkilä et al., 2005; Vainio et al., 1999). *Rspo1* (*Rspondin1*), another female-specific factor, is an activator of the canonical Wnt/β-catenin signaling pathway (Kazanskaya et al., 2004; Tomizuka et al., 2008). An *Rspo1* null mutation in humans results in complete female-to-male sex reversal, uncovering the role of *Rspo1* as a candidate female sex determining gene in mammals (Parma et al., 2006). Subsequent studies in mice lacking *Rspo1* showed a partial female-to-male sex reversal and the presence of ovotestes (Anne Amandine Chassot et al., 2008; Tomizuka et al., 2008). The reduced expression of *Wnt4* in *Rspo1*-null ovaries indicates that RSPO1 is necessary for *Wnt4* and β-catenin expression, but once activated, WNT4 can synergize with RSPO1 to further activate β-catenin activity (Anne Amandine Chassot et al., 2008). The current understanding is that WNT4 is a critical factor that promotes ovarian differentiation in conjunction with RSPO1 by activating a part of the ovarian genetic cascade while also antagonizing the testis pathway and differentiation in mice (Anne Amandine Chassot et al., 2008; Jameson, Lin, & Capel, 2012; Y. Kim et al., 2006; Vainio et al., 1999). *Foxl2/Wnt4* and *Foxl2/Rspo1* double knockout mice have a

more severe ovarian phenotype compared to their single mutant counterparts, suggesting that both pathways are essential for proper ovarian differentiation (Anne Amandine Chassot et al., 2008).

The downstream mediator of canonical *Wnt/Rspo1* signaling, β-catenin, has been shown to play a critical role in ovarian development as well. The somatic cell-specific knockout of β-catenin using *Sf1*Cre results in ovaries with molecular and morphological defects, such as the formation of the testis-specific coelomic vessel, ablation of oocytes before birth, and the presence of androgen-producing adrenal-like cells (C.-F. Liu, Bingham, Parker, & Yao, 2009). This phenotype is similar to both the *Rspo1* and *Wnt4* knockout ovaries, further connecting its role as a downstream mediator in this common pathway. Conversely, the expression of stabilized, constitutively active β-catenin in XY gonads is sufficient to cause male-to-female sex reversal, indicating β-catenin itself has pro-ovarian and anti-testis activity (Maatouk et al., 2008). **Figure 1.3** outlines key phenotypes in mouse knockout models of this pathway.

Multiple factors are hypothesized to be regulated by β-catenin mediated transcription in the developing ovary, but few direct targets have been identified. *Irx3* and *Irx5* double knockout ovaries show a similar phenotype to *Wnt4*$^{-/-}$, *Rspo1*$^{-/-}$, and somatic β-catenin cKO mice, suggesting there may be a link between this critical ovarian pathway and *Irx3* and *Irx5* expression. **Chapter 2** and **Chapter 3** explore this connection in both the somatic and germ cell compartments of the ovary.

Mutual Antagonism

The bipotential gonad can differentiate into a testis or an ovary depending on the signaling cues within the supporting cell population. These cells then push a particular fate forward and guide other cells, including germ cells, towards the same sex-specific result. One might think this is irreversible, but some studies suggest this is not the case. Multiple factors have been shown to both promote sex determination and counteract the factors supporting the opposite sex. The absence of primary sex determination genes results in the ectopic expression of factors specific to the opposite sex. For example, *Sox9* or *Fgf9* (or its receptor *Fgfr2*) deletions in the male cause partial or complete male to female sex reversal and upregulation of female-specific factors (Bagheri-Fam et al., 2008; Chaboissier et al., 2004; Colvin et al., 2001; Y. Kim et al., 2006; Siggers et al., 2014). This antagonism is also demonstrated in the female, where the loss of *Rspo1/Wnt4/Ctnnb1* individually or in combination results in the increased expression of male factors *Sox9* and *Fgf9* and partial female to male sex reversal (A. A. Chassot, Gillot, & Chaboissier, 2014; Y. Kim et al., 2006). **Figure 1.1** outlines some of the known antagonistic pathways present during gonad differentiation.

Epigenetic landscape within the gonad

Somatic cells contain approximately 2 meters of DNA (Bloom & Joglekar, 2010), which is highly compacted into tightly regulated structures called nucleosomes. This octameric protein complex contains two of each core histone (H2A, H2B, H3, and H4) (Bentley, Lewit-Bentley, Finch, Podjarny, & Roth, 1984; Kornberg & Thomas, 1974; Luger, Mäder, Richmond, Sargent, & Richmond, 1997) with 145-147bp of DNA wrapped

around the exterior of the structure. Generally, nucleosomes impede DNA transcription (Lee, Hayes, Pruss, & Wolffe, 1993; Wasylyk & Chambon, 1979) via physical obstruction or bending of DNA. However, post-translational modifications of histones play an enormous role that can influence compaction and accessibility of DNA, which can then impact gene expression. The most common post-translational modifications - acetylation, methylation, and phosphorylation - occur on the N-terminal tail region of histones, which is accessible on its surface (Luger et al., 1997). Histone tail modifications can serve to recruit additional factors by precise recognition of modified histones by way of protein domains, which are specialized for these purposes (Jenuwein & Allis, 2001).

In past years, it has come to light that epigenetics plays a significant role in the dynamic gene expression regulation in many tissues and systems. The gonad is no exception – there is increasing evidence for the role of epigenetics in regulating essential sex determination and differentiation factors (Garcia-Moreno, Futtner, et al., 2019; Garcia-Moreno, Lin, et al., 2019; Garcia-Moreno, Plebanek, & Capel, 2018; Gonen et al., 2018). The accessibility of both enhancer and promoter regions is a fundamental mechanism of gene regulation, and it involves DNA conformation, chromatin modifications, and DNA methylation. Modern techniques such as DNAseI-seq, ATAC-seq, Native ChIP-seq, ChIP-seq, and single-cell transcriptomics are being utilized to tease out the complicated processes that underlie sex determination and differentiation.

Although the exact mechanisms that drive the precise spatiotemporal expression of *Sry* are not clear, recent studies have started to elucidate some critical cellular

pathways involved (Hiramatsu et al., 2009). Histone and DNA methylation status at two regions upstream of *Sry* have been shown to coincide with *Sry* expression (Gierl, Gruhn, von Seggern, Maltry, & Niehrs, 2012; Nishino et al., 2011; Nishino, Hattori, Tanaka, & Shiota, 2004). Both areas exhibit CpG hypermethylation before sex determination and *Sry* expression. Both regions are hypomethylated in the gonad at the time of sex determination but remain hypermethylated in other tissues (Gierl et al., 2012; Nishino et al., 2004). Additionally, histone methylation has been shown to play a role in *Sry* expression. H3K9me2 marks around the *Sry* promoter require histone demethylase JMJD1A for proper *Sry* expression in the testis. Disruption of *Jmjd1a* results in the accumulation of H3K9me2, leading to lower *Sry* expression (Kuroki et al., 2013). Permissive histone markers H3K4me3 and H3ac enrichment have also been reported in the *Sry* promoter to facilitate *Sry* expression (Gierl et al., 2012).

The testis-specific enhancer TESCO was discovered to influence the expression of *Sox9* during testis determination (Sekido & Lovell-Badge, 2008). The deletion of this enhancer resulted in a 50% reduction of *Sox9* expression but did not elicit sex reversal in XY mice (Gonen, Quinn, O'Neill, Koopman, & Lovell-Badge, 2017). Recently, our collaborators combined ATAC-seq with ChIP-seq to screen for additional *Sox9* enhancers and found a 557bp element located 565kb upstream of *Sox9* that, when deleted, resulted in complete male-to-female sex reversal (Gonen et al., 2018). (Chapter 2 will present more information on these datasets).

Because the supporting cell population in both XY and XX gonads arise from a common precursor, questions arise about how transcription factors and epigenetics intertwine to control cell fate decision. One protein, CBX2, has recently come to light as

a potential major player to influence cell fate in the gonad. CBX2 is a member of the polycomb repressive complex 1 (PRC1), which binds to H3K27me3 to maintain chromatin compaction status and to repress gene expression (Lau et al., 2017). *Cbx2* was mentioned earlier as an essential gene for the bipotential gonad and this gene, when disrupted, results in ovary development in XY mice (Katoh-Fukui et al., 2012; Katoh-Fukui et al., 1998). It was initially thought that *Cbx2* acted as a pro-testis factor by indirect positive regulation of *Sry* (Garcia-Moreno et al., 2018; Katoh-Fukui et al., 2012), but it turns out that this is not the case. Recent studies suggest that instead, *Cbx2* blocks the upregulation of female-determining genes, therefore stabilizing the male fate (Garcia-Moreno, Lin, et al., 2019). This study confirmed CBX2 enrichment at the *Lef1* promoter, a female-specific Wnt target gene, blocking its transcription. In testes lacking *Cbx2*, *Lef1* is upregulated, promoting the female pathways that actively antagonize male factors, allowing for somatic differentiation into pregranulosa cells (Garcia-Moreno, Lin, et al., 2019).

Our knowledge about the epigenetic influence on gonad development and sex differentiation is still minimal, and these genome-wide sequencing studies will play an enormous role in many important discoveries in the years to come. Until recently, most of our understanding of sex determination and differentiation was limited to targeted knockout genes. These data, alongside chromatin status screens and transcription factor binding maps, will be the foundation to uncover the vital regulatory networks that control this complicated process and will lead this field into uncharted territories.

Because the regulation of *Irx3* and *Irx5* varies between species and tissues, one of our goals was to elucidate regulatory regions within the *IrxB* locus using the available

epigenetic datasets and histone markers as a starting point. We used histone markers such as H3K27ac and H3K27me3 to identify active and repressive regions, respectively, within cell populations of the gonad during development. We hypothesize that histone modifications, in coordination with canonical *Wnt/Rspo1/β-catenin* signaling in the ovary, lead to increased *Irx3* and *Irx5* expression, meanwhile absence of β-catenin and the presence of repressive histones in the testis results in the lack of *Irx3* and *Irx5* expression. **Chapter 2** explores these connections, and how both epigenetics and β-catenin play sex-specific roles in *Irx3* and *Irx5* regulation.

β-catenin and its multiple roles in the cell

β-catenin, a multifaceted and evolutionary conserved protein, has numerous functions in the cell. Specifically, β-catenin is an integral component of cadherin-based adherens junctions, but also is the critical nuclear effector of canonical Wnt signaling (**Figure 1.2**). During development, β-catenin contributes to the establishment of the body axis while additionally orchestrating the development of many tissues and organs. In the adult, β-catenin plays roles in tissue homeostasis, cell renewal, and regeneration.

In the 1980s, the Kemler group isolated β-catenin together with two other proteins (now known as α-catenin and γ-catenin) as proteins associated with E-cadherin, which is a critical molecule in calcium-dependent cell adhesion. The name ‘catenin' comes from the Latin word ‘Catena,' which means chain. This name reflects their linking of E-cadherin to cytoskeletal structures (Ozawa, Baribault, & Kemler, 1989). β-catenin’s structure is the reason it can mediate both adhesive and signaling roles

independently – the protein (781aa residues in human) consists of 12 imperfect Armadillo repeats that are flanked by N- and C-terminal domains. A conserved Helix-C is located proximal to the C-terminal domain, next to the last armadillo repeat (Xing et al., 2008). The terminal domains are structurally flexible, where the central region forms a relatively rigid scaffold. This rigid scaffold is where β-catenin can interact to its binding partners on the membrane, in the cytoplasm, and the nucleus (Huber, Nelson, & Weis, 1997). Both biochemical and crystal structure analysis showed that many binding partners of β-catenin share overlapping binding sites within this region, which means that these partners cannot bind simultaneously (Eklof Spink, Fridman, & Weis, 2001; Graham, Weaver, Mao, Kimelman, & Xu, 2000; Huber & Weis, 2001; Poy, Lepourcelet, Shivdasani, & Eck, 2001).

In the absence of Wnt signaling, most β-catenin is at the cytoplasmic side of the membrane as a component of the cadherin complex. Cadherins are single-pass transmembrane glycoproteins that link β-catenin through their cytoplasmic tails. β-catenin can interact with both E-cadherins and N-cadherins, but the most extensively studied are the β-catenin and E-cadherin interactions. The interaction between β-catenin and E-cadherin is constitutive; newly synthesized E-cadherin links with β-catenin while still in the endoplasmic reticulum, and then both proteins move together to the membrane. Interference between the β-catenin/E-cadherin interaction results in the degradation of E-cadherin due to the exposure of a PEST sequence on E-cadherin usually shielded by β-catenin. This motif is recognized by a ubiquitin ligase, marking E-cadherin for degradation (Hinck, Näthke, Papkoff, & Nelson, 1994).

Cadherin-catenin junctions are highly dynamic complexes, and loss of cell adhesion via cadherins can promote the release of β-catenin and its signaling activity. Conversely, cadherins can act as a trap for free β-catenin as well (reviewed in (Heuberger & Birchmeier, 2010)). Proteases can also cleave the intracellular domain of cadherins, affecting the integrity of adherins junctions and β-catenin activity (Maretzky et al., 2005; Reiss et al., 2005). Both somatic and germ cell-specific knockouts of E-cadherin in the gonad result in germ cell death, suggesting that *Cdh1* is necessary for germ cell survival (Piprek, Kolasa, Podkowa, Kloc, & Kubiak, 2019). This study did not investigate the effect of *Cdh1* loss on β-catenin activity, which would be an important question for future studies.

Free β-catenin (not bound by E-cadherin) in the cytoplasm is short-lived in the absence of Wnt signaling. Axin almost immediately recognizes β-catenin and APC in its free state, establishing a platform for kinases CK1α and GSK3β to phosphorylate residues Ser45, Thr41, Ser37, and Ser33 on β-catenin (C. Liu et al., 2002; Roberts et al., 2011; Xing, Clements, Kimelman, & Xu, 2003). Phosphorylated β-catenin can then interact with the E3 ubiquitin ligase machinery and it is ultimately degraded by the 26S proteasome (Hart et al., 1999). Activation of Wnt signaling at the membrane via the Frizzled (FZD) receptor or co-receptors LRP5/6 result in the disassembly of the destruction complex, which blocks the kinase activity by GSK3β on β-catenin. This disassembly is thought to occur based on the recruitment of Dishevelled (Dvl) to the ligand-activated FZD receptor, ultimately recruiting Axin and other associated proteins (such as CK1α and GSK3β) thereby destabilizing the entire complex (Bilic et al., 2007;

Schwarz-Romond, Metcalfe, & Bienz, 2007). β-catenin then remains unphosphorylated, accumulates in the cytoplasm, and then translocates to the nucleus. Nuclear β-catenin can subsequently associate with TCF/LEF DNA binding family members, converting the TCF/LEF proteins from transcriptional repressors to activators (van Noort & Clevers, 2002). See **Figure 1.2** for a simplified model.

The identification of β-catenin/TCF/LEF binding sites specific to the female during gonad differentiation plays a central role in **Chapter 2**. Our genes of interest, *Irx3* and *Irx5*, show a positive correlation to β-catenin expression in the developing ovary, and we hypothesize that these highly conserved genes are direct targets of this pathway.

Iroquois Genes

The Iroquois (Iro) genes were first discovered in *Drosophila* when researchers were identifying genes that affected the patterning of external sensory organs (Dambly-Chaudière & Leyns, 1992; Leyns, Gómez-Skarmeta, & Dambly-Chaudière, 1996). The phenotype that arose in *Drosophila* after mutation of *iro* resembled the hairstyle of the Iroquois American Indians (more commonly known as the Mohawk); hence, the name was given to the gene locus. Characterization of these genes in *Drosophila* by Gómez-Skarmeta *et al*. and McNeill *et al.* (Gomez-Skarmeta, Diez del Corral, de la Calle-Mustienes, Ferré-Marcó, & Modolell, 1996; McNeill, Yang, Brodsky, Ungos, & Simon, 1997) led to the identification of homologs in *C. elegans*, *Xenopus*, zebrafish, mouse, and human (Bao, Bruneau, Seidman, Seidman, & Cepko, 1999; Bellefroid et al., 1998; Bosse et al., 2000; Bosse et al., 1997; Christoffels, Keijser, Houweling, Clout, & Moorman, 2000; Cohen, Cheng, Cheng, & Hui, 2000; Funayama, Sato, Matsumoto,

Ogura, & Takahashi, 1999; Goriely, Diez del Corral, & Storey, 1999; JL, 1998; T. Peters, R. Dildrop, K. Ausmeier, & U. Rüther, 2000; Tan, Korzh, & Gong, 1999). All Iroquois proteins conform to the TALE (Three Amino Acid Loop Extension) structure and contain an Iro box domain, which is a motif with an unknown function, but most likely mediates protein-protein interactions (Bürglin, 1997; J. L. Gómez-Skarmeta & Modolell, 2002; Mukherjee & Bürglin, 2007). *Drosophila* has three Iro genes (*ara, caup, mirror*), and mammals have six Iro genes organized by two clusters (*Irx1-6*). The mammalian Iro genes are clustered in two groups of three with the A cluster (*Irx1, 2, 4*) and the B cluster (*Irx3, 5, 6*) located on chromosomes 5 and 16 in the human and chromosomes 8 and 13 in the mouse (Bosse et al., 2000; Thomas Peters, Renate Dildrop, Katrin Ausmeier, & Ulrich Rüther, 2000). The organization of these genes most likely arose from a duplication event in an ancestral lineage, as the mouse and human organization are strikingly similar.

Most functional studies of the *Iro* gene family have been performed in *Drosophila* and have provided important insight for vertebrate research. One of the first systems studied in connection with the Iroquois complex (Iro-C) was *Drosophila* eye development. One group analyzed the loss of *mirr* in the dorsal region of the eye (McNeill et al., 1997), which induced ectopic barriers at the border between *mirr* positive and negative cells. Following this study, multiple groups demonstrated that the mis-expression of any genes within Iro-C in the eye disc led to a loss-of-eye phenotype (Cavodeassi, Diez Del Corral, Campuzano, & Domínguez, 1999; Cho & Choi, 1998; Domínguez & de Celis, 1998). Similarly, Iro-C helps confer identity and patterning of tissues at the Iro-C expression and non-expression boundary in the *Drosophila* dorsal

mesothorax (Diez del Corral, Aroca, G mez-Skarmeta, Cavodeassi, & Modolell, 1999). Overall, the *Drosophila* studies conclude that the Iro-C genes play a role in the dorsoventral organization in multiple tissues throughout the body.

In early *Xenopus* development, *Xiro1* and *Xiro2* are essential for neural plate development. Injection of mRNA that encodes wild-type or mutated Xiro proteins show abnormal neural crest development in the mutant samples, and overexpression of *Xiro1* and *Xiro2* results in an enlarged neural plate and a reduction in neural crests (Bellefroid et al., 1998; J. Gómez-Skarmeta, de La Calle-Mustienes, & Modolell, 2001; JL, 1998). One of the key findings in early neural fate development is the regulation of *Xiro1* by Wnt signaling and its role in the repression of *Bmp-4*. Overexpression of *Xiro1* reduces *Bmp-4* and, conversely, the presence of dominant negative *Xiro1* results in ectopic *Bmp-4* expression (J. Gómez-Skarmeta et al., 2001).

Iro genes are also necessary for heart patterning and function. Mice with a disruption of *Irx4* develop a normal heart but exhibit abnormal ventricular gene expression, and these mice eventually develop cardiomyopathy as adults (Bruneau et al., 2001). *Irx* genes are essential for some postnatal cardiac function in mice, such as cardiac repolarization (*Irx5*) and rapid ventricular conduction (*Irx3*) (Costantini et al., 2005; Zhang, Kim, Rosen, Smyth, & Sakuma, 2011). Additionally, *Irx3* has been shown to ensure proper expression of gap junction proteins *Gja5* and *Gja1* in the postnatal ventricular conduction system (VCS); mice lacking *Irx3* in these tissues develop morphological defects in the VCS (K. H. Kim et al., 2016; Zhang et al., 2011).

The control of *Iro* gene expression is an elusive journey – the emerging conclusion is that although some signaling pathways commonly control these genes,

the details of this regulation varies widely between tissues. In the *Drosophila* eye, Iro genes are activated by Wg (Wingless) and Hh (Hedgehog) signaling (Cavodeassi et al., 1999), while the JAK/STAT pathway has been shown to positively regulate *mirr* (Zeidler, Perrimon, & Strutt, 1999). The EGFR pathway has also been implicated in activating Iro-C in the wing (Wang, Simcox, & Campbell, 2000). In early vertebrate development, both Wnt and BMP-4 have been involved (J. Gómez-Skarmeta et al., 2001), but many questions about the control of the postnatal expression of the Irx genes remain unanswered. Some groups have claimed postnatal expression relies on Hh signaling (*Xenopus*, Chick) or FGF factors in the brain (*Xenopus*), but these claims require further investigation (Bellefroid et al., 1998; Briscoe, Pierani, Jessell, & Ericson, 2000; JL, 1998).

Irx3 **and** ***Irx5*** **role in Ovarian Development**

Our laboratory discovered that *Irx3,* an *IrxB* cluster member, is specifically expressed in the ovary (and not the testis) during gonad development using an Affymetrix GeneChip. *Irx3* expression is abundant in the ovary during development and early adulthood (Jorgensen & Gao, 2005). This expression pattern is similar for *Irx5*, another *IrxB* cluster member, which is also ovary-specific (B. Kim, Kim, Sakuma, et al., 2011).

The first mouse model we explored was the *Fused Toes* (*Ft*) mouse. This mouse lacked the *IrxB* cluster (*Irx3, 5, 6*) and three *Ft* genes (*Ftm, Fts, Fto*). *Ft* mutant ovaries exhibit fewer germ cells caused by a progressive decrease in germ cell proliferation (B. Kim, Kim, Sakuma, et al., 2011). These mutant ovaries also show improper follicle

development and have few surviving immature follicles, ultimately leading to the conclusion that the disruption of these genes stunt follicle maturation in *Ft* mutant ovaries (B. Kim, Kim, Cooke, Rüther, & Jorgensen, 2011).

The *Ft* mutant mice established that *IrxB* and or *Ft* loci were critical for ovary development. Next, we obtained mutant mouse models that allowed us to focus on *Irx3* and *Irx5*. Ovaries lacking both *Irx3* and *Irx5* had abnormal granulosa cell morphology within the follicle and disrupted granulosa/oocyte interactions (Fu et al., 2018). Another mouse with a complex genotype that included global knockout of *Irx5,* a single allele knockout of *Irx3* (Δ), and a single floxed allele of *Irx3* (*Irx3/5* Hypomorph mouse), failed to respond to hormonal signals dedicated for ovulation. These ovaries had fewer oocytes retrieved in IVF, supported by the presence of fewer corpora lutea (CL), which are present at a 1:1 ratio of ovulated oocytes (Fu et al., 2018).

Finally, individual knockouts of either *Irx3* ($Irx3^{LacZ/LacZ}$) or *Irx5* ($Irx5^{EGFP/EGFP}$) showed that both strains were sub-fertile, but in different ways. *Irx3* knockout mice gave birth to fewer pups throughout the breeding period but *Irx5* knockout mice did not produce fewer pups until 4 months into the 6-month long breeding study. These data led us to conclude that while both factors are essential for optimal fertility, they potentially have different roles in the ovary (Fu et al., 2018), which may be explained by their differential expression patterns. Both *Irx3* and *Irx5* are expressed solely in the somatic, pre-granulosa cells within germline nests during development, but their expression transitions to the germ cell (while remaining on in the somatic compartment) during primordial follicle formation. Once primordial follicles form and then initiate follicle

maturation, *Irx3* is confined to the germ cell, while *Irx5* reverts back into the granulosa cells before diminishing completely (Fu et al., 2018).

Because *Irx3* and *Irx5* are expressed in both cell types during distinct time frames, we explored both somatic (**Chapter 2**) and germ cell (**Chapter 3**) connections between *Irx3*, *Irx5*, and the canonical *Wnt/Rspo1/β-catenin* signaling pathway. In addition, the overexpression of *Irx3* in both cell types is examined in **Chapter 4** with intriguing results.

In summary, a delicate balance between signaling pathways and epigenetic markers coordinate sex differentiation and regulation in the ovary, and we sought to explore this coordination in connection to *Irx3* and *Irx5* expression in the ovary, along with the effects of *Irx3* overexpression in both sexes. While we have come a long way with this project, there are future avenues for this study that could answer some critical questions pertaining to the important roles of *Irx3* and *Irx5* and overall ovarian health throughout the life of a woman, and how *Irx3* and *Irx5* may be linked to the pathogenesis of POI in humans (**Chapter 5**).

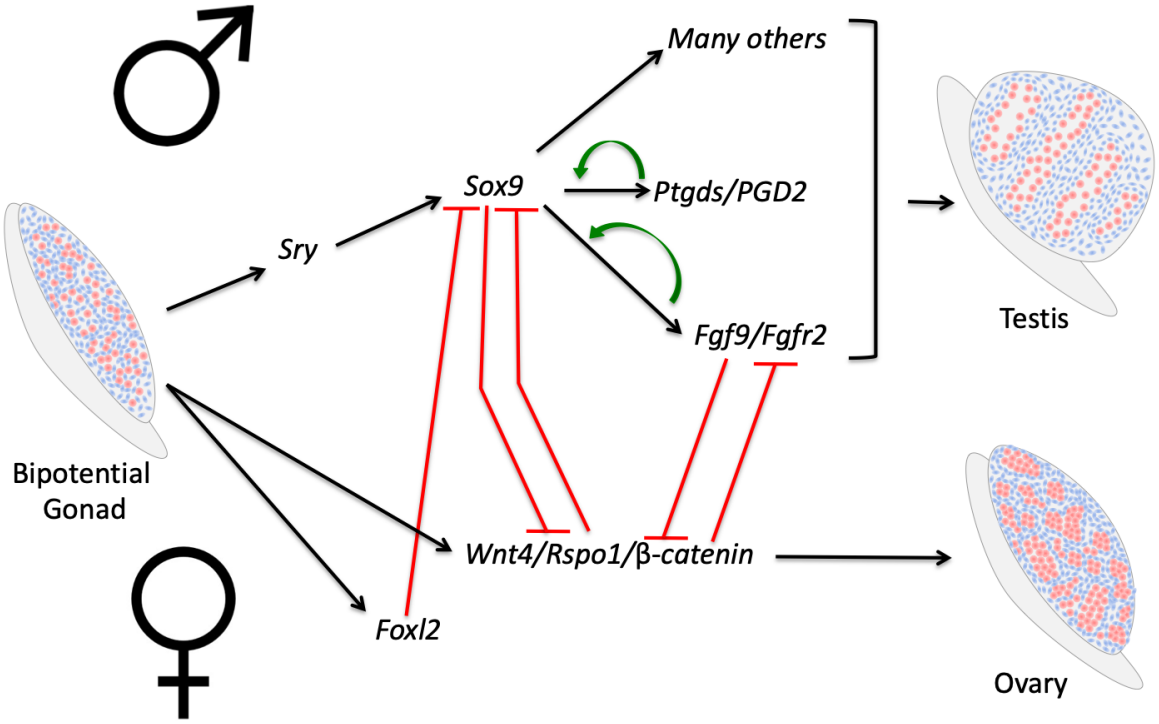

Figure 1.1

Factors underlying sex determination in the gonad

Gonad development in the mouse begins at a bipotential state and can differentiate into either a testis or an ovary depending on the activation of certain genes/pathways. Mutual antagonism between many of these factors ensure the proper formation of either a testis or an ovary. Red lines indicate antagonism, green lines indicate a positive feedback loop.

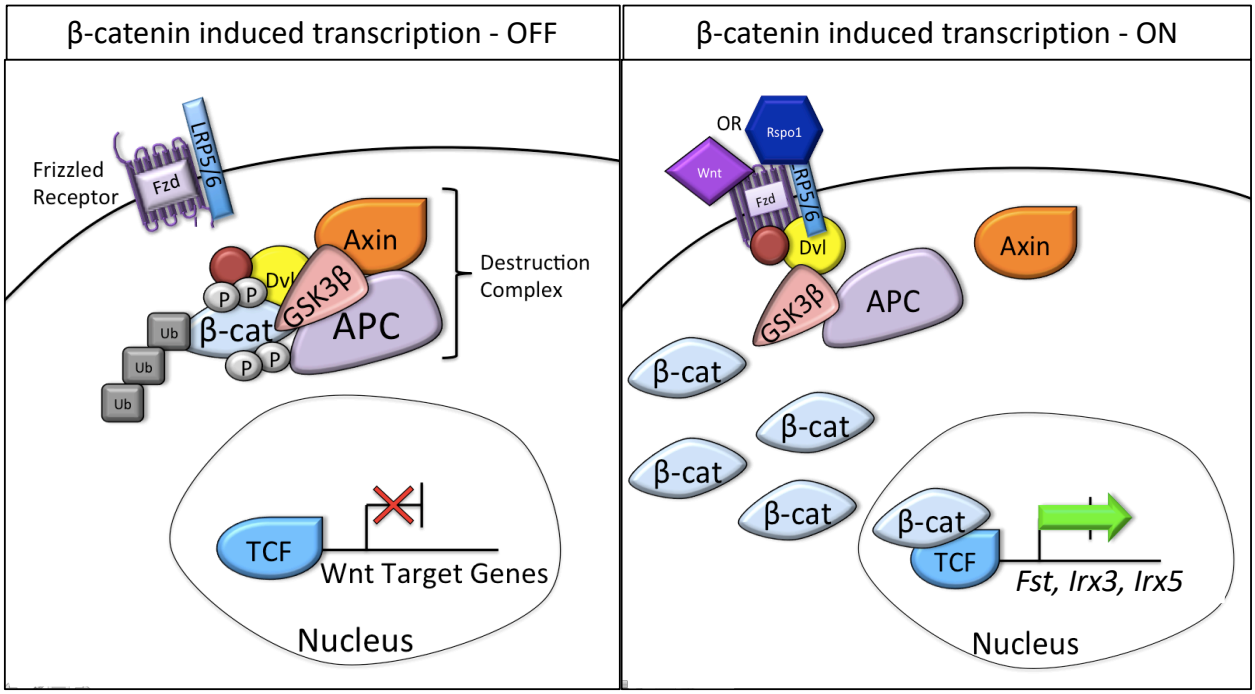

Figure 1.2:

Canonical Wnt/Rspo1 signaling leads to β-catenin induced transcription

Left panel: Without a WNT or RSPO1 ligand present at the membrane at the Frizzled (FZD) or LRP5/6 receptors, the destruction complex forms, leading to β-catenin degradation by the 26S proteasome, keeping Wnt target genes in an "off" state. Right panel: If a WNT or RSPO1 ligand binds to its membrane receptor(s), the destruction complex does not form, allowing β-catenin to accumulate, translocate to the nucleus, bind to its DNA binding partners TCF/LEF family members, and turn on Wnt target genes (ovary examples: *Fst, Irx3, Irx5*).

Gene-Altered	Loss or Gain	Ovary Phenotype	Testis Phenotype	Sex reversal?	Reference
Wnt4	Knockout	Testis vasculature, Leydig cell markers are shown, depletion of oocytes	Possible abnormal Sertoli cell differentiation (conflicting evidence)	Partial	(Jeays-Ward, Dandonneau, & Swain, 2004; Vainio et al., 1999; H. H. C. Yao et al., 2004)
Rspo1	Knockout	Testis vasculature, seminiferous tubules, Sertoli and Leydig cells present, loss of oocytes, meiosis impaired	None reported	Partial	(A.-A. Chassot et al., 2011; Anne Amandine Chassot et al., 2008; Tomizuka et al., 2008)
Ctnnb1	Somatic Loss	Coelomic vessel formation, Leydig cell markers are shown, loss of germ cells	None reported	Partial	(C.-F. Liu et al., 2009; Manuylov, Smagulova, Leach, & Tevosian, 2008)
Ctnnb1	Somatic Gain	Hemorrhagic areas present, previously described in another model. Infertile.	No cord formation resemble ovary lacking oocytes, disruption of Sertoli cell lineage. Infertile.	Full	(Boerboom et al., 2005; Maatouk et al., 2008)

Figure 1.3:

Phenotypes of Canonical Wnt/Rspo1/β-catenin manipulation in mouse gonads.

Previous literature reported effects of the indicated manipulation.

References

Bagheri-Fam, S., Sim, H., Bernard, P., Jayakody, I., Taketo, M. M., Scherer, G., & Harley, V. R. (2008). Loss of Fgfr2 leads to partial XY sex reversal. *Dev Biol, 314*(1), 71-83. doi:10.1016/j.ydbio.2007.11.010

Bao, Z. Z., Bruneau, B. G., Seidman, J. G., Seidman, C. E., & Cepko, C. L. (1999). Regulation of chamber-specific gene expression in the developing heart by Irx4. *Science, 283*(5405), 1161-1164. Retrieved from https://www.ncbi.nlm.nih.gov/pubmed/10024241

Barrionuevo, F., Bagheri-Fam, S., Klattig, J., Kist, R., Taketo, M. M., Englert, C., & Scherer, G. (2006). Homozygous inactivation of Sox9 causes complete XY sex reversal in mice. *Biol Reprod, 74*(1), 195-201. doi:10.1095/biolreprod.105.045930

Bellefroid, E. J., Kobbe, A., Gruss, P., Pieler, T., Gurdon, J. B., & Papalopulu, N. (1998). Xiro3 encodes a Xenopus homolog of the Drosophila Iroquois genes and functions in neural specification. *EMBO J, 17*(1), 191-203. doi:10.1093/emboj/17.1.191

Bentley, G. A., Lewit-Bentley, A., Finch, J. T., Podjarny, A. D., & Roth, M. (1984). Crystal structure of the nucleosome core particle at 16 A resolution. *J Mol Biol, 176*(1), 55-75. Retrieved from https://www.ncbi.nlm.nih.gov/pubmed/6737479

Berta, P., Hawkins, J. R., Sinclair, A. H., Taylor, A., Griffiths, B. L., Goodfellow, P. N., & Fellous, M. (1990). Genetic evidence equating SRY and the testis-determining factor. *Nature, 348*(6300), 448-450. doi:10.1038/348448A0

Bilic, J., Huang, Y. L., Davidson, G., Zimmermann, T., Cruciat, C. M., Bienz, M., & Niehrs, C. (2007). Wnt induces LRP6 signalosomes and promotes dishevelled-dependent LRP6 phosphorylation. *Science, 316*(5831), 1619-1622. doi:10.1126/science.1137065

Birk, O. S., Casiano, D. E., Wassif, C. A., Cogliati, T., Zhao, L., Zhao, Y., Grinberg, A., Huang, S., Kreidberg, J. A., Parker, K. L., Porter, F. D., & Westphal, H. (2000). The LIM homeobox gene Lhx9 is essential for mouse gonad formation. *Nature, 403*(6772), 909-913. doi:10.1038/35002622

Bishop, C. E., Whitworth, D. J., Qin, Y., Agoulnik, A. I., Agoulnik, I. U., Harrison, W. R., Behringer, R. R., & Overbeek, P. A. (2000). A transgenic insertion upstream of sox9 is associated with dominant XX sex reversal in the mouse. *Nat Genet, 26*(4), 490-494. doi:10.1038/82652

Bloom, K., & Joglekar, A. (2010). Towards building a chromosome segregation machine. *Nature, 463*(7280), 446-456. doi:10.1038/nature08912

Boerboom, D., Paquet, M., Hsieh, M., Liu, J., Jamin, S. P., Behringer, R. R., Sirois, J., Taketo, M. M., & Richards, J. S. (2005). Misregulated Wnt/beta-catenin signaling leads to ovarian granulosa cell tumor development. *Cancer Res, 65*(20), 9206-9215. doi:10.1158/0008-5472.CAN-05-1024

Bosse, A., Stoykova, A., Nieselt-Struwe, K., Chowdhury, K., Copeland, N. G., Jenkins, N. A., & Gruss, P. (2000). Identification of a novel mouse Iroquois homeobox gene, Irx5, and chromosomal localisation of all members of the mouse Iroquois gene family. *Dev Dyn, 218*(1), 160-174. doi:10.1002/(SICI)1097-0177(200005)218:1<160::AID-DVDY14>3.0.CO;2-2

Bosse, A., Zülch, A., Becker, M. B., Torres, M., Gómez-Skarmeta, J. L., Modolell, J., & Gruss, P. (1997). Identification of the vertebrate Iroquois homeobox gene family with overlapping expression during early development of the nervous system. *Mech Dev, 69*(1-2), 169-181. Retrieved from https://www.ncbi.nlm.nih.gov/pubmed/9486539

Brennan, J., Tilmann, C., & Capel, B. (2003). Pdgfr-alpha mediates testis cord organization and fetal Leydig cell development in the XY gonad. *Genes Dev, 17*(6), 800-810. doi:10.1101/gad.1052503

Briscoe, J., Pierani, A., Jessell, T. M., & Ericson, J. (2000). A homeodomain protein code specifies progenitor cell identity and neuronal fate in the ventral neural tube. *Cell, 101*(4), 435-445. Retrieved from http://www.ncbi.nlm.nih.gov/pubmed/10830170

Bruneau, B. G., Bao, Z. Z., Fatkin, D., Xavier-Neto, J., Georgakopoulos, D., Maguire, C. T., Berul, C. I., Kass, D. A., Kuroski-de Bold, M. L., de Bold, A. J., Conner, D. A., Rosenthal, N., Cepko, C. L., Seidman, C. E., & Seidman, J. G. (2001). Cardiomyopathy in Irx4-deficient mice is preceded by abnormal ventricular gene expression. *Mol Cell Biol, 21*(5), 1730-1736. doi:10.1128/MCB.21.5.1730-1736.2001

Bürglin, T. R. (1997). Analysis of TALE superclass homeobox genes (MEIS, PBC, KNOX, Iroquois, TGIF) reveals a novel domain conserved between plants and animals. *Nucleic Acids Res, 25*(21), 4173-4180. Retrieved from https://www.ncbi.nlm.nih.gov/pubmed/9336443

Cavodeassi, F., Diez Del Corral, R., Campuzano, S., & Domínguez, M. (1999). Compartments and organising boundaries in the Drosophila eye: the role of the homeodomain Iroquois proteins. *Development, 126*(22), 4933-4942. Retrieved from https://www.ncbi.nlm.nih.gov/pubmed/10529412

Chaboissier, M. C., Kobayashi, A., Vidal, V. I., Lützkendorf, S., van de Kant, H. J., Wegner, M., de Rooij, D. G., Behringer, R. R., & Schedl, A. (2004). Functional analysis of Sox8 and Sox9 during sex determination in the mouse. *Development, 131*(9), 1891-1901. doi:10.1242/dev.01087

Chassot, A.-A., Gregoire, E. P., Lavery, R., Taketo, M. M., de Rooij, D. G., Adams, I. R., & Chaboissier, M.-C. (2011). RSPO1/β-catenin signaling pathway regulates oogonia differentiation and entry into meiosis in the mouse fetal ovary. *PloS one, 6*(10), e25641-e25641. doi:10.1371/journal.pone.0025641

Chassot, A. A., Gillot, I., & Chaboissier, M. C. (2014). R-spondin1, WNT4, and the CTNNB1 signaling pathway: strict control over ovarian differentiation. *Reproduction, 148*(6), R97-110. doi:10.1530/REP-14-0177

Chassot, A. A., Ranc, F., Gregoire, E. P., Roepers-Gajadien, H. L., Taketo, M. M., Camerino, G., de Rooij, D. G., Schedl, A., & Chaboissier, M. C. (2008). Activation of β-catenin signaling by Rspo1 controls differentiation of the mammalian ovary. *Hum Mol Genet, 17*(9), 1264-1277. doi:10.1093/hmg/ddn016

Cho, K. O., & Choi, K. W. (1998). Fringe is essential for mirror symmetry and morphogenesis in the Drosophila eye. *Nature, 396*(6708), 272-276. doi:10.1038/24394

Christoffels, V. M., Keijser, A. G., Houweling, A. C., Clout, D. E., & Moorman, A. F. (2000). Patterning the embryonic heart: identification of five mouse Iroquois homeobox genes in the developing heart. *Dev Biol, 224*(2), 263-274. doi:10.1006/dbio.2000.9801

Clements, A., Poux, A. N., Lo, W. S., Pillus, L., Berger, S. L., & Marmorstein, R. (2003). Structural basis for histone and phosphohistone binding by the GCN5 histone acetyltransferase. *Mol Cell, 12*(2), 461-473. Retrieved from https://www.ncbi.nlm.nih.gov/pubmed/14536085

Cohen, D. R., Cheng, C. W., Cheng, S. H., & Hui, C. C. (2000). Expression of two novel mouse Iroquois homeobox genes during neurogenesis. *Mech Dev, 91*(1-2), 317-321. Retrieved from https://www.ncbi.nlm.nih.gov/pubmed/10704856

Colvin, J. S., Green, R. P., Schmahl, J., Capel, B., & Ornitz, D. M. (2001). Male-to-female sex reversal in mice lacking fibroblast growth factor 9. *Cell, 104*(6), 875-889. Retrieved from https://www.ncbi.nlm.nih.gov/pubmed/11290325

Conway, G. S. (2010). Premature ovarian failure and FMR1 gene mutations: an update. *Ann Endocrinol (Paris), 71*(3), 215-217. doi:10.1016/j.ando.2010.02.009

Cooper, G. S., & Sandler, D. P. (1997). Long-term effects of reproductive-age menstrual cycle patterns on peri- and postmenopausal fracture risk. *Am J Epidemiol, 145*(9), 804-809. Retrieved from https://www.ncbi.nlm.nih.gov/pubmed/9143210

Cooper, G. S., & Sandler, D. P. (1998). Age at natural menopause and mortality. *Ann Epidemiol, 8*(4), 229-235. Retrieved from https://www.ncbi.nlm.nih.gov/pubmed/9590601

Cordts, E. B., Christofolini, D. M., Dos Santos, A. A., Bianco, B., & Barbosa, C. P. (2011). Genetic aspects of premature ovarian failure: a literature review. *Arch Gynecol Obstet, 283*(3), 635-643. doi:10.1007/s00404-010-1815-4

Costantini, D. L., Arruda, E. P., Agarwal, P., Kim, K. H., Zhu, Y., Zhu, W., Lebel, M., Cheng, C. W., Park, C. Y., Pierce, S. A., Guerchicoff, A., Pollevick, G. D., Chan, T. Y., Kabir, M. G., Cheng, S. H., Husain, M., Antzelevitch, C., Srivastava, D., Gross, G. J., Hui, C. C., Backx, P. H., & Bruneau, B. G. (2005). The homeodomain transcription factor Irx5 establishes the mouse cardiac ventricular repolarization gradient. *Cell, 123*(2), 347-358. doi:10.1016/j.cell.2005.08.004

Coulam, C. B., Adamson, S. C., & Annegers, J. F. (1986). Incidence of premature ovarian failure. *Obstet Gynecol, 67*(4), 604-606. Retrieved from https://www.ncbi.nlm.nih.gov/pubmed/3960433

Cramer, D. W. (1990). Epidemiologic aspects of early menopause and ovarian cancer. *Ann N Y Acad Sci, 592*, 363-375; discussion 390-364. Retrieved from https://www.ncbi.nlm.nih.gov/pubmed/2197952

Dambly-Chaudière, C., & Leyns, L. (1992). The determination of sense organs in Drosophila: a search for interacting genes. *Int J Dev Biol, 36*(1), 85-91. Retrieved from https://www.ncbi.nlm.nih.gov/pubmed/1627479

Datta, J., Palmer, M. J., Tanton, C., Gibson, L. J., Jones, K. G., Macdowall, W., Glasier, A., Sonnenberg, P., Field, N., Mercer, C. H., Johnson, A. M., & Wellings, K. (2016). Prevalence of infertility and help seeking among 15 000 women and men. *Hum Reprod, 31*(9), 2108-2118. doi:10.1093/humrep/dew123

Diez del Corral, R., Aroca, P., G mez-Skarmeta, J. L., Cavodeassi, F., & Modolell, J. (1999). The Iroquois homeodomain proteins are required to specify body wall identity in Drosophila. *Genes Dev, 13*(13), 1754-1761. doi:10.1101/gad.13.13.1754

DiNapoli, L., Batchvarov, J., & Capel, B. (2006). FGF9 promotes survival of germ cells in the fetal testis. *Development, 133*(8), 1519-1527. doi:10.1242/dev.02303

Domínguez, M., & de Celis, J. F. (1998). A dorsal/ventral boundary established by Notch controls growth and polarity in the Drosophila eye. *Nature, 396*(6708), 276-278. doi:10.1038/24402

Eklof Spink, K., Fridman, S. G., & Weis, W. I. (2001). Molecular mechanisms of beta-catenin recognition by adenomatous polyposis coli revealed by the structure of an APC-beta-catenin complex. *EMBO J, 20*(22), 6203-6212. doi:10.1093/emboj/20.22.6203

Fu, A., Oberholtzer, S. M., Bagheri-Fam, S., Rastetter, R. H., Holdreith, C., Caceres, V. L., John, S. V., Shaw, S. A., Krentz, K. J., Zhang, X., Hui, C. C., Wilhelm, D., & Jorgensen, J. S. (2018). Dynamic expression patterns of Irx3 and Irx5 during germline nest breakdown and primordial follicle formation promote follicle survival in mouse ovaries. *PLoS Genet, 14*(8), e1007488. doi:10.1371/journal.pgen.1007488

Funayama, N., Sato, Y., Matsumoto, K., Ogura, T., & Takahashi, Y. (1999). Coelom formation: binary decision of the lateral plate mesoderm is controlled by the

ectoderm. *Development, 126*(18), 4129-4138. Retrieved from https://www.ncbi.nlm.nih.gov/pubmed/10457021

Garcia-Moreno, S. A., Futtner, C. R., Salamone, I. M., Gonen, N., Lovell-Badge, R., & Maatouk, D. M. (2019). Gonadal supporting cells acquire sex-specific chromatin landscapes during mammalian sex determination. *Dev Biol, 446*(2), 168-179. doi:10.1016/j.ydbio.2018.12.023

Garcia-Moreno, S. A., Lin, Y. T., Futtner, C. R., Salamone, I. M., Capel, B., & Maatouk, D. M. (2019). CBX2 is required to stabilize the testis pathway by repressing Wnt signaling. *PLoS Genet, 15*(5), e1007895. doi:10.1371/journal.pgen.1007895

Garcia-Moreno, S. A., Plebanek, M. P., & Capel, B. (2018). Epigenetic regulation of male fate commitment from an initially bipotential system. *Mol Cell Endocrinol, 468*, 19-30. doi:10.1016/j.mce.2018.01.009

Gierl, M. S., Gruhn, W. H., von Seggern, A., Maltry, N., & Niehrs, C. (2012). GADD45G functions in male sex determination by promoting p38 signaling and Sry expression. *Dev Cell, 23*(5), 1032-1042. doi:10.1016/j.devcel.2012.09.014

Gökmen, O., Seçkin, N. C., Sener, A. B., Ozakşit, G., & Ekmekçi, S. (1995). A study of premature ovarian failure in Turkish women. *Gynecol Endocrinol, 9*(4), 283-287. Retrieved from https://www.ncbi.nlm.nih.gov/pubmed/8629455

Golbabapour, S., Majid, N. A., Hassandarvish, P., Hajrezaie, M., Abdulla, M. A., & Hadi, A. H. (2013). Gene silencing and Polycomb group proteins: an overview of their structure, mechanisms and phylogenetics. *OMICS, 17*(6), 283-296. doi:10.1089/omi.2012.0105

Gold, E. B., Bromberger, J., Crawford, S., Samuels, S., Greendale, G. A., Harlow, S. D., & Skurnick, J. (2001). Factors associated with age at natural menopause in a multiethnic sample of midlife women. *Am J Epidemiol, 153*(9), 865-874. Retrieved from https://www.ncbi.nlm.nih.gov/pubmed/11323317

Gómez-Skarmeta, J., de La Calle-Mustienes, E., & Modolell, J. (2001). The Wnt-activated Xiro1 gene encodes a repressor that is essential for neural development and downregulates Bmp4. *Development, 128*(4), 551-560. Retrieved from https://www.ncbi.nlm.nih.gov/pubmed/11171338

Gomez-Skarmeta, J. L., Diez del Corral, R., de la Calle-Mustienes, E., Ferré-Marcó, D., & Modolell, J. (1996). Araucan and caupolican, two members of the novel iroquois complex, encode homeoproteins that control proneural and vein-forming genes. *Cell, 85*(1), 95-105. Retrieved from https://www.ncbi.nlm.nih.gov/pubmed/8620542

Gómez-Skarmeta, J. L., & Modolell, J. (2002). Iroquois genes: genomic organization and function in vertebrate neural development. *Curr Opin Genet Dev, 12*(4), 403-408. Retrieved from https://www.ncbi.nlm.nih.gov/pubmed/12100884

Gonen, N., Futtner, C. R., Wood, S., Garcia-Moreno, S. A., Salamone, I. M., Samson, S. C., Sekido, R., Poulat, F., Maatouk, D. M., & Lovell-Badge, R. (2018). Sex reversal following deletion of a single distal enhancer of. *Science, 360*(6396), 1469-1473. doi:10.1126/science.aas9408

Gonen, N., Quinn, A., O'Neill, H. C., Koopman, P., & Lovell-Badge, R. (2017). Normal Levels of Sox9 Expression in the Developing Mouse Testis Depend on the TES/TESCO Enhancer, but This Does Not Act Alone. *PLoS Genet, 13*(1), e1006520. doi:10.1371/journal.pgen.1006520

Goriely, A., Diez del Corral, R., & Storey, K. G. (1999). c-Irx2 expression reveals an early subdivision of the neural plate in the chick embryo. *Mech Dev, 87*(1-2), 203-206. Retrieved from https://www.ncbi.nlm.nih.gov/pubmed/10495288

Goswami, D., & Conway, G. S. (2005). Premature ovarian failure. *Hum Reprod Update, 11*(4), 391-410. doi:10.1093/humupd/dmi012

Graham, T. A., Weaver, C., Mao, F., Kimelman, D., & Xu, W. (2000). Crystal structure of a beta-catenin/Tcf complex. *Cell, 103*(6), 885-896. Retrieved from https://www.ncbi.nlm.nih.gov/pubmed/11136974

Hacker, A., Capel, B., Goodfellow, P., & Lovell-Badge, R. (1995). Expression of Sry, the mouse sex determining gene. *Development, 121*(6), 1603-1614. Retrieved from https://www.ncbi.nlm.nih.gov/pubmed/7600978

Harlow, B. L., & Signorello, L. B. (2000). Factors associated with early menopause. *Maturitas, 35*(1), 3-9. Retrieved from https://www.ncbi.nlm.nih.gov/pubmed/10802394

Hart, M., Concordet, J. P., Lassot, I., Albert, I., del los Santos, R., Durand, H., Perret, C., Rubinfeld, B., Margottin, F., Benarous, R., & Polakis, P. (1999). The F-box protein beta-TrCP associates with phosphorylated beta-catenin and regulates its activity in the cell. *Curr Biol, 9*(4), 207-210. Retrieved from https://www.ncbi.nlm.nih.gov/pubmed/10074433

Hatano, O., Takayama, K., Imai, T., Waterman, M. R., Takakusu, A., Omura, T., & Morohashi, K. (1994). Sex-dependent expression of a transcription factor, Ad4BP, regulating steroidogenic P-450 genes in the gonads during prenatal and postnatal rat development. *Development, 120*(10), 2787-2797. Retrieved from https://www.ncbi.nlm.nih.gov/pubmed/7607070

Heikkilä, M., Prunskaite, R., Naillat, F., Itäranta, P., Vuoristo, J., Leppäluoto, J., Peltoketo, H., & Vainio, S. (2005). The partial female to male sex reversal in Wnt-4-deficient females involves induced expression of testosterone biosynthetic genes and testosterone production, and depends on androgen action. *Endocrinology, 146*(9), 4016-4023. doi:10.1210/en.2005-0463

Heuberger, J., & Birchmeier, W. (2010). Interplay of cadherin-mediated cell adhesion and canonical Wnt signaling. *Cold Spring Harb Perspect Biol, 2*(2), a002915. doi:10.1101/cshperspect.a002915

Hinck, L., Näthke, I. S., Papkoff, J., & Nelson, W. J. (1994). Dynamics of cadherin/catenin complex formation: novel protein interactions and pathways of complex assembly. *J Cell Biol, 125*(6), 1327-1340. doi:10.1083/jcb.125.6.1327

Hiramatsu, R., Matoba, S., Kanai-Azuma, M., Tsunekawa, N., Katoh-Fukui, Y., Kurohmaru, M., Morohashi, K., Wilhelm, D., Koopman, P., & Kanai, Y. (2009). A critical time window of Sry action in gonadal sex determination in mice. *Development, 136*(1), 129-138. doi:10.1242/dev.029587

Hirshfield, A. N. (1991). Development of follicles in the mammalian ovary. *Int Rev Cytol, 124*, 43-101. Retrieved from https://www.ncbi.nlm.nih.gov/pubmed/2001918

Hjerrild, B. E., Mortensen, K. H., & Gravholt, C. H. (2008). Turner syndrome and clinical treatment. *Br Med Bull, 86*, 77-93. doi:10.1093/bmb/ldn015

Huber, A. H., Nelson, W. J., & Weis, W. I. (1997). Three-dimensional structure of the armadillo repeat region of beta-catenin. *Cell, 90*(5), 871-882. Retrieved from https://www.ncbi.nlm.nih.gov/pubmed/9298899

Huber, A. H., & Weis, W. I. (2001). The structure of the beta-catenin/E-cadherin complex and the molecular basis of diverse ligand recognition by beta-catenin. *Cell, 105*(3), 391-402. Retrieved from https://www.ncbi.nlm.nih.gov/pubmed/11348595

Ikeda, Y., Shen, W. H., Ingraham, H. A., & Parker, K. L. (1994). Developmental expression of mouse steroidogenic factor-1, an essential regulator of the steroid hydroxylases. *Mol Endocrinol, 8*(5), 654-662. doi:10.1210/mend.8.5.8058073

Jameson, S. A., Lin, Y. T., & Capel, B. (2012). Testis development requires the repression of Wnt4 by Fgf signaling. *Dev Biol, 370*(1), 24-32. doi:10.1016/j.ydbio.2012.06.009

Jeays-Ward, K., Dandonneau, M., & Swain, A. (2004). Wnt4 is required for proper male as well as female sexual development. *Developmental biology, 276*(2), 431-440. doi:10.1016/j.ydbio.2004.08.049

JL, G.-S. (1998). Xiro, a Xenopus homolog of the Drosophila Iroquois complex genes, controls development at the neural plate. In G. A (Ed.), (Vol. 17, pp. 181-190). EMBO J.

Joakimsen, O., Bønaa, K. H., Stensland-Bugge, E., & Jacobsen, B. K. (2000). Population-based study of age at menopause and ultrasound assessed carotid atherosclerosis: The Tromsø Study. *J Clin Epidemiol, 53*(5), 525-530. Retrieved from https://www.ncbi.nlm.nih.gov/pubmed/10812326

Jorgensen, J. S., & Gao, L. (2005). Irx3 is differentially up-regulated in female gonads during sex determination. *Gene expression patterns : GEP, 5*(6), 756-762. doi:10.1016/j.modgep.2005.04.011

Jost, A. (1972). A new look at the mechanisms controlling sex differentiation in mammals. *Johns Hopkins Med J, 130*(1), 38-53. Retrieved from https://www.ncbi.nlm.nih.gov/pubmed/4481103

Katoh-Fukui, Y., Miyabayashi, K., Komatsu, T., Owaki, A., Baba, T., Shima, Y., Kidokoro, T., Kanai, Y., Schedl, A., Wilhelm, D., Koopman, P., Okuno, Y., & Morohashi, K. (2012). Cbx2, a polycomb group gene, is required for Sry gene expression in mice. *Endocrinology, 153*(2), 913-924. doi:10.1210/en.2011-1055

Katoh-Fukui, Y., Tsuchiya, R., Shiroishi, T., Nakahara, Y., Hashimoto, N., Noguchi, K., & Higashinakagawa, T. (1998). Male-to-female sex reversal in M33 mutant mice. *Nature, 393*(6686), 688-692. doi:10.1038/31482

Kazanskaya, O., Glinka, A., del Barco Barrantes, I., Stannek, P., Niehrs, C., & Wu, W. (2004). R-Spondin2 is a secreted activator of Wnt/beta-catenin signaling and is required for Xenopus myogenesis. *Dev Cell, 7*(4), 525-534. doi:10.1016/j.devcel.2004.07.019

Kent, J., Wheatley, S. C., Andrews, J. E., Sinclair, A. H., & Koopman, P. (1996). A male-specific role for SOX9 in vertebrate sex determination. *Development, 122*(9), 2813-2822. Retrieved from https://www.ncbi.nlm.nih.gov/pubmed/8787755

Kim, B., Kim, Y., Cooke, P. S., Rüther, U., & Jorgensen, J. S. (2011). The fused toes locus is essential for somatic-germ cell interactions that foster germ cell maturation in developing gonads in mice. *Biology of reproduction, 84*(5), 1024-1032. doi:10.1095/biolreprod.110.088559

Kim, B., Kim, Y., Sakuma, R., Hui, C. C., Rüther, U., & Jorgensen, J. S. (2011). Primordial germ cell proliferation is impaired in Fused Toes mutant embryos. *Developmental biology, 349*(2), 417-426. doi:10.1016/j.ydbio.2010.10.010

Kim, K. H., Rosen, A., Hussein, S. M., Puviindran, V., Korogyi, A. S., Chiarello, C., Nagy, A., Hui, C. C., & Backx, P. H. (2016). Irx3 is required for postnatal maturation of the mouse ventricular conduction system. *Sci Rep, 6*, 19197. doi:10.1038/srep19197

Kim, Y., Kobayashi, A., Sekido, R., DiNapoli, L., Brennan, J., Chaboissier, M. C., Poulat, F., Behringer, R. R., Lovell-Badge, R., & Capel, B. (2006). Fgf9 and Wnt4 act as antagonistic signals to regulate mammalian sex determination. *PLoS Biol, 4*(6), e187. doi:10.1371/journal.pbio.0040187

Koopman, P., Gubbay, J., Vivian, N., Goodfellow, P., & Lovell-Badge, R. (1991). Male development of chromosomally female mice transgenic for Sry. *Nature, 351*(6322), 117-121. doi:10.1038/351117a0

Koopman, P., Münsterberg, A., Capel, B., Vivian, N., & Lovell-Badge, R. (1990). Expression of a candidate sex-determining gene during mouse testis differentiation. *Nature, 348*(6300), 450-452. doi:10.1038/348450a0

Kornberg, R. D., & Thomas, J. O. (1974). Chromatin structure; oligomers of the histones. *Science, 184*(4139), 865-868. doi:10.1126/science.184.4139.865

Kreidberg, J. A., Sariola, H., Loring, J. M., Maeda, M., Pelletier, J., Housman, D., & Jaenisch, R. (1993). WT-1 is required for early kidney development. *Cell, 74*(4), 679-691. Retrieved from https://www.ncbi.nlm.nih.gov/pubmed/8395349

Kritz-Silverstein, D., & Barrett-Connor, E. (1993). Early menopause, number of reproductive years, and bone mineral density in postmenopausal women. *Am J Public Health, 83*(7), 983-988. Retrieved from https://www.ncbi.nlm.nih.gov/pubmed/8328621

Kuroki, S., Matoba, S., Akiyoshi, M., Matsumura, Y., Miyachi, H., Mise, N., Abe, K., Ogura, A., Wilhelm, D., Koopman, P., Nozaki, M., Kanai, Y., Shinkai, Y., & Tachibana, M. (2013). Epigenetic regulation of mouse sex determination by the histone demethylase Jmjd1a. *Science, 341*(6150), 1106-1109. doi:10.1126/science.1239864

Lakhal, B., Braham, R., Berguigua, R., Bouali, N., Zaouali, M., Chaieb, M., Veitia, R. A., Saad, A., & Elghezal, H. (2010). Cytogenetic analyses of premature ovarian failure using karyotyping and interphase fluorescence in situ hybridization (FISH) in a group of 1000 patients. *Clin Genet, 78*(2), 181-185. doi:10.1111/j.1399-0004.2009.01359.x

Lau, M. S., Schwartz, M. G., Kundu, S., Savol, A. J., Wang, P. I., Marr, S. K., Grau, D. J., Schorderet, P., Sadreyev, R. I., Tabin, C. J., & Kingston, R. E. (2017). Mutation of a nucleosome compaction region disrupts Polycomb-mediated axial patterning. *Science, 355*(6329), 1081-1084. doi:10.1126/science.aah5403

Lee, D. Y., Hayes, J. J., Pruss, D., & Wolffe, A. P. (1993). A positive role for histone acetylation in transcription factor access to nucleosomal DNA. *Cell, 72*(1), 73-84. Retrieved from https://www.ncbi.nlm.nih.gov/pubmed/8422685

Leyns, L., Gómez-Skarmeta, J. L., & Dambly-Chaudière, C. (1996). iroquois: a prepattern gene that controls the formation of bristles on the thorax of Drosophila. *Mech Dev, 59*(1), 63-72. Retrieved from https://www.ncbi.nlm.nih.gov/pubmed/8892233

Liu, C., Li, Y., Semenov, M., Han, C., Baeg, G. H., Tan, Y., Zhang, Z., Lin, X., & He, X. (2002). Control of beta-catenin phosphorylation/degradation by a dual-kinase mechanism. *Cell, 108*(6), 837-847. Retrieved from https://www.ncbi.nlm.nih.gov/pubmed/11955436

Liu, C.-F., Bingham, N., Parker, K., & Yao, H. H. C. (2009). Sex-specific roles of beta-catenin in mouse gonadal development. *Hum Mol Genet, 18*(3), 405-417. doi:10.1093/hmg/ddn362

Liu, C. F., Liu, C., & Yao, H. H. (2010). Building pathways for ovary organogenesis in the mouse embryo. *Curr Top Dev Biol, 90*, 263-290. doi:10.1016/S0070-2153(10)90007-0

Loffler, K. A., Zarkower, D., & Koopman, P. (2003). Etiology of ovarian failure in blepharophimosis ptosis epicanthus inversus syndrome: FOXL2 is a conserved, early-acting gene in vertebrate ovarian development. *Endocrinology, 144*(7), 3237-3243. doi:10.1210/en.2002-0095

Logan, C. Y., & Nusse, R. (2004). The Wnt signaling pathway in development and disease. *Annu Rev Cell Dev Biol, 20*, 781-810. doi:10.1146/annurev.cellbio.20.010403.113126

Lovell-Badge, R., & Robertson, E. (1990). XY female mice resulting from a heritable mutation in the primary testis-determining gene, Tdy. *Development, 109*(3), 635-646. Retrieved from https://www.ncbi.nlm.nih.gov/pubmed/2401216

Luborsky, J. L., Meyer, P., Sowers, M. F., Gold, E. B., & Santoro, N. (2003). Premature menopause in a multi-ethnic population study of the menopause transition. *Hum Reprod, 18*(1), 199-206. Retrieved from https://www.ncbi.nlm.nih.gov/pubmed/12525467

Luger, K., Mäder, A. W., Richmond, R. K., Sargent, D. F., & Richmond, T. J. (1997). Crystal structure of the nucleosome core particle at 2.8 A resolution. *Nature, 389*(6648), 251-260. doi:10.1038/38444

Luo, X., Ikeda, Y., & Parker, K. L. (1994). A cell-specific nuclear receptor is essential for adrenal and gonadal development and sexual differentiation. *Cell, 77*(4), 481-490. Retrieved from https://www.ncbi.nlm.nih.gov/pubmed/8187173

Maatouk, D. M., Dinapoli, L., Alvers, A., Parker, K. L., Taketo, M. M., & Capel, B. (2008). Stabilization of β-catenin in XY gonads causes male-to-female sex-reversal. *Hum Mol Genet, 17*(19), 2949-2955. doi:10.1093/hmg/ddn193

Malki, S., Nef, S., Notarnicola, C., Thevenet, L., Gasca, S., Méjean, C., Berta, P., Poulat, F., & Boizet-Bonhoure, B. (2005). Prostaglandin D2 induces nuclear import of the sex-determining factor SOX9 via its cAMP-PKA phosphorylation. *EMBO J, 24*(10), 1798-1809. doi:10.1038/sj.emboj.7600660

Manuylov, N. L., Smagulova, F. O., Leach, L., & Tevosian, S. G. (2008). Ovarian development in mice requires the GATA4-FOG2 transcription complex. *Development (Cambridge, England), 135*(22), 3731-3743. doi:10.1242/dev.024653

Maretzky, T., Reiss, K., Ludwig, A., Buchholz, J., Scholz, F., Proksch, E., de Strooper, B., Hartmann, D., & Saftig, P. (2005). ADAM10 mediates E-cadherin shedding and regulates epithelial cell-cell adhesion, migration, and beta-catenin translocation. *Proc Natl Acad Sci U S A, 102*(26), 9182-9187. doi:10.1073/pnas.0500918102

Mascarenhas, M. N., Flaxman, S. R., Boerma, T., Vanderpoel, S., & Stevens, G. A. (2012). National, regional, and global trends in infertility prevalence since 1990: a systematic analysis of 277 health surveys. *PLoS Med, 9*(12), e1001356. doi:10.1371/journal.pmed.1001356

McLaren, A. (2000). Germ and somatic cell lineages in the developing gonad. *Mol Cell Endocrinol, 163*(1-2), 3-9. Retrieved from https://www.ncbi.nlm.nih.gov/pubmed/10963867

McNeill, H., Yang, C. H., Brodsky, M., Ungos, J., & Simon, M. A. (1997). mirror encodes a novel PBX-class homeoprotein that functions in the definition of the dorsal-

ventral border in the Drosophila eye. *Genes Dev, 11*(8), 1073-1082. Retrieved from https://www.ncbi.nlm.nih.gov/pubmed/9136934

Miyamoto, N., Yoshida, M., Kuratani, S., Matsuo, I., & Aizawa, S. (1997). Defects of urogenital development in mice lacking Emx2. *Development, 124*(9), 1653-1664. Retrieved from https://www.ncbi.nlm.nih.gov/pubmed/9165114

Monaghan, K. G., Lyon, E., Spector, E. B., & Genomics, e. C. o. M. G. a. (2013). ACMG Standards and Guidelines for fragile X testing: a revision to the disease-specific supplements to the Standards and Guidelines for Clinical Genetics Laboratories of the American College of Medical Genetics and Genomics. *Genet Med, 15*(7), 575-586. doi:10.1038/gim.2013.61

Morais da Silva, S., Hacker, A., Harley, V., Goodfellow, P., Swain, A., & Lovell-Badge, R. (1996). Sox9 expression during gonadal development implies a conserved role for the gene in testis differentiation in mammals and birds. *Nat Genet, 14*(1), 62-68. doi:10.1038/ng0996-62

Mukherjee, K., & Bürglin, T. R. (2007). Comprehensive analysis of animal TALE homeobox genes: new conserved motifs and cases of accelerated evolution. *J Mol Evol, 65*(2), 137-153. doi:10.1007/s00239-006-0023-0

Nef, S., Verma-Kurvari, S., Merenmies, J., Vassalli, J. D., Efstratiadis, A., Accili, D., & Parada, L. F. (2003). Testis determination requires insulin receptor family function in mice. *Nature, 426*(6964), 291-295. doi:10.1038/nature02059

Nelson, L. M., Covington, S. N., & Rebar, R. W. (2005). An update: spontaneous premature ovarian failure is not an early menopause. *Fertil Steril, 83*(5), 1327-1332. doi:10.1016/j.fertnstert.2004.11.059

Nishino, K., Hattori, N., Sato, S., Arai, Y., Tanaka, S., Nagy, A., & Shiota, K. (2011). Non-CpG methylation occurs in the regulatory region of the Sry gene. *J Reprod Dev, 57*(5), 586-593. Retrieved from https://www.ncbi.nlm.nih.gov/pubmed/21636956

Nishino, K., Hattori, N., Tanaka, S., & Shiota, K. (2004). DNA methylation-mediated control of Sry gene expression in mouse gonadal development. *J Biol Chem, 279*(21), 22306-22313. doi:10.1074/jbc.M309513200

Ohta, H., Sugimoto, I., Masuda, A., Komukai, S., Suda, Y., Makita, K., Takamatsu, K., Horiguchi, F., & Nozawa, S. (1996). Decreased bone mineral density associated with early menopause progresses for at least ten years: cross-sectional comparisons between early and normal menopausal women. *Bone, 18*(3), 227-231. Retrieved from https://www.ncbi.nlm.nih.gov/pubmed/8703577

Otsuka, F., McTavish, K. J., & Shimasaki, S. (2011). Integral role of GDF-9 and BMP-15 in ovarian function. *Mol Reprod Dev, 78*(1), 9-21. doi:10.1002/mrd.21265

Ottolenghi, C., Omari, S., Garcia-Ortiz, J. E., Uda, M., Crisponi, L., Forabosco, A., Pilia, G., & Schlessinger, D. (2005). Foxl2 is required for commitment to ovary differentiation. *Hum Mol Genet, 14*(14), 2053-2062. doi:10.1093/hmg/ddi210

Ottolenghi, C., Pelosi, E., Tran, J., Colombino, M., Douglass, E., Nedorezov, T., Cao, A., Forabosco, A., & Schlessinger, D. (2007). Loss of Wnt4 and Foxl2 leads to female-to-male sex reversal extending to germ cells. *Hum Mol Genet, 16*(23), 2795-2804. doi:10.1093/hmg/ddm235

Ozawa, M., Baribault, H., & Kemler, R. (1989). The cytoplasmic domain of the cell adhesion molecule uvomorulin associates with three independent proteins structurally related in different species. *EMBO J, 8*(6), 1711-1717. Retrieved from https://www.ncbi.nlm.nih.gov/pubmed/2788574

Parma, P., Radi, O., Vidal, V., Chaboissier, M. C., Dellambra, E., Valentini, S., Guerra, L., Schedl, A., & Camerino, G. (2006). R-spondin1 is essential in sex determination, skin differentiation and malignancy. *Nat Genet, 38*(11), 1304-1309. doi:10.1038/ng1907

Persani, L., Rossetti, R., Cacciatore, C., & Fabre, S. (2011). Genetic defects of ovarian TGF-β-like factors and premature ovarian failure. *J Endocrinol Invest, 34*(3), 244-251. doi:10.1007/BF03347073

Peters, T., Dildrop, R., Ausmeier, K., & Rüther, U. (2000). Organization of mouse Iroquois homeobox genes in two clusters suggests a conserved regulation and function in vertebrate development. *Genome Res, 10*(10), 1453-1462. Retrieved from https://www.ncbi.nlm.nih.gov/pubmed/11042145

Peters, T., Dildrop, R., Ausmeier, K., & Rüther, U. (2000). Organization of mouse Iroquois homeobox genes in two clusters suggests a conserved regulation and

function in vertebrate development. *Genome Research, 10*(10), 1453-1462. doi:10.1101/gr.144100

Piprek, R. P., Kolasa, M., Podkowa, D., Kloc, M., & Kubiak, J. Z. (2019). Tissue-specific knockout of E-cadherin (Cdh1) in developing mouse gonads causes germ cells loss. *Reproduction*. doi:10.1530/REP-18-0621

Poy, F., Lepourcelet, M., Shivdasani, R. A., & Eck, M. J. (2001). Structure of a human Tcf4-beta-catenin complex. *Nat Struct Biol, 8*(12), 1053-1057. doi:10.1038/nsb720

Reiss, K., Maretzky, T., Ludwig, A., Tousseyn, T., de Strooper, B., Hartmann, D., & Saftig, P. (2005). ADAM10 cleavage of N-cadherin and regulation of cell-cell adhesion and beta-catenin nuclear signalling. *EMBO J, 24*(4), 742-752. doi:10.1038/sj.emboj.7600548

Roberts, D. M., Pronobis, M. I., Poulton, J. S., Waldmann, J. D., Stephenson, E. M., Hanna, S., & Peifer, M. (2011). Deconstructing the ßcatenin destruction complex: mechanistic roles for the tumor suppressor APC in regulating Wnt signaling. *Mol Biol Cell, 22*(11), 1845-1863. doi:10.1091/mbc.E10-11-0871

Schmahl, J., Kim, Y., Colvin, J. S., Ornitz, D. M., & Capel, B. (2004). Fgf9 induces proliferation and nuclear localization of FGFR2 in Sertoli precursors during male sex determination. *Development, 131*(15), 3627-3636. doi:10.1242/dev.01239

Schmidt, D., Ovitt, C. E., Anlag, K., Fehsenfeld, S., Gredsted, L., Treier, A. C., & Treier, M. (2004). The murine winged-helix transcription factor Foxl2 is required for granulosa cell differentiation and ovary maintenance. *Development, 131*(4), 933-942. doi:10.1242/dev.00969

Schwarz-Romond, T., Metcalfe, C., & Bienz, M. (2007). Dynamic recruitment of axin by Dishevelled protein assemblies. *J Cell Sci, 120*(Pt 14), 2402-2412. doi:10.1242/jcs.002956

Sekido, R., Bar, I., Narváez, V., Penny, G., & Lovell-Badge, R. (2004). SOX9 is up-regulated by the transient expression of SRY specifically in Sertoli cell precursors. *Dev Biol, 274*(2), 271-279. doi:10.1016/j.ydbio.2004.07.011

Sekido, R., & Lovell-Badge, R. (2008). Sex determination involves synergistic action of SRY and SF1 on a specific Sox9 enhancer. *Nature, 453*(7197), 930-934. doi:10.1038/nature06944

Senöz, S., Direm, B., Gülekli, B., & Gökmen, O. (1996). Estrogen deprivation, rather than age, is responsible for the poor lipid profile and carbohydrate metabolism in women. *Maturitas, 25*(2), 107-114. Retrieved from https://www.ncbi.nlm.nih.gov/pubmed/8905601

Siggers, P., Carré, G. A., Bogani, D., Warr, N., Wells, S., Hilton, H., Esapa, C., Hajihosseini, M. K., & Greenfield, A. (2014). A novel mouse Fgfr2 mutant, hobbyhorse (hob), exhibits complete XY gonadal sex reversal. *PloS one, 9*(6), e100447. doi:10.1371/journal.pone.0100447

Sinclair, A. H., Berta, P., Palmer, M. S., Hawkins, J. R., Griffiths, B. L., Smith, M. J., Foster, J. W., Frischauf, A. M., Lovell-Badge, R., & Goodfellow, P. N. (1990). A gene from the human sex-determining region encodes a protein with homology to a conserved DNA-binding motif. *Nature, 346*(6281), 240-244. doi:10.1038/346240a0

Smith, S., Pfeifer, S. M., & Collins, J. A. (2003). Diagnosis and management of female infertility. *JAMA, 290*(13), 1767-1770. doi:10.1001/jama.290.13.1767

Spicer, L. J., Aad, P. Y., Allen, D. T., Mazerbourg, S., Payne, A. H., & Hsueh, A. J. (2008). Growth differentiation factor 9 (GDF9) stimulates proliferation and inhibits steroidogenesis by bovine theca cells: influence of follicle size on responses to GDF9. *Biol Reprod, 78*(2), 243-253. doi:10.1095/biolreprod.107.063446

Swain, A., & Lovell-Badge, R. (1999). Mammalian sex determination: a molecular drama. *Genes Dev, 13*(7), 755-767. Retrieved from https://www.ncbi.nlm.nih.gov/pubmed/10197976

Tan, J. T., Korzh, V., & Gong, Z. (1999). Expression of a zebrafish iroquois homeobox gene, Ziro3, in the midline axial structures and central nervous system. *Mech Dev, 87*(1-2), 165-168. Retrieved from https://www.ncbi.nlm.nih.gov/pubmed/10495280

Tomizuka, K., Horikoshi, K., Kitada, R., Sugawara, Y., Iba, Y., Kojima, A., Yoshitome, A., Yamawaki, K., Amagai, M., Inoue, A., Oshima, T., & Kakitani, M. (2008). R-

spondin1 plays an essential role in ovarian development through positively regulating Wnt-4 signaling. *Hum Mol Genet, 17*(9), 1278-1291. doi:10.1093/hmg/ddn036

TW, S. (2000). *Langman's Medical Embryology* (IX ed.). Baltimore: Lippincott Williams&Wilkins.

TW, S. (2012). *Langman's Medical Embryology* (XII ed.). Baltimore: Lippincott Williams&Wilkins.

Uda, M., Ottolenghi, C., Crisponi, L., Garcia, J. E., Deiana, M., Kimber, W., Forabosco, A., Cao, A., Schlessinger, D., & Pilia, G. (2004). Foxl2 disruption causes mouse ovarian failure by pervasive blockage of follicle development. *Hum Mol Genet, 13*(11), 1171-1181. doi:10.1093/hmg/ddh124

Uhlenhaut, N. H., Jakob, S., Anlag, K., Eisenberger, T., Sekido, R., Kress, J., Treier, A.-C., Klugmann, C., Klasen, C., Holter, N. I., Riethmacher, D., Schütz, G., Cooney, A. J., Lovell-Badge, R., & Treier, M. (2009). Somatic sex reprogramming of adult ovaries to testes by FOXL2 ablation. *Cell, 139*(6), 1130-1142. doi:10.1016/j.cell.2009.11.021

Vainio, S., Heikkilä, M., Kispert, A., Chin, N., & McMahon, A. P. (1999). Female development in mammals is regulated by Wnt-4 signalling. *Nature, 397*(6718), 405-409. doi:10.1038/17068

Val, P., Lefrançois-Martinez, A. M., Veyssière, G., & Martinez, A. (2003). SF-1 a key player in the development and differentiation of steroidogenic tissues. *Nucl Recept, 1*(1), 8. doi:10.1186/1478-1336-1-8

van der Schouw, Y. T., van der Graaf, Y., Steyerberg, E. W., Eijkemans, J. C., & Banga, J. D. (1996). Age at menopause as a risk factor for cardiovascular mortality. *Lancet, 347*(9003), 714-718. Retrieved from https://www.ncbi.nlm.nih.gov/pubmed/8602000

van Noort, M., & Clevers, H. (2002). TCF transcription factors, mediators of Wnt-signaling in development and cancer. *Dev Biol, 244*(1), 1-8. doi:10.1006/dbio.2001.0566

Vettese-Dadey, M., Grant, P. A., Hebbes, T. R., Crane- Robinson, C., Allis, C. D., & Workman, J. L. (1996). Acetylation of histone H4 plays a primary role in enhancing transcription factor binding to nucleosomal DNA in vitro. *EMBO J, 15*(10), 2508-2518. Retrieved from https://www.ncbi.nlm.nih.gov/pubmed/8665858

Vidal, V. P., Chaboissier, M. C., de Rooij, D. G., & Schedl, A. (2001). Sox9 induces testis development in XX transgenic mice. *Nat Genet, 28*(3), 216-217. doi:10.1038/90046

Wang, S. H., Simcox, A., & Campbell, G. (2000). Dual role for Drosophila epidermal growth factor receptor signaling in early wing disc development. *Genes Dev, 14*(18), 2271-2276. Retrieved from https://www.ncbi.nlm.nih.gov/pubmed/10995384

Wasylyk, B., & Chambon, P. (1979). Transcription by eukaryotic RNA polymerases A and B of chromatin assembled in vitro. *Eur J Biochem, 98*(2), 317-327. Retrieved from https://www.ncbi.nlm.nih.gov/pubmed/226362

Wilhelm, D., & Englert, C. (2002). The Wilms tumor suppressor WT1 regulates early gonad development by activation of Sf1. *Genes Dev, 16*(14), 1839-1851. doi:10.1101/gad.220102

Wilhelm, D., Martinson, F., Bradford, S., Wilson, M. J., Combes, A. N., Beverdam, A., Bowles, J., Mizusaki, H., & Koopman, P. (2005). Sertoli cell differentiation is induced both cell-autonomously and through prostaglandin signaling during mammalian sex determination. *Dev Biol, 287*(1), 111-124. doi:10.1016/j.ydbio.2005.08.039

Wittenberger, M. D., Hagerman, R. J., Sherman, S. L., McConkie-Rosell, A., Welt, C. K., Rebar, R. W., Corrigan, E. C., Simpson, J. L., & Nelson, L. M. (2007). The FMR1 premutation and reproduction. *Fertil Steril, 87*(3), 456-465. doi:10.1016/j.fertnstert.2006.09.004

Xing, Y., Clements, W. K., Kimelman, D., & Xu, W. (2003). Crystal structure of a beta-catenin/axin complex suggests a mechanism for the beta-catenin destruction complex. *Genes Dev, 17*(22), 2753-2764. doi:10.1101/gad.1142603

Xing, Y., Takemaru, K., Liu, J., Berndt, J. D., Zheng, J. J., Moon, R. T., & Xu, W. (2008). Crystal structure of a full-length beta-catenin. *Structure, 16*(3), 478-487. doi:10.1016/j.str.2007.12.021

Yao, H. H., Whoriskey, W., & Capel, B. (2002). Desert Hedgehog/Patched 1 signaling specifies fetal Leydig cell fate in testis organogenesis. *Genes Dev, 16*(11), 1433-1440. doi:10.1101/gad.981202

Yao, H. H. C., Matzuk, M. M., Jorgez, C. J., Menke, D. B., Page, D. C., Swain, A., & Capel, B. (2004). Follistatin operates downstream of Wnt4 in mammalian ovary organogenesis. *Developmental dynamics : an official publication of the American Association of Anatomists, 230*(2), 210-215. doi:10.1002/dvdy.20042

Zeidler, M. P., Perrimon, N., & Strutt, D. I. (1999). Polarity determination in the Drosophila eye: a novel role for unpaired and JAK/STAT signaling. *Genes Dev, 13*(10), 1342-1353. doi:10.1101/gad.13.10.1342

Zhang, S.-s., Kim, K.-h., Rosen, A., Smyth, J. W., & Sakuma, R. (2011). Iroquois homeobox gene 3 establishes fast conduction in the cardiac His – Purkinje network Irx3 deficient mice viable. 1-6. doi:10.1073/pnas.1106911108/-/DCSupplemental.www.pnas.org/cgi/doi/10.1073/pnas.1106911108

Chapter 2: Canonical Wnt/β-catenin Activity and Differential Epigenetic Marks Direct Sexually Dimorphic Regulation of *Irx3* and *Irx5* in Developing Gonads

Megan L Koth[1]; Annie Novak[1]; Kirsten A. Holthusen[2]; Anbarasi Kothandapani[1]; Keer Jiang[1]; Makoto Mark Taketo[3]; Barbara Nicol[4]; Humphrey H-C Yao[4]; S. Alexandra Garcia-Moreno[5*]; Christopher R. Futtner[5]; Danielle M. Maatouk[5 †] ; Joan S. Jorgensen[1*]

[1]Department of Comparative Biosciences, School of Veterinary Medicine, University of Wisconsin – Madison, Madison, Wisconsin, USA

[2]Department of Comparative Biosciences, College of Veterinary Medicine, University of Illinois, Urbana, Illinois, USA

[3]Department of Pharmacology, Kyoto University Graduate School of Medicine, Kyoto Japan

[4]Reproductive and Developmental Biology Laboratory, National Institute of Environmental Health Sciences, Research Triangle Park, North Carolina, USA

[5]Department of Obstetrics and Gynecology, Northwestern University, Chicago, Illinois, USA. *Current location: Department of Cell Biology, Duke University Medical Center.

† Deceased

*Corresponding author

Abstract

Members of the Iroquois B (*IrxB*) homeodomain cluster genes, specifically *Irx3* and *Irx5*, are critical for heart, limb, and bone development. Recently, we reported their importance for follicle health and oocyte survival within the developing ovary. Within developing gonads, *Irx3* and *Irx5* are expressed shortly after sex determination in the ovary but are absent in the fetal testis. Mutually antagonistic molecular signals ensure ovary vs testis differentiation with canonical Wnt/β-catenin signals at the forefront for promoting the ovary pathway in XX gonads. Notably, few direct downstream targets have been identified within the ovary. Here, we report that the canonical Wnt/β-catenin signaling pathway directly stimulates *Irx3* and *Irx5* transcription in the developing ovary. Using *in silico* analysis of ATAC- and ChIP-Seq databases in conjunction with gonad explant transfection assays, we identified TCF/LEF binding sequences within two distal enhancers of the *IrxB* locus that promote β-catenin-responsive ovary expression. Meanwhile, *Irx3* and *Irx5* transcription is suppressed within the developing testis by the presence of H3K27me3 on these same two enhancer sequences. In summary, our results have uncovered two enhancer sequences that resolve sexually dimorphic regulation of *Irx3* and *Irx5* that are also direct targets of β-catenin transcriptional control. Together, they mediate oocyte and follicle survival to promote ovarian health.

Introduction

Early in development, the bipotential mammalian gonad can transform into a testis or an ovary depending on the activation or repression of signaling cascades in the somatic cell lineage (reviewed in (Svingen & Koopman, 2013)). In the ovary, the canonical Wnt4/Rspo1/β-catenin pathway plays a crucial role for proper differentiation and development (reviewed in (Nicol & Yao, 2014)). In XX mouse embryos, knockouts of *Wnt4* (Jeays-Ward, Dandonneau, & Swain, 2004; Vainio, Heikkilä, Kispert, Chin, & McMahon, 1999), *Rspo1* (A. A. Chassot et al., 2008; Tomizuka et al., 2008) or somatic cell loss of the downstream mediator, β-catenin, (Liu, Bingham, Parker, & Yao, 2009; Manuylov, Smagulova, Leach, & Tevosian, 2008) results in a partial ovary to testis sex reversal and subsequent loss of 90% of the germ cell population by birth. Conversely, stabilization of β-catenin in the somatic cell population of the XY gonad leads to male-to-female sex reversal, suggesting that β-catenin is a crucial regulator of the sex identity of the somatic cell lineage (Danielle M. Maatouk et al., 2008). Multiple ovarian factors are thought to be regulated by β-catenin and its cognate DNA binding partners TCF/LEF, but a direct relationship in the ovary has yet to be elucidated.

Previously, we reported that two Iroquois homeobox transcription factors *Irx3* and *Irx5* are expressed in the ovary beginning shortly after sex differentiation. Each exhibits a dynamic profile during the course of germline nest establishment and breakdown through primordial follicle formation suggesting they play important roles in ovarian development (Fu et al., 2018; B. Kim et al., 2011). Iroquois factors are highly conserved factors that are known for their roles in patterning and embryogenesis, along with

organization of the spinal cord, limb, bone, and heart (Bruneau et al., 2001; Diez del Corral, Aroca, G mez-Skarmeta, Cavodeassi, & Modolell, 1999; J. Gómez-Skarmeta, de La Calle-Mustienes, & Modolell, 2001; J. L. Gómez-Skarmeta & Modolell, 2002; Lovrics et al., 2014). Developmental regulation of these factors within these systems is context-specific as a number of signaling pathways have been described. Recently, we showed that null mutation of both *Irx3* and *Irx5* resulted in improper somatic-germ cell connections within follicles, which culminated in oocyte death (Fu et al., 2018). Notably, it was previously reported that the *Wnt4* knockout mouse also exhibited physical gaps between germ and somatic cells within follicles (Vainio et al., 1999), suggesting that Wnt and Iroquois factors may lie in the same pathway. *Irx3* and *Irx5* expression have been attributed to the canonical Wnt signaling pathway in other tissues including the developing mouse ovary (F. Naillat et al., 2010; Naillat et al., 2015), but a direct link to β-catenin/TCF/LEF transcriptional regulation has not been made.

Based on results from our and other studies, we hypothesized that *Irx3* and *Irx5* are direct transcriptional targets of the canonical Wnt/β-catenin pathway in the developing ovary. We detected no sex-specific regulatory activity within the proximal promoter regions using *ex vivo* gonad transfection assays. Instead, we uncovered two distant regulatory sequences within the *IrxB* locus that promote sexually dimorphic expression during critical stages of gonad differentiation. Herein, we report that active histone marks work together with β-catenin/TCF/LEF to bind and activate at least two enhancer regions within the *IrxB* locus to stimulate *Irx3* and *Irx5* transcription in the ovary. Meanwhile, these same sites were enriched for repressor H3K27me3 chromatin marks

that actively repressed their transcription in developing testes. Together, these findings increase our perspective of the complex networks that are in place to ensure appropriate sex differentiation of gonads that include cooperation between epigenetic marks and transcription factors on promoter and distant regulatory sequences. In addition, this report uncovers mechanisms by which bipotential regulation can be achieved on the *IrxB* locus. These data provide a foundation for new discoveries of mechanisms by which canonical Wnt and other regulatory pathways work together to promote IRX3 and IRX5 function in a spatiotemporal manner within the developing ovary and during organogenesis of other systems including the heart, limb, bone and spinal cord.

Results

β-catenin activity correlates with *Irx3* and *Irx5* expression

Wnt4/Rspo1/β-catenin regulated transcription plays an essential role in ovarian development in somatic cells during sex differentiation. Our lab previously reported that *Irx3* and *Irx5* expression increased upon the onset of sex differentiation in the ovary (Fu et al., 2018) and these factors have been linked to canonical Wnt/β-catenin signaling in other tissues (Janssens, Denayer, Deroo, Van Roy, & Vleminckx, 2010; F. Naillat et al., 2010; Naillat et al., 2015). Therefore, we hypothesized that canonical β-catenin regulates *Irx3* and *Irx5* in the somatic cells of the ovary at this time. To test this hypothesis, *ex vivo* and *in vivo* approaches were used to manipulate β-catenin activity to cause loss and gain-of-function in the developing ovary and testis, respectively. Embryonic day 11.5 (E11.5) wild-type ovaries were cultured with two different dosages

of iCRT14, a small molecule that inhibits the interaction between β-catenin and TCF/LEF family members to block β-catenin mediated gene transcription (M. Yan, Li, & An, 2017). As expected, treatment did not change the expression of *Rps29*, a ribosomal protein used as a negative control but inhibited β-catenin-responsive transcription in a dose-responsive manner. The 50μM dose decreased expression of known β-catenin target genes *Axin2* (0.23 fold) and *Fst* (0.13 fold) and caused a significant decrease in *Irx3* (0.27 fold) and *Irx5* (0.24 fold) transcripts (**Figure 2-1A)**. Next, we evaluated *Irx3* and *Irx5* transcript accumulation in embryonic ovaries lacking somatic cell β-catenin activity that were generated by crossing *Sf1*Cre to *Ctnnb1*$^{F/F}$ mice (**Supplementary Figure 2-1**). *Rps29* transcripts from E14.5 control (*Sf1*Cre; *Ctnnb1*$^{F/+}$) and mutant (*Sf1Cre; Ctnnb1*$^{F/F}$) ovaries were not changed while *Axin2* and *Fst* were significantly decreased in mutant ovaries (0.24 and 0.04 fold, respectively). In support of the *ex vivo* culture findings, *Irx3* and *Irx5* transcripts were also significantly decreased (0.35 and 0.40-fold, respectively) in the mutant ovaries compared to the controls (**Figure 2-1B)**. Together, *ex vivo* and *in vivo* results showed that the loss of β-catenin and its transcriptional activity in the developing ovary significantly diminished *Irx3* and *Irx5* expression.

Canonical Wnt/β-catenin is actively repressed in the developing testis (Y. Kim et al., 2006; Uhlenhaut et al., 2009). Indeed, it has been shown that stabilization of β-catenin within the somatic cell population was sufficient to cause male-to-female sex reversal (Danielle M. Maatouk et al., 2008). Therefore, we evaluated whether β-catenin

stabilization in the developing testis influenced *Irx3* and *Irx5* expression. Wild-type E11.5 testes were cultured *ex vivo* for 24 hours with Lithium Chloride (LiCl) to stabilize β-catenin. Results from treated testes showed no change for *Rps29* and significantly increased expression of positive controls *Axin2* (4 fold) and *Fst* (10 fold). *Irx3* and *Irx5* transcripts also increased 9- and 5-fold, respectively, compared to vehicle control (**Figure 2-1C**). Previously it was reported that stabilized β-catenin activity in somatic cells of developing testes from *Sf1*Cre;*Ctnnb1*$^{\Delta ex3/+}$ (Harada et al., 1999) embryos caused sex reversal (Danielle M. Maatouk et al., 2008). Transcripts from control (No Cre;*Ctnnb1*$^{\Delta ex3/+}$) and mutant (*Sf1*Cre;*Ctnnb1*$^{\Delta ex3/+}$) testes (**Supplementary Figure 2-1**) at E14.5 displayed no significant change in *Rps29* transcript levels but exhibited significantly increased expression of *Axin2* (11 fold), *Fst* (7 fold), *Irx3* (16 fold), and *Irx5* (20 fold) (**Figure 1D**) *Bmp2* was also used to test for Wnt/β-catenin specificity due to its role as a pro-ovarian gene that is not regulated by Wnt signaling.

Later in ovarian development, upon germline nest breakdown, *Irx3* expression expands to include both somatic cells and oocytes (Fu et al., 2018). β-catenin is also present in oocytes at this stage as shown by our immunohistochemistry results from ovaries at E14.5 and P7 and supported by previous reports (**Supplementary Figures 2-1, 2-2**) (Bothun & Woods, 2019; A.-A. Chassot et al., 2011; Jameson et al., 2012; Kumar et al., 2016; Usongo, Rizk, & Farookhi, 2012; H. Yan et al., 2019). To test whether β-catenin activity regulates expression of *Irx3* within oocytes during the stage of nest breakdown and primordial follicle formation, we targeted loss of *Ctnnb1* in oocytes using *Figla*Cre (Lin, Jimenez-Movilla, & Dean, 2014) and evaluated ovaries at P0 and P7 . Germ-cell

specific loss of β-catenin using *Figla*Cre was confirmed (**Supplementary Figure 2-2A**); however, immunohistochemistry analysis indicated no obvious change in IRX3 within oocytes of mutant compared to control mice (**Supplementary Figure 2-2B**). Altogether these data suggest that canonical β-catenin transcriptional activity promotes *Irx3* and *Irx5* expression within somatic cells of the germline nest but does not regulate their transcription within oocytes upon their appearance during germline nest breakdown.

β-catenin responsive enhancer sites are present within the *IrxB* locus

Irx3 and *Irx5* are on opposing strands of DNA located 550kb apart within the *IrxB* cluster on chromosome 8 in the mouse (Cavodeassi, Modolell, & Gómez-Skarmeta, 2001; Peters, Dildrop, Ausmeier, & Rüther, 2000). Given their proximity, we set out to identify accessible regions of chromatin within the *IrxB* locus. Previously, we performed DNaseI- and ATAC-seq on male and female somatic cell populations sorted from embryonic gonads at E10.5 (pre-sex differentiation) and E13.5 (post-sex differentiation) (Garcia-Moreno, Futtner, et al., 2019; D. M. Maatouk et al., 2017). These datasets were used to interrogate chromosome 8 spanning 600kb on either side of the *Irx3* transcription start site (tss) to search for areas of open chromatin that also included the consensus motif for β-catenin binding partners TCF/LEF (TCAAAG) (van de Wetering et al., 1997). Those sites that were used for further evaluation included those that were either resolved (R) by- or derived *de novo* (D) by E13.5 in the ovary (Garcia-Moreno, Futtner, et al., 2019). Five sites of interest were identified and named based on their distances from the *Irx3* tss: +205kb, +86kb, -305kb, and -580kb (**see boxed peaks in Figure 2-2A**). The site at -305kb contained two separate TCF/LEF binding motifs, labeled ‘A’ and

'B'; all others harbored a single consensus element. A map detailing the approximate location of each site relative to *Irx3* and *Irx5* is outlined in **Figure 2-2B**.

To evaluate these open chromatin sites, we harvested ovaries and testes from E13.5-14.5 embryos to perform chromatin immunoprecipitation (ChIP) qPCR using antibodies for H3K27ac to mark active enhancer sites, and TCF7L2 to identify TCF/LEF binding sites relevant to the developing ovary. Of TCF/LEF factors, TCF7L2 was chosen for the following reasons: robust ChIP-seq data are available on the ENCODE database, microarray data indicating TCF7L2 is expressed predominantly in the somatic cells of the gonad (Jameson et al., 2012), and the GUDMAP database showed that TCF7L2 expression was detected in the ovary via *in situ* hybridization, whereas other TCF/LEF factors were negative (Harding et al., 2011; McMahon et al., 2008). For each replicate, whole gonad ChIP was first validated by showing RNA Polymerase II enrichment at the GAPDH promoter and TCF7L2 presence at a known β-catenin/TCF complex target, the SP5 promoter (Kennedy et al., 2016) in ovaries and testes (**Supplementary Figure 2-3**). Ovary (XX) ChIP results showed that H3K27ac was significantly enriched at the +86kb (20.1 fold enrichment), and trended towards significant enrichment at the -580kb (11.1 fold enrichment) sites suggesting that they are potential enhancers (**Figure 2-3A**). Only the -305kb (B) site showed a trend for H3K27ac enrichment in the testis (XY) (6.8 fold enrichment) (**Figure 2-3B**). Next, ChIP PCR indicated that significant enrighment for TCF7L2 was observed on ovarian sites +86kb (2.2 fold enrichment) and -580kb (2.7 fold enrichment) and trended for enrichment at +205kb (2.0 fold enrichment), -305kb (A) (1.7 fold enrichment), and -305kb (B) (3.6 fold enrichment). Unlike the ovary, the only

site that had potential TCF7L2 enrichment in the testis was the +205kb site (6.1 fold enrichment) (**Figure 2-3A, B**). These data suggest that β-catenin/TCF/LEF transcription factors bind and act on enhancer sequences at the +86kb and -580kb sites to regulate *Irx3* and *Irx5* expression within developing ovaries. These results also suggest the potential for sex-specific regulation.

Constitutively active β-catenin defines the +86kb and -580kb sites as Wnt responsive enhancers in the *IrxB* locus

To test β-catenin responsive enhancer activity, each potential regulatory site was cloned into a luciferase reporter vector containing a minimal E1b promoter (Huang, Jia, Yan, Guo, & Li, 2006). In addition, each reporter vector was altered to include a single point mutation of the TCF/LEF binding motif (**T**CAAAG to **C**CAAAG), which is the same mutation that differentiates the TOPflash (active) versus FOPflash (inactive) β-catenin reporter plasmids (Korinek et al., 1997) (**Supplementary Table 2-1**). Reporter plasmids were transfected into HEK293 cells along with a constitutively active β-catenin expression vector, CMV-S37A (Jordan, Shen, Olaso, Ingraham, & Vilain, 2003). Specific β-catenin activity of the CMV-S37A expression vector was confirmed using co-transfection with positive and negative control reporter vectors, TOPflash and FOPflash, respectively (**Supplementary Figure 2-4**). Among all reporter vectors including +250kb, +86kb, -305kb (A, B), and -580kb, only the +86kb and -580kb plasmids exhibited a significant increase in reporter activity that was specific to the putative TCF/LEF binding site. Of note, the larger plasmid containing wild type -305ABkb sequences, which includes A and B TCF/LEF binding sites, was not responsive to CMV-S37A, and the

double mutation of (A) and (B) had no effect (**Figure 2-4A**). To test whether the +86kb and -580kb DNA enhancers (together equals 209bp) could stimulate promoter activity, both were cloned into the pGL3 basic luciferase reporter in front of 2,080bp of the mouse *Irx3* promoter (+86kb;-580kb;-1634/+446bp m*Irx3* pGL3). Constitutively active CMV-S37A cotransfected with the enhancer plus promoter reporter stimulated a 3 fold increase in activity compared to promoter alone. In addition, single base pair point mutations of the TCF/LEF binding site in each enhancer sequence completely disrupted enhancer activity (**Figure 2-4B**). Together, these data suggest that the +86kb and -580kb enhancer sequences confer β-catenin specific regulatory activity within the context of the *Irx3* promoter.

+86kb and -580kb enhancers promote β-catenin specific activity in transfected fetal ovaries

Based on ovary-specific expression of *Irx3*, we reasoned that sequences within the *Irx3* promoter would confer ovary-specific expression. To test this hypothesis, three different sized segments of the mouse *Irx3* promoter (-351/+446bp, -603/+446bp, and -1634/+446bp) were cloned into a luciferase reporter plasmid and transfected into ovaries and testes from E13.5 embryos. While reporter activity increased along with longer promoter sequences, none of the promoters exhibited a significant difference when testis and ovary reporter activities were compared (**Figure 2-5A**). Next, we tested whether β-catenin specific activity within the +86kb and -580kb enhancer sequences would promote ovary specific expression. Both enhancers and their mutated counterparts were cloned in front of the most active promoter (-1634/+446bp

mIrx3pGL3) reporter vector and transfected into E14.5 gonads. While the enhancer plus m*Irx3* promoter was equally expressed in both ovary and testes, only ovary expression was disrupted upon mutation of the TCF/LEF binding sites (60% decrease from wild type enhancers) (**Figure 2-5B**). Based on these results we conclude that the +86kb and -580kb enhancer sequences promote β-catenin responsive activity only within the ovary.

+86kb and -580kb regions in the male are enriched for H3K27me3, which results in sex-specific repression of the enhancer activity

Plasmid vectors containing the enhancer sequences linked to the m*Irx3* promoter did not confer ovary versus testis specific reporter activity as expected; however, one limitation to this analysis is that the reporter vectors lack epigenetic decorations that may have a profound impact on enhancer and/or promoter activity. Thus, we hypothesized that repressor histones suppress the +86kb and -580kb enhancer sequences within the developing testis. To test this hypothesis, we mined H3K27me3 ChIP-Seq data (Garcia-Moreno, Lin, et al., 2019) to identify sequences enriched for H3K27me3 using the same somatic cell populations described previously for ATAC-Seq (**Figure 2-2)** (Garcia-Moreno, Futtner, et al., 2019). Results show that H3K27me3 marks are enriched in both the +86kb and -580kb sites in the testis but are completely absent in the ovary (see boxed regions within **Figure 2-6A**). Next, to test whether the H3K27me3 marks actively repress *Irx3* and *Irx5* expression in the testes, wild-type gonads were harvested at E11.5 and cultured for 48 hours with 500nM Tazemetostat (TAZ), a potent EZH2 inhibitor that has been shown to diminish H3K27me3 presence in

ovary chromatin during development (Prokopuk, Hogg, & Western, 2018). To validate TAZ activity in developing gonads, we compared *Rps29* and *p21* transcripts between treated versus control cultures. *In silico* analysis of ovary and testis sequences showed that H3K27me3 was absent at the *Rps29* locus, but present at the *p21* locus, as has been reported in other cell types (**Supplementary Figure 2-5**) (Garcia-Moreno, Lin, et al., 2019; Knutson et al., 2014). Results showed no change in *Rps29* transcripts in both gonads subject toTAZ treatment. As expected, transcripts of *p21* increased in treated gonads in both sexes, but the increase was more robust in treated ovaries (XX 4-fold versus XY 2.5-fold) (**Figure 2-6B**). In contrast, TAZ treatment appeared to have a relatively greater impact on *Irx3* and *Irx5* transcript levels in cultured testes versus ovaries. *Irx3* and *Irx5* increased to only 25-30% of the positive control value in ovaries (*Irx3* 1.8-fold and *Irx5* 1.6-fold increase) but approached 100% of *p21* values in treated testes (2.4-fold increase for both transcripts) suggesting release of epigenetic repression in testes. Taken together, our data uncovers two specific enhancers within the *IrxB* locus that confer ovary versus testis specific promoter activity. In the ovary, canonical β-catenin activity stimulates the +86kb and -580kb enhancers while expression is silenced in the testis due to the combined effects of histone methylation repression and the lack of functional β-catenin activity.

Discussion

Canonical Wnt/β-catenin signaling has been reported to promote *Irx3* and *Irx5* expression in the ovary (Florence Naillat et al., 2010; Naillat et al., 2015) and other tissues such as the brain (Braun, Etheridge, Bernard, Robertson, & Roelink, 2003), lung

(Bell et al., 2008), neural axis (Janssens et al., 2010), kidney (Holmquist Mengelbier et al., 2019), and in colon cancer (Hovanes et al., 2001), but evidence for direct trans-acting regulation via DNA binding partners has not been elucidated. Here we used *in vitro, ex vivo*, and *in vivo* approaches to provide a direct link between canonical Wnt/β-catenin signaling and *Irx3* and *Irx5* expression within the somatic cell population of the developing ovary. In addition, we previously showed that both Iroquois factors emerge in germ cells in late stages of ovarian development (Fu et al., 2018), but here we report that their regulation in this cell type is independent of β-catenin. Specific to *Irx3* and *Irx5* expression within the somatic cell population, we uncovered two enhancer sequences that, although distant from the transcription start site, provided the focus for regulation within the ovary and testis. Our data indicate that chromatin enhancer marks work in conjunction with β-catenin/TCF/LEF at these sites to stimulate the *IrxB* locus in the ovary, while the absence of activated β-catenin in somatic cells along with repressive histone marks enriched at these same sites functionally antagonize expression of *Irx3* and *Irx5* in the testis. Together, these findings highlight interactions between signaling pathways and epigenetic marks that regulate *Irx3* and *Irx5* to ensure appropriate expression based on time, sex, and cellular environments within developing gonads.

It has long been established that the fate of the developing gonad depends on a cadre of active transcription factors and epigenetic marks within the somatic cell population during the sex differentiation window (Garcia-Moreno, Futtner, et al., 2019; Garcia-Moreno, Plebanek, & Capel, 2018; Hiramatsu et al., 2009; Katoh-Fukui et al., 2012; Morais da Silva et al., 1996). β-catenin interacts with its DNA binding partners

(TCF/LEF) in response to canonical Wnt/Rspo1 signals within somatic cells to promote ovary formation while antagonizing testis-promoting factors (A. A. Chassot et al., 2008; Liu et al., 2009; Danielle M. Maatouk et al., 2008). Our previous study showed that the onset of *Irx3* and *Irx5* expression in the ovary is just after sex differentiation and is localized to the somatic cell population that surround germline nests and will eventually be marked by FOXL2, a granulosa cell marker (Fu et al., 2018). This profile indicated that both factors were good candidates for direct regulation by activated β-catenin at this time. Indeed, our transcript analyses of ovaries and testes subjected to pharmacological treatments in hanging drop culture or obtained from gain- and loss-of-function genetic mouse models supported the association of *Irx3* and *Irx5* expression with stabilized β-catenin.

As the ovary continues development, the germline nests break down and primordial follicles assemble to form the ovarian reserve. β-catenin expression has been documented in both somatic and germ cells at this time (A.-A. Chassot et al., 2011; Liu et al., 2009). *Irx3* expression is maintained within somatic cells as germline nests began to breakdown, but we were surprised to find that it is also present within oocytes beginning at the time of nest breakdown and lasting until follicles reached the primary stage (Fu et al., 2018). Once the follicle matures to the primary stage, *Irx3* transitions exclusively to the germ cell where it remains, even in mature follicles within the adult ovary (Fu et al., 2018). To test whether β-catenin also controlled *Irx3* expression within the oocyte during this critical transition, we crossed *Ctnnb1*$^{flox/flox}$ to *Figla*Cre mouse lines (Lin et al., 2014). We verified germ cell-specific elimination of β-catenin but

observed no impact on IRX3 expression, suggesting that *Irx3* is regulated by a separate pathway in the oocyte. Besides canonical Wnt/β-catenin signaling, *Irx3* has also been shown to be controlled by other pathways including TGFβ (Cavodeassi et al., 2001; JL, 1998), SHH (Briscoe, Pierani, Jessell, & Ericson, 2000; Kobayashi et al., 2002), FGF (Kobayashi et al., 2002), and Retinoic acid (Sirbu, Gresh, Barra, & Duester, 2005). Currently, little is known about signals that impact the oocyte during germline nest breakdown, follicle formation, and early maturation. These data highlight new directions of research that need exploration including the intriguing expression profiles of *Irx3* and *Irx5* within the oocyte at a critical phase of ovary development.

We examined ~1200kb of chromosome 8, which included the *IrxB* and *Fto* loci, for female-specific open chromatin sites that could also mediate canonical β-catenin regulation within somatic cells after sex differentiation. Altogether, our ATAC- (D. M. Maatouk et al., 2017) and DNAse1-Seq (Garcia-Moreno, Futtner, et al., 2019) data, along with results from ENCODE ChIP-Seq derived TCF/LEF enrichment in human cell lines (Consortium, 2012) illuminated five putative sites that met these criteria. Notably, none were identified within the proximal promoters of either *Irx3* or *Irx5*. Open chromatin sites were evaluated in the context of sex-specific somatic cells before and after sex determination, which allowed us to envision nucleosome depleted regions that became ovary specific over time. Two sites, +205kb and +86kb were shown to be nucleosome depleted in somatic cells of both sexes before sex determination but resolved into sites specific to ovarian somatic cells after sex determination. The other three sites at -305Akb, -305Bkb, and -580kb represented nucleosome depleted regions

that arised *de novo* only in cells from differentiated ovaries. All five regions had one transcription factor binding site in common, TCF7L2. One limitation to this study is that only perfect matches to the TCF/LEF binding domains were explored. HMG box transcription factors, such as TCF/LEF, can also bind to DNA motifs that do not match the perfect consensus sequence; therefore, all potential binding regions were not explored. In addition, the nucleosome depleted regions also harbor a variety of other putative binding sites according to the JASPAR database (**Appendix 2**) (Khan et al., 2018). These *in silico* analyses did not distinguish any common suite of transcription factor binding sites within either the resolved or *de novo* open chromatin regions. In particular, the two sites that we identified as the most promising β-catenin-responsive enhancers in the ovary, +86kb and -580kb, were characterized as resolved and *de novo* sites, respectively. Notably, besides TCF7L2, the +86kb site harbors sequences that also bind CTCF, p300, and YY1, factors that are important for facilitating higher order chromatin structures (Chan & La Thangue, 2001; Deng, Cao, Wan, & Sui, 2010; Ghirlando & Felsenfeld, 2016). These findings, in combination with the significant distance between enhancer sites and our results that show that 20-40% of *Irx3* and *Irx5* transcripts remain after elimination of β-catenin suggest that chromatin encompassing the *IrxB* locus loops and undergoes extensive remodeling in response to sex-specific signals and developmental time. As noted above, this activity may also incorporate alternative time-sensitive signals that are currently under intense investigation.

We used ChIP-PCR followed by transient transfection assays to identify which of the five nucleosome depleted sites qualified as putative TCF-bound enhancer sequences

that were also responsive to β-catenin activity. Of the five sites, both +86kb and -580kb regions achieved these criteria. Together, they significantly elevated reporter activity when cloned in front of ~2,000bp of the mouse *Irx3* promoter and a single base pair mutation specific to β-catenin/TCF binding in each site completely abrogated this effect. Our next goal was to determine the relevance of these sequences in promoting ovary-specific expression of *Irx3* and *Irx5*. To that end, we used our previously described microinjection and electroporation technique to transfect reporter plasmids into embryonic gonads (Gao et al., 2011) focusing on the mouse *Irx3* promoter (mIrx3-pGL3). We cloned between 1,000 – 2,000bp of the mIrx3 promoter and added both +86kb and -580kb enhancers into a luciferase reporter. *Ex vivo* gonad transfection analysis failed to detect any sex-specific reporter activity. Point mutation of each β-catenin/TCF binding site, however, turned out to be critical to uncover ovary-specific regulation.

At first, we were surprised that the enhancer/m*Irx3* promoter reporters were equally active in ovaries and testes. We noted however, that in general, reporter plasmids are inherently devoid of epigenetic information. Enrichment of the active enhancer mark, H3K27Ac, was detected at the +86kb site in ovaries, with a trend towards positive enrichment at the -580kb site, while neither of these sites were enriched in testes. Meanwhile, our ChIP-Seq data showed substantial coverage by the repressor mark, H3K27me3 (Ringrose & Paro, 2007; Schuettengruber, Chourrout, Vervoort, Leblanc, & Cavalli, 2007) on both sites only in testes (Garcia-Moreno, Lin, et al., 2019). To test the relevance of these marks, we treated gonads *ex vivo* with Tazemetostat, a

pharmacological inhibitor of EZH2 mediated methyl transferase onto H3K27 (Knutson et al., 2014). Although we observed individual variability between gonads, we found that TAZ effectively increased the positive control, *p21*, transcripts in both ovaries and testes. The impact on *Irx3* and *Irx5* expression, however, appeared more profound in testis compared to ovary samples relative to *p21* responses in each. It is possible that Tazemetostat treatment may cause release of another factor that could then stimulate *Iroquois* transcripts in testes; however, the results reported here are in the context of testis culture that lack aggressive epigenetic or transcription factor activation of other ovary-specific factors. Thus, taken together, we conclude that both +86kb and -560kb open sites are subject to changing epigenetic landscapes. In newly differentiated ovarian somatic cells, active β-catenin/TCF complexes accumulate on the *IrxB* locus to stimulate *Irx3* and *Irx5* transcription. In contrast, somatic cells that are destined for the testis phenotype lack β-catenin and instead, recruit epigenetic decorations consistent with transcriptional repression.

The results of this study highlight the importance of transcription factor binding and local epigenetic landscape in illuminating cell and sex-defining fates during gonadogenesis. Previous studies have focused on epigenetic events at the proximal promoter, demonstrating *Cbx2* binding at female specific-gene promoters to repress transcription of female factors during male sex differentiation. (Garcia-Moreno, Lin, et al., 2019). Our study highlights a similar mechanism, where repressive histone mark H3K27me3 and EZH2 activity represses transcriptional activity in the testis, but in this example, at female-specific enhancers, not promoters. Distant enhancer sites have long been

implicated in gene control in the gonad and new technologies are improving our capacity to identify and validate their importance (Gonen et al., 2018; Gonen, Quinn, O'Neill, Koopman, & Lovell-Badge, 2017; Sekido & Lovell-Badge, 2008). Here, we describe two distal enhancer sites on the *IrxB* locus that are actively repressed in developing testes while at the same time, are engaged with active chromatin marks and β-catenin/TCF to stimulate *Irx3* and *Irx5* expression within the developing ovary. Thus, *Irx3* and *Irx5* are bonafide downstream targets of Wnt/Rspo1/β-catenin that together, are critical mediators of ovary development and oocyte survival. These findings allow us to begin to unravel the means by which specific cell environments control *Irx3* and *Irx5* expression within the fetal ovary. We suggest that these same principles could be applied to the developing brain, spinal cord, lung, kidney, or to abnormal cellular activity in Iroquois-positive cancers.

Methods & Materials

Animals

Mouse strains included CD1 outbred mice (Crl:CD1(ICR), Charles River, MA), *Sf1*Cre mice that were originally obtained from the Keith Parker Lab (Bingham, Verma-Kurvari, Parada, & Parker, 2006), *Ctnnb1* conditional loss-of-function (LOF) mice (B6.129-*Ctnnb1*^{tm2Kem}/KnwJ, Jackson Labs), and *Ctnnb1* conditional gain-of-function (GOF) mice (*β-cat*$^{fl.ex3}$) obtained from Dr. Makoto Mark Taketo, Kyoto University, Kyoto, Japan (Harada et al., 1999). Timed mating was identified by the presence of a vaginal plug, which was designated as embryonic day 0.5 (E0.5). Animals were dissected at the appropriate time and genomic DNA was isolated from tails or ear notches and subjected

to PCR using gene specific primers: *Sf1*Cre: 5′-GAGTGAACGAACCTGGTCGAAATCAGTGCG-3′ and 5′-GCATTACCGGTCGATGCAACGAGTGATGAG-3′; *Ctnnb1* wild-type and floxed (LOF) allele 5′-AAGGTAGAGTG ATGAAAGTTGTT-3′ and 5′-CACCATTGTCCTCTGTCTATTC -3′; *Ctnnb1* wild-type and β-*cat*$^{fl.ex3}$ (GOF) allele 5'-GCTGCGTGGACAATGGCTACTCAA-3' and 5'-GCCATGTCCAACTCCATCAGGTCA-3'. In the case where sex could not be determined visually, PCR for SRY was performed: 5'-TGCAGCTCTACTCCAGTCTTG-3' and 5'-GATCTTGATTTTTAGTGTTC-3'.

Animal housing and all procedures described were reviewed and approved by the Institutional Animal Care and Use Committee at the University of Wisconsin-Madison and were performed in accordance with the National Institute of Health Guiding Principles for the Care and Use of Laboratory Animals. Mice were housed in disposable, ventilated cages (Innovive, San Diego, CA). Rooms were maintained at 22 ±2 degrees Celsius and 30–70% humidity on a 12 hour light/dark cycle.

Organ culture using the droplet method

Gonad cultures were performed using a modified version of previously described protocols (Danielle M. Maatouk et al., 2008; Martineau, Nordqvist, Tilmann, Lovell-Badge, & Capel, 1997). Briefly, E11.5 gonad/mesonephros complexes were cultured at 37°C with 5%CO_2/95% air in ~20µl droplet of culture media (DMEM F-12 (Fisher, SH3002301)) supplemented with 10% fetal bovine serum (Fisher, SH3091003) and 1%

Penicillin-Streptomycin (Fisher, ICN1670249). Sex of the gonads was determined by genotyping PCR for SRY (see above). Gonad/mesonephros complexes were placed in round droplets of media on an inverted lid of a 100mm Petri dish within a humidified chamber. Gonads (XX and XY) were cultured in a droplet supplemented with either vehicle control DMSO, the indicated concentrations of iCRT14 (XX gonads, Sigma SML0203), or LiCl (XY gonads, Fisher L121-100) for 24 hours, rinsed with PBS and then harvested for RNA extraction and qPCR analysis. Tazemetostat (EPZ-6438) (Selleckchem, S7128) treated gonads were cultured for 48 hours (media change at 24 hours) before harvest.

RNA Extraction and qPCR

RNA was extracted using Trizol (Invitrogen, ca#: 15596026) according to the manufacturer's instructions and quantified using a NanoDrop 2000. 500ng RNA from each sample was used for First-Strand cDNA synthesis by SuperScriptII-RT (Invitrogen, AM9515). cDNA was diluted 1:5 and then 2 µl was added to 5 µl SYBR green PCR mixture (Applied Biosystems), 2.4 µl water, and 1.25 pmol primer mix. PCR reactions were carried out using the ABI Prism 7000 Sequence Detection System (Applied Biosystems). RNA transcripts were quantified using the $\Delta\Delta$Ct method (Livak & Schmittgen, 2001). Briefly, to control for overall gene expression in each time point, the average cycle threshold (aveCt) for 36B4 was subtracted from the aveCt value for each gene to generate ΔCt. Next, ΔCt for each gene was compared to ΔCt of that same gene for the mutant genotype (e.g. ΔCt $Irx3_{female\ control} - \Delta$Ct $Irx3_{female\ mutant}$), to generate ΔΔCt.

Finally, fold change was calculated as 2 to the −ΔΔCt power ($2^{-\Delta\Delta Ct}$). Primers are listed in **Supplementary Table 2-2**.

DNase-I seq, ATAC-seq cluster analysis, and ChIP-seq

DNAse-I, ATAC-seq, and H3K27me3 data were mined from these studies: (Garcia-Moreno, Futtner, et al., 2019; Garcia-Moreno, Lin, et al., 2019; D. M. Maatouk et al., 2017). These data were analyzed for open chromatin regions within 600kb on either side of the *Irx3* transcription start site (tss) of chromosome 8 in the mouse. Open chromatin region sequences that were specific to the female after sex determination were explored for TCF/LEF binding motifs using the JASPAR database (jaspar.genereg.net). The sequences containing the highest scores for binding potential were chosen for further investigation.

Chromatin Immunoprecipitation

E13.5-E14.5 CD1 ovaries and testes without mesonephros were harvested, snap frozen, and stored at -80°C. 100-150 pairs of snap-frozen gonads were thawed and fixed in 1% formaldehyde for 15 min at room temperature with gentle shaking. The reaction was quenched with 160 µL of 1.25 M glycine for 5 min at room temp with gentle shaking. Samples were washed 2x with PBS and cOmplete™ protease inhibitor (CPI) tablets (Roche, Basel, Switzerland; catalog #04693116001) then resuspended in 400 µL RIPA lysis buffer + CPI tablets. Samples were homogenized with a pestle, then chromatin shearing was performed by lightly sonicating via probe-based sonication to fully lyse cells and the nuclear envelope followed by 1 minute incubation at 37°C using

1000 gel units of Micrococcal Nuclease (MNase) (New England Biolabs; catalog #M0247S). A separate 5µL sample was incubated with Proteinase K to validate efficient shearing of DNA (between 300 bp–900 bp). The MNase reaction was stopped with 1.25 µmol EGTA. Debris was removed by centrifugation at 15,000 g for 10 m at 4 °C and then 100 µL of each lysate was diluted in 200 µL IP buffer (PBS + 0.05% Triton X-100) and incubated overnight with 2 µg of antibody. After overnight antibody incubation, 25 µL of Dynabeads protein G magnetic beads (Life Technologies; catalog #10004D) was added and mixed for 2 hours at 4 °C with gentle rocking. Samples were washed sequentially with 500 µL Low Salt, 500 µL High Salt, and 500 µL TE Buffers, then resuspended in Digestion Buffer (50 mM Tris, 10 mM EDTA, 0.5% SDS, pH 8.0) + Proteinase K for 2 hours at 62 °C. DNA was isolated via ethanol precipitation. qPCR analysis was performed to quantify relative amounts of DNA enrichment; immunoprecipitated (IP) samples were normalized to input and IgG. Antibodies used: Anti-phospo RNA PolII (Ser2), clone 3 (Millipore MABE954), Normal Mouse IgG (Sigma, M8695), TCF4 (C4H811) (Cell Signaling Technology, #2569S), and Histone H3K27Ac (Active Motif, Cat#39133).

Plasmid Constructs

Luciferase reporters were generated from mouse genomic sequences of the enhancers at +205kb, +86kb, -305kb, and -580kb from the *Irx3* tss specific to the region containing the TCF/LEF binding motif via PCR with the addition of the KpnI and XhoI restriction enzyme sequences (**Supplementary Table 2-1**). Each sequence was digested and inserted into the pGL3 basic vector containing a minimal E1b promoter (Huang et al.,

2006) digested at the KpnI and XhoI sites. The QuikChangeII site-directed mutagenesis kit was used to make a single base pair mutation for each TCF/LEF binding site as directed in the manufacturer's protocol (Stratagene) (**Supplementary Table 2-1**). The mouse *Irx3* promoter construct was generated from mouse genomic sequence using primers specific to 1634bp upstream and 446bp downstream of the *Irx3* tss and placed into the pGL3 basic vector. The +86kb and -580kb sequences were inserted in front of the mouse *Irx3* promoter using the NEBuilder HiFi DNA Assembly Cloning Kit according the manufacturer's instructions (New England BioLabs, E5520S). Each reporter construct was sequenced for accuracy after initial construction and proper mutation following mutagenesis (Sanger sequencing, UW Madison Biotech Center).

Plasmids containing promoter regions of *Irx3* were constructed via the Ensembl *Irx3* gene sequence and primer design software (Primer Designer version 1.01). PCR primers targeted the promoter region 5' of the *Irx3* tss. Genomic DNA was amplified, and inserts were blunt-end ligated into the pST-blue Accepter vector (Novagen). Sequencing was then performed (Keck Center, University of Illinois); the insert sequence was compared to the archived DNA sequence (NT_078586.1) and validated for accuracy.

Cell culture and Transient Transfection

80,000 HEK293 cells were plated in 24 well plates (Thermo Scientific, catalog #12565163) for transfection assays. Plasmids were prepped using column based mini or midi prep kits (Qiagen, cat#27104, cat#12143) and quantified using a NanoDrop

2000. Cells were transfected using Lipofectamine 2000 (Invitrogen, cat#11668019) with plasmid DNA diluted in OPTI-MEM media (Fisher, cat#31985070) according to the manufacturer's instructions. Luciferase reporter vectors were transfected at 0.8μg/well along with 50ng/well co-expression vector CMV-EGFP (Addgene #11153) or CMV-S37A-β-catenin (Jordan et al., 2003) (kindly provided by Dr. Vincent Harley, Hudson Institute for Medical Research, Monash University, Melbourne, Australia) for normalization or treatment, respectively. The lipofectamine 2000 mixture was incubated with the cells for 16-18 hours followed by a media change. After 24 hours, the cells were lysed using 1X Passive lysis buffer and read using the Dual Luciferase Reporter Assay (Promega, E1910). Treatment groups were plated in triplicate and experiments were repeated at least three times. Luciferase values from the treatment group were normalized to the non-treatment group and also normalized to the empty vector control.

Gonad Injection and Electroporation

Transient transfection assays in urogenital ridge explant cultures were based on previously reported methods of the explant culture system (Jorgensen & Gao, 2005). The sex of the gonad tissue was determined by characteristic findings of a coelomic vessel and testicular cords in the male and the lack of these in the female. Urogenital ridges were harvested from embryos at E14.5 and injected with approximately 0.5μL of a DNA cocktail containing 4 μg/μl pGL3, wild type +86kb/-580kb/mIrx3 promoter pGL3, or mutated +86kb/-580kb/mIrx3 promoter pGL3 plus 2 μg/μl SV40-Renilla luciferase in Dulbecco phosphate-buffered saline (PBS; Sigma D8537). An additional aliquot of 25 μl of sterile PBS was placed on the gonad for electroporation. Immediately thereafter, five

square electrical pulses of 65 V, 50 msec each at 100-msec intervals, were delivered through platinum electrodes from an electroporator. After electroporation, urogenital ridges were placed back into the culture for 24 hours. Explant cultures were maintained at 37°C with 5% CO_2/95% air in 50 µl of Dulbecco minimal Eagle medium (DMEM) supplemented with 10% FBS (fetal bovine serum) and 1% Penicillin/Streptomycin. Transfected gonad explants were harvested in 50µl passive lysis buffer, snap frozen, subjected to three freeze-thaw cycles, and then processed for dual luciferase assays. Data were calculated by taking the ratio of luciferase to renilla expression with at least 3 biological replicates for each injected plasmid.

Statistics

Statistics between groups were carried out using a two-tailed t-test assuming unequal variances. Results were considered statistically significant if p-values were ≤ 0.05. One-way ANOVA Post-hoc Tukey was performed where appropriate.

Acknowledgements

Special thanks to all members of the Jorgensen lab for ideas and support throughout this work. We are extremely grateful for the technical support from Dr. Camila Lopez-Anido and Dr. John Svaren in our. ChIP experiments. Also, thank you to Janelle Ryan and Dr. Vincent Harley for the CMV-S37A active β-catenin plasmid. We have an immense amount of gratitude to the cohort of undergraduates that helped with immunofluorescence, genotyping, and sectioning, especially Linda Wang, Ann Turcotte, and Rebekah Schroeder. In addition, thanks to the University of Wisconsin Biotron for the exemplary mouse husbandry help.

Dedicated to Danielle M. Maatouk, a wonderful colleague, scientist, and friend.

Funding Support

This work was supported by the National Institutes of Health: R21HD48911, R01HD075079, and R01HD090660 to JSJ; R01HD090660-Reentry Supplement to AK; T32GM008688 to MLK; T32GM008061 to SAGM. In addition, this research was also supported in part by the Intramural Research Program of the National Institutes of Health at the National Institute of Environmental Health Sciences (NIH-ZIAES102965 to H.H-C.Y.).

References

Bell, S. M., Schreiner, C. M., Wert, S. E., Mucenski, M. L., Scott, W. J., & Whitsett, J. a. (2008). R-spondin 2 is required for normal laryngeal-tracheal, lung and limb morphogenesis. *Development (Cambridge, England), 135*(6), 1049-1058. doi:10.1242/dev.013359

Bingham, N. C., Verma-Kurvari, S., Parada, L. F., & Parker, K. L. (2006). Development of a steroidogenic factor 1/Cre transgenic mouse line. *Genesis (New York, N.Y. : 2000), 44*(9), 419-424. doi:10.1002/dvg.20231

Bothun, A. M., & Woods, D. C. (2019). Dynamics of WNT signaling components in the human ovary from development to adulthood. *Histochem Cell Biol, 151*(2), 115-123. doi:10.1007/s00418-018-1729-y

Braun, M. M., Etheridge, A., Bernard, A., Robertson, C. P., & Roelink, H. (2003). Wnt signaling is required at distinct stages of development for the induction of the posterior forebrain. *Development (Cambridge, England), 130*(23), 5579-5587. doi:10.1242/dev.00685

Briscoe, J., Pierani, A., Jessell, T. M., & Ericson, J. (2000). A homeodomain protein code specifies progenitor cell identity and neuronal fate in the ventral neural tube. *Cell, 101*(4), 435-445. Retrieved from http://www.ncbi.nlm.nih.gov/pubmed/10830170

Bruneau, B. G., Bao, Z. Z., Fatkin, D., Xavier-Neto, J., Georgakopoulos, D., Maguire, C. T., Berul, C. I., Kass, D. A., Kuroski-de Bold, M. L., de Bold, A. J., Conner, D. A., Rosenthal, N., Cepko, C. L., Seidman, C. E., & Seidman, J. G. (2001). Cardiomyopathy in Irx4-deficient mice is preceded by abnormal ventricular gene expression. *Mol Cell Biol, 21*(5), 1730-1736. doi:10.1128/MCB.21.5.1730-1736.2001

Cavodeassi, F., Modolell, J., & Gómez-Skarmeta, J. L. (2001). The Iroquois family of genes: from body building to neural patterning. *Development, 128*(15), 2847-2855. Retrieved from https://www.ncbi.nlm.nih.gov/pubmed/11532909

Chan, H. M., & La Thangue, N. B. (2001). p300/CBP proteins: HATs for transcriptional bridges and scaffolds. *J Cell Sci, 114*(Pt 13), 2363-2373. Retrieved from https://www.ncbi.nlm.nih.gov/pubmed/11559745

Chassot, A.-A., Gregoire, E. P., Lavery, R., Taketo, M. M., de Rooij, D. G., Adams, I. R., & Chaboissier, M.-C. (2011). RSPO1/β-catenin signaling pathway regulates oogonia differentiation and entry into meiosis in the mouse fetal ovary. *PloS one, 6*(10), e25641-e25641. doi:10.1371/journal.pone.0025641

Chassot, A. A., Ranc, F., Gregoire, E. P., Roepers-Gajadien, H. L., Taketo, M. M., Camerino, G., de Rooij, D. G., Schedl, A., & Chaboissier, M. C. (2008). Activation of β-catenin signaling by Rspo1 controls differentiation of the mammalian ovary. *Hum Mol Genet, 17*(9), 1264-1277. doi:10.1093/hmg/ddn016

Consortium, E. P. (2012). An integrated encyclopedia of DNA elements in the human genome. *Nature, 489*(7414), 57-74. doi:10.1038/nature11247

Deng, Z., Cao, P., Wan, M. M., & Sui, G. (2010). Yin Yang 1: a multifaceted protein beyond a transcription factor. *Transcription, 1*(2), 81-84. doi:10.4161/trns.1.2.12375

Diez del Corral, R., Aroca, P., G mez-Skarmeta, J. L., Cavodeassi, F., & Modolell, J. (1999). The Iroquois homeodomain proteins are required to specify body wall identity in Drosophila. *Genes Dev, 13*(13), 1754-1761. doi:10.1101/gad.13.13.1754

Fu, A., Oberholtzer, S. M., Bagheri-Fam, S., Rastetter, R. H., Holdreith, C., Caceres, V. L., John, S. V., Shaw, S. A., Krentz, K. J., Zhang, X., Hui, C. C., Wilhelm, D., & Jorgensen, J. S. (2018). Dynamic expression patterns of Irx3 and Irx5 during germline nest breakdown and primordial follicle formation promote follicle survival in mouse ovaries. *PLoS Genet, 14*(8), e1007488. doi:10.1371/journal.pgen.1007488

Gao, L., Kim, Y., Kim, B., Lofgren, S. M., Schultz-Norton, J. R., Nardulli, A. M., Heckert, L. L., & Jorgensen, J. S. (2011). Two regions within the proximal steroidogenic factor 1 promoter drive somatic cell-specific activity in developing gonads of the female mouse. *Biology of reproduction, 84*(3), 422-434. doi:10.1095/biolreprod.110.084590

Garcia-Moreno, S. A., Futtner, C. R., Salamone, I. M., Gonen, N., Lovell-Badge, R., & Maatouk, D. M. (2019). Gonadal supporting cells acquire sex-specific chromatin landscapes during mammalian sex determination. *Dev Biol, 446*(2), 168-179. doi:10.1016/j.ydbio.2018.12.023

Garcia-Moreno, S. A., Lin, Y. T., Futtner, C. R., Salamone, I. M., Capel, B., & Maatouk, D. M. (2019). CBX2 is required to stabilize the testis pathway by repressing Wnt signaling. *PLoS Genet, 15*(5), e1007895. doi:10.1371/journal.pgen.1007895

Garcia-Moreno, S. A., Plebanek, M. P., & Capel, B. (2018). Epigenetic regulation of male fate commitment from an initially bipotential system. *Mol Cell Endocrinol, 468*, 19-30. doi:10.1016/j.mce.2018.01.009

Ghirlando, R., & Felsenfeld, G. (2016). CTCF: making the right connections. *Genes Dev, 30*(8), 881-891. doi:10.1101/gad.277863.116

Gómez-Skarmeta, J., de La Calle-Mustienes, E., & Modolell, J. (2001). The Wnt-activated Xiro1 gene encodes a repressor that is essential for neural development and downregulates Bmp4. *Development, 128*(4), 551-560. Retrieved from https://www.ncbi.nlm.nih.gov/pubmed/11171338

Gómez-Skarmeta, J. L., & Modolell, J. (2002). Iroquois genes: genomic organization and function in vertebrate neural development. *Curr Opin Genet Dev, 12*(4), 403-408. Retrieved from https://www.ncbi.nlm.nih.gov/pubmed/12100884

Gonen, N., Futtner, C. R., Wood, S., Garcia-Moreno, S. A., Salamone, I. M., Samson, S. C., Sekido, R., Poulat, F., Maatouk, D. M., & Lovell-Badge, R. (2018). Sex reversal following deletion of a single distal enhancer of. *Science, 360*(6396), 1469-1473. doi:10.1126/science.aas9408

Gonen, N., Quinn, A., O'Neill, H. C., Koopman, P., & Lovell-Badge, R. (2017). Normal Levels of Sox9 Expression in the Developing Mouse Testis Depend on the TES/TESCO Enhancer, but This Does Not Act Alone. *PLoS Genet, 13*(1), e1006520. doi:10.1371/journal.pgen.1006520

Harada, N., Tamai, Y., Ishikawa, T., Sauer, B., Takaku, K., Oshima, M., & Taketo, M. M. (1999). Intestinal polyposis in mice with a dominant stable mutation of the beta-catenin gene. *The EMBO journal, 18*(21), 5931-5942. doi:10.1093/emboj/18.21.5931

Harding, S. D., Armit, C., Armstrong, J., Brennan, J., Cheng, Y., Haggarty, B., Houghton, D., Lloyd-MacGilp, S., Pi, X., Roochun, Y., Sharghi, M., Tindal, C., McMahon, A. P., Gottesman, B., Little, M. H., Georgas, K., Aronow, B. J., Potter, S. S., Brunskill, E. W., Southard-Smith, E. M., Mendelsohn, C., Baldock, R. A.,

Davies, J. A., & Davidson, D. (2011). The GUDMAP database--an online resource for genitourinary research. *Development, 138*(13), 2845-2853. doi:10.1242/dev.063594

Hiramatsu, R., Matoba, S., Kanai-Azuma, M., Tsunekawa, N., Katoh-Fukui, Y., Kurohmaru, M., Morohashi, K., Wilhelm, D., Koopman, P., & Kanai, Y. (2009). A critical time window of Sry action in gonadal sex determination in mice. *Development, 136*(1), 129-138. doi:10.1242/dev.029587

Holmquist Mengelbier, L., Lindell-Munther, S., Yasui, H., Jansson, C., Esfandyari, J., Karlsson, J., Lau, K., Hui, C. C., Bexell, D., Hopyan, S., & Gisselsson, D. (2019). The Iroquois homeobox proteins IRX3 and IRX5 have distinct roles in Wilms tumour development and human nephrogenesis. *J Pathol, 247*(1), 86-98. doi:10.1002/path.5171

Hovanes, K., Li, T. W., Munguia, J. E., Truong, T., Milovanovic, T., Lawrence Marsh, J., Holcombe, R. F., & Waterman, M. L. (2001). Beta-catenin-sensitive isoforms of lymphoid enhancer factor-1 are selectively expressed in colon cancer. *Nat Genet, 28*(1), 53-57. doi:10.1038/88264

Huang, M., Jia, F. J., Yan, Y. C., Guo, L. H., & Li, Y. P. (2006). Transactivated minimal E1b promoter is capable of driving the expression of short hairpin RNA. *J Virol Methods, 134*(1-2), 48-54. doi:10.1016/j.jviromet.2005.11.016

Jameson, S. A., Natarajan, A., Cool, J., DeFalco, T., Maatouk, D. M., Mork, L., Munger, S. C., & Capel, B. (2012). Temporal transcriptional profiling of somatic and germ cells reveals biased lineage priming of sexual fate in the fetal mouse gonad. *PLoS Genet, 8*(3), e1002575. doi:10.1371/journal.pgen.1002575

Janssens, S., Denayer, T., Deroo, T., Van Roy, F., & Vleminckx, K. (2010). Direct control of Hoxd1 and Irx3 expression by Wnt/beta-catenin signaling during anteroposterior patterning of the neural axis in Xenopus. *The International journal of developmental biology, 54*(10), 1435-1442. doi:10.1387/ijdb.092985sj

Jeays-Ward, K., Dandonneau, M., & Swain, A. (2004). Wnt4 is required for proper male as well as female sexual development. *Developmental biology, 276*(2), 431-440. doi:10.1016/j.ydbio.2004.08.049

JL, G.-S. (1998). Xiro, a Xenopus homolog of the Drosophila Iroquois complex genes, controls development at the neural plate. In G. A (Ed.), (Vol. 17, pp. 181-190). EMBO J.

Jordan, B. K., Shen, J. H., Olaso, R., Ingraham, H. A., & Vilain, E. (2003). Wnt4 overexpression disrupts normal testicular vasculature and inhibits testosterone synthesis by repressing steroidogenic factor 1/beta-catenin synergy. *Proc Natl Acad Sci U S A, 100*(19), 10866-10871. doi:10.1073/pnas.1834480100

Jorgensen, J. S., & Gao, L. (2005). Irx3 is differentially up-regulated in female gonads during sex determination. *Gene expression patterns : GEP, 5*(6), 756-762. doi:10.1016/j.modgep.2005.04.011

Katoh-Fukui, Y., Miyabayashi, K., Komatsu, T., Owaki, A., Baba, T., Shima, Y., Kidokoro, T., Kanai, Y., Schedl, A., Wilhelm, D., Koopman, P., Okuno, Y., & Morohashi, K. (2012). Cbx2, a polycomb group gene, is required for Sry gene expression in mice. *Endocrinology, 153*(2), 913-924. doi:10.1210/en.2011-1055

Kennedy, M. W., Chalamalasetty, R. B., Thomas, S., Garriock, R. J., Jailwala, P., & Yamaguchi, T. P. (2016). Sp5 and Sp8 recruit β-catenin and Tcf1-Lef1 to select enhancers to activate Wnt target gene transcription. *Proc Natl Acad Sci U S A, 113*(13), 3545-3550. doi:10.1073/pnas.1519994113

Khan, A., Fornes, O., Stigliani, A., Gheorghe, M., Castro-Mondragon, J. A., van der Lee, R., Bessy, A., Chèneby, J., Kulkarni, S. R., Tan, G., Baranasic, D., Arenillas, D. J., Sandelin, A., Vandepoele, K., Lenhard, B., Ballester, B., Wasserman, W. W., Parcy, F., & Mathelier, A. (2018). JASPAR 2018: update of the open-access database of transcription factor binding profiles and its web framework. *Nucleic Acids Res, 46*(D1), D260-D266. doi:10.1093/nar/gkx1126

Kim, B., Kim, Y., Sakuma, R., Hui, C. C., Rüther, U., & Jorgensen, J. S. (2011). Primordial germ cell proliferation is impaired in Fused Toes mutant embryos. *Developmental biology, 349*(2), 417-426. doi:10.1016/j.ydbio.2010.10.010

Kim, Y., Kobayashi, A., Sekido, R., DiNapoli, L., Brennan, J., Chaboissier, M. C., Poulat, F., Behringer, R. R., Lovell-Badge, R., & Capel, B. (2006). Fgf9 and Wnt4 act as antagonistic signals to regulate mammalian sex determination. *PLoS Biol, 4*(6), e187. doi:10.1371/journal.pbio.0040187

Knutson, S. K., Kawano, S., Minoshima, Y., Warholic, N. M., Huang, K. C., Xiao, Y., Kadowaki, T., Uesugi, M., Kuznetsov, G., Kumar, N., Wigle, T. J., Klaus, C. R., Allain, C. J., Raimondi, A., Waters, N. J., Smith, J. J., Porter-Scott, M., Chesworth, R., Moyer, M. P., Copeland, R. A., Richon, V. M., Uenaka, T., Pollock, R. M., Kuntz, K. W., Yokoi, A., & Keilhack, H. (2014). Selective inhibition of EZH2 by EPZ-6438 leads to potent antitumor activity in EZH2-mutant non-Hodgkin lymphoma. *Mol Cancer Ther, 13*(4), 842-854. doi:10.1158/1535-7163.MCT-13-0773

Kobayashi, D., Kobayashi, M., Matsumoto, K., Ogura, T., Nakafuku, M., & Shimamura, K. (2002). Early subdivisions in the neural plate define distinct competence for inductive signals. *Development, 129*(1), 83-93. Retrieved from https://www.ncbi.nlm.nih.gov/pubmed/11782403

Korinek, V., Barker, N., Morin, P. J., van Wichen, D., de Weger, R., Kinzler, K. W., Vogelstein, B., & Clevers, H. (1997). Constitutive transcriptional activation by a beta-catenin-Tcf complex in APC-/- colon carcinoma. *Science, 275*(5307), 1784-1787. doi:10.1126/science.275.5307.1784

Kumar, M., Camlin, N. J., Holt, J. E., Teixeira, J. M., McLaughlin, E. A., & Tanwar, P. S. (2016). Germ cell specific overactivation of WNT/βcatenin signalling has no effect on folliculogenesis but causes fertility defects due to abnormal foetal development. *Sci Rep, 6*, 27273. doi:10.1038/srep27273

Lin, R. S., Jimenez-Movilla, M., & Dean, J. (2014). Figla-Cre transgenic mice expressing myristoylated EGFP in germ cells provide a model for investigating perinatal oocyte dynamics. *PloS one, 9*(1), e84477. doi:10.1371/journal.pone.0084477

Liu, C.-F., Bingham, N., Parker, K., & Yao, H. H. C. (2009). Sex-specific roles of beta-catenin in mouse gonadal development. *Hum Mol Genet, 18*(3), 405-417. doi:10.1093/hmg/ddn362

Livak, K. J., & Schmittgen, T. D. (2001). Analysis of relative gene expression data using real-time quantitative PCR and the 2(-Delta Delta C(T)) Method. *Methods, 25*(4), 402-408. doi:10.1006/meth.2001.1262

Lovrics, A., Gao, Y., Juhász, B., Bock, I., Byrne, H. M., Dinnyés, A., & Kovács, K. A. (2014). Boolean modelling reveals new regulatory connections between transcription factors orchestrating the development of the ventral spinal cord. *PloS one, 9*(11), e111430. doi:10.1371/journal.pone.0111430

Maatouk, D. M., Dinapoli, L., Alvers, A., Parker, K. L., Taketo, M. M., & Capel, B. (2008). Stabilization of β-catenin in XY gonads causes male-to-female sex-reversal. *Hum Mol Genet, 17*(19), 2949-2955. doi:10.1093/hmg/ddn193

Maatouk, D. M., Natarajan, A., Shibata, Y., Song, L., Crawford, G. E., Ohler, U., & Capel, B. (2017). Genome-wide identification of regulatory elements in Sertoli cells. *Development, 144*(4), 720-730. doi:10.1242/dev.142554

Manuylov, N. L., Smagulova, F. O., Leach, L., & Tevosian, S. G. (2008). Ovarian development in mice requires the GATA4-FOG2 transcription complex. *Development (Cambridge, England), 135*(22), 3731-3743. doi:10.1242/dev.024653

Martineau, J., Nordqvist, K., Tilmann, C., Lovell-Badge, R., & Capel, B. (1997). Male-specific cell migration into the developing gonad. *Curr Biol, 7*(12), 958-968. Retrieved from https://www.ncbi.nlm.nih.gov/pubmed/9382843

McMahon, A. P., Aronow, B. J., Davidson, D. R., Davies, J. A., Gaido, K. W., Grimmond, S., Lessard, J. L., Little, M. H., Potter, S. S., Wilder, E. L., Zhang, P., & project, G. (2008). GUDMAP: the genitourinary developmental molecular anatomy project. *J Am Soc Nephrol, 19*(4), 667-671. doi:10.1681/ASN.2007101078

Morais da Silva, S., Hacker, A., Harley, V., Goodfellow, P., Swain, A., & Lovell-Badge, R. (1996). Sox9 expression during gonadal development implies a conserved role for the gene in testis differentiation in mammals and birds. *Nat Genet, 14*(1), 62-68. doi:10.1038/ng0996-62

Naillat, F., Prunskaite-Hyyrylainen, R., Pietila, I., Sormunen, R., Jokela, T., Shan, J., & Vainio, S. J. (2010). Wnt4/5a signalling coordinates cell adhesion and entry into meiosis during presumptive ovarian follicle development. *Hum Mol Genet, 19*(8), 1539-1550. doi:10.1093/hmg/ddq027

Naillat, F., Prunskaite-Hyyryläinen, R., Pietilä, I., Sormunen, R., Jokela, T., Shan, J., & Vainio, S. J. (2010). Wnt4/5a signalling coordinates cell adhesion and entry into meiosis during presumptive ovarian follicle development. *Hum Mol Genet, 19*(8), 1539-1550. doi:10.1093/hmg/ddq027

Naillat, F., Yan, W., Karjalainen, R., Liakhovitskaia, A., Samoylenko, A., Xu, Q., Sun, Z., Shen, B., Medvinsky, A., Quaggin, S., & Vainio, S. J. (2015). Identification of the genes regulated by Wnt-4, a critical signal for commitment of the ovary. *Experimental Cell Research, 2*. doi:10.1016/j.yexcr.2015.01.010

Nicol, B., & Yao, H. H. (2014). Building an ovary: insights into establishment of somatic cell lineages in the mouse. *Sex Dev, 8*(5), 243-251. doi:10.1159/000358072

Peters, T., Dildrop, R., Ausmeier, K., & Rüther, U. (2000). Organization of mouse Iroquois homeobox genes in two clusters suggests a conserved regulation and function in vertebrate development. *Genome Research, 10*(10), 1453-1462. doi:10.1101/gr.144100

Prokopuk, L., Hogg, K., & Western, P. S. (2018). Pharmacological inhibition of EZH2 disrupts the female germline epigenome. *Clin Epigenetics, 10*, 33. doi:10.1186/s13148-018-0465-4

Ringrose, L., & Paro, R. (2007). Polycomb/Trithorax response elements and epigenetic memory of cell identity. *Development, 134*(2), 223-232. doi:10.1242/dev.02723

Schuettengruber, B., Chourrout, D., Vervoort, M., Leblanc, B., & Cavalli, G. (2007). Genome regulation by polycomb and trithorax proteins. *Cell, 128*(4), 735-745. doi:10.1016/j.cell.2007.02.009

Sekido, R., & Lovell-Badge, R. (2008). Sex determination involves synergistic action of SRY and SF1 on a specific Sox9 enhancer. *Nature, 453*(7197), 930-934. doi:10.1038/nature06944

Sirbu, I. O., Gresh, L., Barra, J., & Duester, G. (2005). Shifting boundaries of retinoic acid activity control hindbrain segmental gene expression. *Development, 132*(11), 2611-2622. doi:10.1242/dev.01845

Svingen, T., & Koopman, P. (2013). Building the mammalian testis: origins, differentiation, and assembly of the component cell populations. *Genes Dev, 27*(22), 2409-2426. doi:10.1101/gad.228080.113

Tomizuka, K., Horikoshi, K., Kitada, R., Sugawara, Y., Iba, Y., Kojima, A., Yoshitome, A., Yamawaki, K., Amagai, M., Inoue, A., Oshima, T., & Kakitani, M. (2008). R-spondin1 plays an essential role in ovarian development through positively

regulating Wnt-4 signaling. *Hum Mol Genet, 17*(9), 1278-1291. doi:10.1093/hmg/ddn036

Uhlenhaut, N. H., Jakob, S., Anlag, K., Eisenberger, T., Sekido, R., Kress, J., Treier, A.-C., Klugmann, C., Klasen, C., Holter, N. I., Riethmacher, D., Schütz, G., Cooney, A. J., Lovell-Badge, R., & Treier, M. (2009). Somatic sex reprogramming of adult ovaries to testes by FOXL2 ablation. *Cell, 139*(6), 1130-1142. doi:10.1016/j.cell.2009.11.021

Usongo, M., Rizk, A., & Farookhi, R. (2012). ??-Catenin/Tcf signaling in murine oocytes identifies nonovulatory follicles. *Reproduction, 144*(6), 669-676. doi:10.1530/REP-12-0291

Vainio, S., Heikkilä, M., Kispert, A., Chin, N., & McMahon, A. P. (1999). Female development in mammals is regulated by Wnt-4 signalling. *Nature, 397*(6718), 405-409. doi:10.1038/17068

van de Wetering, M., Cavallo, R., Dooijes, D., van Beest, M., van Es, J., Loureiro, J., Ypma, A., Hursh, D., Jones, T., Bejsovec, A., Peifer, M., Mortin, M., & Clevers, H. (1997). Armadillo coactivates transcription driven by the product of the Drosophila segment polarity gene dTCF. *Cell, 88*(6), 789-799. doi:10.1016/s0092-8674(00)81925-x

Yan, H., Wen, J., Zhang, T., Zheng, W., He, M., Huang, K., Guo, Q., Chen, Q., Yang, Y., Deng, G., Xu, J., Wei, Z., Zhang, H., Xia, G., & Wang, C. (2019). Oocyte-derived E-cadherin acts as a multiple functional factor maintaining the primordial follicle pool in mice. *Cell Death Dis, 10*(3), 160. doi:10.1038/s41419-018-1208-3

Yan, M., Li, G., & An, J. (2017). Discovery of small molecule inhibitors of the Wnt/β-catenin signaling pathway by targeting β-catenin/Tcf4 interactions. *Exp Biol Med (Maywood), 242*(11), 1185-1197. doi:10.1177/1535370217708198

Figure legends

Figure 2-1: *β-catenin activity correlates with Irx3 and Irx5 expression*

(**A**) *Ex vivo:* RNA analysis from wild type E11.5 ovaries (XX) that were cultured in 20μL media containing either vehicle (DMSO), 25μM, or 50μM iCRT14. (**B**) *In vivo:* RNA analysis from E14.5 ovaries (XX) from control (*Sf1Cre;Ctnnb1*$^{F/+}$) and mutant (*Sf1Cre;Ctnnb1*$^{F/F}$*)* embryos and subjected to qPCR analysis. (**C**) *Ex vivo:* RNA analysis from wild type E11.5 testes (XY) cultured in 20μL media containing either vehicle (DMSO) or 50mM Lithium Chloride (LiCl). (**D**) *In vivo:* RNA analysis from E14.5 testes (XY) from control (No Cre*;Ctnnb1*$^{\Delta ex3/+}$) and mutant (*Sf1Cre;Ctnnb1*$^{\Delta ex3/+}$*)* embryos and subjected to qPCR analysis. Error bars represent +/- SEM. Student t-test, *p<0.05, **p<0.01, ***p<0.005, ****p<0.001.

Figure 2-2: *Open chromatin regions containing TCF/LEF binding motifs are identified in the IrxB locus*

(**A**) ATAC-seq peaks in isolated somatic cells pre (E10.5) and post (E13.5) sex differentiation from both female (XX) and male (XY) gonads show four highlighted regions that contain a female specific peak at E13.5 and also includes a TCF/LEF binding motif (TCAAAG) (outlined in boxes). Note that for each Seq analysis, there are duplicate assays presented for each age/sex gonad. Site -305 ‘A’ and ‘B’ indicate two separate TCF/LEF binding motifs. Each putative site is labeled based on its distance to the *Irx3* promoter *Irx3* and *Irx5* tss’ position labeled with red arrow. Genes within the same locus include *Fto* and *Crnde* (lncRNA). Transcription direction is labeled with black arrows. (**B**) A model of the *IrxB* locus and each putative enhancer site relative to

the *Irx3* tss. Color coding for each putative enhancer site is maintained throughout. R=resolved, D=de novo peaks within the E13.5 ovary.

Figure 2-3: *Ovary-specific β-catenin responsive enhancer sites reside within the IrxB locus*

(**A**) H3K27ac (active enhancer marker) (left panel) and β-catenin binding partner TCF7L2 (right panel) chromatin immunoprecipitation (ChIP) of E14.5 ovaries (XX) from wild-type mice. (**B**) ChIP using the same markers in E14.5 testes (XY). H3K27ac (left panel) and TCF7L2 (right panel). Data are represented as fold change over IgG, which is normalized to 1. Data are presented as the average +/- SEM. N>3 separate experiments. Student t-test, *p≤0.05, #p≤0.1.

Figure 2-4: *Constitutively active β-catenin defines +86kb and -580kb as Wnt responsive enhancers within the Irx3/5 locus.*

(**A**) Luciferase reporter plasmids containing wild type and mutated DNA sequences of each putative enhancer site were transfected into HEK293 cells along with CMV-S37A, an expression vector that encodes a constitutively active form of β-catenin. Test plasmids were normalized to pGL3 Basic activity. (**B**) -1634/+446bp m*Irx3* pGL3, +86kb WT;-580kb WT; -1634/+446bp m*Irx3* pGL3, or +86kb MUT; -580kb MUT; -1634/+446bp m*Irx3* pGL3 were transfected into HEK293 cells along with a constitutively active β-catenin expression vector, CMV-S37A. Each transfection was repeated at least three times. Data are presented as the average +/- SEM. Student t-test, **p<0.01, ***p<0.005

Figure 2-5: *+86kb and -580kb enhancers promote β-catenin specific activity in transfected fetal ovaries*

(**A**) *Ex vivo* transfections in ovary (white bars) versus testes (black bars) of luciferase reporter vectors containing increasing sequence lengths of the mouse *Irx3* promoter compared to the empty pGL3 Basic control reporter vector. (**B**) *Ex vivo* transfections in ovary (white bars) versus testes (black bars) of +86kb WT; -580kb WT; -1634/+446bp m*Irx3* pGL3 or +86kb MUT; -580kb MUT; -1634/+446bp m*Irx3* pGL3. All data is represented as the fold change over pGL3 Basic, repeated at least three times. Data are represented as the average +/- SEM. Student t-test, *p<0.05.

Figure 2-6: *H3K27me3 represses +86kb and -580kb in the fetal testis*

(**A**) ChIP-seq of H3K27me3 (black bars) aligned to the *IrxB* locus (top panel). *Irx3* and *Irx5* tss sites labeled with arrows. Note that for each Seq analysis, there are duplicate assays presented for each age/sex gonad. Only data from E13.5 analyses are shown. Bottom panel shows increased resolution surrounding the two regions of interest, +86kb (yellow) and -580kb (green). Grey boxes outline H3K27me3 and ATAC-seq peaks at +86kb and -580kb (bottom panel) (**B**) Wild Type E11.5 gonads were cultured in 20μL media containing either vehicle (DMSO) or 500nM Tazemetostat (TAZ) for 48 hrs. RT-qPCR results are displayed as 500nM TAZ treatment normalized to DMSO control for each gene. Data are represented as average +/- SEM. **p≤0.01, ****p≤0.0001

Supplementary Figure Legends

Supplementary Figure 2-1: *Somatic cell manipulation of β-catenin in the developing gonad using genetic mouse models*

(**A**) Control ovary (No Cre;*Ctnnb1*$^{F/F}$) and (**B**) mutant ovary (*Sf1*Cre;*Ctnnb1*$^{F/F}$), both harvested at E14.5. β-catenin green, DAPI blue. The remaining β-catenin in the mutant ovary resides in the germ cell membrane. E14.5 (**C**) Control testis (No Cre;*Ctnnb1*$^{\Delta ex3/+}$) and (**D**) mutant testis (*Sf1*Cre;*Ctnnb1*$^{\Delta ex3/+}$), both harvested at E14.5. β-catenin green, DAPI blue. β-catenin is stabilized in the mutant testis.

Supplementary Figure 2-2: *FiglaCre targeted loss of β-catenin does not affect IRX3 expression in oocytes*

(**A**) Immunofluorescence images of P7 ovaries from No Cre; *Ctnnb1*$^{F/F}$ (control, left panel) and *Figla*Cre*; Ctnnb1*$^{F/F}$ (mutant, right panel). *Figla*Cre targets β-catenin elimination specifically in the oocyte. Inset includes a magnified view of primary or transitioning follicles. White dotted lines outline the membrane of the germ cell. DAPI (blue) and β-catenin (green). (**B**) IHC images of P7 ovaries for DAPI (blue) and IRX3 (green). No difference was observed in IRX3 staining between the oocytes of the control and mutant ovaries. Scale bars set to 50μm.

Supplementary Figure 2-3: *Chromatin Immunoprecipitation controls*

RNA Pol II is enriched at the GAPDH promoter and TCF7L2 is enriched at the SP5 promoter in both ovaries and testes

Supplementary Figure 2-4: *Validate β-catenin specific responsiveness for CMV-S37A expression vector*

TOPflash and FOPflash constructs were co-transfected with 50ng/well CMV-EGFP or CMV-S37A. TOPflash showed a specific and robust increase in luciferase expression in the CMV-S37A treated wells compared to FOPflash. CMV-EGFP or CMV-S37A. TOPflash showed a specific and robust increase in luciferase expression in the CMV-S37A treated wells compared to FOPflash.

Supplementary Figure 2-5: *H3K27me3 ChIP-seq at Rps29 and p21 controls*

H3K27me3 is absent at negative control *Rps29* but enriched at positive control *p21* (*Cdkn1a*) loci in both males and female somatic cell populations.

Supplementary Table S1: Individual potential enhancer sites containing TCF/LEF motif(s) were cloned into the pGL3 Basic backbone using KpnI and XhoI. Primer sequences listed above and the insert size. DNA was generated by PCR with mouse genomic DNA. Wild type and mutated TCF/LEF binding motif for each enhancer site. The mutated base pair is in red bold.

Supplementary Table S2: Real-time qPCR primer sequences

Figure 2-1

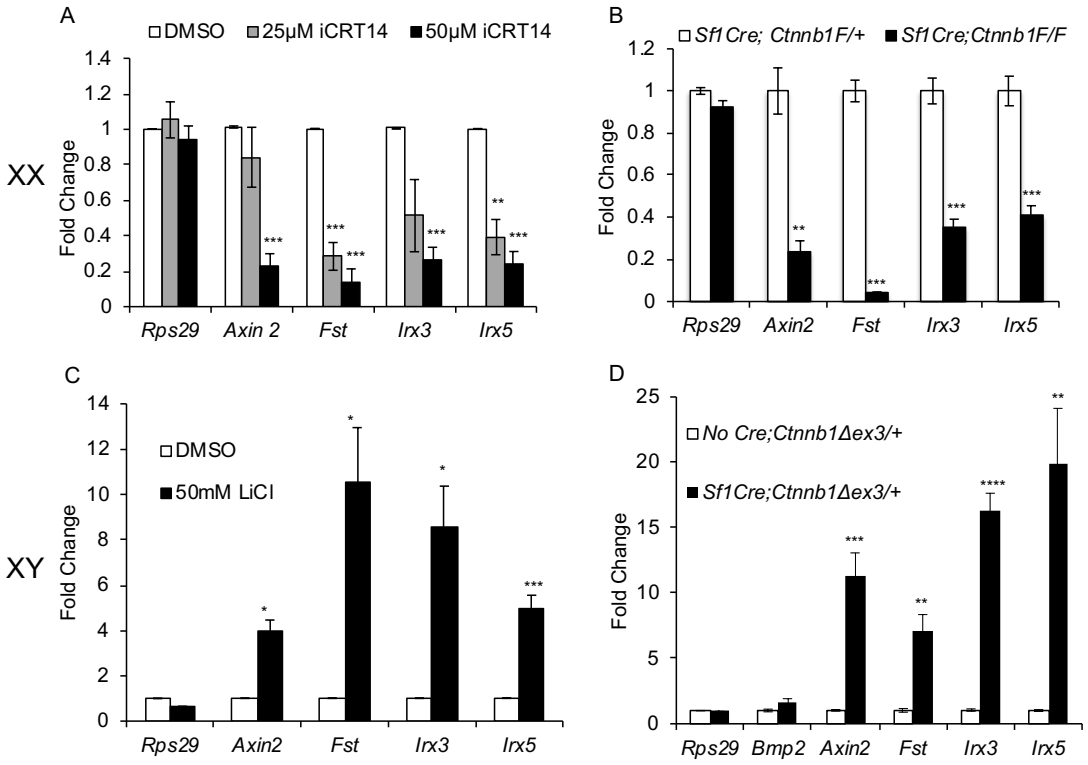
A
DMSO
25μM iCRT14
50μM iCRT14
XX
Fold Change
Rps29
Axin 2
Fst
Irx3
Irx5
B
Sf1Cre; Ctnnb1F/+
Sf1Cre;Ctnnb1F/F
Fold Change
Rps29
Axin2
Fst
Irx3
Irx5
C
DMSO
50mM LiCl
XY
Fold Change
Rps29
Axin2
Fst
Irx3
Irx5
D
No Cre;Ctnnb1Δex3/+
Sf1Cre;Ctnnb1Δex3/+
Fold Change
Rps29
Bmp2
Axin2
Fst
Irx3
Irx5

Figure 2-2

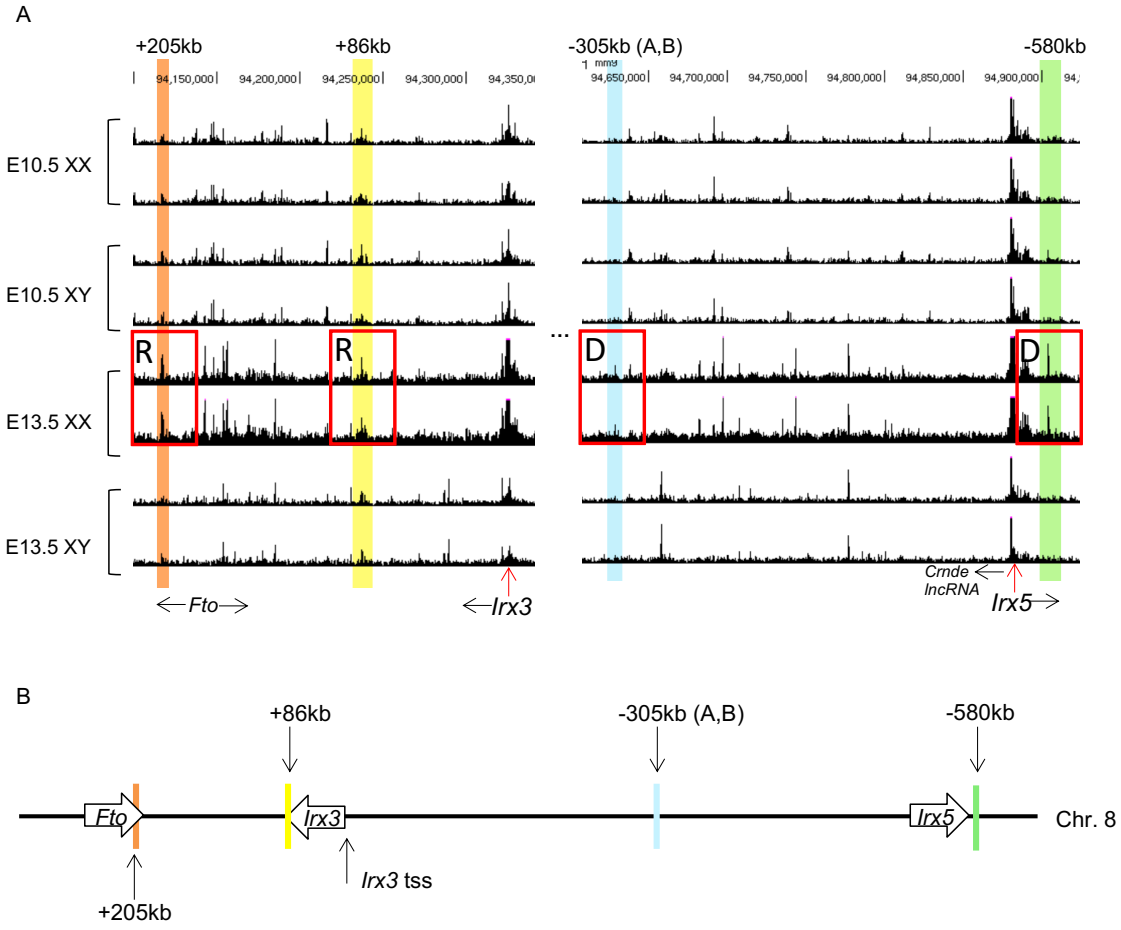
A
+205kb
+86kb
-305kb (A,B)
-580kb
E10.5 XX
E10.5 XY
E13.5 XX
E13.5 XY
R
R
D
D
Fto
Irx3
Crnde lncRNA
Irx5
B
+86kb
-305kb (A,B)
-580kb
Fto
Irx3
Irx5
Chr. 8
Irx3 tss
+205kb

Figure 2-3

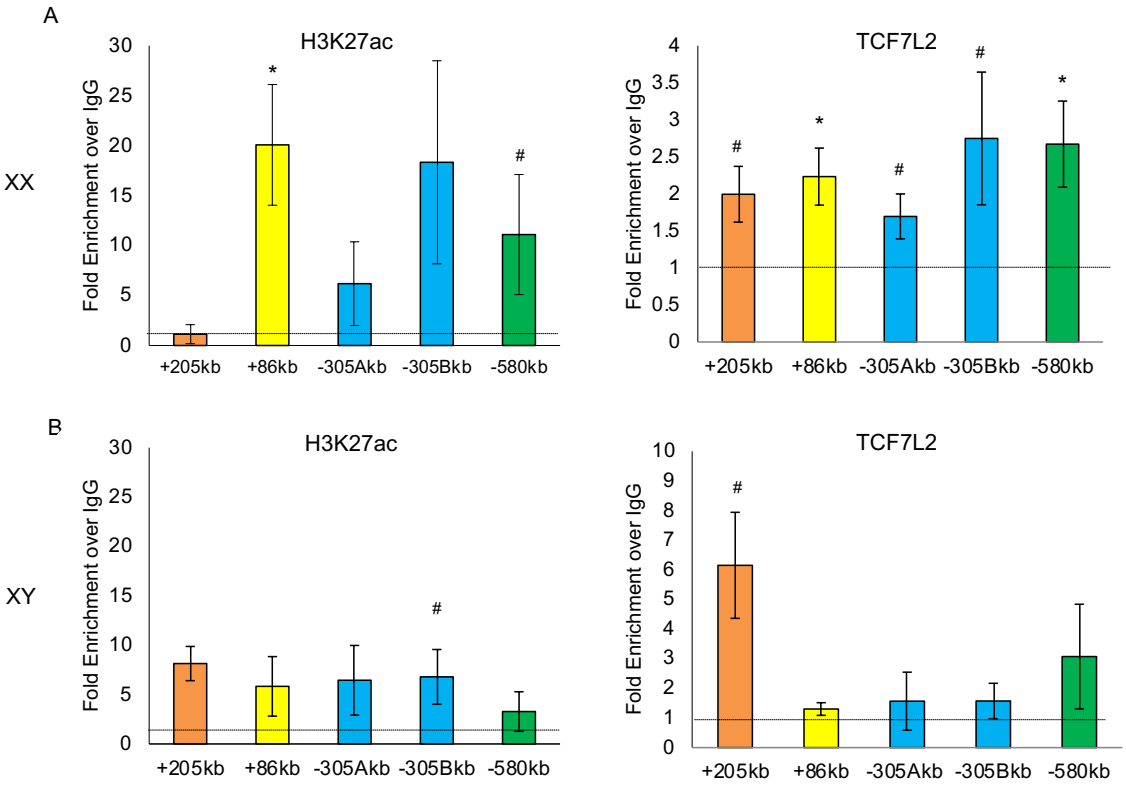
A
XX
H3K27ac
Fold Enrichment over IgG
30
25
20
15
10
5
0
*
#
+205kb
+86kb
-305Akb
-305Bkb
-580kb
TCF7L2
Fold Enrichment over IgG
4
3.5
3
2.5
2
1.5
1
0.5
0
#
*
#
#
*
+205kb
+86kb
-305Akb
-305Bkb
-580kb
B
XY
H3K27ac
Fold Enrichment over IgG
30
25
20
15
10
5
0
#
+205kb
+86kb
-305Akb
-305Bkb
-580kb
TCF7L2
Fold Enrichment over IgG
10
9
8
7
6
5
4
3
2
1
0
#
+205kb
+86kb
-305Akb
-305Bkb
-580kb

Figure 2-4

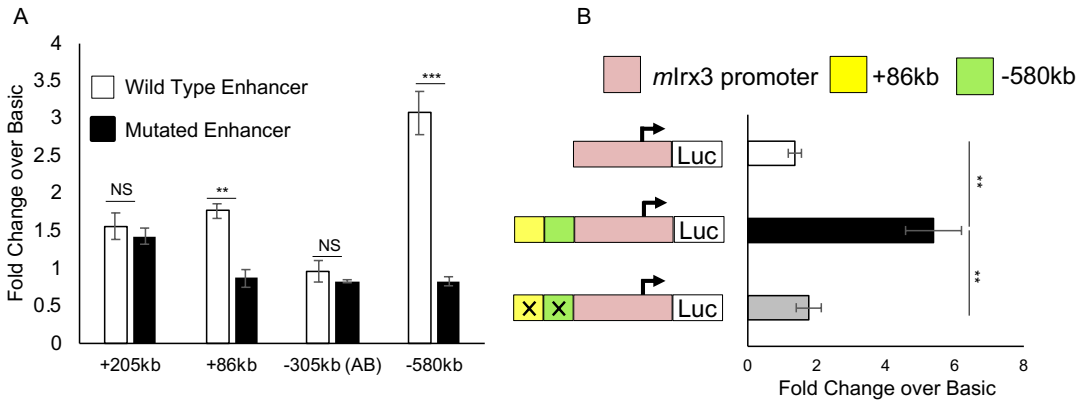
A
Fold Change over Basic
4
3.5
3
2.5
2
1.5
1
0.5
0
Wild Type Enhancer
Mutated Enhancer
NS
**
NS
***
+205kb
+86kb
-305kb (AB)
-580kb
B
mIrx3 promoter
+86kb
-580kb
Luc
Luc
Luc
**
**
0
2
4
6
8
Fold Change over Basic

Figure 2-5

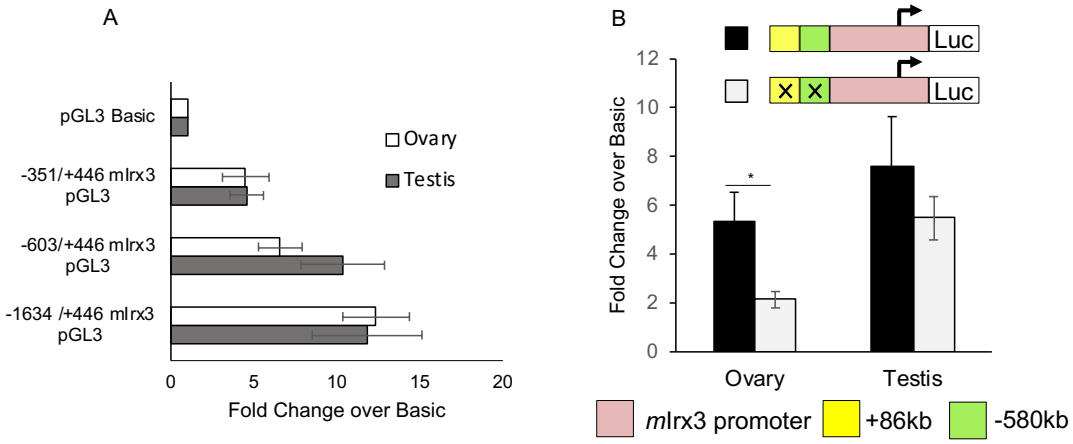
A
pGL3 Basic
-351/+446 mIrx3 pGL3
-603/+446 mIrx3 pGL3
-1634 /+446 mIrx3 pGL3
Ovary
Testis
0
5
10
15
20
Fold Change over Basic
B
Luc
Luc
12
10
8
6
4
2
0
Fold Change over Basic
*
Ovary
Testis
mIrx3 promoter
+86kb
-580kb

Figure 2-6

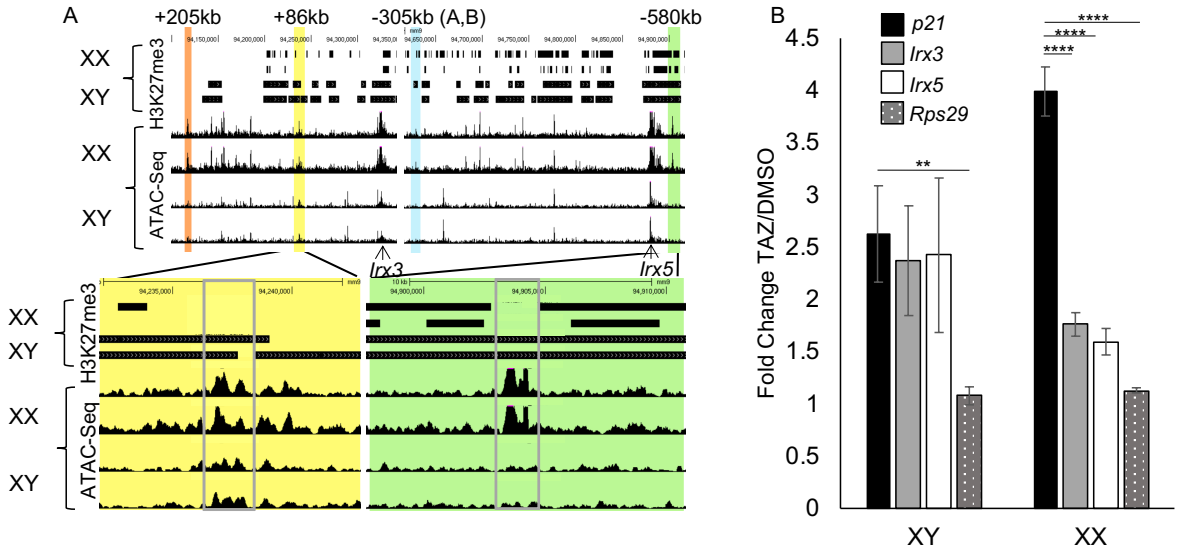
A
+205kb
+86kb
-305kb (A,B)
-580kb
XX
XY
H3K27me3
ATAC-Seq
Irx3
Irx5
B
p21
Irx3
Irx5
Rps29
Fold Change TAZ/DMSO
4.5
4
3.5
3
2.5
2
1.5
1
0.5
0
**
****
****
****
XY
XX

Supplementary Figure 2-1

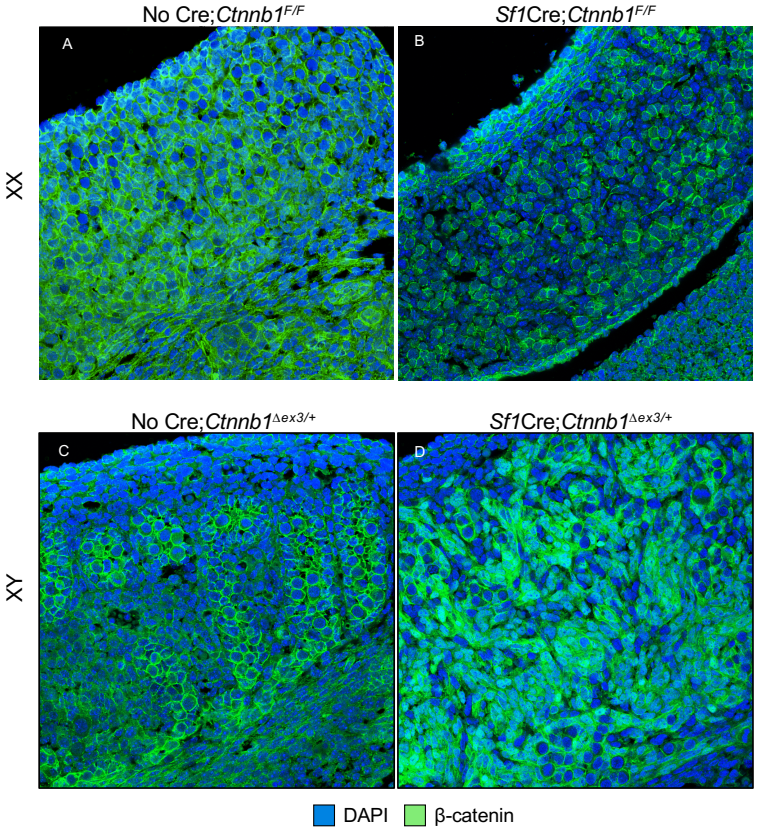

Supplementary Figure 2-2

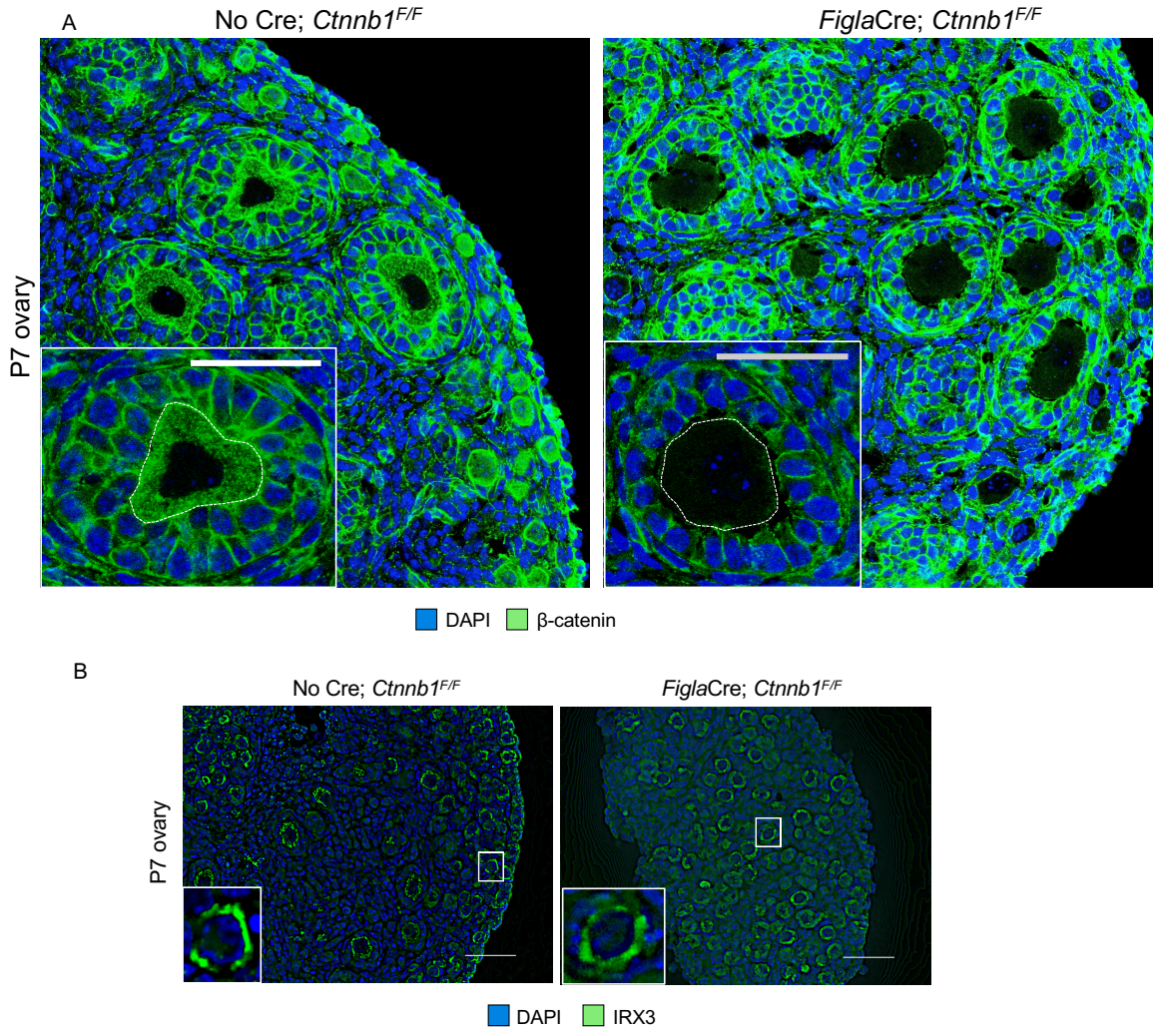

Supplementary Figure 2-3

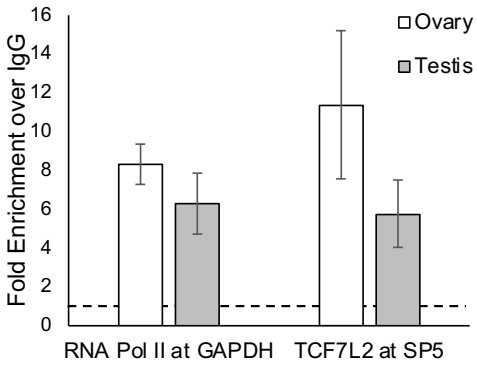

Supplementary Figure 2-4

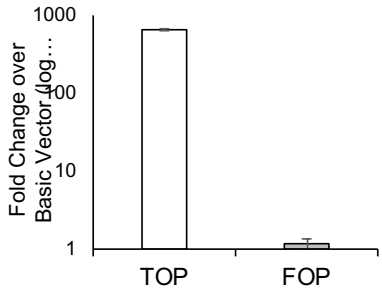

Supplementary Figure 2-5

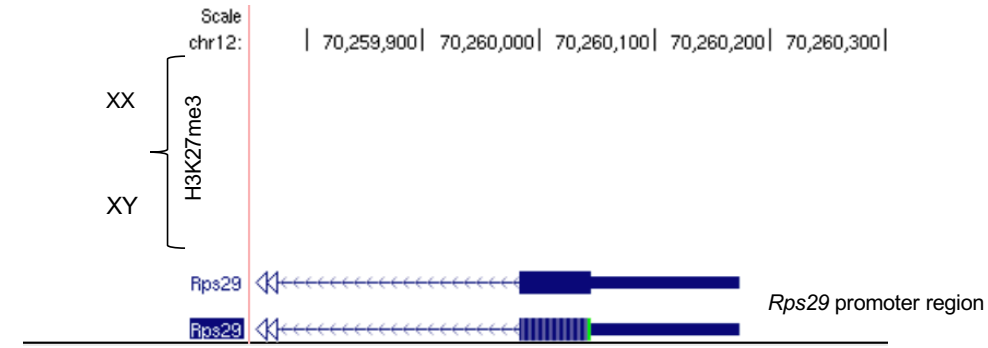

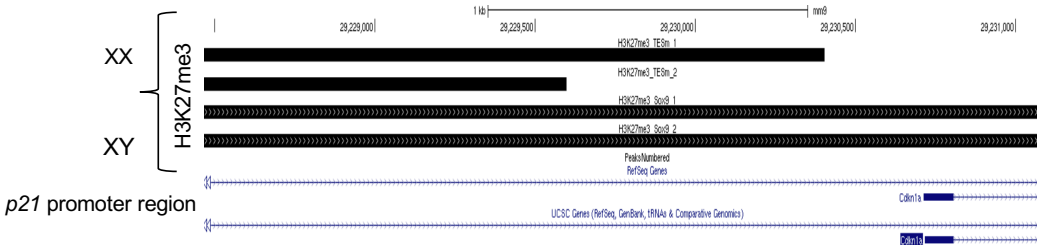

Supplementary Table 2-1

Site Label	Forward Primer	Reverse Primer	Total insert length
+205kb	5'-GCGCGGTACCTCACCTGGTAACTTTGTGCTGT-3'	5'-GCGCCTCGAGCCAAGGCTTCCGGTATCAGC-3'	108bp
+86kb	5'-GCGCGGTACCTTCCCTTTCCTATTTGTTCAGAAG-3'	5'-GCGCCTCGAGTTCCCTCGGCTGACAGAG-3'	59bp
-305AB kb	5'-GCGCGGTACCGGTTTCAAAAAGCCCAAGTG-3'	5'-GCGCCTCGAGTTATTTCTCTCTTTCTCTCTCTCCA-3'	250bp
-580kb	5'-GCGCGGTACCCCGCCATGATAGGAGTCAAC-3'	5'-GCGCCTCGAGGGCAGCCCTTTGTAAATGTT-3'	89bp

Mutation Site	+205kb	+86kb	-305kb (AB)	-580kb
Wild Type Sequence	GTTCAAAGGC	GTTCAAAGCG	(A) GTTCAAAGTC (B) TTTCAAAGGG	CATCAAAGAC
Mutated Sequence	GT**C**CAAAGGC	GT**C**CAAAGCG	(A) GT**C**CAAAGTC (B) TT**C**CAAAGGG	CA**C**CAAAGAC

Supplementary Table 2-2

Gene	Forward Primer	Reverse Primer
36B4	5’ – CGACCTGGAAGTCCAACTAC – 3’	5’ – ATCTGCTGCATCTGCTTG - 3’
Gapdh	5’ – TTCACCACCATGGAGAAGGC – 3’	5’ – GGCATGGACTGTGGTCATGA – 3’
Rps29	5' - TGAAGGCAAGATGGGTCAC - 3'	3' - GCACATGTTCAGCCCGTATT - 5'
Axin2	5’ – CCAGGCTGGAGAAACTGAAACT - 3'	5’ – CCTGCTCAGACCCCTCCTTT - 3'
Fst	5' - AAAACCTACCGCAACGAATG - 3'	5' - TTCAGAAGAGGAGGGCTCTG - 3'
Bmp2	5’ – CGGACTGCGGTCTCCTAA – 3’	5’ – GGGGAAGCAGCAACACTAGA – 3’
Irx3	5' - CGCCTCAAGAAGGAGAACAAGA - 3'	5' - CGCTCGCTCCCATAAGCAT - 3'
Irx5	5' - GGCTACAACTCGCACCTCCA - 3'	5' - CCAAGGAACCTGCCATACCG - 3'

Chapter 3

Loss of β-catenin in the oocyte does not impact *Irx3* expression or ovarian development

Koth, ML and Jorgensen, JS

Department of Comparative Biosciences, School of Veterinary Medicine, University of Wisconsin – Madison, Madison, Wisconsin, USA

Abstract

β-catenin is critical for proper ovarian development and lies downstream of canonical Wnt/Rspo1 signaling during development. The somatic cell expression of β-catenin has been extensively studied, and its primary roles are to repress male-specific factors and to promote the female lineage. The role of β-catenin, however, in the germ cell has been harder to define based on the tools available. Using the newly developed *Figla*Cre-EGFP mouse line, we asked if knocking out β-catenin in the early oocyte would affect oocyte development, follicle formation, and ovarian morphology. We previously confirmed that β-catenin regulates *Irx3* in the somatic cell compartment. Therefore, we hypothesized that β-catenin regulates *Irx3* within the oocyte as well. Results indicate oocyte expression of β-catenin is not essential for ovarian function, oocyte health, follicle growth, or *Irx3* expression.

Introduction

β-catenin plays an integral role in ovarian development, which is clear based on the evidence presented in Chapter 1. This role is established in the somatic cell population of the ovary, with the conditional knockout exhibiting male-specific features (Liu, Bingham, Parker, & Yao, 2009; Manuylov, Smagulova, Leach, & Tevosian, 2008). Additionally, somatic cell stabilization of β-catenin in the testis overrides the male pathway and instead, promotes a male-to-female sex reversal (Maatouk et al., 2008). While the importance of β-catenin in the somatic cell compartment of the ovary is evident, the role of β-catenin in the oocyte remains elusive.

β-catenin is expressed in the oocyte as early as E12.5 and is transcriptionally active due to the detection of β-galactosidase in oocytes of *Axin2*$^{+/LacZ}$ reporter mice (A.-A. Chassot et al., 2011; A. A. Chassot et al., 2008). Furthermore, *Rspo1* is necessary for the expression of β-catenin in the oocyte due to the lack of nuclear β-catenin staining in *Rspo1*$^{-/-}$ oocytes (A.-A. Chassot et al., 2011). Meiosis is affected in *Rspo1*$^{-/-}$ oocytes, where early meiotic marker *Stra8* and entry into meiosis is impaired. This ovarian phenotype occurs prior to detectable Sertoli cell differentiation, a feature of this mouse model, indicating that β-catenin expression in the germ cells promotes oocytes toward an XX fate and entry into meiosis (A.-A. Chassot et al., 2011). Moreover, overexpression of β-catenin in oocytes using *Ddx4*Cre showed a sub-fertile phenotype due to defects in ectoderm differentiation and abnormal fetal development, but no defects in ovarian function, oocyte number, ovulation ability, or embryonic development (Kumar et al., 2016).

β-catenin directly regulates transcription factors *Irx3* and *Irx5* in the somatic cells of the ovary (Chapter 2). Because *Irx3* and *Irx5* are expressed in the oocyte starting shortly after birth (Fu et al., 2018) and β-catenin is detected in the oocyte starting E12.5 (A.-A. Chassot et al., 2011; A. A. Chassot et al., 2008), we hypothesize the regulatory mechanism is consistent with the somatic cell compartment. Iroquois genes have a wide array of pathways associated with their regulation, which includes Wnt, Hedgehog, JAK/STAT, EGFR, and FGF (Briscoe, Pierani, Jessell, & Ericson, 2000; Cavodeassi, Diez Del Corral, Campuzano, & Domínguez, 1999; Gómez-Skarmeta, de La Calle-Mustienes, & Modolell, 2001; JL, 1998; Wang, Simcox, & Campbell, 2000; Zeidler, Perrimon, & Strutt, 1999). Therefore, we aimed to generate an oocyte-specific conditional knockout of β-catenin using the newly developed *Figla*Cre-EGFP to elucidate the importance of β-catenin in the developing oocyte and whether *Irx3* expression is regulated by β-catenin in the oocyte. We also hypothesized knocking out β-catenin in the early oocyte would affect follicle formation, meiosis, or proliferation in the ovary during early stages of development.

Multiple labs, including our own, have attempted to generate a knockout mouse that targets β-catenin loss specific to oocytes within the developing ovary. Attempts to eliminate β-catenin in oocytes at early embryonic stages using *TNAP*Cre or *Ddx4*Cre studies have either failed due to embryonic lethality (*TNAP*Cre (A.-A. Chassot et al., 2011)) or have remained unpublished, most likely due to the same issues (*Ddx4*Cre). One study was successful in knocking out β-catenin in oocytes using *Zp3*Cre, but this cre is not expressed until early postnatal development in growing oocytes (de Vries et

al., 2000; Takezawa et al., 2011). In *Zp3*Cre β-catenin conditional knockout females, oocytes from control and mutant mice were super-ovulated and sperm-oocyte adhesion was examined *in vitro*, revealing a sperm-oocyte adhesion defect (Takezawa et al., 2011). While this study reported valuable information regarding the importance of β-catenin at the oocyte membrane, this group did not examine ovaries and the lack of phenotype could be due to cre recombinase activity turning on after follicle formation and after the onset of meiosis, when *Irx3* is first detected in the oocyte. Although their results suggest β-catenin deficient oocytes do not affect ovarian development in females, our study would be the first to directly observe this conditional knockout and its effects on ovarian and follicle development.

The conditional knockout of β-catenin in the oocyte utilizing *Figla*Cre-EGFP was successful, however, mutant mice exhibited ovaries indistinguishable from controls. Our factor of interest, *Irx3*, was not affected in the knockout mouse, indicating that a pathway other than β-catenin is responsible for its expression in the oocyte. Mutant oocytes were able to enter into meiosis properly and follicle development was not impaired. Further, while the ovarian somatic cell knockout of β-catenin exhibits germ cell death around birth, the germ cell knockout of β-catenin did not display any major phenotype.

Three major conclusions can be drawn from this study: First, our results suggest that oocyte activity of β-catenin is not necessary for ovary development and follicle maturation, which is a similar conclusion drawn in a previous study using a cre expressed at a later stage. Second, the outcome of Cre-Lox recombination is highly

dependent on the flox lines used. To our knowledge, *Figla*Cre-EGFP has been bred to three different flox lines: *mTomato/mEGFP*, *TdTomato*, and *Ctnnb1^{flox}*. The original *Figla*Cre-EGFP study highlighted cre activity starting at E14.5 using *mTomato/mEGFP* mice. Dr. Humphrey Yao's lab presented evidence of *Figla*cre-EGFP activity beginning in early postnatal gonads using *TdTomato* mice, and we also did not see cre activity until early postnatal ovaries using *Ctnnb1^{flox}* mice. Finally, important and useful new information gives us reason to conclude that *Irx3* is not regulated by β-catenin in the oocyte as we hypothesized. Even though we show critical evidence that *Irx3* is directly regulated by β-catenin in the somatic cells of the ovary, the oocyte expression of *Irx3* is independent of β-catenin.

Results

Conclusion 1: β-catenin in the oocyte is not required for proper ovarian development or follicle maturation

It is well established that β-catenin is necessary in the ovarian somatic cell and, therefore, ovary development, starting in the bipotential gonad (Chapter 1). Besides somatic cell expression, β-catenin is detected within germ cells of the ovary starting as early as E12.5 (A.-A. Chassot et al., 2011; A. A. Chassot et al., 2008). Elimination of β-catenin in the oocyte starting at post-natal, primary follicle stage had no impact on female fertility (Takezawa et al., 2011). Therefore, our goal was to evaluate whether loss of β-catenin in the oocyte at an earlier time point within the fetal ovary would have an impact on ovarian development.

Ovarian and follicle development is unaffected in mutant females

Histological analysis of ovaries in early postnatal (P0, P3, P7, P21) and preweaning stages confirms proper ovarian development in both control (No Cre; *Ctnnb1*$^{f/f}$) and mutant (*Figla*Cre-EGFP; *Ctnnb1*$^{f/f}$) mice. Follicles at all stages were present, indicating proper follicle maturation in mutant ovaries (**Figure 3-1**). Overall, the loss of β-catenin in the oocyte does not seem to affect ovarian development and follicle formation and maturation in the ovary (n=2-3 of each genotype and age).

Germ cells initiate meiosis in the early mutant ovary

β-catenin expression in the oocyte is important for proper entry into meiosis (A.-A. Chassot et al., 2011), therefore we used SCP3, which encodes synaptonemal complex protein 3 functions within a complex that forms between homologous chromosomes during prophase of meiosis (Yuan et al., 2002) to detect oocytes undergoing meiosis in E16.5 ovaries. Our results showed that there was no difference in staining between control (No Cre; *Ctnnb1*$^{F/F}$) and mutant (*Figla*Cre; *Ctnnb1*$^{F/F}$) ovaries. Most germ cells stained positive for SCP3 in both genotypes, indicating that mutant oocytes initiated meiosis similar to controls (n=2 ovaries for each genotype and age) (**Figure 3-2**).

Germ cells remain abundant at birth

Massive germ cell death curing early ovarian development is a shared phenotype in *Wnt4* null (Vainio, Heikkilä, Kispert, Chin, & McMahon, 1999), *Rspo1*$^{-/-}$ (Tomizuka et

al., 2008), and β-catenin somatic cKO mice (Liu et al., 2009). We hypothesized that β-catenin depletion in the oocyte would also result in germ cell death. Ovary sections were stained with a germ cell-specific marker, Tra98, at P0 in control (No Cre; *Ctnnb1*$^{F/F}$) and mutant (*Figla*Cre; *Ctnnb1*$^{F/F}$) ovaries. Quantification indicated that germ cell numbers were comparable between mutant and control ovaries (n=2-3 ovaries per genotype) (**Figure 3-3**).

The proliferation of somatic cells is unaltered

β-catenin is implicated in many cell types as a proliferative marker and is shown to regulate Wnt4 expression in the ovary, a paracrine signal that affects downstream events, such as proliferation (Hernandez Gifford, 2015; Liu et al., 2009; Liu, Parker, & Yao, 2010). This function of Wnt4 leads to the question of whether loss of β-catenin in the oocyte could affect proliferation in other ovarian cell types. Postnatal day 7 (P7) ovaries were examined for proliferation differences using Ki67 (**Figure 3-4A**). Average Ki67 positive granulosa cells per follicle were quantified, and there was no significant difference between control and mutant animals (n=8 follicles of similar size/stage, 2-3 animals per genotype) (**Figure 3-4B**).

Follicle number is not affected in adult mutant females

Although our restuls indicate that early ovarian development is comparable between control and mutant mice up to preweaning age, we hypothesized that the loss of β-catenin in the oocyte might have an effect on germ/somatic cell contacts in larger follicles, which could potentially trigger follicle death. To quantify follicles in adult mice,

eight-week-old control and mutant females were collected for histological analysis. Follicle types were quantified and presented as the percentage of total follicles counted. No significant difference was seen at any follicle stage between the control and mutant ovaries: Primordial (29.0% vs 22.1%), primary (10.2% vs 9.4%), secondary (4.9% vs 4.0%), preantral (14.8% vs 19.9%), antral (7.4% vs 7.7%), small atretic (25.2% vs 29.7%) and large atretic (8.5% vs 7.3%). Based on these results, we conclude that follicle formation and growth are independent of β-catenin expression in the oocyte. (**Figure 3-5**)

Conclusion 2: Flox lines respond to Cre activity differently

Loss of β-catenin using FiglaCre-EGFP confirmed via immunohistochemistry

According to the original publication of the *Figla*Cre-EGFP mouse (Lin, Jimenez-Movilla, & Dean, 2014), cre recombinase activity was observed beginning at E14.5 (shown by EGFP expression) and in newborn ovaries and testes of *mTomato/mEGFP* reporter lines. *Figla*Cre-EGFP was also bred to the *TdTomato* line, and EGFP expression was not detected in embryonic gonad tissue but was observed in early postnatal gonads starting at P1, courtesy of Dr. Paula Brown and Dr. Humphrey Yao (NIEHS) (**Supplementary Figure 3-1**). In our study, *Figla*Cre-EGFP were bred to *Ctnnb1*^{flox} mice in two generations to generate mutant samples (see methods). We did not observe differences in β-catenin expression in oocytes of mutant mice (*Figla*Cre-EGFP; *Ctnnb1*$^{flox/flox}$) until postnatal day 3 (**Figure 3-1**). The most notable effect on β-catenin was observed by postnatal day 7, with oocytes of all stages harboring β-catenin in control but were absent in the mutant ovaries (**Figure 3-1**). Our data are similar to

*Figla*Cre-EGFP x *TdTomato* reporter, indicating that the timing of *Figla*Cre onset is occurring at a later stage than anticipated. This may explain why our phenotype is similar to the *Zp3*Cre knockout of β-catenin, as *Zp3*Cre is not efficient until after follicle formation in early postnatal oocytes.

Conclusion 3: Irx3 is not regulated by β-catenin in the oocyte

Irx3 expression in oocyte is unaffected

Even though we did not detect any defect in ovarian development or follicle maturation using *Figla*Cre-EGFP x *Ctnnb1*^{flox} females, we were still determined to assess its role in regulating *Irx3*. We have demonstrated that β-catenin controls the expression of *Irx3* (and *Irx5*) in the somatic cells of the ovary (Chapter 2), therefore it was hypothesized that β-catenin controls the expression of these genes in the oocytes as well. Immunohistochemistry using an antibody for IRX3 indicate that IRX3 is expressed at similar levels within oocytes of control (No Cre; *Ctnnb1*$^{F/F}$) and mutant (*Figla*Cre; *Ctnnb1*$^{F/F}$) ovaries at P7, despite the absence of β-catenin in the oocyte (**Figure 3-7**). These results suggest that IRX3 expression in the oocyte is independent of β-catenin activity, and further investigation is necessary to uncover the regulatory mechanism of *Irx3* and *Irx5* in the oocyte.

Discussion

β-catenin is critical for proper ovarian development, and has been shown to play roles in both the somatic and germ cell compartments during gestation (A.-A. Chassot et al., 2011; Liu et al., 2009). The role of β-catenin in the oocyte during development has remained elusive due to the lack of efficient cre mouse models, therefore we aimed to generate an oocyte-specific knockout of β-catenin utilizing the newly developed *Figla*Cre-EGFP (Lin et al., 2014). In addition, we previously determined that β-catenin is responsible for *Irx3* regulation in the somatic cells of the ovary (Chapter 2) and therefore hypothesized that loss of β-catenin in the oocyte would result in loss of *Irx3* expression in the oocyte. Altogether, this study provided additional insight into the role of β-catenin in the germ cell and gave us key information regarding the regulation of *Irx3* in a critical ovarian cell type.

We generated three conclusions from this study: β-catenin in the oocyte is not required for proper ovarian development or follicle maturation, flox lines respond to *Figla*Cre-EGFP activity differently, and *Irx3* is not regulated by β-catenin in the oocyte. First, we found that *Figla*Cre-EGFP; *Ctnnb1*$^{flox/flox}$ ovaries had a normal phenotype and female mice were fertile. Germ cell numbers, proliferation rate, and follicle counts were comparable between our control and mutant ovaries, indicating mutant ovaries did not exhibit any major defects. β-catenin is crucial for the entry of meiosis in oocytes (A.-A. Chassot et al., 2011), but oocytes in our mutant mice were able to initiate meiosis comparable to control oocytes. We discovered that in contrast to previous reports using *Figla*Cre-EGFP mice, β-catenin was not eliminated until after birth, around P3. For

example, meiosis initiates during ovarian development and would likely be affected if the cre initiated excision of β-catenin by E14.5, but based on our expression data, *Figla*Cre-EGFP is not expressed until after this process has already initiated. We were able to mimic the phenotype reported in a previous study using *Zp3*Cre that knocked out β-catenin in the oocyte. *Zp3*Cre is active in growing oocytes, generally starting at about the secondary follicle stage. The authors used IVF to study the sperm-oocyte adhesion defects in these oocytes lacking β-catenin, and they reported similar numbers of oocytes were collected from control and mutant animals, suggesting no ovarian defects in mutant females (Takezawa et al., 2011). Ovarian development was not examined in the *Zp3*Cre; *Ctnnb1*$^{flox/flox}$ mutant mice, and we were able to confirm that there are no defects in ovarian development or follicle maturation when β-catenin is knocked out in the oocyte.

Next, the outcome of *Figla*Cre depends on the applied flox line. In the original study, *Figla*Cre-EGFP activity was reported at E14.5 utilizing the EGFP tag (Lin et al., 2014). *mTomato/mEGFP*, an additional reporter line used in this study, reported *Figla*Cre-EGFP activity in newborn gonads of both sexes. It was not clear if the authors examined the reporter strain at an earlier time point, yet it would be an important finding to disclose in the study. Our collaborators Dr. Humphrey Yao and Dr. Pamela Brown performed an expression test using *TdTomato* and did not see *Figla*Cre-EGFP activity via EGFP staining until early postnatal life. Our results emulated the results from the Yao lab, showing no obvious loss of β-catenin in the oocyte in the *Figla*Cre-EGFP; *Ctnnb1*$^{f/f}$ oocytes until postnatal age points.

Finally, we were able to conclude that β-catenin does not regulate *Irx3* in the oocyte. IRX3 is expressed in the somatic cells of the ovary during development, and is expressed solely in the oocyte around birth in the mouse (Fu et al., 2018). Our previous work has shown that *Irx3* is directly regulated by the canonical Wnt/Rspo1/β-catenin signaling pathway in the somatic cells of the ovary early in development (Chapter 2) and we hypothesized that this pathway may also be responsible for the expression of *Irx3* in the oocyte. Our results show that IRX3 expression in the oocyte is not affected by oocyte-specific knockout of β-catenin. Thus, regulation of Iroquois factors may be linked to other pathways documented, including Hedgehog (Cavodeassi et al., 1999), JAK/STAT (Zeidler et al., 1999), EGFR (Wang et al., 2000), and TGFβ factors (Cavodeassi, Modolell, & Gómez-Skarmeta, 2001). This important finding requires further examination, as we have reason to believe that IRX3 expression in the oocyte has a large impact on oocyte and follicle health.

Previous reports showed that overexpression of β-catenin in oocytes using *Ddx4*Cre had no impact on oocytes or ovarian function (Kumar et al., 2016). In spite of this finding, mutant females bred to males with known fertility never resulted in pups. The authors showed that β-catenin overexpression in oocytes caused defects in the development of embryonic germ layers, which lead to fetal death (Kumar et al., 2016). We tried to recapitulate this phenotype using *Figla*Cre-EGFP with no success – pups from the F2 generation (*Figla*Cre-EGFP; *Ctnnb1*$^{GOF/+}$ X *Ctnnb1*$^{GOF/GOF}$) were all heterozygous. Further analysis revealed these mutant pups died *in utero*, most likely due to a combination of a leaky cre and a very robust β-catenin gain-of-function model.

Analysis of *Figla*Cre-EGFP; *Ctnnb1*$^{GOF/+}$ mice revealed no distinct phenotype, as they were viable and fertile, indicating the defect most likely occurred during the F2 breeding.

In conclusion, the loss of β-catenin in the oocyte starting at a postnatal stage did not have a significant effect on oocyte and follicle development, maturation, or morphology. Our phenotype was similar to that reported with *Zp3*Cre, which initiated cre-excision at approximately the same time although previous reports indicated robust *Figla*Cre expression by E14.5 in the female (Lin et al., 2014). The *Figla*Cre-EGFP; *Ctnnb1*$^{flox/flox}$ mutant mouse model did not eliminate *Irx3* expression in the oocyte, suggesting that Iroquois factors have a different regulatory mechanism in their expression than in the somatic cell compartment, a critical finding that requires further investigation. To date, there is no model to knock out β-catenin in the oocyte at an early gestational age, indicating a need for this critical resource; perhaps or a novel technique in gene manipulation, such as cell-specific CrisprCas9, would help to reveal the role of β-catenin in the early oocyte.

Methods

Animals

Mouse strains included *Ctnnb1* floxed conditional loss-of-function (LOF) mice (B6.129-*Ctnnb1*^{tm2Kem}/KnwJ, Jackson Labs) and *Figla*Cre-EGFP (FVB/N-Tg(Figla-EGFP-icre)ZP3Dean/Mmjax) obtained from Dr. Jurrien Dean at NIH/NIDDK. Timed mating was identified by the presence of a vaginal plug, which was designated as embryonic day 0.5 (E0.5). Animals were dissected at the appropriate time, and genomic DNA was isolated from tails or ear notches and subjected to PCR using gene-specific

primers: *Ctnnb1* wild-type and floxed (LOF) allele 5′-AAGGTAGAGTG ATGAAAGTTGTT-3′ and 5′-CACCATTGTCCTCTGTCTATTC -3′; *Figla*Cre iCRE F: 5' - CCAGCTCAACATGCTGCACA-3' and iCRE R: 5' - GCCACACCAGACACAGAGAT – 3'.

Animal housing and all procedures described were reviewed and approved by the Institutional Animal Care and Use Committee at the University of Wisconsin-Madison and were performed in accordance with the National Institute of Health Guiding Principles for the Care and Use of Laboratory Animals. Mice were housed in disposable, ventilated cages (Innovive, San Diego, CA). Rooms were maintained at 22 ±2 degrees Celsius and 30–70% humidity on a 12 hour light/dark cycle.

*Figla*Cre-EGFP mice were bred in two generations to generate mutant samples as outlined below.

*Figla*Cre-EGFP X *Ctnnb1*$^{flox/flox}$

|

F1 *Figla*Cre-EGFP; *Ctnnb1*$^{flox/+}$ X *Ctnnb1*$^{flox/flox}$

|

F2 *Figla*Cre-EGFP; *Ctnnb1*$^{flox/flox}$

Histology

Ovaries were harvested at the age indicated, fixed in 4% PFA overnight and embedded in paraffin. Paraffin blocks were sectioned at 8μm thickness and stained with hematoxylin and eosin (H&E) for histological analysis.

Immunofluorescence

Mouse ovaries were harvested at the age indicated, fixed in 4% paraformaldehyde overnight at 4°C, and washed in PBS. Samples were dehydrated through an ethanol gradient, cleared in xylene, and embedded in paraffin. Blocks were sectioned at 8μm thickness. After paraffin clearing, rehydration gradient, antigen retrieval, and blocking, primary antibodies were applied to paraffin sections at 4°C overnight (**Supplementary Table 1**). Secondary antibodies were then incubated at room temperature for 1 hour. DAPI in PBS solution was used as a nuclear counterstain. Images were collected on a Leica SP8 confocal microscope and a Keyence BZ-X700 microscope.

Cell Counting

Blinded to genotype, Ki67 positive granulosa cells of similar-staged follicles were counted using ImageJ. N=8 follicles, 2-3 animals per genotype.

Follicle Quantification

Ovaries were sectioned entirely through. Every 10^{th} section was stained for H&E and used to quantify the numbers for each follicle type. All counting was completed blinded to the ovary genotype.

References

Briscoe, J., Pierani, A., Jessell, T. M., & Ericson, J. (2000). A homeodomain protein code specifies progenitor cell identity and neuronal fate in the ventral neural tube. *Cell, 101*(4), 435-445. Retrieved from http://www.ncbi.nlm.nih.gov/pubmed/10830170

Cavodeassi, F., Diez Del Corral, R., Campuzano, S., & Domínguez, M. (1999). Compartments and organising boundaries in the Drosophila eye: the role of the homeodomain Iroquois proteins. *Development, 126*(22), 4933-4942. Retrieved from https://www.ncbi.nlm.nih.gov/pubmed/10529412

Cavodeassi, F., Modolell, J., & Gómez-Skarmeta, J. L. (2001). The Iroquois family of genes: from body building to neural patterning. *Development, 128*(15), 2847-2855. Retrieved from https://www.ncbi.nlm.nih.gov/pubmed/11532909

Chassot, A.-A., Gregoire, E. P., Lavery, R., Taketo, M. M., de Rooij, D. G., Adams, I. R., & Chaboissier, M.-C. (2011). RSPO1/β-catenin signaling pathway regulates oogonia differentiation and entry into meiosis in the mouse fetal ovary. *PloS one, 6*(10), e25641-e25641. doi:10.1371/journal.pone.0025641

Chassot, A. A., Ranc, F., Gregoire, E. P., Roepers-Gajadien, H. L., Taketo, M. M., Camerino, G., de Rooij, D. G., Schedl, A., & Chaboissier, M. C. (2008). Activation of β-catenin signaling by Rspo1 controls differentiation of the mammalian ovary. *Hum Mol Genet, 17*(9), 1264-1277. doi:10.1093/hmg/ddn016

de Vries, W. N., Binns, L. T., Fancher, K. S., Dean, J., Moore, R., Kemler, R., & Knowles, B. B. (2000). Expression of Cre recombinase in mouse oocytes: a means to study maternal effect genes. *Genesis, 26*(2), 110-112. Retrieved from https://www.ncbi.nlm.nih.gov/pubmed/10686600

Fu, A., Oberholtzer, S. M., Bagheri-Fam, S., Rastetter, R. H., Holdreith, C., Caceres, V. L., John, S. V., Shaw, S. A., Krentz, K. J., Zhang, X., Hui, C. C., Wilhelm, D., & Jorgensen, J. S. (2018). Dynamic expression patterns of Irx3 and Irx5 during germline nest breakdown and primordial follicle formation promote follicle survival in mouse ovaries. *PLoS Genet, 14*(8), e1007488. doi:10.1371/journal.pgen.1007488

Gómez-Skarmeta, J., de La Calle-Mustienes, E., & Modolell, J. (2001). The Wnt-activated Xiro1 gene encodes a repressor that is essential for neural

development and downregulates Bmp4. *Development, 128*(4), 551-560. Retrieved from https://www.ncbi.nlm.nih.gov/pubmed/11171338

Hernandez Gifford, J. A. (2015). The role of WNT signaling in adult ovarian folliculogenesis. *Reproduction (Cambridge, England)*. doi:10.1530/REP-14-0685

JL, G.-S. (1998). Xiro, a Xenopus homolog of the Drosophila Iroquois complex genes, controls development at the neural plate. In G. A (Ed.), (Vol. 17, pp. 181-190). EMBO J.

Kumar, M., Camlin, N. J., Holt, J. E., Teixeira, J. M., McLaughlin, E. A., & Tanwar, P. S. (2016). Germ cell specific overactivation of WNT/βcatenin signalling has no effect on folliculogenesis but causes fertility defects due to abnormal foetal development. *Sci Rep, 6*, 27273. doi:10.1038/srep27273

Lin, R. S., Jimenez-Movilla, M., & Dean, J. (2014). Figla-Cre transgenic mice expressing myristoylated EGFP in germ cells provide a model for investigating perinatal oocyte dynamics. *PloS one, 9*(1), e84477. doi:10.1371/journal.pone.0084477

Liu, C.-F., Bingham, N., Parker, K., & Yao, H. H. C. (2009). Sex-specific roles of beta-catenin in mouse gonadal development. *Hum Mol Genet, 18*(3), 405-417. doi:10.1093/hmg/ddn362

Liu, C.-F., Parker, K., & Yao, H. H. C. (2010). WNT4/beta-catenin pathway maintains female germ cell survival by inhibiting activin betaB in the mouse fetal ovary. *PloS one, 5*(4), e10382-e10382. doi:10.1371/journal.pone.0010382

Maatouk, D. M., Dinapoli, L., Alvers, A., Parker, K. L., Taketo, M. M., & Capel, B. (2008). Stabilization of β-catenin in XY gonads causes male-to-female sex-reversal. *Hum Mol Genet, 17*(19), 2949-2955. doi:10.1093/hmg/ddn193

Manuylov, N. L., Smagulova, F. O., Leach, L., & Tevosian, S. G. (2008). Ovarian development in mice requires the GATA4-FOG2 transcription complex. *Development (Cambridge, England), 135*(22), 3731-3743. doi:10.1242/dev.024653

Takezawa, Y., Yoshida, K., Miyado, K., Sato, M., Nakamura, A., Kawano, N., Sakakibara, K., Kondo, T., Harada, Y., Ohnami, N., Kanai, S., Miyado, M., Saito, H., Takahashi, Y., Akutsu, H., & Umezawa, A. (2011). β-catenin is a molecular

switch that regulates transition of cell-cell adhesion to fusion. *Sci Rep, 1*, 68. doi:10.1038/srep00068

Tomizuka, K., Horikoshi, K., Kitada, R., Sugawara, Y., Iba, Y., Kojima, A., Yoshitome, A., Yamawaki, K., Amagai, M., Inoue, A., Oshima, T., & Kakitani, M. (2008). R-spondin1 plays an essential role in ovarian development through positively regulating Wnt-4 signaling. *Hum Mol Genet, 17*(9), 1278-1291. doi:10.1093/hmg/ddn036

Vainio, S., Heikkilä, M., Kispert, A., Chin, N., & McMahon, A. P. (1999). Female development in mammals is regulated by Wnt-4 signalling. *Nature, 397*(6718), 405-409. doi:10.1038/17068

Wang, S. H., Simcox, A., & Campbell, G. (2000). Dual role for Drosophila epidermal growth factor receptor signaling in early wing disc development. *Genes Dev, 14*(18), 2271-2276. Retrieved from https://www.ncbi.nlm.nih.gov/pubmed/10995384

Yuan, L., Liu, J. G., Hoja, M. R., Wilbertz, J., Nordqvist, K., & Höög, C. (2002). Female germ cell aneuploidy and embryo death in mice lacking the meiosis-specific protein SCP3. *Science, 296*(5570), 1115-1118. doi:10.1126/science.1070594

Zeidler, M. P., Perrimon, N., & Strutt, D. I. (1999). Polarity determination in the Drosophila eye: a novel role for unpaired and JAK/STAT signaling. *Genes Dev, 13*(10), 1342-1353. doi:10.1101/gad.13.10.1342

Figure legends

Figure 3-1: *Histology of mutant ovaries remains grossly unaffected*

Ovaries from P0, P3, P7, and P21 control (No Cre; *Ctnnb1*$^{F/F}$) and mutant (*Figla*Cre-EGFP; *Ctnnb1*$^{F/F}$) mice were stained for H&E and examined. Columns 2 and 4 show higher magnification images of follicles, black boxes indicating the region from the original image. Scale bars set to 50μm.

Figure 3-2: *Meiosis initiation is comparable to between control and mutant ovaries*

Immunohistochemistry for SCP3, a meiosis marker, in E16.5 control (No Cre; *Ctnnb1*$^{F/F}$) and mutant (*Figla*Cre-EGFP; *Ctnnb1*$^{F/F}$) ovaries.

Figure 3-3: *Germ cell numbers are no different between control and mutant ovaries*

Nuclear germ cell marker Tra98 was used to detect oocytes at P0 in both control (No Cre; *Ctnnb1*$^{F/F}$) and mutant (*Figla*Cre-EGFP; *Ctnnb1*$^{F/F}$) ovaries.

Figure 3-4: *Granulosa cell proliferation is no different between control and mutant ovaries*

(A) Immunohistochemistry for Ki67 in P7 control (No Cre; *Ctnnb1*$^{F/F}$) and mutant (*Figla*Cre-EGFP; *Ctnnb1*$^{F/F}$) ovaries. (**B**) The average number of Ki67 positive granulosa cells per follicle. No significant difference was seen between control and mutant follicle proliferation rates. N=8 follicles, 2-3 animals per genotype. Scale bars set to 50μm.

Figure 3-5: *Follicle counts from 8-week old ovaries revealed no difference between control and mutant ovaries*

Percentage of primordial, primary, secondary, preantral, antral, small atretic follicles, and large atretic follicles in 8-week old control (No Cre; *Ctnnb1*$^{F/F}$) and mutant (*Figla*Cre-EGFP; *Ctnnb1*$^{F/F}$) ovaries. No follicle stage was significantly different between genotypes.

Figure 3-6:

β-catenin is eliminated specifically in the oocyte

Immunohistochemistry of mouse ovaries at postnatal day 3 (P3) and postnatal day 7 (P7) ovaries exhibiting loss of β-catenin specifically in the oocyte. The somatic cells surrounding each oocyte are not affected and still express β-catenin. White arrowheads indicate primary follicles containing oocytes in both the P3 and P7 ovary that have lost β-catenin expression. White arrows indicate larger/transitioning follicles with oocytes lacking β-catenin in the P7 ovary.

Figure 3-7: *FiglaCre-EGFP targeted loss of β-catenin does not affect IRX3 expression in oocytes*

Immunofluorescence images of P7 ovaries for DAPI (blue) and IRX3 (green). No difference was observed in IRX3 staining between the oocytes of the control and mutant ovaries. Scale bars set to 50μm.

Supplementary Figures

Supplementary Figure 3-1: *FiglaCre-EGFP expression shows robust activity in early postnatal ovaries when bred to the TdTomato reporter mouse*

Immunofluorescence images of E14.5, P1, and P2 ovaries for DAPI (grey) and Figla (green), Tomato (red) and FoxL2 (blue). Data kindly provided by Dr. Paula Brown and Dr. Humphrey Yao, NIEHS

Supplementary Table 3-1

Antibodies used for immunofluorescence

Figure 3-1

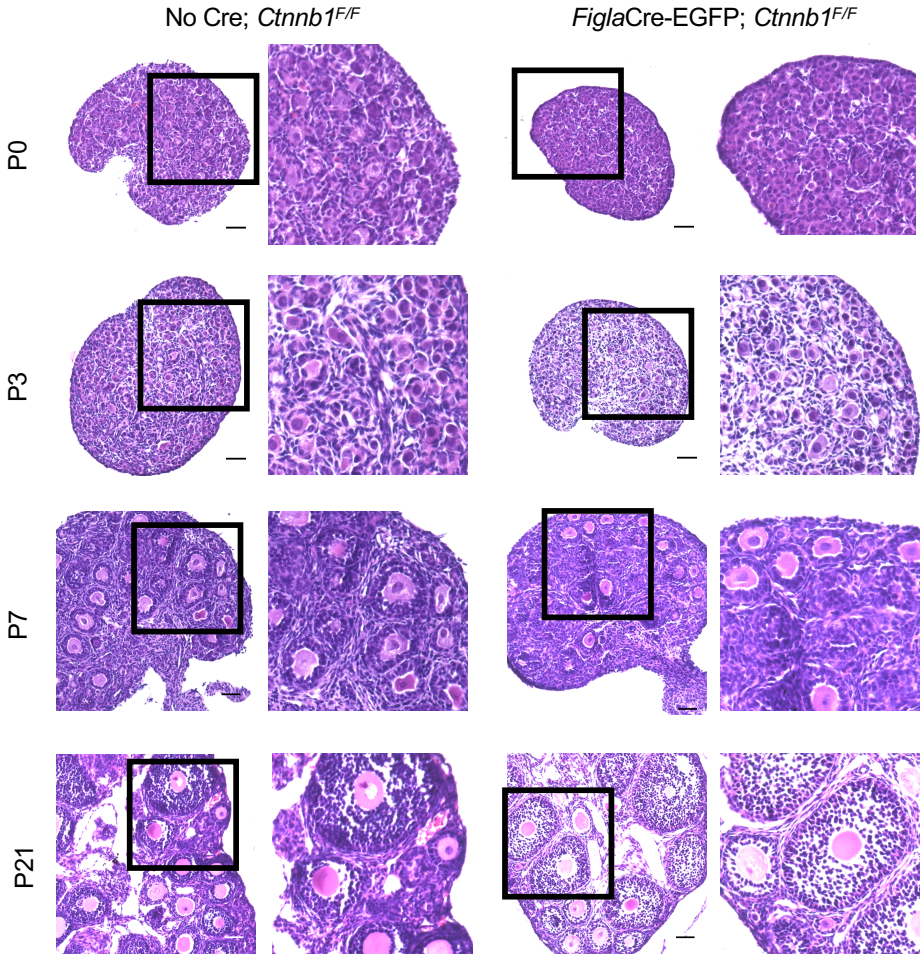

Figure 3-2

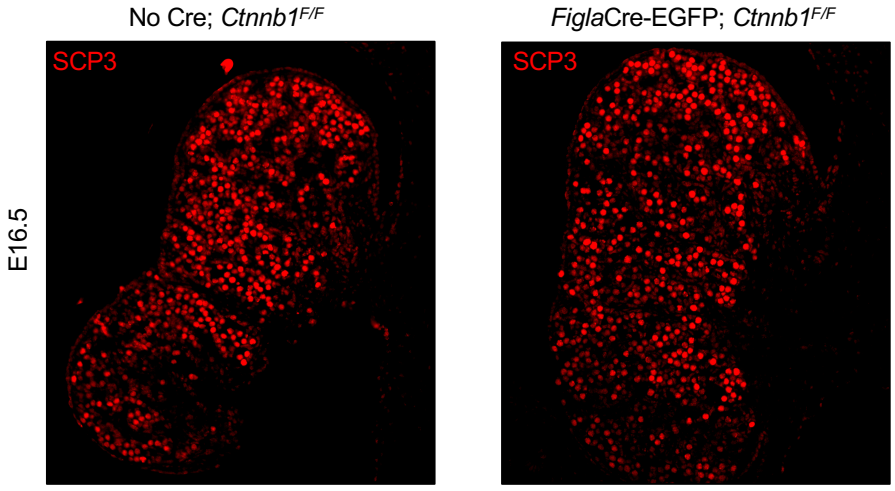

Figure 3-3

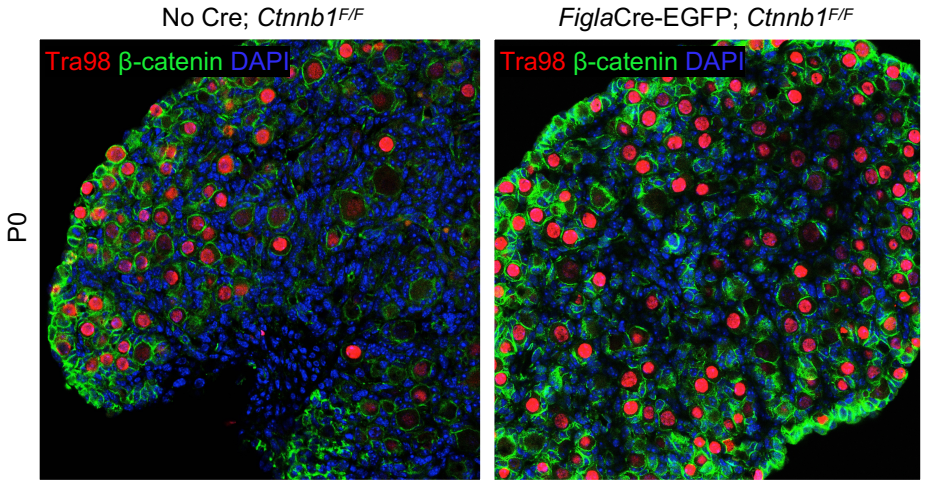
No Cre; Ctnnb1F/F
FiglaCre-EGFP; Ctnnb1F/F
P0
Tra98 β-catenin DAPI
Tra98 β-catenin DAPI

Figure 3-4

A

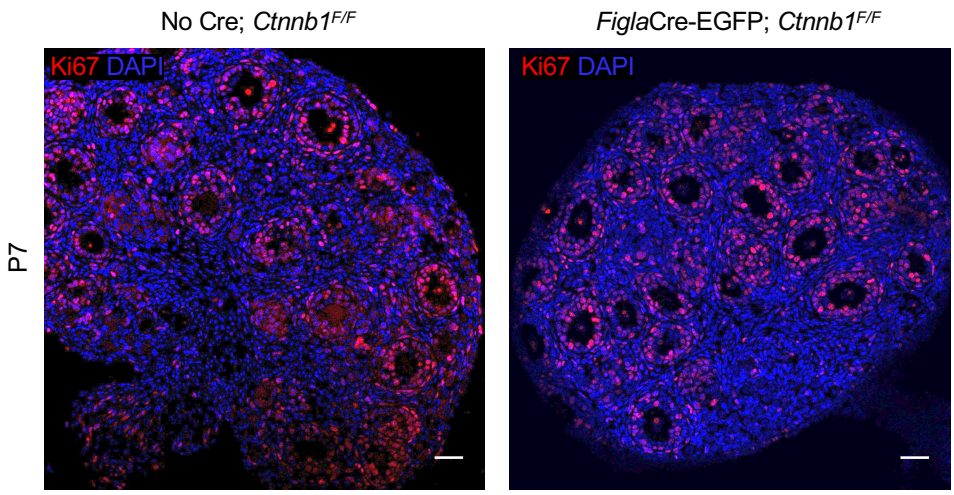
No Cre; Ctnnb1F/F
FiglaCre-EGFP; Ctnnb1F/F
Ki67 DAPI
Ki67 DAPI
P7

B

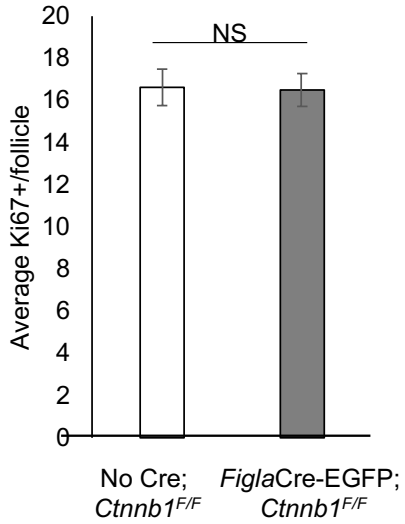
20
18
16
14
12
10
8
6
4
2
0
NS
Average Ki67+/follicle
No Cre; Ctnnb1F/F
FiglaCre-EGFP; Ctnnb1F/F

Figure 3-5

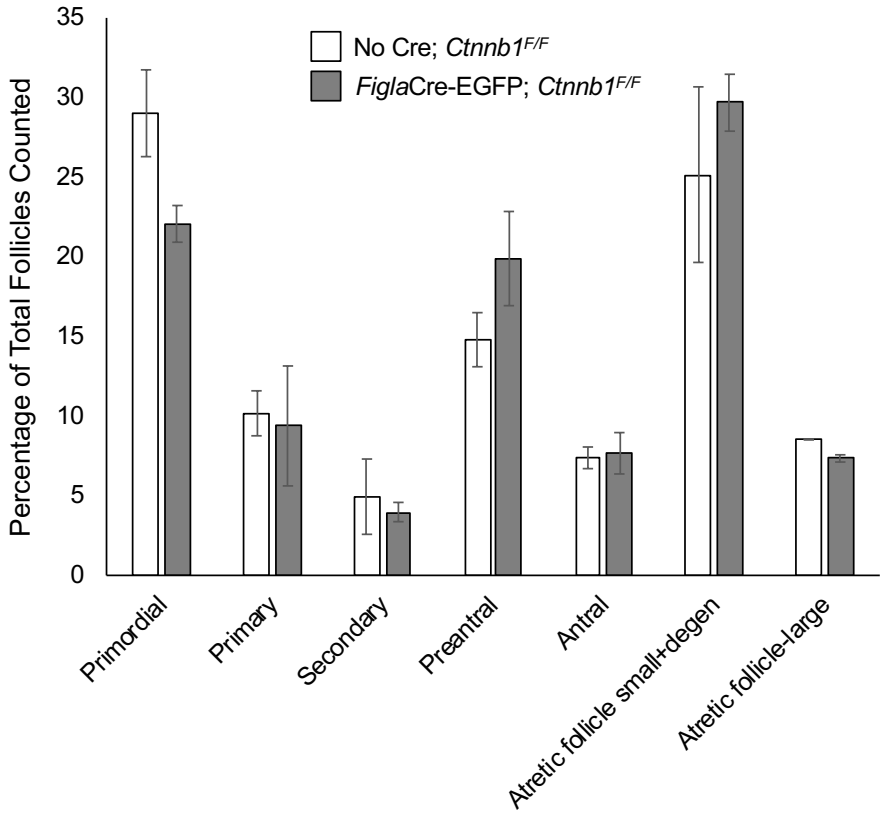
35
30
25
20
15
10
5
0
Percentage of Total Follicles Counted
No Cre; Ctnnb1F/F
FiglaCre-EGFP; Ctnnb1F/F
Primordial
Primary
Secondary
Preantral
Antral
Atretic follicle small+degen
Atretic follicle-large

Figure 3-6

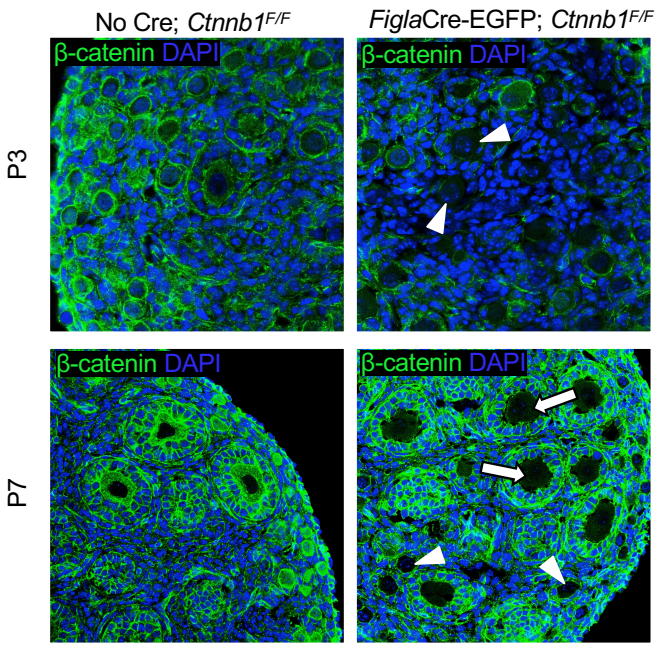
No Cre; Ctnnb1F/F
FiglaCre-EGFP; Ctnnb1F/F
P3
P7
β-catenin DAPI
β-catenin DAPI
β-catenin DAPI
β-catenin DAPI

Figure 3-7

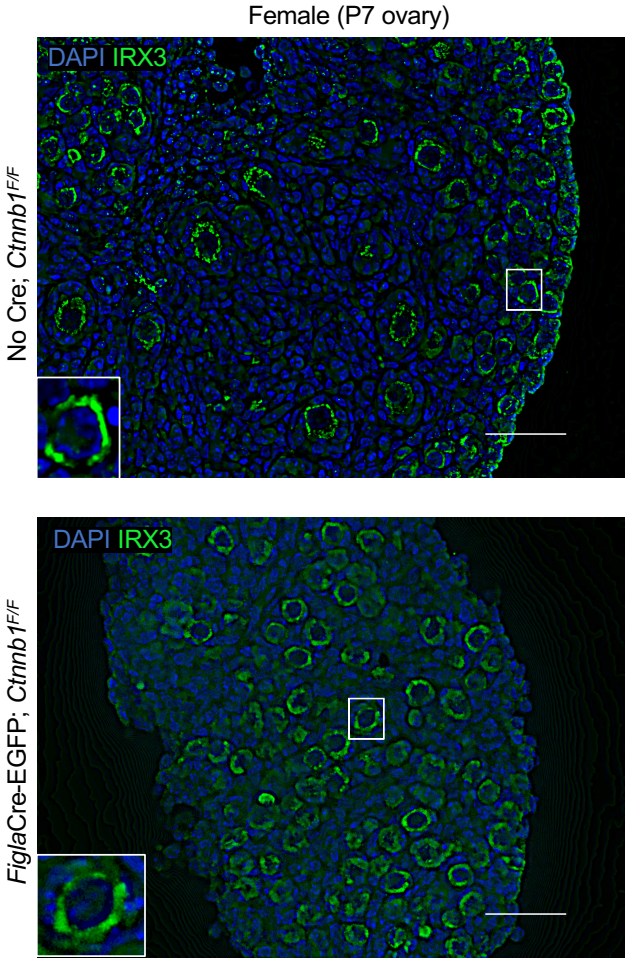
Female (P7 ovary)
DAPI IRX3
No Cre; Ctnnb1F/F
DAPI IRX3
FiglaCre-EGFP; Ctnnb1F/F

Supplementary Figure 3-1

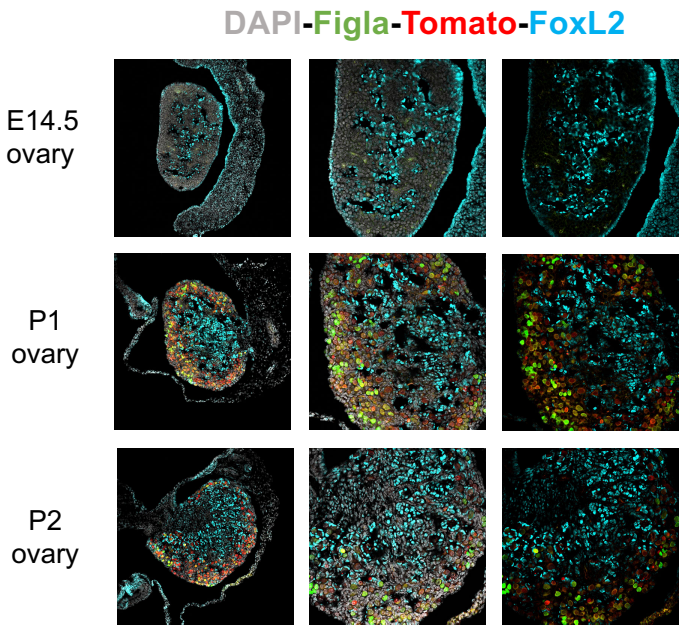

Supplementary Table 3-1

Primary Antibody	Dilution	Source	Catalog #
β-catenin	1:100	BD Biosciences	610153
Tra98	1:150	Cosmo Bio Co. LTD	73-003
SCP3	1:200	Abcam	ab15093
Ki67	1:1000	Abcam	ab15580
Irx3	1:500	Invitrogen	PA5-35149

Chapter 4

Irx3 Overexpression in the Developing Ovary and Testis

Manuscript in preparation

Koth, ML and Jorgensen, JS

Department of Comparative Biosciences, School of Veterinary Medicine, University of Wisconsin – Madison, Madison, Wisconsin, USA

Abstract

Irx3 is expressed in the mouse ovary after sex differentiation and plays an important role in follicle health and female fertility while *Irx3* is not expressed in the testis. A novel *Irx3* overexpression mouse model was used to overexpress *Irx3* in the somatic or germ cells of ovaries and to introduce *Irx3* in testes where expression is normally absent. *Sf1*Cre was used to drive overexpression in somatic cells of the gonad, while *Figla*Cre-EGFP drove germ-cell specific cre recombinase. Our results suggest *Irx3* overexpression in either granulosa cells or oocytes had no impact on ovarian morphology or female fertility. *Irx3* overexpression in the somatic cells of the testes did not affect testis histology or male fertility. In contrast, *Irx3* overexpression in the germ cells of the testis resulted in sub-fertility and a sperm agglutination phenotype. These results suggest that introduction of *Irx3* expression in sperm may be detrimental to sperm health and could give us insight into a potential contributing factor to male infertility.

Introduction

Irx3 and *Irx5*, two transcription factors expressed in the ovary, but not the testis during gonad development, are important for follicle integrity, ovarian health, and fertility (A. Fu et al., 2018; B. Kim, Kim, Cooke, Rüther, & Jorgensen, 2011). Both *Irx3* and *Irx5* are expressed in the somatic cells (pre-granulosa cells) prior to birth, but their expression expands to the germ cell just before germline nest breakdown around E17.5 to postnatal day zero (P0). After follicles have formed, *Irx3* expression transitions to oocyte only, while *Irx5* expression reverts back into the somatic cells for a brief period of time before its expression diminishes (A. Fu et al., 2018). The dynamic expression profile of these genes leads us to question whether overexpression of *Irx3* in the ovary or introduction of *Irx3* in the testis would have any effect on gonad development or fertility.

The gonad consists of two major cell types: somatic and germ. Ovaries consist of both theca and granulosa somatic cells and germ cells called oocytes. Testes are composed of Sertoli, Leydig, and interstitial somatic cells and germ cells called sperm. *Irx3* is not expressed in any testis cell type, while ovarian somatic and germ cells have a dynamic expression pattern of *Irx3*. The expression profile of *Irx3* in ovaries led us to hypothesize whether extending the expression of *Irx3* in the somatic cells of the ovary or increasing *Irx3* in the oocyte would have any effect on ovarian development or fertility. Moreover, we questioned if introduction of *Irx3* in either somatic or germ cells of the testis would have any effect in the male. Utilizing a conditional *Irx3* overexpression mouse model, we were able to overexpress *Irx3* in somatic cells using *Sf1*Cre and germ cells with a newly developed line, *Figla*Cre-EGFP. These mouse models gave us insight

into the role and function of *Irx3* in both ovaries and testes, and how abnormal expression due to genetic defects may have long-term effects on gonad health and fertility later in life.

After histological analysis and breeding studies, we can conclude that *Irx3* overexpression in the somatic or germ cells of the ovary had no impact on ovarian histology and function. *Sf1*Cre driven overexpression of *Irx3* in the somatic cells of the testis did not affect testis morphology or male fertility. *Irx3* overexpression in sperm, however, were sub-fertile; these males were able to generate litters and pups, but litters were inconsistent and fewer pups were produced in total throughout the breeding period. Through sperm analysis, we discovered an intriguing phenotype that suggests *Irx3* overexpression in sperm causes sperm agglutination. Sperm agglutination is commonly seen in men, and *Irx3* has yet to be connected with this phenotype.

Results

Irx3 overexpression mouse model and confirmation of overexpression

Irx3 sequences were inserted downstream of a stop cassette flanked by LoxP sites targeted into the *Rosa26* locus, enabling tissue (cre) specific overexpression of *Irx3.* Cre recombinase excises the stop codon which will allow expression of HA-*Irx3* and EGFP within cre expressing cells (Hui C.C., unpublished). Cre recombinase was targeted to the somatic cells of the gonad with *Sf1*Cre (Bingham, Verma-Kurvari, Parada, & Parker, 2006) or *Figla*Cre-EGFP (Lin, Jimenez-Movilla, & Dean, 2014) to overexpress *Irx3* in ovaries or testes. **Figure 4-1A** shows a diagram of the *Irx3* overexpression mouse model used in these studies.

For clarity, the following nomenclature will be used to classify each mouse model:

- Ovary C-*Irx3*: Control female (No Cre; *Irx3*$^{GOF/GOF}$). This genotype is the control for both somatic and germ cell overexpression within each breeding line.
- Ovary S-*Irx3*: Somatic cell *Irx3* overexpression female (*Sf1*Cre; *Irx3*$^{GOF/GOF}$)
- Ovary G-*Irx3*: Germ cell *Irx3* overexpression female (*Figla*Cre-EGFP; *Irx3*$^{GOF/GOF}$)
- Testis C-*Irx3*: Control male (No Cre; *Irx3*$^{GOF/GOF}$). This genotype is the control for both somatic and germ cell overexpression within each breeding line.
- Testis S-*Irx3*: Somatic cell *Irx3* overexpression male (*Sf1*Cre; *Irx3*$^{GOF/GOF}$)
- Testis G-*Irx3*: Germ cell *Irx3* overexpression male (*Figla*Cre-EGFP; *Irx3*$^{GOF/GOF}$)

Methods to confirm overexpression of *Irx3* in the somatic cells of both ovaries and testes included evaluation of *Irx3* transcripts and immunohistochemistry for EGFP-reporter detection. qPCR was performed using E15.5 gonads. *Irx3* is specific to somatic cells in the ovary at this gestational age and is near its peak expression level. **Ovary**: transcripts from Ovary C-*Irx3* and Ovary S-*Irx3* at E15.5 showed no change in negative control *Rps29* as expected. *Irx3* expression was significantly higher in Ovary S-*Irx3* (2.2 fold over Ovary C-*Irx3*, p=0.016), and *Irx5* was unchanged (**Figure 4-1B**). **Testis**:

Rps29 was unchanged between Testis C-*Irx3* and Testis S-*Irx3*, while *Irx3* was significantly higher in Testis S-*Irx3* (29.5 fold over Testis C-*Irx3*, p=0.0001). It is important to note that because *Irx3* is expressed at extremely low levels in the Testis C-*Irx3*, the relative fold change in the Testis S-*Irx3* is high. When the Testis S-*Irx3* values were normalized to the Ovary C-*Irx3*, the fold change is equivalent to the Ovary S-*Irx3*, at about 2.4-fold. *Irx5* was unchanged in the Testis S-*Irx3* compared to Testis C-*Irx3*. Preliminary results from P0 Testis C-*Irx3* and Testis G-*Irx3* indicate *Irx3* is expressed about 14-fold higher in the Testis G-*Irx3* (**Figure 4-1C**). Ovary G-*Irx3* samples are currently being collected for qPCR analysis at P7 due to endogenous *Irx3* expression in the somatic cells at P0.

*Sf1*Cre drives expression to somatic cells, and it is important to confirm that *Irx3* or EGFP expression is confined to this cell type. Quantitative PCR suggested elevated *Irx3* transcripts in developing ovaries and testes but does not produce localization information. To establish cell specificity, we evaluated gonads by immunohistochemistry (IHC) and *in-situ* hybridization (ISH). To confirm overexpression of *Irx3* specifically to somatic cells, we took advantage of the reporter that was incorporated in the targeted knock-in in gonads from *Sf1*Cre positive animals. IHC was performed using an antibody for EGFP, which is tagged to *Irx3* in the overexpression mouse model. P0 testes show EGFP expression in the somatic cells of Testis S-*Irx3* samples, confirming overexpression of *Irx3* in the correct cell type (**Figure 4-2A**). Previously, we reported that *Irx3* is expressed in the both the somatic and germ cell compartments at postnatal day 0 (P0) (A. Fu et al., 2018). Shortly thereafter, *Irx3* expression transitions in the somatic cells and is confined to the oocyte. Therefore, P21 ovaries from Ovary C-*Irx3*

and Ovary S-*Irx3* were subjected to both ISH for *Irx3* and IHC for EGFP for somatic overexpression analysis. Ovary S-*Irx3* ovaries showed increased *Irx3* mRNA and EGFP expression in the somatic cells of the P21 ovaries compared to Ovary C-*Irx3* (**Figure 4-2B**).

To confirm *Irx3* overexpression did not affect classic sex-specific markers, additional sex-specific controls *Foxl2* (ovary) and *Sox9* (testis) transcripts were analyzed by qPCR. *Foxl2* showed no change between Ovary C-*Irx3* and Ovary S-*Irx3* ovaries. *Sox9* was unchanged between Testis C-*Irx3* and Testis S-*Irx3* testes (**Supplementary Figure 4-1**). Overall, *Irx3* transcripts were elevated in the overexpression models analyzed, and EGFP expression is confined to the correct cell type in the somatic cell models.

Irx3 overexpression in the ovary does not affect ovarian function or female fertility

*Sf1*Cre was bred to *Irx3*$^{GOF/GOF}$ females to generate *Irx3* overexpression confined to the somatic cells of the ovary. Although *Irx3* is endogenously expressed in the somatic cells until the primordial follicle stage, we hypothesized that stabilizing *Irx3* after it is normally absent in the somatic cells could have an effect on follicle health and maturation. Ovary C-*Irx3* and Ovary S-*Irx3* ovaries were harvested from embryonic (E) 16.5, postnatal (P) day 0, P21, and adult mice to follow ovarian development and follicle maturation over time. Of most interest was to observe any defects in later follicle stages, when *Irx3* is normally turned off. Healthy follicles of all stages were present in both Ovary C-*Irx3* and Ovary S-*Irx3* ovaries, indicating there were no defects during follicle formation or development. (**Figure 4-3A**). Next, Ovary S-*Irx3* mice and Ovary C-*Irx3*

controls were set up with wild-type CD1 males for 6 months to assess fertility. Litter dates and pup numbers were recorded throughout the breeding period. No significant difference was seen at any point in the study between Ovary C-*Irx3* and Ovary S-*Irx3* (**Figure 4-3B**).

Likewise, *Figla*Cre-EGFP was bred to *Irx3*$^{GOF/GOF}$ female mice to overexpress *Irx3* in the germ cell. *Irx3* is endogenously expressed in the oocyte beginning at the primordial follicle stage. Stabilized expression of other endogenously expressed genes, such as β-catenin, can disrupt normal ovarian function (Maatouk et al., 2008). Therefore, we questioned whether stabilization of *Irx3* could have an effect on oocyte health, follicle maturation, or female fertility. Ovary C-*Irx3* and Ovary G-*Irx3* ovaries from P0, P7, and P21 were processed for H&E analysis, and no visible defects were seen in follicle development or maturation. (**Figure 4-4A**). Next, to assess fertility, Ovary C-*Irx3* and Ovary G-*Irx3* mice were bred to male wild-type CD1 mice for 5 months and litter dates and pup numbers were recorded. Total pup number accumulation over time was comparable between Ovary C-*Irx3* and Ovary G-*Irx3* mice, indicating no fertility defects (**Figure 4-4B**).

Irx3 overexpression in the somatic cells of the testis does not affect testis function or male fertility

Irx3 is not expressed at any point during testis development; therefore, we hypothesized that aberrant *Irx3* overexpression may cause defects in testis development and/or male fertility. Testes were collected during gestation and into adulthood to analyze testis cord formation and development at E16.5, P0, P21, and

adult in Testis C-*Irx3* and Testis S-*Irx3* mice. Histological analysis shows normal testis cords and seminiferous tubules in Testis S-*Irx3* mice that were comparable to controls throughout development and into adulthood, indicating proper testis formation and development (**Figure 4-5A**). As with studies in female mice, Testis S-*Irx3* males along with Testis C-*Irx3* controls were paired with wild-type CD1 females for a 6-month breeding study. Results showed no difference in litter sizes over time between control and Testis S-*Irx3* mice (**Figure 4-5B**). Overall, *Irx3* overexpression in the somatic cells of the testis had no effect on testis histology and had no effect on male fertility.

Irx3 overexpression in the germ cells of male mice results in a sub-fertile phenotype and sperm agglutination

To assess the effects of *Irx3* overexpression in sperm, we bred *Figla*Cre-EGFP to *Irx3*$^{GOF/GOF}$ mice. Testes were collected at P0, P7, P21, and adult in Testis C-*Irx3* and Testis G-*Irx3* mice and processed for histological analysis. Sections from testes from each time point were stained with H&E. Results show no obvious defects in Testis G-*Irx3* samples when compared to controls (**Figure 4-6A**). Although there was no obvious defect based on histology, a breeding study was required to assess testis function in these mice. Testis C-*Irx3* and Testis G-*Irx3* males were set up with wild-type CD1 females for 4 months. Testis C-*Irx3* males, on average, produced litters of 11 to 18 pups every 23 days. In contrast, Testis G-*Irx3* males failed to produce litters on a regular basis of consistent size. One Testis G-*Irx3* mouse produced litters, but the litter sizes contained fewer pups than the average control litter size (15 vs 5.4 pups). Two other Testis G-*Irx3* males in the study produced one litter within 1-2 months, but then failed to

produce any litters thereafter. Finally, one other Testis G-*Irx3* male has never produced a litter. Overall, Testis G-*Irx3* males showed a phenotype consistent with sub- or complete infertility when *Irx3* was overexpressed in the germ cells of the testis (**Figure 4-6B**).

The results of the breeding study were surprising given that no obvious morphological defect was observed. Thus, we hypothesized that sperm concentration and/or motility were decreased in Testis G-*Irx3* males. Following the breeding study, Testis C-*Irx3* and Testis G-*Irx3* males were euthanized and their epididiymides were aseptically dissected. Mature sperm were released from the epididymides and after brief incubation at 37°C, loaded onto a sperm-counting chamber slide and analyzed using a computer assisted sperm analyzer to assess motility and concentration. Testis C-*Irx3* sperm were normal with high sperm counts and high motility rates. The Testis G-*Irx3* mouse that produced consistent litters of fewer pups showed normal sperm concentration and motility, but displayed numerous clumps of sperm moving around within the sample. The two Testis G-*Irx3* males that produced one litter and then none thereafter showed variable sperm concentration (though nothing of concern) and high motility, but also displayed sperm agglutination throughout the sample. The sperm from the Testis G-*Irx3* male that has produced zero litters will be analyzed after the conclusion of his breeding period. A table displaying sperm counts, motility rate, and phenotype displayed as well as images of a representative sperm analysis image is presented in **Figure 4-7A, B.** In conclusion, Testis G-*Irx3* males exhibit an intriguing phenotype of sperm agglutination that warrants further investigation and the need to fine-tune testicular histological analysis.

Discussion

To disrupt the endogenous expression profile of *Irx3* in the ovary or to introduce *Irx3* expression in the testis, we overexpressed *Irx3* in either the somatic or germ cells of both ovaries and testes. We can conclude that *Irx3* overexpression in the ovary in either somatic or germ cells has no impact on ovarian histology or fertility, and *Irx3* overexpression in the somatic cells of the testis does not affect testis histology or fertility. In the Testis G-*Irx3* model, testis morphology was not histologically different from controls; however, Testis G-*Irx3* mice exhibited a sub-fertile phenotype and sperm agglutination was detected using sperm analysis. Sperm agglutination is not widely seen in mice and warrants further investigation for this project.

In the ovary, *Irx3* expression turns off in the somatic cell compartment after primordial follicle formation. We questioned whether stabilizing *Irx3* expression in the granulosa cells would have an effect on follicle maturation or ovarian function. We did not see any defect in the Ovary S-*Irx3* model, and we reflected on the qPCR transcript levels of *Irx3* compared to Ovary C-*Irx3* mice. Ovary S-*Irx3* mice displayed a 2.2-fold increase in *Irx3* transcripts compared to the control, which may not be sufficient to drive a phenotype in these females, suggesting endogenous *Irx3* expression may be at a point of saturation and overexpression had no effect. This may also be the case in the germ cell compartment, where a slight increase of *Irx3* expression may have no biological consequences *in vivo*.

Irx3 is not expressed in the testis at any point during development; therefore, we hypothesized that aberrant expression of *Irx3* would disrupt testicular development and fertility. The somatic cell overexpression of *Irx3* showed no indication of irregular

testicular cord development, and the breeding study confirmed that these male mice were as fertile as control littermates. In contrast, germ cell overexpression of *Irx3* showed no obvious signs of abnormal testes or sperm by H&E analysis, but the breeding study exposed a significant fertility defect. Some, but not all Testis G-*Irx3* mice were able to produce litters that were inconsistent in timing and litter size. Sperm analysis determined that Testis G-*Irx3* males had normal sperm counts; however, there was significant evidence of sperm agglutination.

Sperm agglutination is defined as sperm adhering to each other without the presence of other cells or debris (Ulrik Kvist, 2002). This phenomenon was first documented in the early 1900s and seen as a relatively uncommon condition (WILSON, 1956). More recent studies show that sperm autoimmunity, the leading cause of sperm agglutination, is thought to be caused by the presence of antibodies against spermatozoa (Friberg, 1980; Friberg & Tilly-Friberg, 1977; Ulrik Kvist, 2002; WILSON, 1956) and is responsible for about 7% of human male infertility (Shlomi Barak, 2016). Sperm are normally protected from sperm antigens by tight junctions of Sertoli cells, which form the blood-testis barrier (Vasan, 2011). We previously showed that Connexin 43 (GJA1) expression is decreased in our *Irx3/5* double knockout ovaries (A. Fu et al., 2018), and *Irx3* was also shown to modulate the transcription of both Cx43 and Cx40 in the heart (K. H. Kim et al., 2016). These data suggest that the presence of *Irx3* within germ cells impacts tight or gap junctions. We plan to analyze tight junctions and the testis-blood barrier of Male G-*Irx3* mice. Defects in the testis-blood barrier has been shown to elicit an immune response that leads to the formation of anti-sperm antibodies (ASAs). ASAs are shown to create clumps of moving sperm in semen samples, which

hinder the passage of sperm through cervical mucus, zonal binding, and passage through the cervix (Mortimer, 1994). One group investigated cognate antigens of agglutinating ASAs and identified 8 potential ASA candidates (Koide, Wang, & Kamada, 2000). Sperm agglutination factors, interestingly, have been proposed as potential contraceptive agents for men (Aggarwal & Prabha, 2006; Naz & Chauhan, 2001). Most agglutination cases in humans can be treated by reproductive assistance and sperm washing, but treatment with proteolytic enzymes has also been proposed to treat this condition (Pattinson, Mortimer, Curtis, Leader, & Taylor, 1990).

Available research suggests that a sperm agglutination phenotype is generally seen in mice that have antibodies against spermatozoon-specific proteins (J. Fu et al., 2012) or if there was any sort of trauma to the genital area by either infection or disease (Kalaydjiev, Dimitrova, Mitov, Dikov, & Nakov, 2007; Shetty, Bronson, & Herr, 2008). The agglutination phenotype seen in the Testis G-*Irx3* sperm is intriguing due to the lack of evidence connecting *Irx3* to sperm agglutination and could be caused by the presence of ASAs. An ELISA assay for ASAs is commercially available and would give us the opportunity to detect ASAs in the serum of Testis G-*Irx3* males. This would give us insight whether ASAs were playing a role in the agglutination phenotype or if there are additional factors involved. Furthermore, we plan to perform RNA-seq on Testis G-*Irx3* sperm to identify genes that are up- or down-regulated in mutant sperm, and whether those genes tie into an auto-immunity pathway.

In conclusion, we successfully overexpressed *Irx3* in distinct cell populations within both ovaries and testes using a novel *Irx3* overexpression mouse line. No significant differences were seen in morphology or fertility between control and mutant

ovaries of either overexpression model, indicating that an increase of *Irx3* expression has no effect on ovarian development or overall health. Next, *Irx3* overexpression in the somatic cells of the developing testis, where *Irx3* is normally absent, had no effect on testis morphology or fertility in males. In contrast, *Irx3* overexpression in sperm had no obvious morphology defects during testis development, but resulted in male sub-fertility, potentially caused by a sperm agglutination phenotype in mutant sperm. In order to build on this study, we need to determine how *Irx3* overexpression in the sperm results in a sperm agglutination phenotype, which could lead to a novel pathogenesis in male infertility.

Methods

Animals

Mouse strains included ROSA26-Stop^{flox}/Irx3-IRES-EGFP mice (referenced as *Irx3*^{GOF}), generated and provided by Dr. Chi-Chung Hui, University of Toronto, with *Irx3* sequences inserted behind the Rosa26 promoter within the Rosa locus with a floxed stop codon (**Figure 4-1A**), *Sf1*Cre, originally obtained from the Keith Parker Lab (Bingham et al., 2006), and *Figla*Cre-EGFP (FVB/N-Tg(Figla-EGFP-icre)ZP3Dean/Mmjax) obtained from Dr. Jurrien Dean at NIH/NIDDK. Genotyping was carried out using primers Q (Irx3 GOF F): 5'-AAAGTCGCTCTGAGTTGTTAT-3', R (Irx3 GOF Mut R): 5'-GGAGCGGGAGAAATGGATATG-3', S (Irx3 GOF WT R): 5'-GCGAAGAGTTTGTCCTCAACC-3'; *Sf1*Cre: 5′-GAGTGAACGAACCTGGTCGAAATCAGTGCG-3′ and 5′-GCATTACCGGTCGATGCAACGAGTGATGAG-3′; *Figla*Cre iCRE F: 5' -

CCAGCTCAACATGCTGCACA-3’ and iCRE R: 5’ - GCCACACCAGACACAGAGAT – 3’. Timed mating was identified by the presence of a vaginal plug, which was designated as embryonic day 0.5 (E0.5).

Animal housing and all procedures described were reviewed and approved by the Institutional Animal Care and Use Committee at the University of Wisconsin-Madison and were performed in accordance with the National Institute of Health Guiding Principles for the Care and Use of Laboratory Animals. Mice were housed in disposable, ventilated cages (Innovive, San Diego, CA). Rooms were maintained at 22 ±2 degrees Celsius and 30–70% humidity on a 12-hour light/dark cycle.

Histology

Ovaries and testes were harvested at the age point indicated, fixed in 4% PFA overnight, and embedded in paraffin. Blocks were sectioned at 8μm thickness and then stained with hematoxylin and eosin (H&E) for histological analysis.

Immunohistochemistry

Mouse ovaries and testes were harvested at the age indicated, fixed in 4% paraformaldehyde overnight at 4°C, and washed in PBS and embedded in paraffin. Blocks were sectioned at 8μm thickness. Biotin anti GFP (Abcam, ab6658, 1:50 dilution) was applied to paraffin sections at 4°C overnight. 2° (Alexa Fluor 488-conjugate IgG fraction monoclonal mouse anti-biotin, Jackson ImmunoResearch, #200-542-211, 1:100 dilution) was then incubated at room temperature for 1 hour. DAPI in PBS solution was

used as a nuclear counterstain. Images were collected on a Keyence BZ-X700 microscope. Images were processed with ImageJ and/or the Keyence BZ-X700 analyzer software.

Section In-situ hybridiziation

Full methods can be found in (Wilhelm et al., 2007). Briefly, sections were deparaffinized and rehydrated with an ethanol gradient and incubated with 5μg/ml Proteinase K for 20 minutes at room temperature. Sections were then re-fixed with fresh 4% PFA and acetylated, and prehybridized with hybridization solution for 2 hours at room temperature. Hybridization (hybridization solution + 0.05μg/ml probe) was performed overnight at 60°C in a hybridization oven. Slides were washed and then incubated with blocking solution for 2 hours in a humidified chamber. Anti-DIG (1:1000) was applied overnight at 4°C. Unbound antibodies were removed with washing and slides were equilibrated and incubated in color solution (3.5μl of 5-bromo-4chloro-3-indolyl phosphate (Roche Applied Science) per mL of NTM buffer until staining was satisfactory (usually overnight at 4°C). Sequences for *Irx3* probes can be found in (Jorgensen & Gao, 2005).

RNA Extraction and qPCR

RNA was extracted using Trizol (Invitrogen, ca#: 15596026) according to the manufacturer's instructions and quantified using a NanoDrop 2000. 500ng RNA from each sample was used for First-Strand cDNA synthesis by SuperScriptII-RT (Invitrogen, AM9515). cDNA was diluted 1:5 and then 2 μl was added to 5 μl SYBR green PCR

mixture (Applied Biosytems), 2.4 µl water, and 1.25 pmol primer mix. PCR reactions were carried out using the ABI Prism 7000 Sequence Detection System (Applied Biosystems). RNA transcripts were quantified using the ΔΔCt method (Livak & Schmittgen, 2001). Briefly, to control for overall gene expression in each time point, the average cycle threshold (aveCt) for 36B4 was subtracted from the aveCt value for each gene to generate ΔCt. Next, ΔCt for each gene was compared to ΔCt of that same gene for the mutant genotype (e.g. $\Delta Ct\ Irx3_{female\ control} - \Delta Ct\ Irx3_{female\ mutant}$), to generate ΔΔCt. Finally, fold change was calculated as 2 to the −ΔΔCt power ($2^{-\Delta\Delta Ct}$).

Breeding Study

Male and female control and mutant mice from all lines (S-*Irx3* and G-*Irx3*) were set up with wild type (CD1) mice of the opposite sex to breed for the times indicated. Litter sizes and birth dates were monitored and recorded throughout the breeding period.

Sperm Analysis

Male mice were sacrificed and cauda epididymides were aseptically dissected. Fat and blood were removed and then the cauda epididymides were transferred to 0.8ul HTF+PVA (poly-vinyl-alcohol) at 37°C. Five to six incisions were made in the epididymides using a micro scissors to release the sperm. After a ten-minute swim-up, a 10ul aliquot was diluted in 90ul HTF+PVA. After 1 minute, sperm was loaded into the computer assisted sperm analyzer (Hamilton Thorne) and analyzed to assess motility and sperm concentration.

References

Aggarwal, J., & Prabha, V. (2006). Contraceptive effect of sperm-agglutinating factor isolated from Staphylococcus aureus in mouse. *BJOG, 113*(9), 1039-1043. doi:10.1111/j.1471-0528.2006.01024.x

Bingham, N. C., Verma-Kurvari, S., Parada, L. F., & Parker, K. L. (2006). Development of a steroidogenic factor 1/Cre transgenic mouse line. *Genesis (New York, N.Y. : 2000), 44*(9), 419-424. doi:10.1002/dvg.20231

Friberg, J. (1980). Autoagglutination in ejaculates caused by sperm-agglutinating antibodies. *Am J Reprod Immunol, 1*(1), 44-48. Retrieved from https://www.ncbi.nlm.nih.gov/pubmed/7337149

Friberg, J., & Tilly-Friberg, I. (1977). Spontaneous spermagglutination in ejaculates from men with head-to-head or tail-to-tail spermagglutinating antibodies in serum. *Fertil Steril, 28*(6), 658-662. Retrieved from https://www.ncbi.nlm.nih.gov/pubmed/862977

Fu, A., Oberholtzer, S. M., Bagheri-Fam, S., Rastetter, R. H., Holdreith, C., Caceres, V. L., John, S. V., Shaw, S. A., Krentz, K. J., Zhang, X., Hui, C. C., Wilhelm, D., & Jorgensen, J. S. (2018). Dynamic expression patterns of Irx3 and Irx5 during germline nest breakdown and primordial follicle formation promote follicle survival in mouse ovaries. *PLoS Genet, 14*(8), e1007488. doi:10.1371/journal.pgen.1007488

Fu, J., Wang, Y., Fok, K. L., Yang, D., Qiu, Y., Chan, H. C., Koide, S. S., Miao, S., & Wang, L. (2012). Anti-ACTL7a antibodies: a cause of infertility. *Fertil Steril, 97*(5), 1226-1233.e1221-1228. doi:10.1016/j.fertnstert.2012.02.023

Jorgensen, J. S., & Gao, L. (2005). Irx3 is differentially up-regulated in female gonads during sex determination. *Gene expression patterns : GEP, 5*(6), 756-762. doi:10.1016/j.modgep.2005.04.011

Kalaydjiev, S., Dimitrova, D., Mitov, I., Dikov, I., & Nakov, L. (2007). Serum sperm antibodies after diarrhoeal diseases. *Andrologia, 39*(3), 101-108. doi:10.1111/j.1439-0272.2007.00772.x

Kim, B., Kim, Y., Cooke, P. S., Rüther, U., & Jorgensen, J. S. (2011). The fused toes locus is essential for somatic-germ cell interactions that foster germ cell maturation in developing gonads in mice. *Biology of reproduction, 84*(5), 1024-1032. doi:10.1095/biolreprod.110.088559

Kim, K. H., Rosen, A., Hussein, S. M., Puviindran, V., Korogyi, A. S., Chiarello, C., Nagy, A., Hui, C. C., & Backx, P. H. (2016). Irx3 is required for postnatal maturation of the mouse ventricular conduction system. *Sci Rep, 6*, 19197. doi:10.1038/srep19197

Koide, S. S., Wang, L., & Kamada, M. (2000). Antisperm antibodies associated with infertility: properties and encoding genes of target antigens. *Proc Soc Exp Biol Med, 224*(3), 123-132. doi:10.1046/j.1525-1373.2000.22410.x

Lin, R. S., Jimenez-Movilla, M., & Dean, J. (2014). Figla-Cre transgenic mice expressing myristoylated EGFP in germ cells provide a model for investigating perinatal oocyte dynamics. *PloS one, 9*(1), e84477. doi:10.1371/journal.pone.0084477

Livak, K. J., & Schmittgen, T. D. (2001). Analysis of relative gene expression data using real-time quantitative PCR and the 2(-Delta Delta C(T)) Method. *Methods, 25*(4), 402-408. doi:10.1006/meth.2001.1262

Maatouk, D. M., Dinapoli, L., Alvers, A., Parker, K. L., Taketo, M. M., & Capel, B. (2008). Stabilization of β-catenin in XY gonads causes male-to-female sex-reversal. *Hum Mol Genet, 17*(19), 2949-2955. doi:10.1093/hmg/ddn193

Mortimer, D. (1994). *Practical laboratory andrology*: Oxford University Press on Demand.

Naz, R. K., & Chauhan, S. C. (2001). Presence of antibodies to sperm YLP(12) synthetic peptide in sera and seminal plasma of immunoinfertile men. *Mol Hum Reprod, 7*(1), 21-26. doi:10.1093/molehr/7.1.21

Pattinson, H. A., Mortimer, D., Curtis, E. F., Leader, A., & Taylor, P. J. (1990). Treatment of spermagglutination with proteolytic enzymes. I. Sperm motility, vitality, longevity and successful disagglutination. *Hum Reprod, 5*(2), 167-173. doi:10.1093/oxfordjournals.humrep.a137063

Shetty, J., Bronson, R. A., & Herr, J. C. (2008). Human sperm protein encyclopedia and alloantigen index: mining novel allo-antigens using sera from ASA-positive infertile patients and vasectomized men. *J Reprod Immunol, 77*(1), 23-31. doi:10.1016/j.jri.2007.04.006

Shlomi Barak, M. H. B., MD, PhD, FRACP. (2016). *Clinical Management of Male Infertility*. Endotext.

Ulrik Kvist, L. B. (2002). Manual on Basic Semen Analysis. *ESHRE Monographs*, 1-4.

Vasan, S. S. (2011). Semen analysis and sperm function tests: How much to test? *Indian J Urol, 27*(1), 41-48. doi:10.4103/0970-1591.78424

Wilhelm, D., Hiramatsu, R., Mizusaki, H., Widjaja, L., Combes, A. N., Kanai, Y., & Koopman, P. (2007). SOX9 regulates prostaglandin D synthase gene transcription in vivo to ensure testis development. *J Biol Chem, 282*(14), 10553-10560. doi:10.1074/jbc.M609578200

WILSON, L. (1956). Sperm agglutination due to autoantibodies; a new cause of sterility. *Fertil Steril, 7*(3), 262-267. Retrieved from https://www.ncbi.nlm.nih.gov/pubmed/13318036

Figure legends

Figure 4-1*: Irx3 transcripts increased in mutant mice*

(**A**) Diagram representing the *Irx3* overexpression mouse model. HA-*Irx3*-IRES-EGFP sequences follow a floxed stop codon an tpA within the *Rosa26* genomic locus. (**B**) qPCR analysis of E15.5 ovaries in Ovary C-*Irx3* or Ovary S-*Irx3* mice (n=3-5 biological replicates for each genotype) (**C**) qPCR analysis of E15.5 testes in Testis C-*Irx3* or Testis S-*Irx3* mice (n=3), and preliminary data of *Irx3* expression in P0 Male C-*Irx3* (n=2) and Male G-*Irx3* testes (n=1). Error bars represent +/- SEM. **p<0.01, ****p<0.001.

Figure 4-2*: Confirmation of Irx3 overexpression in the somatic cells of testes and ovaries in Male S-Irx3 and Female S-Irx3 mice*

(**A**) IHC was performed with anti-EGFP to detect the IRES driven EGFP expression. Both Sertoli and interstitial cells of P0 Testis S-*Irx3* testis were positive for EGFP while no EGFP was detected in Testis C-*Irx3* testes (**B**) ISH for *Irx3* mRNA in p21 Female C-*Irx3* and Female S-*Irx3* ovaries. (**C**) EGFP is detected in the granulosa cells of P21 Ovary S-*Irx3* ovaries and is absent in Ovary C-*Irx3* samples. Scale bars set to 50μm.

Figure 4-3*: Sf1Cre mediated somatic cell overexpression of Irx3 in the ovary has no impact on ovarian development or fertility*

(**A**) H&E staining of Ovary C-*Irx3* and Ovary S-*Irx3* tissues at the ages indicated. Insets are images at higher magnification of the regions outlined by black boxes. Images representative of n=3-4 ovaries from each genotype. Scale bars set to 50μm. (**B**) Ovary

C-*Irx3* (n=5) and Ovary S-*Irx3* (n=4) females were bred to wild-type male mice for 6 months. Data represents total numbers of pups accumulated over time. Data are represented as the average +/- SEM.

Figure 4-4*: FiglaCre mediated germ cell overexpression of Irx3 germ cell has no effect on ovarian development or female fertility*

(**A**) H&E staining of Ovary C-*Irx3* and Ovary G-*Irx3* tissues at the ages indicated. Insets are images at higher magnification of the regions outlined in black boxes. Images are representative of 3 biological replicates. Scale bars set to 50μm. (**B**) Ovary C-*Irx3* (n=4) and Ovary G-*Irx3* (n=3) females were bred to wild-type male mice for 5 months. Data represents total numbers of pups accumulated over time. Data are represented as the average +/- SEM.

Figure 4-5*: Sf1Cre mediated somatic cell Irx3 overexpression in the male does not impact testis development or fertility*

(**A**) H&E staining of Testis C-*Irx3* and Testis S-*Irx3* testes at the ages indicated. Insets are images at higher magnification of the regions outlined by black boxes. Images representative of n=3-4 testes from each genotype. Scale bars set to 50μm. (**B**) Testis C-*Irx3* (n=3) and Testis S-*Irx3* (n=4) males were paired with wild-type CD1 females for 6 months. Data represents total numbers of pups accumulated over time. Data are represented as the average +/- SEM.

Figure 4-6*: FiglaCre mediated germ cell Irx3 overexpression in males shows no defect in testis morphology but reveals a sub-fertile phenotype*

(**A**) H&E staining of Testis C-*Irx3* and Testis G-*Irx3* testes at the ages indicated. Insets are images at higher magnification of the regions outlined by black boxes. Images representative of n=3 testes from each genotype. Scale bars set to 50μm. (**B**) Testis C-*Irx3* (n=3) and Testis G-*Irx3* (n=4) mice were paired with wild-type CD1 females for 4 months. Pup number and litter dates were recorded, data represents total pups over time. *p<0.05, **p<0.01, ***p<0.001. Data are represented as the average +/- SEM.

Figure 4-7*: Sperm analysis reveals agglutination phenotype in mutant males*

(**A**) Sperm count and motility percentage from each mouse of the genotype listed along with notes about each analysis (**B**) Representative sperm analysis pictures from Testis C-*Irx3* and Testis G-*Irx3* males. White structures are live sperm. The large clump in the Testis G-*Irx3* image is a cluster of live sperm, which is seen moving throughout the sample. Several representative images are taken for each sample with a camera attached to the microscope for analysis.

Supplementary Table 4-1*: Primers used for RT-qPCR*

Primers written in the 5’ to 3’ direction

Supplementary Figure 4-1: qPCR analysis of sex-specific controls

(**A**) *Foxl2* transcripts were analyzed from Female C-*Irx3* and Female S-*Irx3* ovaries at E15.5 (**B**) *Sox9* transcripts were analyzed from Male C-*Irx3* and Male S-*Irx3* testes at E15.5. Error bars represent +/- SEM.

Figure 4-1

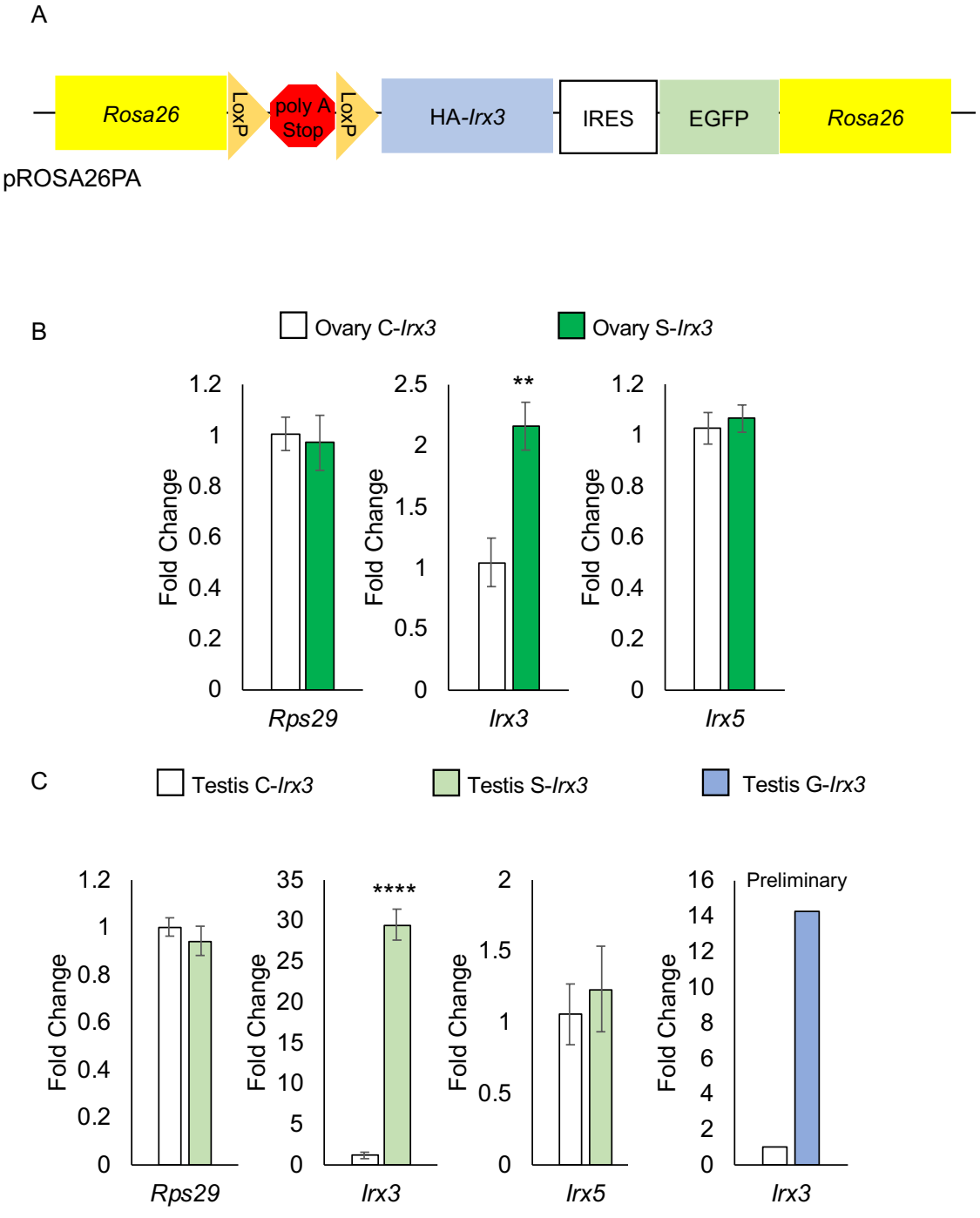
A
Rosa26
LoxP
poly A Stop
LoxP
HA-Irx3
IRES
EGFP
Rosa26
pROSA26PA
B
Ovary C-Irx3
Ovary S-Irx3
Fold Change
Rps29
Irx3
Irx5
**
C
Testis C-Irx3
Testis S-Irx3
Testis G-Irx3
****
Preliminary

Figure 4-2

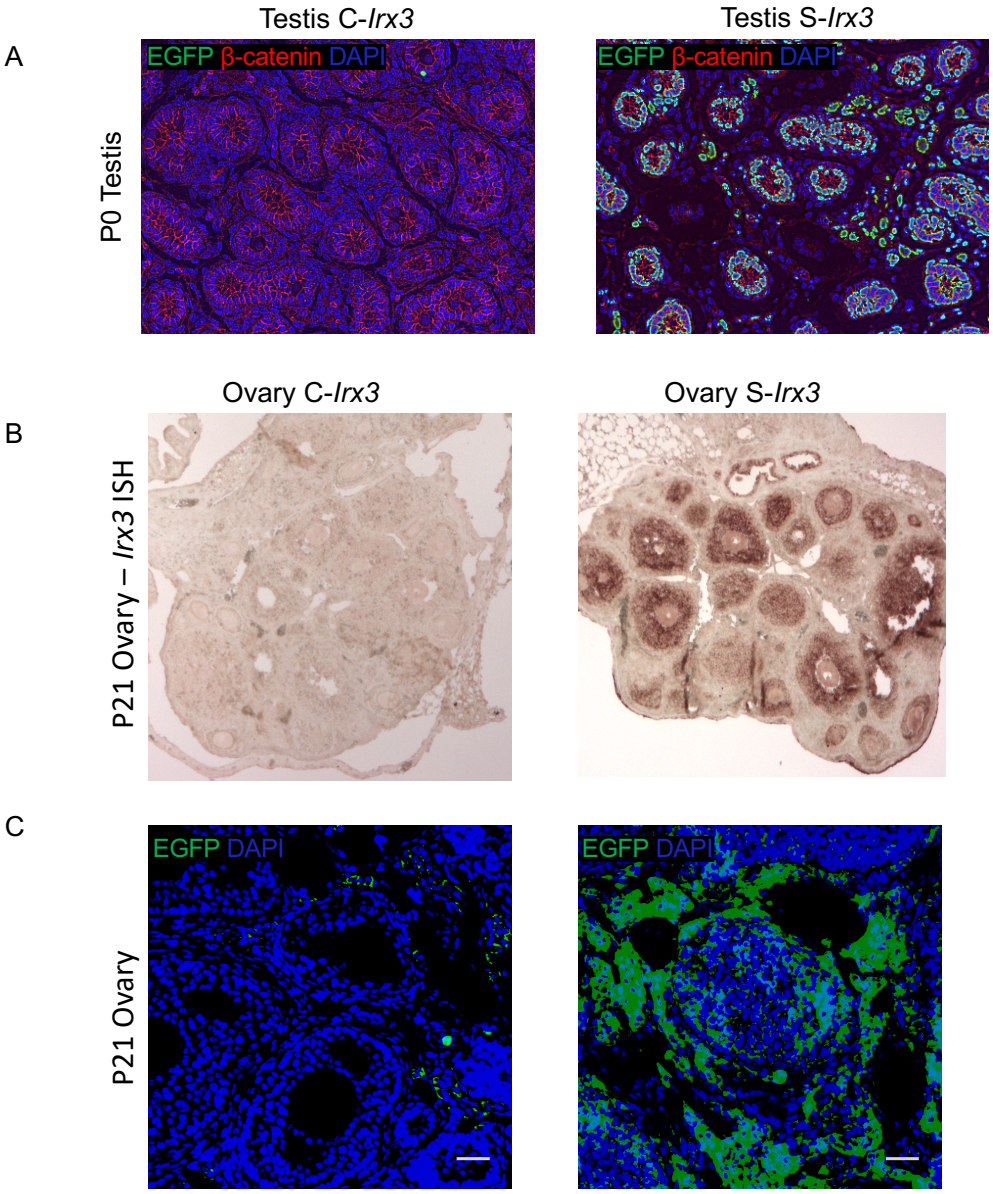
A
Testis C-Irx3
Testis S-Irx3
P0 Testis
EGFP β-catenin DAPI
EGFP β-catenin DAPI
B
Ovary C-Irx3
Ovary S-Irx3
P21 Ovary – Irx3 ISH
C
P21 Ovary
EGFP DAPI
EGFP DAPI

Figure 4-3

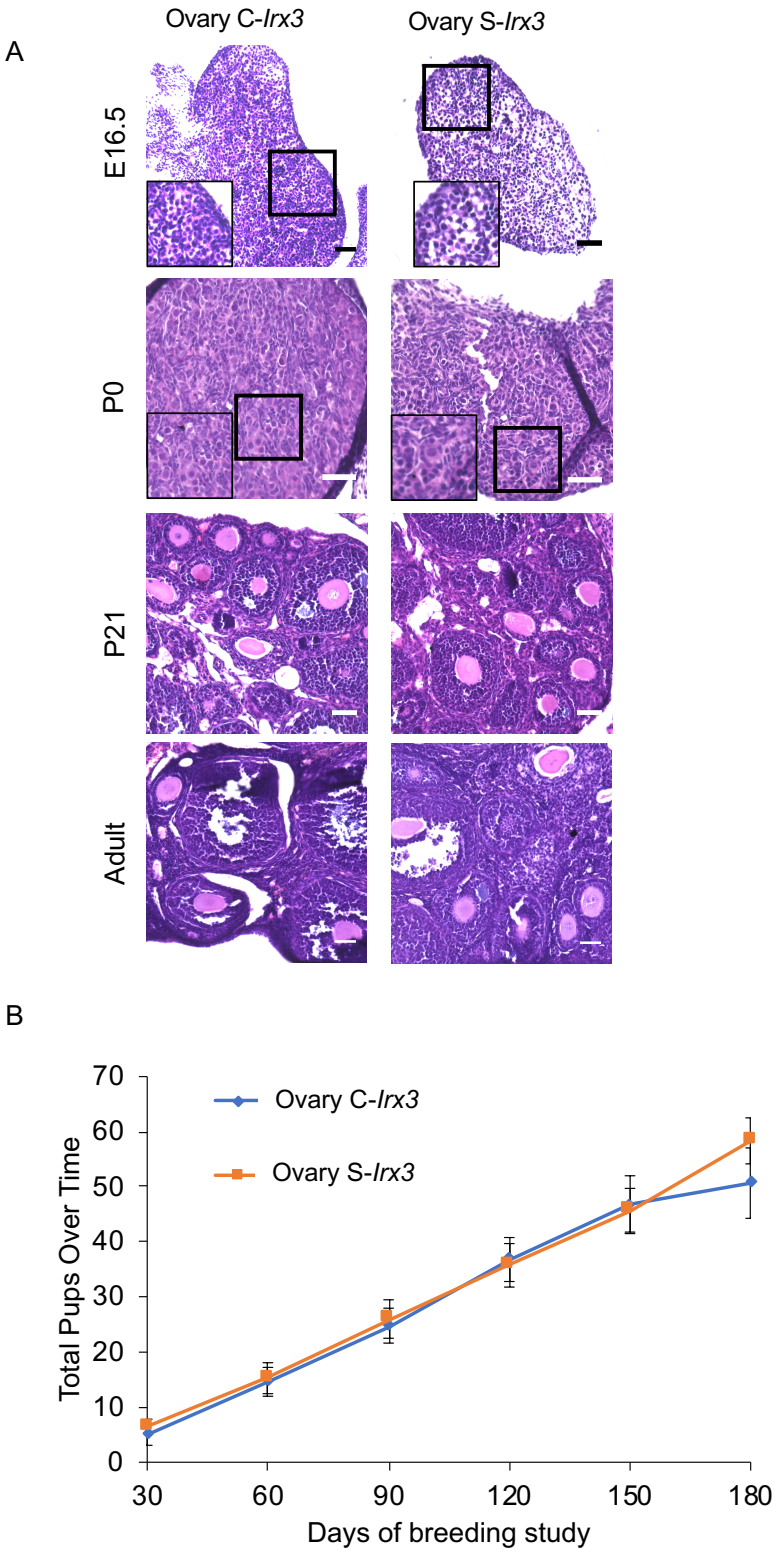
A
Ovary C-Irx3
Ovary S-Irx3
E16.5
P0
P21
Adult
B
Ovary C-Irx3
Ovary S-Irx3
Total Pups Over Time
0
10
20
30
40
50
60
70
30
60
90
120
150
180
Days of breeding study

Figure 4-4

A

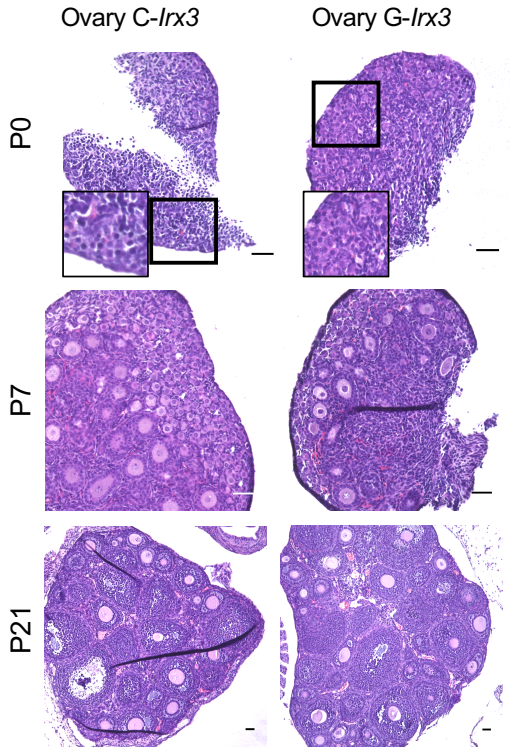
Ovary C-Irx3
Ovary G-Irx3
P0
P7
P21

B

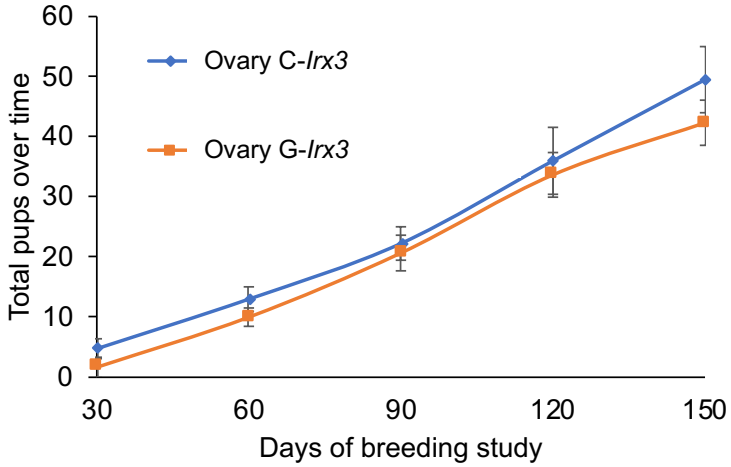
60
50
40
30
20
10
0
Total pups over time
Ovary C-Irx3
Ovary G-Irx3
30
60
90
120
150
Days of breeding study

Figure 4-5

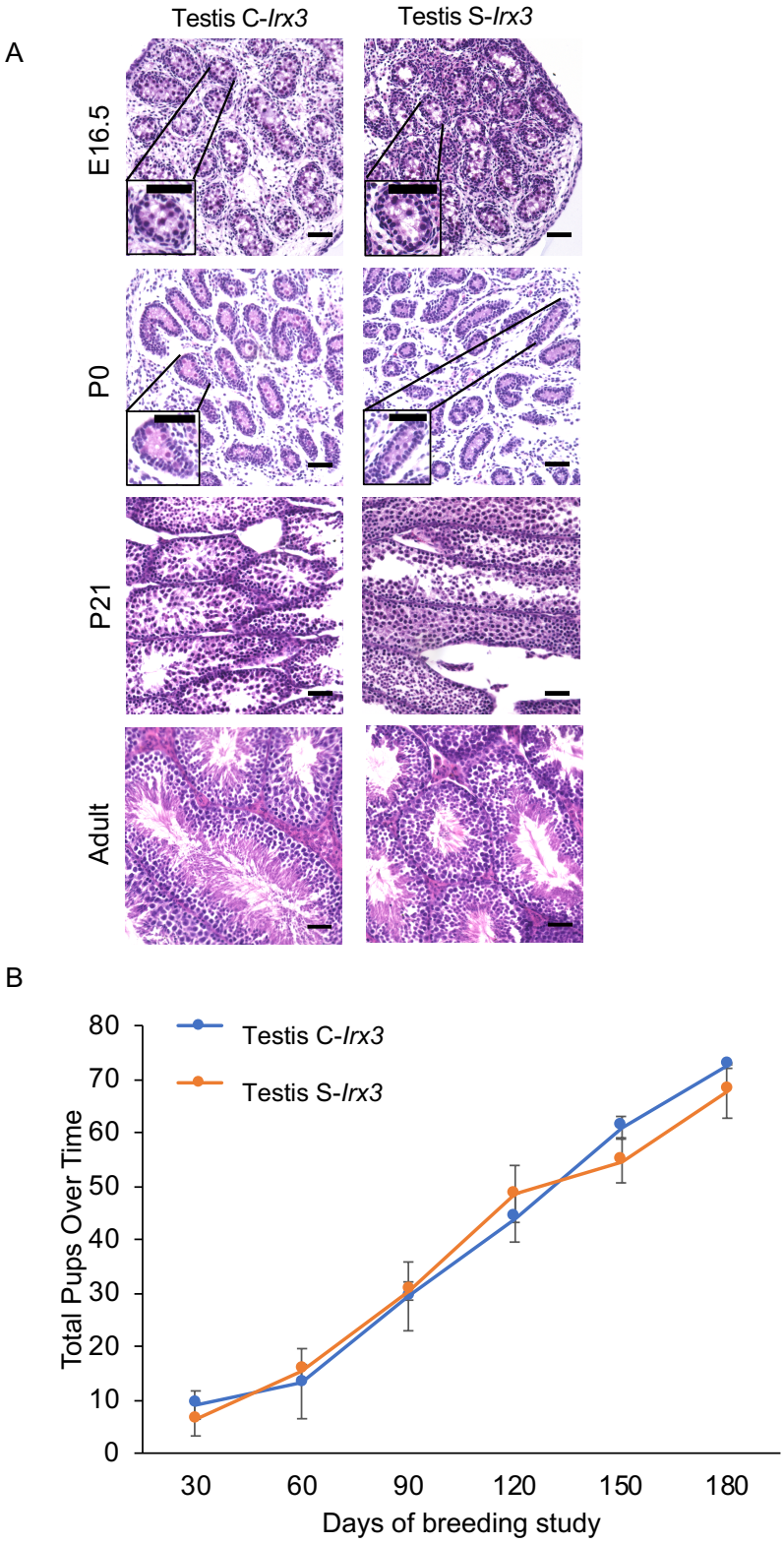
A
Testis C-Irx3
Testis S-Irx3
E16.5
P0
P21
Adult
B
Testis C-Irx3
Testis S-Irx3
Total Pups Over Time
0
10
20
30
40
50
60
70
80
30
60
90
120
150
180
Days of breeding study

Figure 4-6

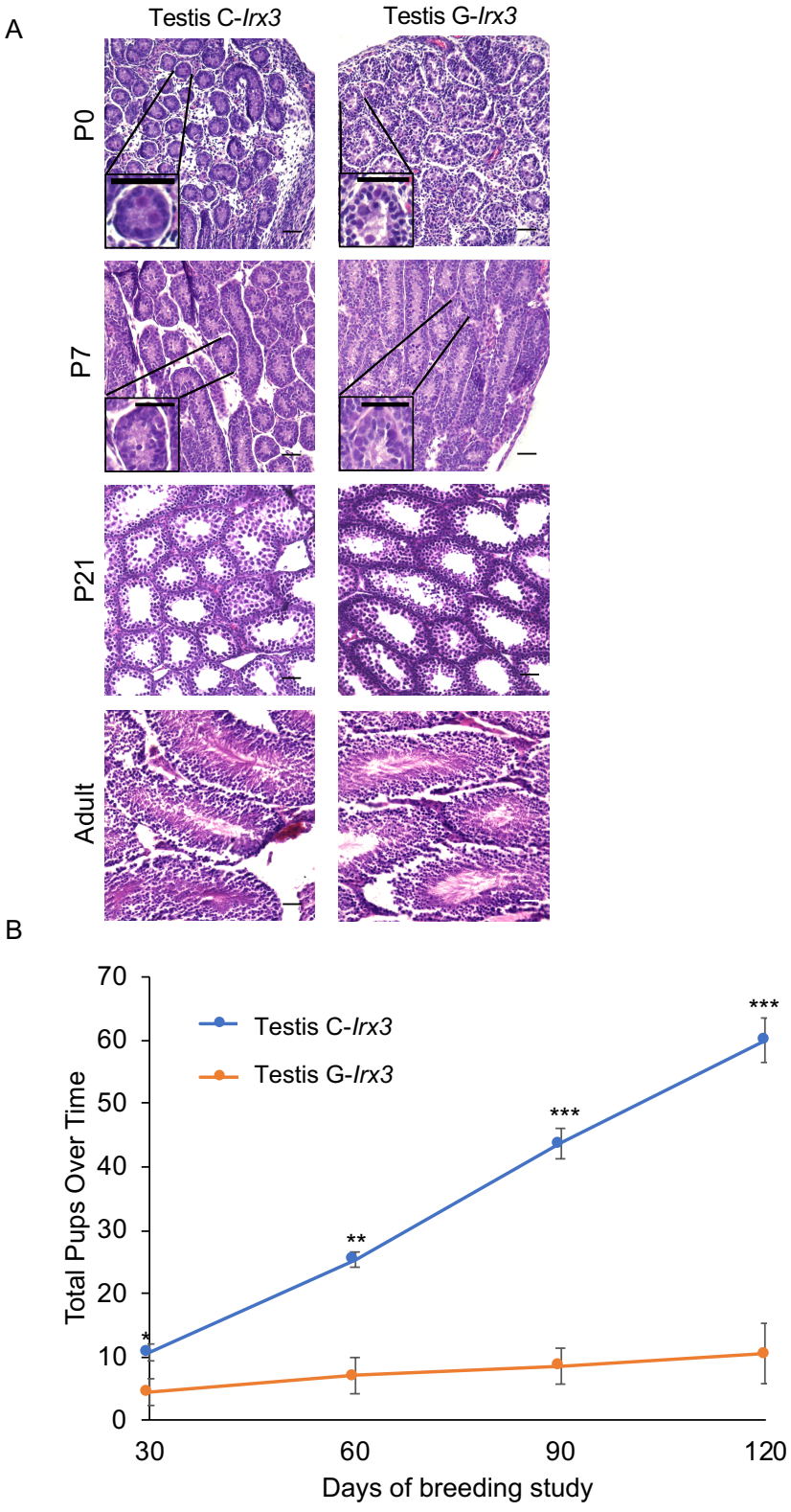
A
Testis C-Irx3
Testis G-Irx3
P0
P7
P21
Adult
B
Testis C-Irx3
Testis G-Irx3
Total Pups Over Time
Days of breeding study
0
10
20
30
40
50
60
70
30
60
90
120
*
**
***
***

Figure 4-7

A

Genotype	Sperm Count (Mil/mL)	Motility	Notes
Testis C-*Irx3* 1	16.6 +/- 0.5	74%	N/A
Testis C-*Irx3* 2	20.4 +/- 1.01	67%	One small agglutination clump
Testis G-*Irx3* 1	20.9 +/- 0.79	76%	Severe agglutination
Testis G-*Irx3* 2	6.9 +/- 1.10	57%	Moderate sperm agglutination
Testis G-*Irx3* 3	33.5 +/- 1.03	85%	Severe agglutination

B

Tetsis C-*Irx3* 2

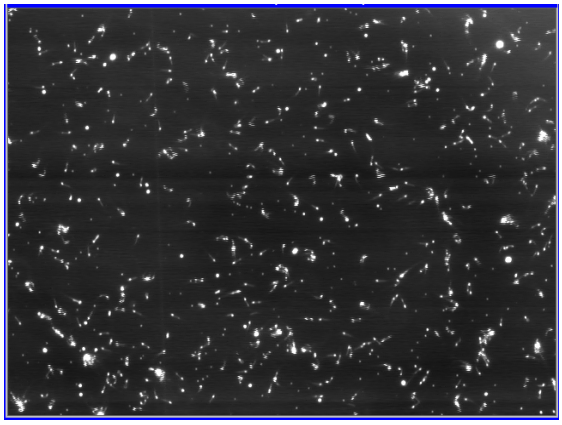

Testis G-*Irx3* 3

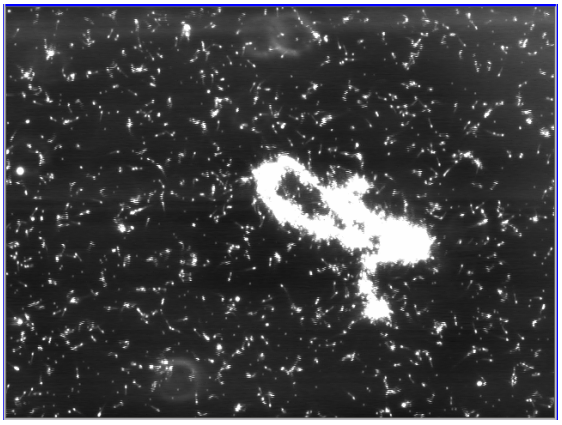

Supplementary Table 4-1

Gene name	Forward Primer	Reverse Primer
36B4	CGACCTGGAAGTCCAACTAC	ATCTGCTGCATCTGCTTG
Rps29	TGAAGGCAAGATGGGTCAC	GCACATGTTCAGCCCGTATT
Foxl2	GCAAGGGAGGCGGGACAACAC	GAACGGGAACTTGGCTATGATGT
Sox9	AGTACCCGCATCTGCACAAC	TACTTGTAATCGGGGTGGTCT
Irx3	CGCCTCAAGAAGGAGAACAAGA	CGCTCGCTCCCATAAGCAT
Irx5	GGCTACAACTCGCACCTCCA	CCAAGGAACCTGCCATACCG

Supplementary Figure 4-2

A

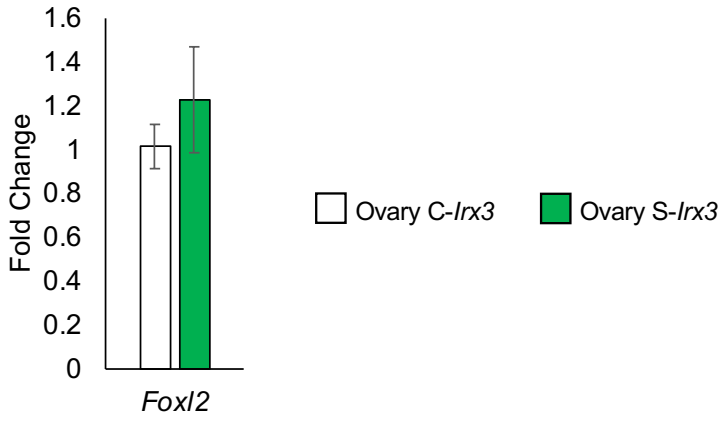

B

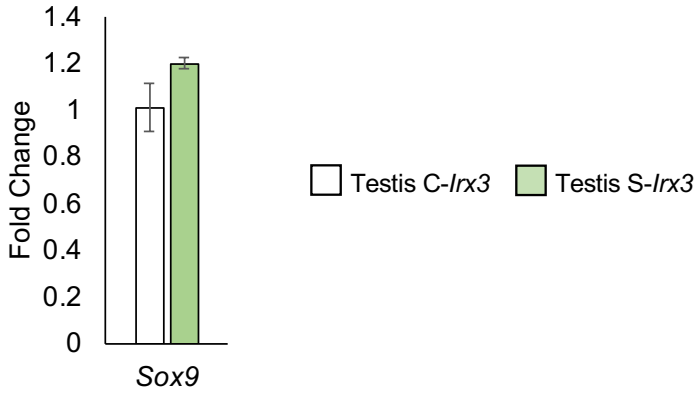

Chapter 5

Concluding Remarks and Future Directions

Summary

The gonad is an extraordinary organ and its development is a fascinating process. Iroquois homeobox transcription factors *Irx3* and *Irx5* play important roles in ovarian health and development in both somatic and germ cells (Fu et al., 2018; Jorgensen & Gao, 2005; Kim, Kim, Cooke, Rüther, & Jorgensen, 2011). The regulation of these factors is largely unexplored, and one of my research objectives was to determine if the canonical Wnt/Rspo1/β-catenin signaling pathway regulated *Irx3* and *Irx5* in either cell type. A further objective was to explore a novel mouse model to determine how the overexpression of *Irx3* affected development of ovaries and testes as well as fertility in mice.

In Chapter 2, I explored the hypothesis that β-catenin was responsible for the transcriptional regulation of *Irx3* and *Irx5* in the somatic cells of the developing ovary. I was able to utilize conditional mouse models to knock out, or stabilize, β-catenin in the somatic cells of the ovary and testis, respectively. I determined that β-catenin expression positively correlates with both *Irx3* and *Irx5* transcripts. Additionally, I applied both DNAseI-seq and ATAC-seq datasets to identify possible regulatory regions of interest that contained β-catenin/TCF/LEF binding elements. Through ChIP-qPCR, transient transfection, and transient gonad transfection, I was able to identify two novel enhancer regions within the *IrxB* locus that responded to β-catenin stimulation and had ovarian-specific loss of activity after mutation of the TCF/LEF consensus motif. Further, we mined an H3K27me3 dataset to find enrichment of this repressive factor in the testis at these same enhancer regions. In our study, inhibition of H3K27me3 in testis cultures significantly upregulated *Irx3* and *Irx5* transcripts supporting this epigenetic repression.

The evidence provided in this chapter led us to conclude that β-catenin is directly regulating *Irx3* and *Irx5* in the somatic cells of the ovary via two enhancers on the *IrxB* locus.

To continue studying the effects of β-catenin in the developing ovary, I shifted to germ cell expression of β-catenin and how its loss could affect *Irx3* expression in Chapter 3. Other groups (Chassot et al., 2011) have attempted to conditionally knock out β-catenin in the oocyte early in development, but have failed to do so due to embryonic lethality and/or inefficient cre mouse models. Others have successfully knocked out β-catenin in the oocyte, but only in the post-natal ovary, long after follicles have formed. These conditional β-catenin knockout mice were fertile. Thus, we used a newly developed germ cell-specific cre, *Figla*Cre, that was reported to be functional during ovarian development. With this cre line, I was able to knock out β-catenin in the oocyte, but cre activity was detected at a much later time than anticipated. Similar to the previous report with *Zp3*Cre, our *Figla*Cre; *Ctnnb1*$^{flox/flox}$ females had no effect on the ovary as a whole, with no defects in meiosis, germ cell number, or follicle development. An important discovery, however, was that the loss of β-catenin in the oocyte had no impact on oocyte expression of *Irx3*. This finding is important because it differentiates Iroquois regulation within neighboring cell types in the ovary.

Irx3 is expressed in the somatic cells of the ovary until primordial follicle formation, but then is solely expressed in the oocyte thereafter. We questioned if *Irx3* overexpression in the somatic cells after primordial follicle formation or *Irx3* overexpression in the germ cells would affect the dynamics of follicle formation or

fertility in females. Furthermore, *Irx3* is never expressed in the testis, and we suspected that its presence could affect testis development and/or fertility. In Chapter 4, with the use of a novel *Irx3* overexpression mouse line, I was able to overexpress *Irx3* in both the somatic (*Sf1*Cre) and the germ (*Figla*Cre-EGFP) cells of both the ovary and testis. *Irx3* overexpression had no effect on ovarian development in either the somatic or the germ cells, displaying normal follicle development and fertility that matched control females in both lines. I also explored *Irx3* overexpression in both the somatic and the germ cells of the developing testis. We found that somatic cell overexpression of *Irx3* had no effect on the testis; however, we were intrigued when *Irx3* overexpression in the sperm had an effect on male fertility. Morphologically, mutant testes look comparable to controls, but mutant male mice did not produce consistent litters and had fewer pups in total compared to control males. We also detected a sperm agglutination phenotype during sperm analysis of these mutant males, which may be a contributing factor to their reduced fertility.

Overall, these data provide insight into the complicated process of gonad development and the role of *Irx3* and *Irx5* therein. This research provides a better understanding of these factors and how they promote overall ovarian health in mice, as well as suggesting multiple directions for future projects. A model is outlined for Chapter 2 (**Figure 5-1**) and a phenotype table is provided for Chapter 4 (**Table 5-1**).

Future Directions

My research offers a better understanding of the regulation our factors of interest, *Irx3* and *Irx5*, in the developing ovary and how the overexpression of *Irx3* affects gonad development, yet additional questions and potential avenues of inquiry remain. These questions could be answered by experiments proposed below, which could lead to additional projects for our lab. Key conclusions for continued experimentation and future research in this area provide valuable information about ovarian development and overall women's health.

Canonical Wnt signaling and *Irx3/5* in the somatic cell

Based on our general conclusion that canonical Wnt signaling regulates *Irx3* and *Irx5* in the somatic cell population of the ovary, I think it would be interesting to treat pregnant dams with a commonly used drug that can inhibit Wnt signaling to see if this would have any effect on ovarian development. NSAIDs (Nonsteroidal anti-inflammatory drugs) have anti-canonical Wnt signaling effects (Castellone, Teramoto, Williams, Druey, & Gutkind, 2005), and their use is therefore generally contraindicated in pregnancy, especially in the first trimester, due to concerns about pregnancy loss and congenital defects (Mayo Clinic). While some women are aware of their pregnancy early in gestation, it is common for others to remain unaware of their pregnancy for multiple weeks, especially if they do not have a regular menstrual cycle. Therefore, many unknowingly pregnant women may be taking regular doses of NSAIDs during a critical window of fetal development. Aspirin, a widely used NSAID, inhibits β-catenin transcriptional activity via inhibition of protein phosphatase A2 (PP2A) (Bos et al., 2006;

Dihlmann, Siermann, & von Knebel Doeberitz, 2001; Ratcliffe, Itoh, & Sokol, 2000). Aspirin has also been shown to reduce β-catenin levels in APC^{min} mice *in vivo* (Mahmoud et al., 1998). Because this drug can inhibit β-catenin transcription, we hypothesize that Aspirin use during ovarian development may have a negative effect on ovarian health and could possibly contribute to fertility issues in female pups exposed to NSAID activity. Data from this study could, for the first time, provide a link between Aspirin usage during pregnancy to defects in the developing ovary that may manifest in reproductive disorders, such as POI, in female offspring.

Because we demonstrated TCF/LEF responsive elements in the ovary (Chapter 2), an additional experiment would explore the effects of TCF/LEF knockouts in ovarian development. TCF7L2 and LEF1 knockout mice are commercially available through Jackson Laboratories; it would be interesting to examine the effects of these knockouts on the ovary as a whole, and also how the knockout would affect *Irx3* and *Irx5* expression. We could also use these mice for either ATAC-seq or ChIP-seq for H3K27ac to see if enhancer regions are affected by these knockouts. We could also perform RNA-seq to identify other target genes of this pathway.

Furthermore, I have also considered performing ChIP-seq for TCF/LEF factors in the wild-type ovary to identify direct target genes other than *Irx3* and *Irx5*. This would be performed both pre- and post-sex determination and binding profiles would be compared, giving insight into the spatio-temporal effects of these transcription factors on female-specific gene regulation.

Finally, we discovered two novel enhancer elements at +86kb and -580kb in the *IrxB* locus; it would be fascinating to knock out one or both of these sequences in a

mouse either using CrisprCas9 technology or with the addition of LoxP sites flanking each region. One limitation to the CrisprCas9 technique is that it would result in a global knockout and could affect regulation in other tissues. The conditional knockout of these regions may be a better choice, as we could study the effect of this conditional knockout specifically in the somatic cells of the ovary and the testis.

Irx3 and *Irx5* expression in the oocyte

Because *Irx3* is not affected when β-catenin is eliminated in the oocyte, this of course leads us to question what is regulating the Iroquois factors in the germ cell. As mentioned in both Chapter 1 and Chapter 3, Iroquois factors have been connected to multiple pathways, such as Wnt and Hedgehog (Briscoe, Pierani, Jessell, & Ericson, 2000; Cavodeassi, Diez Del Corral, Campuzano, & Domínguez, 1999; Kobayashi et al., 2002), JAK/STAT (Zeidler, Perrimon, & Strutt, 1999), FGF (Kobayashi et al., 2002), EGFR (Wang, Simcox, & Campbell, 2000), BMP-4 (Gómez-Skarmeta, de La Calle-Mustienes, & Modolell, 2001), and TGFβ (Cavodeassi, Modolell, & Gómez-Skarmeta, 2001; JL, 1998). Many of these pathways would be good starting points when investigating oocyte regulation, but I found a different gene which has yet to be connected to Iroquois regulation and I hypothesize may be involved in the expression of *Irx3* and *Irx5* in the oocyte.

Nobox is an oocyte-specific homeobox gene that is expressed in oocytes (Suzumori, Yan, Matzuk, & Rajkovic, 2002), at about the same time as *Irx3* and *Irx5* expression is detected (Fu et al., 2018). Transcripts of oocyte genes *Mos*, *Oct4*, *Rfp14, Fgf8, Zar1, Dnmtlo, Gdf9, Bmp15,* and *H100* are downregulated in *Nobox*$^{-/-}$ ovaries

(Rajkovic, Pangas, Ballow, Suzumori, & Matzuk, 2004), suggesting that *Nobox* is important for either the direct or the indirect regulation of these genes crucial for postnatal oocyte development. *Nobox* has been implicated in POI in mice, where a null mutation results in the loss of germ cells by 6 weeks of age (Rajkovic et al., 2004), and 6.2% of human POI cases contain mutations in the *Nobox* gene (Bouilly, Bachelot, Broutin, Touraine, & Binart, 2011; Qin et al., 2007). Furthermore, it was reported that *Nobox* deficient mice have defects in somatic cell invasion and germ cell nest breakdown (Lechowska et al., 2011). This is particularly interesting because preliminary data from our lab shows a potential germ cell nest breakdown defect when *Irx3* is conditionally knocked out in the oocyte. Moreover, a cis-acting NOBOX DNA binding element (TAATTG) (Choi & Rajkovic, 2006) is present 1.3kb from the *Irx3* tss. It would be interesting to examine *Nobox* deficient ovaries to determine if *Irx3* and/or *Irx5* expression are affected in the germ cell, giving us insight into how our factors of interest are regulated in another ovarian cell type.

Could *Irx3* overexpression rescue germ cell loss in the somatic β-catenin conditional knockout model?

The somatic cell conditional knockout of β-catenin in mice results in massive germ cell death around birth (Liu, Bingham, Parker, & Yao, 2009). A leading group in this field demonstrated that canonical WNT4/β-catenin is responsible for germ cell survival via inhibition of Activin βB (*Inhbb*) (Liu, Parker, & Yao, 2010). Results from another graduate student in our lab, Anqi Fu, indicate that *Inhbb* mRNA levels are elevated in *Irx3/Irx5* double knock-out ovaries, suggesting that *Inhbb* may be

downstream from *Irx3* and/or *Irx5* (*manuscript in preparation*). One of our original goals was to induce *Irx3* via the overexpression model used in Chapter 4 in the context of the somatic cell conditional knockout of β-catenin (see Chapter 2) to determine if this resulted in increased germ cell survival. Moreover, we would explore whether *Inhbb* levels decreased in this rescue, further solidifying the conclusion that *Irx3* and *Irx5* lie downstream of β-catenin and upstream of *Inhbb*. Before introducing the *Irx3* overexpression line into the β-catenin cKO, we thought it was necessary to characterize the *Irx3* overexpression alone to isolate any phenotypes seen in this line (Chapter 4). We attempted to initiate this rescue project, but unfortunately, due to a nonspecific genotyping issue in the *Ctnnb1*$^{F/F}$ line, we were unable to complete this study. Because this issue was introduced prior to our receipt of the mice, a new line from Jackson Laboratory would be required in order to complete this experiment.

Overall, multiple avenues have emerged from the conclusions drawn from the studies documented in Chapters 2-4. This will provide our lab with additional exciting experiments to pursue in years to come and expand our knowledge of the complicated processes of gonad development and gene regulation. We look forward to the continued exploration of *Irx3* and *Irx5* in gonad development and how their expression is connected with fertility later in life, which could lead to preventative treatments for POI in humans in the future.

A

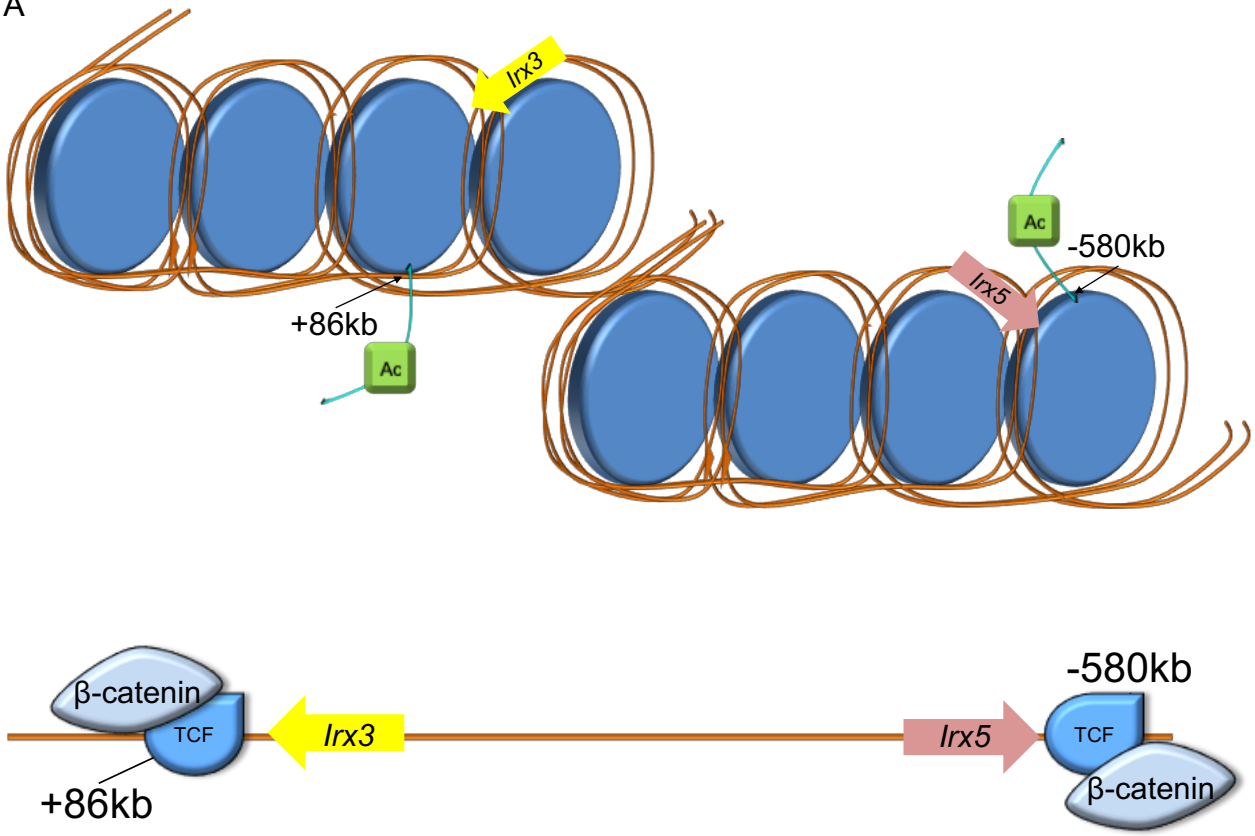
Irx3
+86kb
Ac
Ac
-580kb
Irx5
β-catenin
TCF
+86kb
Irx3
Irx5
-580kb
TCF
β-catenin

B

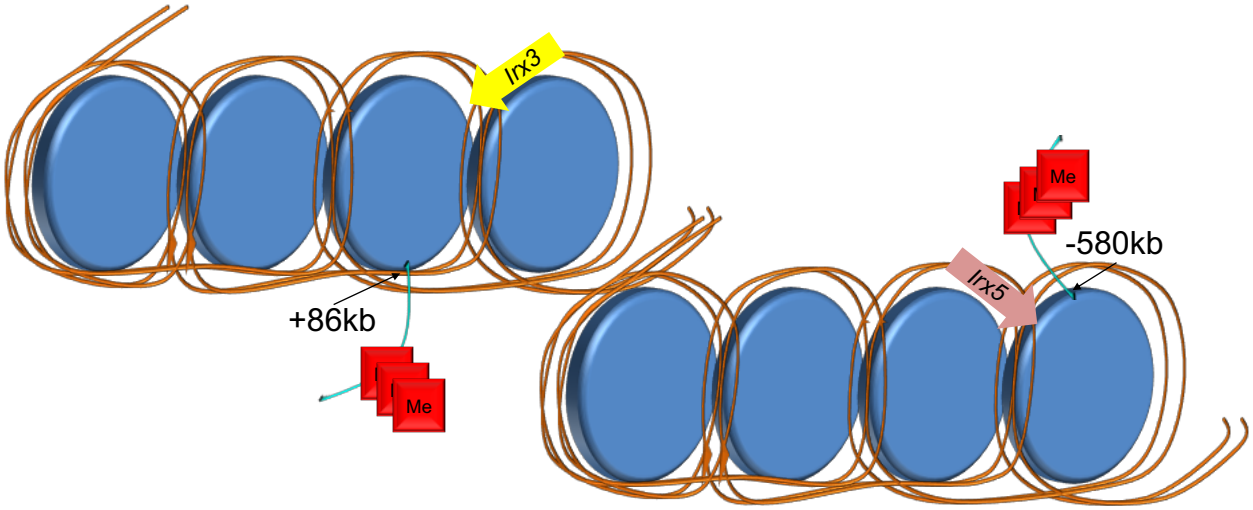
Irx3
+86kb
Me
Me
-580kb
Irx5

Figure 5-1: *Model for Irx3 and Irx5 regulation in the somatic cells of the gonad*

(**A)** Histones (blue) are modified by H3K27ac (green) at +86kb and -580kb sites in the ovary and DNA (orange) is able to open. TCF/LEF and β-catenin factors can bind at these sites, increasing *Irx3* and *Irx5* expression. (**B**) Histones (blue) are modified by H3K27me3 (red) at +86kb and -580kb sites in the testis, leaving histones and DNA tightly compacted, leaving *Irx3* and *Irx5* in a repressed state. This mechanism does not appear to translate to the oocyte population in the ovary.

Sex	Cell type	Histology defect?	Fertility defect?
Female	Somatic	No	No
Female	Germ	No	No
Male	Somatic	No	No
Male	Germ	No	Yes

Table 5-1: *Irx3 Overexpression in the gonad results*

Irx3 overexpression in the gonad did not have any effects in the female (either somatic or germ cell models) or in the somatic cells of the testis. In contrast, *Irx3* overexpression in the germ cells of the male (sperm) resulted in sub-fertility. We are currently investigating the mechanism behind this fertility issue.

References

Bos, C. L., Kodach, L. L., van den Brink, G. R., Diks, S. H., van Santen, M. M., Richel, D. J., Peppelenbosch, M. P., & Hardwick, J. C. (2006). Effect of aspirin on the Wnt/beta-catenin pathway is mediated via protein phosphatase 2A. *Oncogene, 25*(49), 6447-6456. doi:10.1038/sj.onc.1209658

Bouilly, J., Bachelot, A., Broutin, I., Touraine, P., & Binart, N. (2011). Novel NOBOX loss-of-function mutations account for 6.2% of cases in a large primary ovarian insufficiency cohort. *Hum Mutat, 32*(10), 1108-1113. doi:10.1002/humu.21543

Briscoe, J., Pierani, A., Jessell, T. M., & Ericson, J. (2000). A homeodomain protein code specifies progenitor cell identity and neuronal fate in the ventral neural tube. *Cell, 101*(4), 435-445. Retrieved from http://www.ncbi.nlm.nih.gov/pubmed/10830170

Castellone, M. D., Teramoto, H., Williams, B. O., Druey, K. M., & Gutkind, J. S. (2005). Prostaglandin E2 promotes colon cancer cell growth through a Gs-axin-beta-catenin signaling axis. *Science, 310*(5753), 1504-1510. doi:10.1126/science.1116221

Cavodeassi, F., Diez Del Corral, R., Campuzano, S., & Domínguez, M. (1999). Compartments and organising boundaries in the Drosophila eye: the role of the homeodomain Iroquois proteins. *Development, 126*(22), 4933-4942. Retrieved from https://www.ncbi.nlm.nih.gov/pubmed/10529412

Cavodeassi, F., Modolell, J., & Gómez-Skarmeta, J. L. (2001). The Iroquois family of genes: from body building to neural patterning. *Development, 128*(15), 2847-2855. Retrieved from https://www.ncbi.nlm.nih.gov/pubmed/11532909

Chassot, A.-A., Gregoire, E. P., Lavery, R., Taketo, M. M., de Rooij, D. G., Adams, I. R., & Chaboissier, M.-C. (2011). RSPO1/β-catenin signaling pathway regulates oogonia differentiation and entry into meiosis in the mouse fetal ovary. *PloS one, 6*(10), e25641-e25641. doi:10.1371/journal.pone.0025641

Choi, Y., & Rajkovic, A. (2006). Characterization of NOBOX DNA binding specificity and its regulation of Gdf9 and Pou5f1 promoters. *J Biol Chem, 281*(47), 35747-35756. doi:10.1074/jbc.M604008200

Dihlmann, S., Siermann, A., & von Knebel Doeberitz, M. (2001). The nonsteroidal anti-inflammatory drugs aspirin and indomethacin attenuate beta-catenin/TCF-4 signaling. *Oncogene, 20*(5), 645-653. doi:10.1038/sj.onc.1204123

Fu, A., Oberholtzer, S. M., Bagheri-Fam, S., Rastetter, R. H., Holdreith, C., Caceres, V. L., John, S. V., Shaw, S. A., Krentz, K. J., Zhang, X., Hui, C. C., Wilhelm, D., & Jorgensen, J. S. (2018). Dynamic expression patterns of Irx3 and Irx5 during germline nest breakdown and primordial follicle formation promote follicle survival in mouse ovaries. *PLoS Genet, 14*(8), e1007488. doi:10.1371/journal.pgen.1007488

Gómez-Skarmeta, J., de La Calle-Mustienes, E., & Modolell, J. (2001). The Wnt-activated Xiro1 gene encodes a repressor that is essential for neural development and downregulates Bmp4. *Development, 128*(4), 551-560. Retrieved from https://www.ncbi.nlm.nih.gov/pubmed/11171338

JL, G.-S. (1998). Xiro, a Xenopus homolog of the Drosophila Iroquois complex genes, controls development at the neural plate. In G. A (Ed.), (Vol. 17, pp. 181-190). EMBO J.

Jorgensen, J. S., & Gao, L. (2005). Irx3 is differentially up-regulated in female gonads during sex determination. *Gene expression patterns : GEP, 5*(6), 756-762. doi:10.1016/j.modgep.2005.04.011

Kim, B., Kim, Y., Cooke, P. S., Rüther, U., & Jorgensen, J. S. (2011). The fused toes locus is essential for somatic-germ cell interactions that foster germ cell maturation in developing gonads in mice. *Biology of reproduction, 84*(5), 1024-1032. doi:10.1095/biolreprod.110.088559

Kobayashi, D., Kobayashi, M., Matsumoto, K., Ogura, T., Nakafuku, M., & Shimamura, K. (2002). Early subdivisions in the neural plate define distinct competence for inductive signals. *Development, 129*(1), 83-93. Retrieved from https://www.ncbi.nlm.nih.gov/pubmed/11782403

Lechowska, A., Bilinski, S., Choi, Y., Shin, Y., Kloc, M., & Rajkovic, A. (2011). Premature ovarian failure in nobox-deficient mice is caused by defects in somatic cell invasion and germ cell cyst breakdown. *J Assist Reprod Genet, 28*(7), 583-589. doi:10.1007/s10815-011-9553-5

Liu, C.-F., Bingham, N., Parker, K., & Yao, H. H. C. (2009). Sex-specific roles of beta-catenin in mouse gonadal development. *Hum Mol Genet, 18*(3), 405-417. doi:10.1093/hmg/ddn362

Liu, C.-F., Parker, K., & Yao, H. H. C. (2010). WNT4/beta-catenin pathway maintains female germ cell survival by inhibiting activin betaB in the mouse fetal ovary. *PloS one, 5*(4), e10382-e10382. doi:10.1371/journal.pone.0010382

Mahmoud, N. N., Dannenberg, A. J., Mestre, J., Bilinski, R. T., Churchill, M. R., Martucci, C., Newmark, H., & Bertagnolli, M. M. (1998). Aspirin prevents tumors in a murine model of familial adenomatous polyposis. *Surgery, 124*(2), 225-231. Retrieved from https://www.ncbi.nlm.nih.gov/pubmed/9706142

Qin, Y., Choi, Y., Zhao, H., Simpson, J. L., Chen, Z. J., & Rajkovic, A. (2007). NOBOX homeobox mutation causes premature ovarian failure. *Am J Hum Genet, 81*(3), 576-581. doi:10.1086/519496

Rajkovic, A., Pangas, S. A., Ballow, D., Suzumori, N., & Matzuk, M. M. (2004). NOBOX deficiency disrupts early folliculogenesis and oocyte-specific gene expression. *Science, 305*(5687), 1157-1159. doi:10.1126/science.1099755

Ratcliffe, M. J., Itoh, K., & Sokol, S. Y. (2000). A positive role for the PP2A catalytic subunit in Wnt signal transduction. *J Biol Chem, 275*(46), 35680-35683. doi:10.1074/jbc.C000639200

Suzumori, N., Yan, C., Matzuk, M. M., & Rajkovic, A. (2002). Nobox is a homeobox-encoding gene preferentially expressed in primordial and growing oocytes. *Mech Dev, 111*(1-2), 137-141. Retrieved from https://www.ncbi.nlm.nih.gov/pubmed/11804785

Wang, S. H., Simcox, A., & Campbell, G. (2000). Dual role for Drosophila epidermal growth factor receptor signaling in early wing disc development. *Genes Dev, 14*(18), 2271-2276. Retrieved from https://www.ncbi.nlm.nih.gov/pubmed/10995384

Zeidler, M. P., Perrimon, N., & Strutt, D. I. (1999). Polarity determination in the Drosophila eye: a novel role for unpaired and JAK/STAT signaling. *Genes Dev, 13*(10), 1342-1353. doi:10.1101/gad.13.10.1342

Appendix 1

Jorgensen, J. S., Fu, A., & **Hornung, M**. (2018). Female Sex Determination: Molecular. In M. K. Skinner (Ed.), Encyclopedia of Reproduction. vol. 2, pp. 57–64. Academic Press: Elsevier. http://dx.doi.org/10.1016/B978-0-12-801238-3.64393-3

ISBN: 9780128118993

Appendix 2: *Transcription factor binding motifs in addition to TCF/LEF*

-205kb, +86kb, -305kb (A,B), and -580kb sequences were analyzed through the JASPAR database for additional transcription factor binding motifs. Matrices are displayed as highest score to lowest score.

Site +205kb							
Name	**Score**	**Relative score**	**Sequence ID**	**Start**	**End**	**Strand**	**Predicted sequence**
TCF7L1	17.6766	0.95057	seq205	373	384	+	AAAGTTCAAAGG
TCF7L2	17.3015	0.98155	seq205	373	386	+	AAAGTTCAAAGGCA
Tcf7	16.7531	0.93777	seq205	373	384	+	AAAGTTCAAAGG
LEF1	16.5665	0.91007	seq205	373	387	+	AAAGTTCAAAGGCAT
Foxk1	16.0085	0.91036	seq205	448	464	+	GTGATGTAAACAAATGG
FOXP2	15.9346	0.99502	seq205	451	461	+	ATGTAAACAAA
ZNF384	15.5692	0.98008	seq205	142	153	+	GAAAAAAAAAAA
ZNF384	15.4851	0.97879	seq205	141	152	+	AGAAAAAAAAAA
RUNX3	15.2766	0.989	seq205	151	160	+	AAACCACAAA
POU4F1	14.8565	0.90399	seq205	495	508	-	CTGCATATTTTATT
FOXK2	14.5705	0.99405	seq205	451	461	+	ATGTAAACAAA
FOXP1	14.5628	0.97072	seq205	451	462	+	ATGTAAACAAAT
ZNF384	14.5506	0.96449	seq205	140	151	+	GAGAAAAAAAAA
FOXO3	14.5271	1	seq205	453	460	+	GTAAACAA
FOXK1	14.0755	0.94026	seq205	450	463	+	GATGTAAACAAATG
ZNF384	14.0659	0.95707	seq205	143	154	+	AAAAAAAAAAAC
FOXG1	14.0369	1	seq205	453	460	+	GTAAACAA
Atoh1	14.0329	1	seq205	608	615	-	CAGATGGC
FLI1	13.7805	0.96195	seq205	413	422	+	ACCGGAAGCC
RUNX2	13.6374	0.97624	seq205	151	159	+	AAACCACAA
MAFK	13.59	0.92642	seq205	482	496	-	TTAAATCAGCACAAA
Foxj2	13.5645	1	seq205	453	460	+	GTAAACAA

RUNX1	13.5396	0.96208	seq205	151	161	-	ATTTGTGGTTT
ELK4	13.5214	0.97229	seq205	413	421	+	ACCGGAAGC
ERG	13.4558	0.96491	seq205	413	422	+	ACCGGAAGCC
PRDM1	13.3825	0.94979	seq205	180	189	-	TCACTTTCTA
RUNX1	13.2845	0.97352	seq205	151	161	-	ATTTGTGGTTT
ZNF384	13.2793	0.94503	seq205	139	150	+	GGAGAAAAAAAA
FOXO6	13.2574	1	seq205	453	459	+	GTAAACA
Mafb	13.2287	0.93643	seq205	55	66	-	CAAGTGCTGACT
FOXI1	13.2222	1	seq205	453	459	+	GTAAACA
ELK1	13.1541	0.9411	seq205	413	422	+	ACCGGAAGCC
SOX10	13.0791	0.97433	seq205	289	299	+	TGAACAAAGCA
FOXI1	13.0627	0.95114	seq205	92	103	-	TTGTATTTATTT
ETS1	12.9202	0.95151	seq205	413	422	+	ACCGGAAGCC
FEV	12.9067	0.95472	seq205	413	422	+	ACCGGAAGCC
Foxo1	12.7769	0.93675	seq205	452	462	-	ATTTGTTTACA
FOXO4	12.7136	1	seq205	453	459	+	GTAAACA
Rxra	12.7042	0.94732	seq205	569	579	+	CAAAGGGCAAA
ETV1	12.6743	0.95134	seq205	413	422	+	ACCGGAAGCC
NEUROD1	12.5692	0.92608	seq205	606	618	-	ACGCAGATGGCTC
FOXA1	12.5674	0.93478	seq205	571	581	-	TGTTTGCCCTT
FOXA1	12.5447	0.93411	seq205	571	581	-	TGTTTGCCCTT
ELK3	12.5401	0.93625	seq205	413	422	+	ACCGGAAGCC
ERF	12.4825	0.92507	seq205	413	422	+	ACCGGAAGCC
FOXD1	12.3413	0.99436	seq205	453	460	+	GTAAACAA
ETV5	12.2851	0.96925	seq205	413	422	+	ACCGGAAGCC
HNF4G	12.2764	0.90746	seq205	563	577	+	TGGAATCAAAGGGCA
FOXL1	12.2661	1	seq205	453	459	+	GTAAACA
FOXC2	12.2155	0.92408	seq205	450	461	+	GATGTAAACAAA
ETV4	12.1579	0.94305	seq205	413	422	+	ACCGGAAGCC
FOXO3	12.142	1	seq205	452	459	+	TGTAAACA

ETV3	12.1301	0.92247	seq205	413	422	+	ACCGGAAGCC
MYB	12.0887	0.9854	seq205	810	819	-	CTCAACTGCT
GABPA	11.8719	0.93745	seq205	413	422	+	ACCGGAAGCC
ZEB1	11.8641	0.94683	seq205	317	325	+	ATTCACCTG
FOXI1	11.777	0.9201	seq205	773	784	+	GCCTGTTTGGTT
HOXB13	11.7372	0.92487	seq205	555	564	-	CAAATAAAAC
ELK4	11.7353	0.9232	seq205	413	423	-	AGGCTTCCGGT
FOXD2	11.6458	1	seq205	453	459	+	GTAAACA
MAFK	11.6346	0.90353	seq205	52	66	+	TCTAGTCAGCACTTG
NRL	11.6339	0.95181	seq205	56	66	-	CAAGTGCTGAC
RBPJ	11.5987	0.96596	seq205	86	95	+	ACTGGGAAAT
PHOX2A	11.5361	0.90367	seq205	829	839	+	TAAACTGATTA
E2F1	11.5181	0.94131	seq205	676	686	+	AGAGCGGCAAG
VENTX	11.5029	0.95714	seq205	832	840	+	ACTGATTAG
ELF1	11.4812	0.90327	seq205	410	422	+	GATACCGGAAGCC
TWIST1	11.441	0.91205	seq205	352	364	+	CTAACAGATGTAG
Arid3b	11.4295	0.92231	seq205	870	880	-	AAATTAATGAA
FOXP3	11.3004	1	seq205	453	459	+	GTAAACA
Phox2b	11.2993	0.90658	seq205	829	839	+	TAAACTGATTA
ZNF384	11.2793	0.91442	seq205	144	155	+	AAAAAAAAAACC
FIGLA	11.2411	0.94007	seq205	318	327	+	TTCACCTGGT
TEF	11.1731	0.91453	seq205	880	891	-	CATTACGGAATA
Dlx2	11.1434	0.99988	seq205	220	227	-	GCAATTAT
Msx3	11.0881	0.97764	seq205	236	243	-	GCAATTAC
MSX2	11.0241	0.96335	seq205	236	243	-	GCAATTAC
MYB	11.0113	0.96246	seq205	802	811	-	CTCAACTGGC
Dlx2	10.9709	0.99575	seq205	236	243	-	GCAATTAC
NRL	10.9506	0.93711	seq205	482	492	+	TTTGTGCTGAT
Rxra	10.8827	0.92108	seq205	129	139	+	AAGAGTTCAGG
HOXD13	10.8208	0.91674	seq205	493	502	+	TTAATAAAAT

LHX6	10.7952	0.93342	seq205	832	841	-	CCTAATCAGT
VDR	10.7919	0.97121	seq205	130	137	+	AGAGTTCA
MSX1	10.779	0.97643	seq205	236	243	-	GCAATTAC
Msx3	10.7404	0.96986	seq205	220	227	-	GCAATTAT
Dlx4	10.7241	0.99744	seq205	236	243	-	GCAATTAC
HOXD13	10.6858	0.91425	seq205	555	564	-	CAAATAAAAC
HESX1	10.6632	0.94648	seq205	219	228	+	GATAATTGCA
Gata1	10.6323	0.92797	seq205	468	478	-	GGAGATAATGA
DLX6	10.6254	0.98868	seq205	236	243	-	GCAATTAC
HOXA10	10.618	0.91632	seq205	492	502	+	TTTAATAAAAT
RUNX1	10.6035	0.90408	seq205	122	132	-	TCTTGTGGTAT
LIN54	10.6033	0.94785	seq205	386	394	+	ATTTGAAAT
FOXA1	10.602	0.90973	seq205	571	585	-	AGCCTGTTTGCCCTT
Dlx2	10.5678	0.98609	seq205	587	594	+	ACAATTAT
Lhx8	10.5118	0.97579	seq205	833	840	-	CTAATCAG
Arid3b	10.4768	0.90217	seq205	490	500	+	GATTTAATAAA
LIN54	10.4708	0.94522	seq205	847	855	-	ATTTGAACG
ELK1	10.4621	0.95992	seq205	411	420	+	ATACCGGAAG
MSX2	10.4273	0.94961	seq205	220	227	-	GCAATTAT
Dlx4	10.4225	0.98921	seq205	220	227	-	GCAATTAT
RUNX1	10.4091	0.90105	seq205	122	132	-	TCTTGTGGTAT
NKX6-1	10.3889	0.96261	seq205	870	877	+	TTCATTAA
LHX6	10.381	0.92633	seq205	832	841	+	ACTGATTAGG
SRY	10.374	0.95688	seq205	453	461	+	GTAAACAAA
TFAP2A	10.3576	0.91762	seq205	654	664	-	CCCCTGAAGCA
BARX1	10.3515	0.9825	seq205	236	243	-	GCAATTAC
Dlx3	10.3311	0.99485	seq205	236	243	-	GCAATTAC
FOXC1	10.3137	0.90831	seq205	450	460	+	GATGTAAACAA
GATA2	10.2697	0.91406	seq205	468	478	+	TCATTATCTCC
Bhlha15	10.2578	0.9376	seq205	609	616	+	CCATCTGC

Stat5a::Stat5b	10.2436	0.91896	seq205	85	95	-	ATTTCCCAGTG
DLX6	10.2333	0.97851	seq205	220	227	-	GCAATTAT
EN1	10.2322	0.96392	seq205	236	243	-	GCAATTAC
Lhx8	10.1963	0.96983	seq205	833	840	+	CTGATTAG
RUNX2	10.1765	0.91245	seq205	122	130	+	ATACCACAA
MEIS3	10.1662	0.95418	seq205	23	30	-	TTGACAAG
Rxra	10.1451	0.91046	seq205	372	382	+	GAAAGTTCAAA
VDR	10.1321	0.9524	seq205	373	380	+	AAAGTTCA
FOXL1	10.1199	0.9607	seq205	94	100	+	ATAAATA
NFAT5	10.1141	0.91621	seq205	866	875	+	CTTTTTCATT
Dlx3	10.0975	0.98768	seq205	220	227	-	GCAATTAT
DLX6	10.0611	0.97405	seq205	587	594	+	ACAATTAT
CDX1	10.0107	0.93148	seq205	493	501	+	TTAATAAAA
SOX10	10.0019	0.90831	seq205	328	338	-	AGCACAAAGTT
BARX1	9.98862	0.97446	seq205	220	227	-	GCAATTAT
ZEB1	9.98315	0.9213	seq205	318	328	+	TTCACCTGGTA
MSX1	9.97466	0.95651	seq205	220	227	-	GCAATTAT
BSX	9.95934	0.97806	seq205	236	243	-	GCAATTAC
TEAD3	9.95817	0.94656	seq205	546	553	-	TCATTCCA
TEAD3	9.95817	0.94656	seq205	752	759	-	TCATTCCA
Dlx4	9.94644	0.97623	seq205	587	594	+	ACAATTAT
GBX2	9.94215	0.93809	seq205	219	228	-	TGCAATTATC
Msx3	9.89719	0.95101	seq205	587	594	+	ACAATTAT
Arid3a	9.84424	1	seq205	306	311	+	ATTAAA
Arid3a	9.84424	1	seq205	492	497	-	ATTAAA
SNAI2	9.83801	0.94275	seq205	60	68	-	AGCAAGTGC
Atoh1	9.83265	0.9081	seq205	354	363	+	AACAGATGTA
Dlx3	9.80803	0.9788	seq205	587	594	+	ACAATTAT
MEOX2	9.80363	0.9364	seq205	466	475	+	TGTCATTATC
ALX3	9.77368	0.93117	seq205	235	244	-	TGCAATTACA

LMX1A	9.75724	0.92798	seq205	493	500	+	TTAATAAA
MSX2	9.75103	0.93405	seq205	587	594	+	ACAATTAT
BARX1	9.73487	0.96884	seq205	587	594	+	ACAATTAT
Klf4	9.70737	0.94181	seq205	901	910	-	TAGAAGAAGG
Bhlha15	9.69839	0.92713	seq205	355	362	+	ACAGATGT
Bhlha15	9.69839	0.92713	seq205	355	362	-	ACATCTGT
GATA3	9.68518	0.94391	seq205	469	476	-	AGATAATG
Myb	9.68147	0.90725	seq205	240	249	-	CAAACTGCAA
EVX1	9.67635	0.94278	seq205	832	841	+	ACTGATTAGG
NKX6-2	9.65118	0.96631	seq205	870	877	+	TTCATTAA
PDX1	9.63165	0.95717	seq205	236	243	-	GCAATTAC
MNX1	9.6076	0.92933	seq205	492	501	+	TTTAATAAAA
Ahr::Arnt	9.60282	1	seq205	614	619	+	TGCGTG
LIN54	9.58178	0.92759	seq205	848	856	+	GTTCAAATA
MEIS1	9.55709	0.98314	seq205	24	30	-	TTGACAA
OTX2	9.55684	0.94293	seq205	105	112	-	ATAATCTT
TFAP2C(var.2)	9.55662	0.90114	seq205	654	664	-	CCCCTGAAGCA
EVX2	9.55625	0.94072	seq205	832	841	+	ACTGATTAGG
MEIS3	9.53184	0.94013	seq205	186	193	+	GTGACATG
GBX2	9.53041	0.93008	seq205	586	595	+	GACAATTATG
MEOX1	9.51936	0.92174	seq205	466	475	+	TGTCATTATC
Myb	9.50331	0.93952	seq205	810	817	+	AGCAGTTG
LIN54	9.48879	0.92575	seq205	375	383	-	CTTTGAACT
ISX	9.4808	0.94404	seq205	236	243	-	GCAATTAC
STAT3	9.47827	0.91238	seq205	365	375	-	TTTCTGAAAAG
LMX1B	9.46497	0.95236	seq205	493	500	+	TTAATAAA
HESX1	9.4361	0.92291	seq205	586	595	-	CATAATTGTC
RAX	9.42665	0.92102	seq205	873	882	-	ATAAATTAAT
Shox2	9.41377	0.94746	seq205	236	243	-	GCAATTAC
LIN54	9.40722	0.92413	seq205	385	393	-	TTTCAAATG

Hoxd9	9.40264	0.9026	seq205	234	243	-	GCAATTACAA
NOTO	9.40182	0.93399	seq205	873	882	-	ATAAATTAAT
MEIS2	9.39885	0.90971	seq205	23	30	-	TTGACAAG
FOXD2	9.39873	0.95234	seq205	575	581	+	GCAAACA
ISX	9.36775	0.9416	seq205	220	227	-	GCAATTAT
FOXP3	9.35863	0.95115	seq205	575	581	+	GCAAACA
GBX2	9.35367	0.92663	seq205	235	244	-	TGCAATTACA
ALX3	9.35307	0.92001	seq205	219	228	-	TGCAATTATC
EN1	9.34502	0.94464	seq205	833	840	-	CTAATCAG
ISL2	9.29815	0.9294	seq205	220	227	-	GCAATTAT
MEIS1	9.29801	0.97765	seq205	465	471	-	ATGACAT
MEIS3	9.29297	0.93484	seq205	464	471	-	ATGACATC
Lhx4	9.26681	0.93749	seq205	870	877	+	TTCATTAA
ZEB1	9.26193	1	seq205	320	325	+	CACCTG
Dlx1	9.23811	0.93773	seq205	586	595	+	GACAATTATG
MSX1	9.22115	0.93784	seq205	587	594	+	ACAATTAT
Sox17	9.20908	0.92082	seq205	586	594	-	ATAATTGTC
NKX6-1	9.20497	0.93688	seq205	467	474	+	GTCATTAT
Dux	9.20471	0.92077	seq205	833	840	-	CTAATCAG
LBX1	9.20056	0.91946	seq205	207	214	+	TTAACAAG
Nobox	9.19413	0.92847	seq205	586	593	-	TAATTGTC
FOXD2	9.19033	0.94792	seq205	94	100	+	ATAAATA
ISX	9.17917	0.93754	seq205	587	594	+	ACAATTAT
HOXA5	9.1776	0.9761	seq205	872	879	+	CATTAATT
MIXL1	9.15288	0.94342	seq205	235	244	-	TGCAATTACA
MEIS1	9.15158	0.97455	seq205	584	590	+	CTGACAA
MEIS2	9.13644	0.90376	seq205	583	590	-	TTGTCAGC
PDX1	9.12896	0.94712	seq205	220	227	-	GCAATTAT
Prrx2	9.12437	1	seq205	221	225	-	AATTA
Prrx2	9.12437	1	seq205	237	241	-	AATTA

Prrx2	9.12437	1	seq205	315	319	-	AATTA
Prrx2	9.12437	1	seq205	589	593	+	AATTA
Prrx2	9.12437	1	seq205	875	879	-	AATTA
GBX1	9.1215	0.9138	seq205	219	228	-	TGCAATTATC
BSX	9.11224	0.9594	seq205	833	840	+	CTGATTAG
PRRX1	9.09576	0.93712	seq205	236	243	-	GCAATTAC
Prrx2	9.09319	0.95022	seq205	236	243	-	GCAATTAC
EN1	9.09046	0.93911	seq205	220	227	-	GCAATTAT
NOTO	9.08124	0.92832	seq205	869	878	+	TTTCATTAAT
BSX	9.07896	0.95866	seq205	220	227	-	GCAATTAT
SOX15	9.07642	0.9019	seq205	289	298	-	GCTTTGTTCA
LMX1A	9.06403	0.90909	seq205	874	881	-	TAAATTAA
GATA5	9.06236	0.94325	seq205	469	476	-	AGATAATG
SOX15	9.05578	0.90144	seq205	454	463	-	CATTTGTTTA
MNX1	9.04806	0.91651	seq205	219	228	-	TGCAATTATC
PDX1	9.0316	0.94517	seq205	870	877	+	TTCATTAA
Barhl1	9.03034	0.94347	seq205	219	228	+	GATAATTGCA
Arid3a	9.01498	0.96765	seq205	567	572	+	ATCAAA
Shox2	9.01181	0.93844	seq205	220	227	-	GCAATTAT
Dlx1	9.01168	0.932	seq205	219	228	-	TGCAATTATC
ISL2	9.01012	0.92191	seq205	236	243	-	GCAATTAC
MNX1	9.00115	0.91543	seq205	235	244	-	TGCAATTACA
RAX	8.99926	0.91159	seq205	219	228	-	TGCAATTATC
Nkx2-5	8.99637	0.98708	seq205	220	226	+	ATAATTG
Nkx2-5	8.99637	0.98708	seq205	588	594	-	ATAATTG
MNX1	8.98821	0.91513	seq205	869	878	-	ATTAATGAAA
MEOX2	8.97858	0.91577	seq205	219	228	-	TGCAATTATC
RAX	8.97545	0.91107	seq205	586	595	+	GACAATTATG
PDX1	8.96814	0.9439	seq205	467	474	+	GTCATTAT
SPIB	8.96758	0.94869	seq205	413	419	+	ACCGGAA

VAX2	8.95539	0.93082	seq205	1	8	+	TTCATTAC
RAX2	8.93898	0.94189	seq205	236	243	-	GCAATTAC
Klf4	8.93379	0.9191	seq205	900	909	-	AGAAGAAGGG
VAX2	8.92539	0.93002	seq205	870	877	-	TTAATGAA
HOXB2	8.9251	0.94282	seq205	466	475	+	TGTCATTATC
PRRX1	8.91631	0.93242	seq205	220	227	-	GCAATTAT
ZNF354C	8.91578	1	seq205	719	724	-	ATCCAC
MIXL1	8.91076	0.93712	seq205	219	228	-	TGCAATTATC
SOX10	8.90979	1	seq205	292	297	-	CTTTGT
SOX10	8.90979	1	seq205	330	335	+	CTTTGT
EN2	8.90318	0.91832	seq205	219	228	-	TGCAATTATC
NFATC1	8.89726	0.90345	seq205	879	888	+	TTATTCCGTA
EVX2	8.89485	0.92646	seq205	466	475	+	TGTCATTATC
ESX1	8.88273	0.91993	seq205	219	228	-	TGCAATTATC
EVX1	8.85655	0.92413	seq205	466	475	+	TGTCATTATC
PRRX1	8.84645	0.93059	seq205	587	594	+	ACAATTAT
SHOX	8.83511	0.93702	seq205	220	227	+	ATAATTGC
HOXA5	8.82647	0.96374	seq205	155	162	+	CACAAATG
TEAD1	8.8221	0.90389	seq205	545	554	-	ATCATTCCAT
TCF4	8.8141	0.92223	seq205	354	363	-	TACATCTGTT
HOXA2	8.79857	0.92936	seq205	466	475	+	TGTCATTATC
FOXL1	8.79843	0.9365	seq205	575	581	+	GCAAACA
NKX6-2	8.79264	0.94268	seq205	220	227	-	GCAATTAT
Prrx2	8.77709	0.9401	seq205	220	227	-	GCAATTAT
LMX1A	8.77314	0.90116	seq205	870	877	-	TTAATGAA
LMX1B	8.77014	0.93156	seq205	874	881	-	TAAATTAA
Barhl1	8.74891	0.93605	seq205	586	595	-	CATAATTGTC
MNX1	8.74048	0.90946	seq205	586	595	+	GACAATTATG
VAX1	8.73415	0.92805	seq205	870	877	-	TTAATGAA
EN2	8.72996	0.91457	seq205	832	841	-	CCTAATCAGT

Pdx1	8.72988	0.96543	seq205	437	442	-	CTAATG
SPI1	8.72525	0.90612	seq205	181	187	+	AGAAAGT
SPI1	8.72525	0.90612	seq205	371	377	+	AGAAAGT
ZNF354C	8.72314	0.99157	seq205	633	638	-	CTCCAC
Bhlha15	8.71855	0.90881	seq205	609	616	-	GCAGATGG
NKX6-2	8.71403	0.94052	seq205	467	474	+	GTCATTAT
SPI1	8.71068	1	seq205	415	420	+	CGGAAG
LHX9	8.70895	0.93975	seq205	236	243	-	GCAATTAC
EVX1	8.70006	0.92057	seq205	586	595	+	GACAATTATG
SHOX	8.69753	0.93259	seq205	236	243	+	GTAATTGC
NKX2-8	8.69271	0.92772	seq205	11	19	-	TCACTTGAG
HOXA2	8.68361	0.92676	seq205	235	244	-	TGCAATTACA
FOS::JUN	8.68023	0.92759	seq205	793	799	+	TGACTGA
ARNT::HIF1A	8.66409	0.92438	seq205	613	620	+	CTGCGTGC
HOXB2	8.65261	0.93574	seq205	219	228	-	TGCAATTATC
UNCX	8.64742	0.93247	seq205	236	243	-	GCAATTAC
NKX6-2	8.64031	0.93849	seq205	236	243	-	GCAATTAC
GSC2	8.63837	0.90126	seq205	832	841	-	CCTAATCAGT
STAT3	8.63486	0.90216	seq205	224	234	+	TTGCAAGGAAT
Prrx2	8.62979	0.93539	seq205	587	594	+	ACAATTAT
TCF3	8.62533	0.9145	seq205	318	327	+	TTCACCTGGT
Nkx3-2	8.62034	0.92051	seq205	815	823	+	TTGAGTGAA
GSX2	8.61239	0.91715	seq205	235	244	-	TGCAATTACA
SHOX	8.60381	0.92957	seq205	874	881	+	TTAATTTA
HOXB3	8.58871	0.93383	seq205	869	878	+	TTTCATTAAT
PRRX1	8.58079	0.92363	seq205	874	881	-	TAAATTAA
LBX2	8.57445	0.9084	seq205	219	228	-	TGCAATTATC
FOXO4	8.5719	0.91812	seq205	94	100	+	ATAAATA
TCF4	8.57136	0.91852	seq205	318	327	+	TTCACCTGGT
UNCX	8.56279	0.92998	seq205	874	881	-	TAAATTAA

Shox2	8.55548	0.92821	seq205	587	594	+	ACAATTAT
Lhx4	8.55115	0.92103	seq205	493	500	-	TTTATTAA
HOXA2	8.53517	0.9234	seq205	219	228	-	TGCAATTATC
VAX1	8.52941	0.92223	seq205	1	8	+	TTCATTAC
HOXB3	8.52917	0.93244	seq205	235	244	-	TGCAATTACA
RAX2	8.52362	0.9298	seq205	220	227	-	GCAATTAT
HOXA5	8.51074	0.95262	seq205	3	10	-	CGGTAATG
LHX9	8.50846	0.93426	seq205	220	227	-	GCAATTAT
NKX6-1	8.50373	0.92165	seq205	220	227	-	GCAATTAT
HESX1	8.50178	0.90496	seq205	235	244	+	TGTAATTGCA
EMX1	8.49796	0.90189	seq205	869	878	-	ATTAATGAAA
MEOX1	8.48262	0.90038	seq205	219	228	-	TGCAATTATC
HOXB2	8.46724	0.93093	seq205	235	244	-	TGCAATTACA
GSX2	8.46457	0.91306	seq205	869	878	+	TTTCATTAAT
GBX1	8.45986	0.90229	seq205	235	244	-	TGCAATTACA
Nobox	8.44536	0.90378	seq205	221	228	+	TAATTGCA
Nobox	8.44536	0.90378	seq205	237	244	+	TAATTGCA
LHX9	8.4318	0.93217	seq205	587	594	+	ACAATTAT
BSX	8.42728	0.94431	seq205	587	594	+	ACAATTAT
HOXB3	8.4218	0.92994	seq205	466	475	+	TGTCATTATC
PDX1	8.41802	0.93289	seq205	587	594	+	ACAATTAT
EN2	8.41493	0.90774	seq205	235	244	-	TGCAATTACA
NKX6-1	8.4082	0.91957	seq205	493	500	-	TTTATTAA
EN2	8.40169	0.90745	seq205	586	595	+	GACAATTATG
GATA3	8.38812	1	seq205	194	199	-	AGATAG
GATA5	8.38447	0.92601	seq205	834	841	+	TGATTAGG
YY1	8.38313	1	seq205	608	613	+	GCCATC
MNX1	8.37759	0.90114	seq205	492	501	-	TTTTATTAAA
ESX1	8.37012	0.90675	seq205	235	244	-	TGCAATTACA
SHOX	8.36706	0.92194	seq205	587	594	-	ATAATTGT

GSX1	8.36636	0.92077	seq205	869	878	+	TTTCATTAAT
HOXB3	8.36244	0.92856	seq205	219	228	-	TGCAATTATC
NKX6-1	8.35598	0.91844	seq205	236	243	-	GCAATTAC
TCF3	8.33554	0.90962	seq205	354	363	-	TACATCTGTT
Lhx4	8.33176	0.91598	seq205	874	881	-	TAAATTAA
Barhl1	8.32891	0.92498	seq205	235	244	+	TGTAATTGCA
NKX6-2	8.32134	0.92971	seq205	587	594	+	ACAATTAT
EVX2	8.3164	0.91398	seq205	586	595	+	GACAATTATG
HOXB2	8.3041	0.92669	seq205	869	878	+	TTTCATTAAT
ESX1	8.30329	0.90503	seq205	586	595	+	GACAATTATG
Arid3a	8.29923	0.93972	seq205	873	878	+	ATTAAT
Arid3a	8.29923	0.93972	seq205	873	878	-	ATTAAT
Barhl1	8.28985	0.92395	seq205	202	211	-	GTTAATAGCG
EN1	8.2693	0.92127	seq205	587	594	+	ACAATTAT
EVX1	8.25782	0.9105	seq205	219	228	-	TGCAATTATC
MAFG::NFE2L1	8.25357	0.9758	seq205	467	472	-	AATGAC
MAFG::NFE2L1	8.25357	0.9758	seq205	755	760	+	AATGAC
Lhx4	8.2165	0.91333	seq205	833	840	-	CTAATCAG
PDX1	8.19975	0.92853	seq205	1	8	+	TTCATTAC
FOS::JUN	8.18522	0.90952	seq205	670	676	-	TGCCTCA
FOXO4	8.1706	0.91019	seq205	26	32	+	GTCAATA
TEAD3	8.15697	0.91867	seq205	120	127	+	GAATACCA
RHOXF1	8.15566	0.96148	seq205	914	921	-	ATTATCCC
GATA5	8.13697	0.91972	seq205	192	199	-	AGATAGCA
NKX6-2	8.13271	0.92452	seq205	1	8	+	TTCATTAC
NKX6-1	8.13257	0.91358	seq205	1	8	+	TTCATTAC
RAX2	8.12482	0.91819	seq205	587	594	+	ACAATTAT
GSX1	8.12351	0.91417	seq205	235	244	-	TGCAATTACA
FOXP3	8.12264	0.92005	seq205	94	100	+	ATAAATA
LMX1B	8.1116	0.91185	seq205	236	243	-	GCAATTAC

NKX6-2	8.11042	0.9239	seq205	493	500	-	TTTATTAA
Pdx1	8.10589	0.93975	seq205	314	319	+	TTAATT
Pdx1	8.10589	0.93975	seq205	874	879	+	TTAATT
GATA3	8.10267	0.90752	seq205	192	199	-	AGATAGCA
Lhx8	8.09772	0.93019	seq205	236	243	-	GCAATTAC
GATA3	8.09247	0.9876	seq205	797	802	+	TGATAG
Nkx2-5	8.05931	0.94936	seq205	204	210	-	TTAATAG
Nkx2-5	8.05931	0.94936	seq205	282	288	+	TTAATAG
EVX2	8.05786	0.9084	seq205	219	228	-	TGCAATTATC
Lhx8	8.04895	0.92927	seq205	236	243	+	GTAATTGC
GSX2	8.04212	0.90137	seq205	492	501	-	TTTTATTAAA
NKX6-2	8.03755	0.9219	seq205	203	210	+	GCTATTAA
LMX1B	8.03265	0.90949	seq205	874	881	+	TTAATTTA
MEIS1	8.01588	0.9505	seq205	186	192	+	GTGACAT
BARX1	7.98037	0.92997	seq205	833	840	+	CTGATTAG
UNCX	7.95119	0.91198	seq205	220	227	-	GCAATTAT
MZF1	7.93851	0.94768	seq205	740	745	+	AGGGGA
HIC2	7.92989	0.90517	seq205	66	74	-	ATGCACAGC
RAX2	7.92158	0.91227	seq205	874	881	-	TAAATTAA
THAP1	7.91911	0.91	seq205	897	905	+	TTGCCCTTC
LMX1B	7.9108	0.90584	seq205	493	500	-	TTTATTAA
VAX2	7.90553	0.90306	seq205	870	877	+	TTCATTAA
Shox2	7.89919	0.91348	seq205	874	881	-	TAAATTAA
HLTF	7.89775	0.95851	seq205	457	466	-	ATCCATTTGT
Pdx1	7.89619	0.93112	seq205	236	241	+	GTAATT
HOXB2	7.88605	0.91583	seq205	832	841	+	ACTGATTAGG
HOXB2	7.86094	0.91518	seq205	586	595	+	GACAATTATG
THAP1	7.8401	0.90758	seq205	570	578	-	TTGCCCTTT
HOXB3	7.83829	0.91635	seq205	832	841	+	ACTGATTAGG
NKX6-1	7.83514	0.90712	seq205	203	210	+	GCTATTAA

LHX9	7.82688	0.91562	seq205	870	877	-	TTAATGAA
FOXP3	7.82529	0.91257	seq205	206	212	+	ATTAACA
LMX1B	7.81132	0.90286	seq205	870	877	-	TTAATGAA
Mafb	7.81018	0.92685	seq205	54	61	-	GCTGACTA
MIXL1	7.80683	0.90839	seq205	586	595	+	GACAATTATG
ETS1	7.79718	1	seq205	415	420	-	CTTCCG
HOXA2	7.79075	0.90657	seq205	832	841	-	CCTAATCAGT
LMX1B	7.78661	0.90212	seq205	220	227	-	GCAATTAT
LHX9	7.77961	0.91433	seq205	870	877	+	TTCATTAA
UNCX	7.75546	0.90622	seq205	587	594	+	ACAATTAT
HOXB3	7.75061	0.91431	seq205	873	882	-	ATAAATTAAT
Lhx4	7.74739	0.90254	seq205	1	8	+	TTCATTAC
EMX2	7.74736	0.90128	seq205	219	228	-	TGCAATTATC
BSX	7.74734	0.92933	seq205	870	877	+	TTCATTAA
Nkx2-5	7.73959	0.93648	seq205	874	880	+	TTAATTT
Prrx2	7.71838	0.90623	seq205	874	881	-	TAAATTAA
EMX2	7.7119	0.90068	seq205	235	244	-	TGCAATTACA
Lhx4	7.70689	0.90161	seq205	833	840	+	CTGATTAG
Lhx4	7.70045	0.90146	seq205	874	881	+	TTAATTTA
EMX2	7.70011	0.90048	seq205	586	595	+	GACAATTATG
Pax2	7.69337	0.94611	seq205	184	191	-	TGTCACTT
RAX2	7.68733	0.90545	seq205	833	840	+	CTGATTAG
LHX9	7.67724	0.91153	seq205	874	881	-	TAAATTAA
OTX1	7.66796	0.90882	seq205	105	112	-	ATAATCTT
HOXA2	7.66024	0.90362	seq205	832	841	+	ACTGATTAGG
NKX6-1	7.65767	0.90327	seq205	587	594	+	ACAATTAT
UNCX	7.65625	0.9033	seq205	874	881	+	TTAATTTA
Pax2	7.65616	0.94464	seq205	754	761	-	AGTCATTC
UNCX	7.64898	0.90308	seq205	314	321	-	TGAATTAA
MIXL1	7.64838	0.90427	seq205	832	841	+	ACTGATTAGG

BARX1	7.6376	0.92237	seq205	467	474	+	GTCATTAT
MIXL1	7.62382	0.90363	seq205	873	882	-	ATAAATTAAT
LHX9	7.61064	0.90971	seq205	1	8	-	GTAATGAA
BSX	7.60538	0.9262	seq205	467	474	+	GTCATTAT
RAX2	7.60296	0.90299	seq205	833	840	-	CTAATCAG
NFIC	7.58675	0.92931	seq205	117	122	+	TTGGAA
NFIC	7.58675	0.92931	seq205	562	567	+	TTGGAA
FOXL1	7.57323	0.91406	seq205	26	32	+	GTCAATA
NKX6-2	7.56625	0.90893	seq205	282	289	-	ACTATTAA
FOXD2	7.55347	0.91321	seq205	26	32	+	GTCAATA
UNCX	7.54888	0.90014	seq205	833	840	+	CTGATTAG
NOTO	7.5245	0.90079	seq205	873	882	+	ATTAATTTAT
BARHL2	7.5242	0.90666	seq205	832	841	-	CCTAATCAGT
BSX	7.52382	0.9244	seq205	1	8	+	TTCATTAC
HOXB3	7.50953	0.90869	seq205	586	595	+	GACAATTATG
Mafb	7.48594	0.9128	seq205	583	590	+	GCTGACAA
Arid3a	7.46997	0.90737	seq205	275	280	+	ATCAAT
FOXL1	7.46152	0.94319	seq205	303	310	-	TTAATATA
NFIX	7.43319	0.9205	seq205	683	691	+	CAAGCCAGG
GATA3	7.42236	0.95948	seq205	277	282	-	AGATTG
HOXB2	7.42135	0.90376	seq205	873	882	-	ATAAATTAAT
NKX2-8	7.40955	0.90452	seq205	714	722	-	CCACTCTAA
ETS1	7.39347	0.98138	seq205	267	272	+	TATCCG
GATA5	7.389	0.90069	seq205	161	168	+	TGATAAAT
Pax2	7.38498	0.934	seq205	14	21	-	CGTCACTT
Nkx2-5	7.37953	0.92199	seq205	12	18	+	TCAAGTG
HLTF	7.37298	0.94002	seq205	863	872	+	TACCTTTTTC
ZNF354C	7.33082	0.93063	seq205	152	157	+	AACCAC
Mafb	7.31731	0.9055	seq205	407	414	+	GCTGATAC
NKX6-2	7.31016	0.90188	seq205	493	500	+	TTAATAAA

LHX9	7.30519	0.90135	seq205	833	840	-	CTAATCAG
Nkx2-5	7.28167	0.91805	seq205	311	317	-	TTAAGTT
BARHL2	7.27728	0.90206	seq205	586	595	-	CATAATTGTC
FOXD2	7.27635	0.90733	seq205	299	305	-	ATAAACT
Pdx1	7.2659	0.90519	seq205	872	877	-	TTAATG
NKX2-8	7.23216	0.90131	seq205	60	68	+	GCACTTGCT
ETS1	7.22918	0.9738	seq205	596	601	+	CATCCT
YY1	7.21934	0.94056	seq205	703	708	-	GCCATG
NFIC	7.21893	0.91699	seq205	685	690	-	CTGGCT
NFIC	7.21893	0.91699	seq205	801	806	-	CTGGCT
RHOXF1	7.2103	0.94326	seq205	105	112	-	ATAATCTT
GATA3	7.18943	0.94971	seq205	218	223	+	AGATAA
GATA3	7.18943	0.94971	seq205	471	476	-	AGATAA
BARX1	7.12761	0.91107	seq205	870	877	+	TTCATTAA
Lhx8	7.10659	0.91147	seq205	220	227	+	ATAATTGC
SOX10	7.09699	0.91952	seq205	639	644	+	CTGTGT
Pax2	7.08024	0.92203	seq205	166	173	+	AATCATGC
PDX1	7.06914	0.90591	seq205	833	840	+	CTGATTAG
HLTF	7.06722	0.92924	seq205	111	120	+	ATACATTTGG
FOXL1	7.03459	0.92384	seq205	93	100	+	AATAAATA
Nkx2-5	7.01286	0.90723	seq205	236	242	+	GTAATTG
HLTF	6.98239	0.92625	seq205	710	719	+	CTCCTTAGAG
HLTF	6.96796	0.92574	seq205	567	576	-	GCCCTTTGAT
MAFG::NFE2L1	6.93186	0.91856	seq205	167	172	-	CATGAT
Gata1	6.92224	0.99006	seq205	609	614	-	AGATGG
En1	6.92078	0.90138	seq205	852	862	+	AAATAGTCTTC
GATA3	6.89378	0.93731	seq205	161	166	+	TGATAA
NFIX	6.82283	0.90613	seq205	799	807	+	ATAGCCAGT
SOX10	6.81243	0.90689	seq205	262	267	+	CAGTGT
Gata1	6.6862	0.97722	seq205	595	600	-	GGATGC

BARX1	6.67074	0.90095	seq205	1	8	+	TTCATTAC
Lhx8	6.65855	0.90301	seq205	220	227	-	GCAATTAT
GATA2	6.65143	1	seq205	267	271	-	GGATA
GATA2	6.65143	1	seq205	915	919	+	GGATA
RHOXF1	6.3782	0.92722	seq205	840	847	-	GAAAGCCC
RHOXF1	6.33348	0.92636	seq205	744	751	+	GAGAGCCC
RHOXF1	6.23484	0.92446	seq205	705	712	-	GAGAGCCA
GATA2	6.23202	0.97565	seq205	195	199	-	AGATA
GATA2	6.23202	0.97565	seq205	218	222	+	AGATA
GATA2	6.23202	0.97565	seq205	472	476	-	AGATA
GATA3	6.22367	0.9092	seq205	106	111	+	AGATTA
MEIS1	6.15813	0.91116	seq205	723	729	-	AAGACAT
ETS1	6.14179	0.92364	seq205	881	886	+	ATTCCG
Gata1	6.06648	0.9435	seq205	194	199	-	AGATAG
MEIS1	6.05784	0.90903	seq205	792	798	+	TTGACTG
RHOXF1	6.01836	0.92029	seq205	520	527	+	GTGAGCTC
GATA2	5.9783	0.96092	seq205	463	467	+	GGATG
GATA2	5.9783	0.96092	seq205	596	600	-	GGATG
GATA2	5.9783	0.96092	seq205	721	725	+	GGATG
ETS1	5.97749	0.91606	seq205	229	234	-	ATTCCT
Gata1	5.9664	0.93806	seq205	463	468	+	GGATGT
Gata1	5.9664	0.93806	seq205	721	726	+	GGATGT
MEIS1	5.95216	0.90679	seq205	16	22	+	GTGACGG
RHOXF1	5.90668	0.91813	seq205	470	477	+	ATTATCTC
ETS1	5.89604	0.91231	seq205	462	467	-	CATCCA
ETS1	5.89604	0.91231	seq205	720	725	-	CATCCA
Gata1	5.85733	0.93212	seq205	797	802	+	TGATAG
Gata1	5.83043	0.93066	seq205	266	271	-	GGATAC
FOXC1	5.82267	0.90776	seq205	261	268	+	ACAGTGTA
FOXC1	5.82267	0.90776	seq205	342	349	-	CCCGTGTA

Gata1	5.78377	0.92812	seq205	357	362	+	AGATGT
GATA2	5.77818	0.9493	seq205	161	165	+	TGATA
GATA2	5.77818	0.9493	seq205	409	413	+	TGATA
GATA2	5.77818	0.9493	seq205	797	801	+	TGATA
ETS1	5.77712	0.90682	seq205	89	94	-	TTTCCC
FOXC1	5.76378	0.90447	seq205	538	545	+	AATGAGTA
Gata1	5.61263	0.91881	seq205	277	282	-	AGATTG
Gata1	5.57462	0.91674	seq205	273	278	-	TGATGT
Gata1	5.57462	0.91674	seq205	449	454	+	TGATGT
Gata1	5.57462	0.91674	seq205	551	556	+	TGATGT
GATA2	5.55889	0.93657	seq205	357	361	+	AGATG
GATA2	5.55889	0.93657	seq205	610	614	-	AGATG
Gata1	5.43865	0.90935	seq205	409	414	+	TGATAC
RHOXF1	5.21196	0.90474	seq205	217	224	-	ATTATCTT
RHOXF1	5.18259	0.90418	seq205	821	828	+	GAAATCTC
GATA2	5.10505	0.91022	seq205	274	278	-	TGATG
GATA2	5.10505	0.91022	seq205	449	453	+	TGATG
GATA2	5.10505	0.91022	seq205	551	555	+	TGATG

Site +86kb

Name	Score	Relative score	Sequence ID	Start	End	Strand	Predicted sequence
ESRRB	17.6847	0.984412218	seq86	383	393	-	TCAAGGTCATC
Esrra	17.6616	0.965852512	seq86	384	394	-	CTCAAGGTCAT
Esrrg	16.5745	0.999999988	seq86	384	393	-	TCAAGGTCAT
FLI1	16.3648	0.98692939	seq86	680	690	-	ACAGGAAGTGA
Ets1	16.33	0.950352654	seq86	679	693	+	CTCACTTCCTGTCAG
Erg	16.2355	0.988892865	seq86	680	690	-	ACAGGAAGTGA
Esrrb	15.7311	0.979846369	seq86	385	396	-	CTCTCAAGGTCA
Esrrb	15.6722	0.979301446	seq86	385	396	-	CTCTCAAGGTCA
TCF7L2	15.0871	0.950943586	seq86	314	327	+	AAAGTTCAAAGCGC
ZBTB18	14.9894	0.944889298	seq86	628	640	+	TTTGCAGATGTTG
Tcf7	14.7702	0.908452796	seq86	314	325	+	AAAGTTCAAAGC
FOXC2	14.6894	0.962770673	seq86	210	221	-	TAAATAAATAAA
Rhox11	14.5997	0.932881555	seq86	226	242	-	AATAAGCTGTAAATAAA
KLF16	14.5432	0.948681808	seq86	76	86	-	GCCACCCCCCC
FOXC1	14.5169	0.971404558	seq86	207	217	-	TAAATAAATAT
ZNF740	14.4548	0.957972845	seq86	72	81	-	CCCCCCCCAA
ESRRA	14.3892	0.944945268	seq86	383	393	-	TCAAGGTCATC
SP8	14.3676	0.945821472	seq86	75	86	-	GCCACCCCCCCC
ZEB1	14.1968	0.986437111	seq86	467	475	+	GCTCACCTG
ZNF740	14.139	0.952151273	seq86	74	83	-	ACCCCCCCCC
FOXC2	14.1239	0.953927371	seq86	214	225	-	TACGTAAATAAA
Meis1	13.8753	0.924325196	seq86	685	699	+	TCCTGTCAGGCTCCC
EHF	13.7853	0.999252193	seq86	682	689	+	ACTTCCTG
FOXC1	13.7056	0.959226672	seq86	211	221	-	TAAATAAATAA
FOXB1	13.6956	0.939814946	seq86	207	217	-	TAAATAAATAT
EGR1	13.6318	0.926165566	seq86	366	379	+	CTCCAGCCCCCGCC
ELF1	13.4488	0.928672569	seq86	681	693	-	CTGACAGGAAGTG

ERF	13.4355	0.943818256	seq86	681	690	-	ACAGGAAGTG
ELK4	13.2902	0.947299308	seq86	680	690	+	TCACTTCCTGT
Bhlhe40	13.2705	0.962265825	seq86	129	139	+	CTCACATGCAG
FOXC1	13.2327	0.952128083	seq86	607	617	+	AATATAAATAA
FOXC1	13.2313	0.952106238	seq86	215	225	-	TACGTAAATAA
ETS1	13.1541	0.95547997	seq86	681	690	-	ACAGGAAGTG
FOXI1	13.001	0.949647383	seq86	205	216	+	ACATATTTATTT
ZBTB7A	12.9674	0.918371586	seq86	679	691	-	GACAGGAAGTGAG
ETV6	12.9531	0.949815738	seq86	681	690	-	ACAGGAAGTG
Rxra	12.8913	0.950016314	seq86	456	466	+	CAGGGGTCAGG
FOXB1	12.8671	0.926771591	seq86	607	617	+	AATATAAATAA
Foxa2	12.753	0.950801231	seq86	205	216	+	ACATATTTATTT
ERG	12.7522	0.953197441	seq86	681	690	-	ACAGGAAGTG
Stat4	12.7367	0.925223694	seq86	680	693	-	CTGACAGGAAGTGA
Bhlhe40	12.6962	0.954516995	seq86	426	436	-	CACACATGCAG
FLI1	12.6413	0.946423659	seq86	681	690	-	ACAGGAAGTG
ZNF740	12.6032	0.923841679	seq86	73	82	-	CCCCCCCCCA
FOXI1	12.6011	0.939992654	seq86	221	232	+	ACGTATTTATTT
Foxd3	12.4852	0.918653689	seq86	209	220	+	ATTTATTTATTT
FOXB1	12.472	0.920551275	seq86	211	221	-	TAAATAAATAA
TWIST1	12.4516	0.931909803	seq86	628	640	+	TTTGCAGATGTTG
FOXI1	12.4387	0.93607148	seq86	209	220	+	ATTTATTTATTT
NR2F2	12.3751	0.941108976	seq86	383	393	-	TCAAGGTCATC
HNF4A	12.2287	0.906272771	seq86	309	321	+	AGGGAAAAGTTCA
FEV	12.0971	0.941150166	seq86	681	690	-	ACAGGAAGTG
Gabpa	12.0642	0.916517221	seq86	679	689	-	CAGGAAGTGAG
SP3	12.0518	0.925810786	seq86	76	86	-	GCCACCCCCCC
Foxd3	12.0255	0.909481951	seq86	652	663	+	TAATGTTTGTGT
FOXC2	11.985	0.920477981	seq86	607	618	+	AATATAAATAAG
FOXB1	11.9457	0.912266027	seq86	215	225	-	TACGTAAATAA

FEV	11.8515	0.993173383	seq86	682	689	-	CAGGAAGT
FOXA1	11.8425	0.923591372	seq86	606	620	-	TACTTATTTATATTT
ETV3	11.8407	0.916547172	seq86	681	690	-	ACAGGAAGTG
FOXC2	11.7625	0.916997932	seq86	206	217	-	TAAATAAATATG
Foxa2	11.7592	0.925346606	seq86	209	220	+	ATTTATTTATTT
Nr2e3	11.6651	0.999999995	seq86	346	352	-	CAAGCTT
ELK3	11.6291	0.919304353	seq86	681	690	-	ACAGGAAGTG
FOXC1	11.6255	0.928002091	seq86	223	233	-	TAAATAAATAC
FOXI1	11.5552	0.914740605	seq86	608	619	-	ACTTATTTATAT
SPI1	11.5428	1.00000001	seq86	682	688	-	AGGAAGT
RORA	11.513	0.921253286	seq86	385	394	-	CTCAAGGTCA
ZEB1	11.5128	0.949510187	seq86	468	478	+	CTCACCTGAGG
ZNF740	11.5078	0.903648929	seq86	75	84	-	CACCCCCCCC
FOXI1	11.4935	0.913250675	seq86	652	663	+	TAATGTTTGTGT
RUNX2	11.4392	0.935725729	seq86	281	289	-	GAACCGCAA
Crx	11.3607	0.907822851	seq86	546	556	+	AATGGGCTTAA
GABPA	11.3569	0.920921435	seq86	681	690	-	ACAGGAAGTG
ETV1	11.3546	0.926428175	seq86	681	690	-	ACAGGAAGTG
Foxo1	11.3239	0.914574436	seq86	107	117	+	TGTTGTTTTTA
SOX10	11.323	0.936649655	seq86	144	154	+	TGCACAAAGCC
FOXA1	11.3126	0.913255956	seq86	626	636	+	TGTTTGCAGAT
FOXA1	11.2997	0.912482324	seq86	626	636	+	TGTTTGCAGAT
NR4A1	11.2949	0.92981064	seq86	384	393	-	TCAAGGTCAT
ETV4	11.2489	0.925297135	seq86	681	690	-	ACAGGAAGTG
FOXA1	11.1107	0.915411706	seq86	204	218	+	CACATATTTATTTAT
Tcf12	11.0756	0.93551049	seq86	240	250	-	CACAGCTGAAT
FOXI1	11.0751	0.903149533	seq86	39	50	+	TCGTATTTGTTG
BARHL2	11.0537	0.972360548	seq86	403	412	+	ACTAAACGGC
MEIS2	10.959	0.945102011	seq86	576	583	-	CTGACAGG
MEIS2	10.959	0.945102011	seq86	686	693	-	CTGACAGG

Myog	10.8999	0.940056157	seq86	240	250	-	CACAGCTGAAT
Stat5a::Stat5b	10.8968	0.926943374	seq86	3	13	-	TGTTCCATGAA
SP1	10.768	0.962467113	seq86	74	83	+	GGGGGGGGGT
TFAP4	10.6871	0.900284494	seq86	241	250	-	CACAGCTGAA
SP1	10.6764	0.900172836	seq86	73	82	-	CCCCCCCCCA
Bhlha15	10.6601	0.945119182	seq86	631	638	+	GCAGATGT
ELK1	10.5796	0.905109633	seq86	681	690	-	ACAGGAAGTG
FOXI1	10.5742	0.949410085	seq86	216	222	-	GTAAATA
FOXI1	10.5742	0.949410085	seq86	228	234	-	GTAAATA
FOXL1	10.4667	0.96704791	seq86	216	222	-	GTAAATA
FOXL1	10.4667	0.96704791	seq86	228	234	-	GTAAATA
ELF5	10.3908	0.907549506	seq86	681	691	-	GACAGGAAGTG
ETV5	10.3713	0.928324494	seq86	681	690	-	ACAGGAAGTG
FOXK2	10.3419	0.90202496	seq86	214	224	-	ACGTAAATAAA
HOXD13	10.3372	0.907823794	seq86	600	609	+	TCCATAAAAT
Nr2e3	10.321	0.951985795	seq86	345	351	+	AAAGCTT
VDR	10.2768	0.956524889	seq86	61	68	+	AGGGTTCA
FOXK2	10.2674	0.900403562	seq86	608	618	+	ATATAAATAAG
FOXK2	10.2638	0.900324195	seq86	226	236	-	CTGTAAATAAA
FOXO4	10.2484	0.951264677	seq86	216	222	-	GTAAATA
FOXO4	10.2484	0.951264677	seq86	228	234	-	GTAAATA
Klf4	10.2365	0.957338079	seq86	90	99	+	AAAGAGAAGG
NFAT5	10.2361	0.918698646	seq86	308	317	-	CTTTTCCCTT
FOXD2	10.2358	0.97009674	seq86	216	222	-	GTAAATA
FOXD2	10.2358	0.97009674	seq86	228	234	-	GTAAATA
SNAI2	10.229	0.950554061	seq86	573	581	-	GACAGGTTT
FOXC1	10.2172	0.90686218	seq86	109	119	-	AATAAAAACAA
EBF1	10.1965	0.923738406	seq86	69	79	-	CCCCCCAAGGA
LIN54	10.1887	0.939626339	seq86	566	574	-	TTTTAAACA
FOXA1	10.1821	0.90503363	seq86	208	222	+	TATTTATTTATTTAC

GMEB2	10.1478	0.931287157	seq86	219	226	-	ATACGTAA
VDR	10.1321	0.952398492	seq86	314	321	+	AAAGTTCA
FOXL1	10.1199	0.960696958	seq86	208	214	-	ATAAATA
FOXL1	10.1199	0.960696958	seq86	212	218	-	ATAAATA
FOXL1	10.1199	0.960696958	seq86	224	230	-	ATAAATA
FOXL1	10.1199	0.960696958	seq86	610	616	+	ATAAATA
LIN54	10.0506	0.936888155	seq86	541	549	+	CTTTGAATG
Smad4	10.0421	0.931268904	seq86	668	675	+	AGTCTGGA
PITX3	10.0406	0.93562362	seq86	549	557	-	ATTAAGCCC
Rxra	10.0193	0.908648163	seq86	313	323	+	AAAAGTTCAAA
FOXA1	10.0135	0.903149156	seq86	220	234	+	TACGTATTTATTTAC
Rxra	9.95886	0.90777716	seq86	473	483	+	CTGAGGCCAGC
MEIS1	9.94789	0.991412464	seq86	330	336	-	CTGACAG
MEIS1	9.94789	0.991412464	seq86	577	583	-	CTGACAG
MEIS1	9.94789	0.991412464	seq86	687	693	-	CTGACAG
CDX1	9.93029	0.929843924	seq86	600	608	+	TCCATAAAA
MEIS3	9.86652	0.947539472	seq86	47	54	-	TTGACAAC
NFAT5	9.85618	0.91095379	seq86	644	653	+	GTTTTTCATA
NKX3-1	9.80297	0.936114631	seq86	615	621	-	GTACTTA
NKX3-1	9.80297	0.936114631	seq86	618	624	+	GTACTTA
FOXA1	9.76744	0.900398779	seq86	622	636	+	TTACTGTTTGCAGAT
ELF5	9.72717	0.939117735	seq86	681	689	+	CACTTCCTG
SNAI2	9.71729	0.940346843	seq86	23	31	-	GGCAGGTAC
SP1	9.67554	0.902870111	seq86	164	174	-	GCCCCTCCTAG
KLF5	9.63717	0.925851215	seq86	165	174	-	GCCCCTCCTA
MEIS1	9.55709	0.983136445	seq86	48	54	-	TTGACAA
Pitx1	9.55553	0.932695878	seq86	549	556	-	TTAAGCCC
MEIS2	9.50625	0.912150502	seq86	47	54	-	TTGACAAC
SPIB	9.50433	0.967023633	seq86	684	690	-	ACAGGAA
LIN54	9.48879	0.925749108	seq86	316	324	-	CTTTGAACT

SNAI2	9.44899	0.934995027	seq86	422	430	-	TGCAGGTTT
Foxj2	9.40707	0.916367258	seq86	215	222	-	GTAAATAA
Foxj2	9.40707	0.916367258	seq86	227	234	-	GTAAATAA
FOXD2	9.39873	0.952343109	seq86	626	632	-	GCAAACA
FOXO3	9.37963	0.907205504	seq86	228	235	-	TGTAAATA
FOXP3	9.35863	0.951146459	seq86	626	632	-	GCAAACA
Foxj2	9.3367	0.91495166	seq86	109	116	-	AAAAACAA
Foxj2	9.3367	0.91495166	seq86	642	649	-	AAAAACAA
Hic1	9.26747	0.906394332	seq86	27	35	+	CTGCCAGCC
ZEB1	9.26193	0.999999993	seq86	470	475	+	CACCTG
LIN54	9.22066	0.920432764	seq86	519	527	-	TTTTAAAAA
FOXD2	9.19033	0.947923446	seq86	208	214	-	ATAAATA
FOXD2	9.19033	0.947923446	seq86	212	218	-	ATAAATA
FOXD2	9.19033	0.947923446	seq86	224	230	-	ATAAATA
FOXD2	9.19033	0.947923446	seq86	610	616	+	ATAAATA
Foxj2	9.18772	0.911954634	seq86	211	218	-	ATAAATAA
Foxj2	9.18772	0.911954634	seq86	610	617	+	ATAAATAA
NFATC2	9.18689	0.91986211	seq86	310	316	-	TTTTCCC
NFATC2	9.18689	0.91986211	seq86	341	347	-	TTTTCCC
FOXO6	9.14239	0.929554737	seq86	216	222	-	GTAAATA
FOXO6	9.14239	0.929554737	seq86	228	234	-	GTAAATA
RHOXF1	9.0868	0.979430196	seq86	549	556	-	TTAAGCCC
MZF1	9.08528	0.999999979	seq86	188	193	+	TGGGGA
SOX15	9.07543	0.901876057	seq86	54	63	-	CCTTTATTTT
TCF3	9.06488	0.921885499	seq86	630	639	-	AACATCTGCA
Tcf3	9.05429	0.905685392	seq86	629	639	-	AACATCTGCAA
FOXP3	8.97718	0.941549102	seq86	216	222	-	GTAAATA
FOXP3	8.97718	0.941549102	seq86	228	234	-	GTAAATA
MEIS2	8.97559	0.900114101	seq86	329	336	-	CTGACAGA
Klf4	8.95105	0.919605218	seq86	308	317	+	AAGGGAAAAG

SOX10	8.90979	0.999999997	seq86	147	152	-	CTTTGT
Myc	8.89061	0.905310836	seq86	428	437	+	GCATGTGTGT
ELF5	8.8857	0.911617305	seq86	274	282	+	AGTTTCCTT
Stat5a::Stat5b	8.88543	0.902361654	seq86	1	11	+	ATTTCATGGAA
TCF4	8.88311	0.923286462	seq86	630	639	-	AACATCTGCA
LIN54	8.80711	0.912233091	seq86	567	575	+	GTTTAAAAA
FOXL1	8.79843	0.936497447	seq86	626	632	-	GCAAACA
OTX1	8.69566	0.928859055	seq86	549	556	-	TTAAGCCC
MAFG::NFE2L1	8.69154	0.994771697	seq86	383	388	+	GATGAC
LIN54	8.63254	0.908771966	seq86	520	528	+	TTTTAAAAG
NFIX	8.60672	0.94812998	seq86	26	34	+	CCTGCCAGC
FOXO4	8.5719	0.91811942	seq86	208	214	-	ATAAATA
FOXO4	8.5719	0.91811942	seq86	212	218	-	ATAAATA
FOXO4	8.5719	0.91811942	seq86	224	230	-	ATAAATA
FOXO4	8.5719	0.91811942	seq86	610	616	+	ATAAATA
Myod1	8.5512	0.900140269	seq86	241	253	+	TTCAGCTGTGGAA
STAT3	8.54183	0.90103524	seq86	2	12	+	TTTCATGGAAC
FOXP3	8.5041	0.929646506	seq86	655	661	-	ACAAACA
Mafb	8.49364	0.956444112	seq86	330	337	-	GCTGACAG
OTX2	8.48202	0.921063494	seq86	549	556	-	TTAAGCCC
FOXL1	8.45163	0.930146495	seq86	655	661	-	ACAAACA
NFIC	8.39594	0.956408629	seq86	28	33	-	CTGGCA
YY1	8.38313	0.999999988	seq86	33	38	+	GCCATC
YY1	8.38313	0.999999988	seq86	198	203	-	GCCATC
FOXD2	8.35322	0.930169815	seq86	655	661	-	ACAAACA
Bhlha15	8.31813	0.901319065	seq86	631	638	-	ACATCTGC
RHOXF1	8.26734	0.963635238	seq86	465	472	-	GTGAGCCC
FOS::JUN	8.18522	0.909521262	seq86	260	266	+	TGCCTCA
SPI1	8.18402	0.977897674	seq86	683	688	-	AGGAAG
FOXL1	8.17045	0.924997273	seq86	566	572	-	TTAAACA

FOXP3	8.12264	0.920049149	seq86	208	214	-	ATAAATA
FOXP3	8.12264	0.920049149	seq86	212	218	-	ATAAATA
FOXP3	8.12264	0.920049149	seq86	224	230	-	ATAAATA
FOXP3	8.12264	0.920049149	seq86	610	616	+	ATAAATA
THAP1	8.00733	0.912696679	seq86	27	35	+	CTGCCAGCC
FOXD2	7.81576	0.918771522	seq86	110	116	-	AAAAACA
FOXD2	7.81576	0.918771522	seq86	643	649	-	AAAAACA
SNAI2	7.73248	0.900755059	seq86	469	477	-	CTCAGGTGA
SPI1	7.72714	0.95872444	seq86	286	291	-	GGGAAC
HLTF	7.63455	0.949236052	seq86	311	320	-	GAACTTTTCC
ETS1	7.63289	0.992421538	seq86	276	281	+	TTTCCT
ETS1	7.63289	0.992421538	seq86	292	297	+	TTTCCT
ETS1	7.63289	0.992421538	seq86	683	688	+	CTTCCT
FOXL1	7.60784	0.949825232	seq86	609	616	+	TATAAATA
NKX2-8	7.5649	0.90733147	seq86	596	604	+	ACACTCCAT
TFAP2A	7.5598	0.907584799	seq86	471	479	-	GCCTCAGGT
HLTF	7.51332	0.944963675	seq86	191	200	-	ATCCTTGTCC
TFAP2A	7.50998	0.905959225	seq86	478	486	+	GCCAGCAGC
HLTF	7.48939	0.944120224	seq86	522	531	-	TCCCTTTTAA
FOXL1	7.33813	0.937601423	seq86	605	612	+	AAAATATA
HLTF	7.32104	0.938187129	seq86	612	621	-	GTACTTATTT
HLTF	7.23644	0.935205381	seq86	554	563	-	GACCATATTA
ETS1	7.22918	0.973799495	seq86	67	72	+	CATCCT
ETS1	7.22918	0.973799495	seq86	196	201	-	CATCCT
FOXC1	7.20856	0.98528652	seq86	619	626	-	AGTAAGTA
Gata1	7.10487	0.99999999	seq86	197	202	+	GGATGG
SOX10	7.09357	0.919368595	seq86	193	198	-	CCTTGT
HLTF	7.07346	0.92946128	seq86	92	101	-	AACCTTCTCT
FOXL1	7.03459	0.923844532	seq86	208	215	-	AATAAATA
FOXL1	7.03459	0.923844532	seq86	212	219	-	AATAAATA

FOXL1	7.03459	0.923844532	seq86	224	231	-	AATAAATA
YY1	7.02748	0.930762288	seq86	557	562	-	ACCATA
HOXA5	7.01785	0.900039382	seq86	204	211	+	CACATATT
FOXD2	6.94322	0.900266554	seq86	42	48	-	ACAAATA
FOXD2	6.94322	0.900266554	seq86	297	303	-	ACAAATA
Gata1	6.92224	0.990063527	seq86	34	39	-	AGATGG
RHOXF1	6.88328	0.936957995	seq86	148	155	+	CAAAGCCC
ZEB1	6.83073	0.903487042	seq86	24	29	+	TACCTG
FOXL1	6.80431	0.913407369	seq86	116	123	-	TTAAAATA
HLTF	6.58511	0.91225017	seq86	68	77	+	ATCCTTGGGG
SPI1	6.48328	0.906524284	seq86	157	162	+	TGGAAG
SPI1	6.48328	0.906524284	seq86	249	254	+	TGGAAG
HLTF	6.31391	0.902691911	seq86	203	212	+	CCACATATTT
ETS1	6.29975	0.930928106	seq86	157	162	-	CTTCCA
ETS1	6.29975	0.930928106	seq86	249	254	-	CTTCCA
RHOXF1	6.1529	0.92288009	seq86	234	241	-	ATAAGCTG
RHOXF1	6.01836	0.920286824	seq86	14	21	-	GTGAGCTC
FOXC1	5.98617	0.916908949	seq86	613	620	+	AATAAGTA
GATA2	5.9783	0.960920821	seq86	67	71	-	GGATG
GATA2	5.9783	0.960920821	seq86	197	201	+	GGATG
FOXC1	5.79353	0.906132868	seq86	24	31	-	GGCAGGTA
Gata1	5.78377	0.928122717	seq86	633	638	+	AGATGT
ETS1	5.77712	0.906820739	seq86	310	315	-	TTTCCC
ETS1	5.77712	0.906820739	seq86	341	346	-	TTTCCC
RHOXF1	5.71679	0.914474309	seq86	582	589	+	AGAATCCC
GATA2	5.55889	0.93657158	seq86	35	39	-	AGATG
GATA2	5.55889	0.93657158	seq86	382	386	+	CGATG
GATA2	5.55889	0.93657158	seq86	633	637	+	AGATG
Gata1	5.49794	0.912571735	seq86	66	71	-	GGATGA
Gata1	5.40951	0.907760629	seq86	382	387	+	CGATGA

Gata1	5.37659	0.905969296	seq86	583	588	-	GGATTC

Site -305kb

Name	Score	Relative score	Sequence ID	Start	End	Strand	Predicted sequence
Gata4	14.8275	0.984969128	seq305	93	103	+	CCTTATCTGCT
Gata1	14.632	0.968310582	seq305	92	102	+	CCCTTATCTGC
Tal1::Gata1	14.242	0.92569652	seq305	94	111	-	GGGGGCCCAGCAGATAAG
SMAD2::SMAD3::SMAD4	13.9203	0.91206672	seq305	372	384	-	CTGTCTCTCTCCC
Gata1	13.8691	0.987216504	seq305	92	102	-	GCAGATAAGGG
TCF7L2	13.4512	0.928335706	seq305	51	64	+	TGAGATGAAAGGCT
TCF7L2	13.3869	0.927447316	seq305	152	165	+	AAAGTTCAAAGTCG
GATA3	13.3741	0.979436859	seq305	93	100	-	AGATAAGG
ZEB1	13.2187	0.969830656	seq305	47	55	-	TCTCACCTG
ZEB1	13.1361	0.979453823	seq305	44	54	-	CTCACCTGGGC
GATA2	13.0399	0.970913157	seq305	92	102	+	CCCTTATCTGC
ID4	13.0152	0.974646404	seq305	247	256	+	TACACCTGTG
ZNF384	12.9883	0.940578703	seq305	165	176	-	GTTCAAAAAAAC
Gata1	12.919	0.944839538	seq305	197	207	+	TGTTTATCTGT
TCF3	12.7606	0.984017868	seq305	247	256	+	TACACCTGTG
GATA6	12.7295	0.933181039	seq305	91	103	-	AGCAGATAAGGGG
SOX13	12.5778	0.969609787	seq305	182	192	+	GCACAATGGAG
Gfi1b	12.5576	0.930472523	seq305	250	260	-	AAATCACAGGT
TCF4	12.5562	0.979462293	seq305	247	256	+	TACACCTGTG
Gata1	12.3975	0.960281867	seq305	197	207	-	ACAGATAAACA
Sox2	12.3713	0.971709574	seq305	183	190	-	CCATTGTG
ZEB1	12.2105	0.952713497	seq305	246	254	+	CTACACCTG
FOXP2	12.2097	0.930858721	seq305	195	205	-	AGATAAACACA
FIGLA	11.9313	0.953817958	seq305	247	256	+	TACACCTGTG
FOXL1	11.9193	0.993649047	seq305	197	203	-	ATAAACA
Nkx2-5(var.2)	11.8811	0.932942288	seq305	80	90	+	GACCACTCAGA
FOXG1	11.7804	0.957206753	seq305	196	203	-	ATAAACAC
GATA3	11.7346	0.99103868	seq305	93	100	-	AGATAAGG

Foxa2	11.679	0.909096166	seq305	28	39	-	TGTGTACACAGC
Nr2e3	11.6651	0.999999995	seq305	286	292	-	CAAGCTT
FOXK2	11.6538	0.930576271	seq305	195	205	-	AGATAAACACA
GATA2	11.5917	0.909635663	seq305	89	102	+	GACCCCTTATCTGC
FOXA1	11.4828	0.919570246	seq305	29	43	-	TGTGTGTGTACACAG
SNAI2	11.4422	0.974753399	seq305	248	256	-	CACAGGTGT
Gfi1	11.4369	0.965625064	seq305	252	261	-	AAAATCACAG
GATA3	11.3728	0.947947393	seq305	198	205	-	AGATAAAC
GATA2	11.2871	0.90548316	seq305	194	207	+	GTGTGTTTATCTGT
Foxj2	11.1684	0.951799006	seq305	196	203	-	ATAAACAC
FOXO4	11.037	0.966854746	seq305	197	203	-	ATAAACA
FOXO6	10.993	0.961235516	seq305	197	203	-	ATAAACA
NKX2-3	10.9927	0.944849295	seq305	130	139	-	CCCACTTGGG
GATA5	10.9309	0.990764543	seq305	93	100	-	AGATAAGG
NFYA	10.855	0.900826512	seq305	80	90	+	GACCACTCAGA
Sox6	10.845	0.921216027	seq305	181	190	-	CCATTGTGCT
GATA2	10.7077	0.923048512	seq305	197	207	+	TGTTTATCTGT
OTX2	10.6185	0.964535603	seq305	302	309	+	TTAATCTT
FOXD2	10.6003	0.977826697	seq305	197	203	-	ATAAACA
Nr2e3	10.5748	0.961052005	seq305	285	291	+	TAAGCTT
Sox17	10.569	0.964756332	seq305	183	191	-	TCCATTGTG
Sox3	10.5622	0.921970017	seq305	181	190	-	CCATTGTGCT
LIN54	10.5427	0.94664493	seq305	169	177	+	TTTTGAACA
SOX15	10.5099	0.93408617	seq305	181	190	-	CCATTGTGCT
FOXP3	10.4458	0.978500055	seq305	197	203	-	ATAAACA
Gata4	10.4379	0.921858926	seq305	198	208	+	GTTTATCTGTT
ZEB1	10.4332	0.929596302	seq305	247	257	+	TACACCTGTGA
Myod1	10.3531	0.923303798	seq305	247	259	+	TACACCTGTGATT
SOX9	10.2133	0.920195595	seq305	182	190	-	CCATTGTGC
FOXI1	10.1939	0.942144757	seq305	197	203	-	ATAAACA

Rxra	10.1451	0.9104605	seq305	151	161	+	GAAAGTTCAAA
VDR	10.1321	0.952398492	seq305	152	159	+	AAAGTTCA
TBX4	10.0971	0.928308475	seq305	48	55	+	AGGTGAGA
NFATC3	9.70016	0.905446098	seq305	147	156	-	ACTTTCCGCC
NFATC1	9.63197	0.924393464	seq305	147	156	-	ACTTTCCGCC
LIN54	9.60874	0.928127344	seq305	119	127	-	TTTTGAAAC
Ahr::Arnt	9.60282	0.999999989	seq305	321	326	+	TGCGTG
Tcf12	9.55296	0.914252098	seq305	246	256	-	CACAGGTGTAG
CEBPA	9.51453	0.91197437	seq305	203	213	-	ATTTCAACAGA
LIN54	9.48879	0.925749108	seq305	154	162	-	CTTTGAACT
TBX5	9.47292	0.91260284	seq305	48	55	+	AGGTGAGA
GSC2	9.43167	0.920804767	seq305	301	310	+	CTTAATCTTC
Myog	9.39229	0.919858281	seq305	246	256	-	CACAGGTGTAG
FOXO3	9.37963	0.907205504	seq305	30	37	-	TGTACACA
FOXO3	9.37963	0.907205504	seq305	32	39	+	TGTACACA
MGA	9.36487	0.912521087	seq305	48	55	+	AGGTGAGA
ZEB1	9.26193	0.999999993	seq305	47	52	-	CACCTG
ZEB1	9.26193	0.999999993	seq305	249	254	+	CACCTG
Sox3	9.2226	0.902143536	seq305	406	415	-	TCTTTCTTCT
GSC	9.10946	0.90359822	seq305	301	310	+	CTTAATCTTC
TCF4	9.09149	0.926473436	seq305	45	54	-	CTCACCTGGG
Pitx1	9.08354	0.920931861	seq305	302	309	+	TTAATCTT
GATA3	8.99808	0.928111674	seq305	198	205	-	AGATAAAC
ZNF354C	8.91578	1.000000021	seq305	336	341	-	ATCCAC
GATA5	8.85401	0.937949439	seq305	198	205	-	AGATAAAC
NKX2-8	8.81684	0.929969532	seq305	130	138	-	CCACTTGGG
PITX3	8.80964	0.90652538	seq305	301	309	+	CTTAATCTT
TCF3	8.7288	0.916235451	seq305	45	54	-	CTCACCTGGG
SOX10	8.62523	0.987366854	seq305	184	189	-	CATTGT
SOX10	8.62523	0.987366854	seq305	274	279	-	CATTGT

FOXP3	8.5041	0.929646506	seq305	291	297	-	ACAAACA
Klf4	8.4528	0.904979561	seq305	53	62	+	AGATGAAAGG
FOXL1	8.45163	0.930146495	seq305	291	297	-	ACAAACA
OTX1	8.41815	0.92344899	seq305	302	309	+	TTAATCTT
Nkx3-2	8.371	0.911200407	seq305	81	89	-	CTGAGTGGT
FOXD2	8.35322	0.930169815	seq305	291	297	-	ACAAACA
Klf4	8.33191	0.901430834	seq305	405	414	+	AAGAAGAAAG
Klf4	8.32785	0.901311719	seq305	398	407	+	CAGAGAAAAG
FOXO6	8.23405	0.914004601	seq305	30	36	-	GTACACA
FOXO6	8.23405	0.914004601	seq305	33	39	+	GTACACA
Nkx3-2	8.17752	0.903980197	seq305	131	139	+	CCAAGTGGG
GATA5	8.12127	0.919316278	seq305	227	234	+	AGATATCA
MZF1	7.93851	0.947676606	seq305	370	375	+	AGGGGA
FOXP3	7.86599	0.913591958	seq305	364	370	+	ATAAAGA
ETS1	7.79718	0.999999999	seq305	149	154	-	TTTCCG
Dlx1	7.76788	0.900526719	seq305	211	220	-	CCTAAATATT
HLTF	7.73934	0.952929429	seq305	91	100	+	CCCCTTATCT
FOXO4	7.68615	0.90060836	seq305	30	36	-	GTACACA
FOXO4	7.68615	0.90060836	seq305	33	39	+	GTACACA
GATA5	7.54409	0.904638878	seq305	301	308	-	AGATTAAG
HLTF	7.40562	0.941167785	seq305	338	347	-	CTCCATATCC
BARHL2	7.31347	0.902735242	seq305	211	220	-	CCTAAATATT
RHOXF1	7.19648	0.942994759	seq305	302	309	+	TTAATCTT
GATA3	7.18943	0.949713117	seq305	95	100	-	AGATAA
GATA3	7.18943	0.949713117	seq305	200	205	-	AGATAA
RHOXF1	7.16677	0.942422184	seq305	125	132	+	AAAAGCCC
SOX10	7.09699	0.91952059	seq305	29	34	+	CTGTGT
SOX10	7.09699	0.91952059	seq305	39	44	-	CTGTGT
HLTF	7.05105	0.928671472	seq305	328	337	-	ACCCTTTGAA
HLTF	6.98464	0.926330955	seq305	111	120	+	CTCCATAGGT

NFIC	6.9364 5	0.907525186	seq305	145	15 0	+	CTGGCG
FOXL1	6.8043 1	0.913407369	seq305	207	21 4	+	TTGAAATA
GATA2	6.6514 3	1.000000007	seq305	338	34 2	+	GGATA
NFIX	6.5963	0.900799646	seq305	144	15 2	-	TCCGCCAGC
HLTF	6.4625 7	0.907931427	seq305	232	24 1	+	TCACTTTGAC
GATA3	6.4229 6	0.917558655	seq305	227	23 2	+	AGATAT
FOXC1	6.3487 4	0.937190221	seq305	28	35	+	GCTGTGTA
HLTF	6.2686	0.901095204	seq305	308	31 7	-	GCCCATTGAA
GATA2	6.2320 2	0.975650738	seq305	96	10 0	-	AGATA
GATA2	6.2320 2	0.975650738	seq305	201	20 5	-	AGATA
GATA2	6.2320 2	0.975650738	seq305	227	23 1	+	AGATA
GATA3	6.2236 7	0.90919803	seq305	303	30 8	-	AGATTA
RHOXF1	6.1885 7	0.923567578	seq305	60	67	-	CAAAGCCT
GATA3	6.1273 2	0.905155835	seq305	229	23 4	-	TGATAT
RHOXF1	6.1240 8	0.922324638	seq305	14	21	-	CTTAGCCT
FOXC1	5.9861 7	0.916908949	seq305	34	41	-	TGTGTGTA
ETS1	5.8960 4	0.912306063	seq305	337	34 2	-	TATCCA
RHOXF1	5.8734 4	0.91749361	seq305	284	29 1	+	CTAAGCTT
MEIS1	5.8607 6	0.904858957	seq305	378	38 4	+	GAGACAG
MEIS1	5.8607 6	0.904858957	seq305	384	39 0	+	GAGACAG
MEIS1	5.8607 6	0.904858957	seq305	394	40 0	+	GAGACAG
RHOXF1	5.8396 7	0.916842683	seq305	337	34 4	-	CATATCCA
GATA2	5.7781 8	0.949302466	seq305	230	23 4	-	TGATA
GATA2	5.5588 9	0.93657158	seq305	53	57	+	AGATG
Gata1	5.3153 1	0.902635271	seq305	53	58	+	AGATGA
RHOXF1	5.1941 1	0.904399682	seq305	199	20 6	+	TTTATCTG

Site -580kb							
Name	**Score**	**Relative score**	**Sequence ID**	**Start**	**End**	**Strand**	**Predicted sequence**
ZNF143	20.2126	0.945545626	seq580	610	625	-	TACCCATGATGCCCTG
TCF7L2	16.9205	0.97628276	seq580	168	181	+	GAACATCAAAGACA
EBF1	16.0805	0.990653052	seq580	630	640	-	CTCCCCAGGGA
Tcf7	15.5295	0.919680504	seq580	168	179	+	GAACATCAAAGA
Spi1	14.4999	0.924285059	seq580	683	697	+	GGAGGGAGGAAGAGA
Crx	14.2039	0.952278211	seq580	200	210	+	AAGGAGATTAA
Tcf12	13.9954	0.976273397	seq580	849	859	-	AACAGCTGGGA
Gfi1b	13.8469	0.949825523	seq580	544	554	-	CAATCTCTGCT
E2F6	13.794	0.964535168	seq580	682	692	+	GGGAGGGAGGA
Myog	13.772	0.978535971	seq580	849	859	-	AACAGCTGGGA
Stat6	13.4054	0.92289124	seq580	236	250	+	CTATTCCTGTGAATT
POU3F2	13.3683	0.913187185	seq580	190	201	-	TTATGCTAAAGA
EBF1	13.3138	0.959189267	seq580	82	92	-	CTCTCCAGGGG
NFIC	13.2177	0.974851037	seq580	802	812	-	GACTTGGCATG
POU3F1	13.1713	0.919653959	seq580	190	201	-	TTATGCTAAAGA
Klf4	13.1305	0.959594272	seq580	9	18	-	GGGGTGGGGT
KLF5	13.047	0.969229524	seq580	9	18	+	ACCCCACCCC
NEUROD1	13.0076	0.934447922	seq580	282	294	-	AGGCAGATGGGTG
Arid3b	12.9393	0.954225306	seq580	271	281	-	ATATTAATTGT
HESX1	12.7548	0.986665491	seq580	881	890	+	GATAATTGGC
NFIA	12.616	0.986425833	seq580	802	811	+	CATGCCAAGT
YY2	12.5166	0.923384207	seq580	138	148	+	CTCCGCCATGA
Tcf3	12.4032	0.950231913	seq580	850	860	+	CCCAGCTGTTG
Myod1	12.4029	0.949654772	seq580	850	862	+	CCCAGCTGTTGGA
HMBOX1	12.2381	0.964420821	seq580	892	901	+	ATTAGTTAAA
ELF1	12.1073	0.911354507	seq580	684	696	+	GAGGGAGGAAGAG
NFIA	12.0532	0.977750606	seq580	884	893	-	ATTGCCAATT

EBF1	12.0458	0.951252925	seq580	630	639	-	TCCCCAGGGA
TFAP4	12.0199	0.921757914	seq580	850	859	+	CCCAGCTGTT
EBF1	12.008	0.944339117	seq580	453	463	+	CTCTCCAGGGC
SP1	11.9832	0.931902901	seq580	634	644	-	GCTCCTCCCCA
KLF5	11.9702	0.955530194	seq580	635	644	-	GCTCCTCCCC
Erg	11.924	0.930115945	seq580	687	697	+	GGAGGAAGAGA
POU2F1	11.8027	0.900952586	seq580	191	202	-	CTTATGCTAAAG
GBX2	11.7919	0.974115394	seq580	888	897	+	GGCAATTAGT
GBX1	11.7848	0.960158478	seq580	888	897	+	GGCAATTAGT
E2F6	11.7519	0.934405911	seq580	379	389	-	GAGAGGGAGAG
POU3F4	11.7297	0.9276272	seq580	192	200	-	TATGCTAAA
GBX1	11.7064	0.958794238	seq580	881	890	-	GCCAATTATC
Msx3	11.661	0.990445593	seq580	889	896	+	GCAATTAG
ZBTB18	11.6392	0.901541192	seq580	848	860	+	CTCCCAGCTGTTG
RAX	11.5498	0.967863967	seq580	881	890	-	GCCAATTATC
TFAP4	11.5478	0.914152773	seq580	850	859	-	AACAGCTGGG
POU5F1B	11.4655	0.929631477	seq580	192	200	-	TATGCTAAA
MSX2	11.43	0.972687623	seq580	882	889	-	CCAATTAT
GBX2	11.3743	0.965981991	seq580	881	890	-	GCCAATTATC
NFIA	11.323	0.966494047	seq580	247	256	-	TCTGCCAATT
HESX1	11.2879	0.958483829	seq580	888	897	-	ACTAATTGCC
TFEB	11.2401	0.925377232	seq580	798	807	+	ACCACATGCC
MSX2	11.1944	0.96726676	seq580	889	896	+	GCAATTAG
RAX	11.1806	0.959719426	seq580	270	279	+	GACAATTAAT
Esrrb	11.1452	0.902609928	seq580	225	236	-	GGCTGAAGGGCA
BARX1	11.1413	1.000000008	seq580	889	896	+	GCAATTAG
Msx3	11.1168	0.97827838	seq580	882	889	-	CCAATTAT
Esrrb	11.1089	0.901621146	seq580	225	236	-	GGCTGAAGGGCA
CDX2	11.0842	0.919548731	seq580	311	321	-	ATATAATAAAG
Mycn	11.0817	0.944118138	seq580	798	805	+	ACCACATG

EN1	11.0519	0.981728045	seq580	889	896	+	GCAATTAG
Nobox	11.0124	0.988437709	seq580	883	890	+	TAATTGGC
SREBF1	10.9911	0.910229733	seq580	57	66	-	CTCACCTCAG
MSX1	10.9908	0.981673241	seq580	889	896	+	GCAATTAG
LHX2	10.9782	0.947734746	seq580	881	890	-	GCCAATTATC
MSX2	10.9377	0.961357382	seq580	271	278	+	ACAATTAA
RAX	10.9006	0.953541928	seq580	888	897	+	GGCAATTAGT
Hand1::Tcf3	10.884	0.944253715	seq580	301	310	+	CTTCTGGCAT
Dlx2	10.8753	0.993455598	seq580	889	896	+	GCAATTAG
Msx3	10.8686	0.972729172	seq580	271	278	+	ACAATTAA
PDX1	10.8617	0.981777978	seq580	889	896	+	GCAATTAG
FIGLA	10.8398	0.93207918	seq580	850	859	+	CCCAGCTGTT
TFAP2B(var.2)	10.8022	0.913944385	seq580	290	300	-	ACCCCAAGGCA
TFAP2B	10.7698	0.911155608	seq580	290	301	-	GACCCCAAGGCA
ESX1	10.751	0.967958072	seq580	881	890	-	GCCAATTATC
SP1	10.7362	0.916214697	seq580	922	932	+	CCTCCTCCCCA
Dlx2	10.7357	0.99010986	seq580	882	889	-	CCAATTAT
MSX1	10.7146	0.974832857	seq580	882	889	-	CCAATTAT
DLX6	10.6699	0.989833489	seq580	882	889	-	CCAATTAT
FOXO6	10.6653	0.955625989	seq580	154	160	+	GTCAACA
ISX	10.6487	0.969222039	seq580	889	896	+	GCAATTAG
EMX2	10.6374	0.950153662	seq580	888	897	+	GGCAATTAGT
FOXO4	10.6357	0.958921266	seq580	154	160	+	GTCAACA
FIGLA	10.62	0.927702831	seq580	850	859	-	AACAGCTGGG
EN2	10.5999	0.955089348	seq580	881	890	-	GCCAATTATC
ISX	10.5876	0.96790471	seq580	882	889	-	CCAATTAT
ISX	10.5874	0.967900885	seq580	271	278	+	ACAATTAA
Dlx2	10.5728	0.986206304	seq580	271	278	+	ACAATTAA
LBX2	10.5623	0.963025562	seq580	881	890	-	GCCAATTATC
BARX1	10.5546	0.987001563	seq580	271	278	+	ACAATTAA

RBPJ	10.5388	0.943800853	seq580	163	172	+	TTTGGGAACA
SOX10	10.5369	0.919784843	seq580	213	223	+	TTTACAAAGGG
Erg	10.5263	0.911060642	seq580	705	715	-	TCAGGAAGCCG
Dlx4	10.5162	0.991771283	seq580	882	889	-	CCAATTAT
Nobox	10.4832	0.970986025	seq580	888	895	-	TAATTGCC
SP1	10.4743	0.91291918	seq580	9	19	+	ACCCCACCCCA
Shox2	10.474	0.971244438	seq580	889	896	+	GCAATTAG
Tcf3	10.451	0.924263998	seq580	284	294	+	CCCATCTGCCT
LBX1	10.4399	0.945923716	seq580	882	889	+	ATAATTGG
ISL2	10.398	0.958015376	seq580	889	896	+	GCAATTAG
TCF3	10.389	0.944146761	seq580	850	859	-	AACAGCTGGG
EN2	10.3697	0.95010162	seq580	888	897	+	GGCAATTAGT
Nr2e1	10.3629	0.905674278	seq580	150	158	+	AGGAGTCAA
NFIX	10.3416	0.988972683	seq580	802	810	+	CATGCCAAG
GSC	10.2923	0.929539217	seq580	202	211	-	GTTAATCTCC
OTX2	10.2843	0.957734892	seq580	203	210	-	TTAATCTC
KLF5	10.28	0.934028304	seq580	32	41	-	GCCCCACCTT
GBX2	10.2689	0.944457112	seq580	270	279	+	GACAATTAAT
Dlx3	10.2651	0.99282943	seq580	882	889	-	CCAATTAT
Bhlha15	10.2578	0.937595627	seq580	285	292	+	CCATCTGC
TFAP2A	10.2407	0.915781416	seq580	290	300	-	ACCCCAAGGCA
FOXO3	10.2323	0.935849513	seq580	909	916	-	TCTAAACA
DLX6	10.2297	0.978419204	seq580	271	278	+	ACAATTAA
Shox2	10.2282	0.965729978	seq580	882	889	-	CCAATTAT
Hic1	10.2157	0.926036658	seq580	803	811	+	ATGCCAAGT
Hoxd9	10.1927	0.92086673	seq580	271	280	+	ACAATTAATA
PRRX1	10.1722	0.965305739	seq580	271	278	+	ACAATTAA
EMX1	10.1533	0.948401394	seq580	888	897	-	ACTAATTGCC
TFE3	10.1468	0.918481963	seq580	798	807	+	ACCACATGCC
HESX1	10.1458	0.93654274	seq580	270	279	-	ATTAATTGTC

MNX1	10.1327	0.941363047	seq580	270	279	+	GACAATTAAT
SP1	10.1028	0.939263917	seq580	9	18	-	GGGGTGGGGT
MSX1	10.0952	0.95949168	seq580	271	278	+	ACAATTAA
KLF5	10.0811	0.931498537	seq580	922	931	+	CCTCCTCCCC
CDX1	10.0701	0.932690071	seq580	311	319	-	ATAATAAAG
USF2	10.0691	0.910822972	seq580	797	807	-	GGCATGTGGTA
Dlx1	10.0669	0.958704934	seq580	881	890	-	GCCAATTATC
Shox2	10.0634	0.96203252	seq580	271	278	+	ACAATTAA
Dlx4	10.0351	0.978643719	seq580	889	896	+	GCAATTAG
TFAP2A(var.2)	10.0325	0.908671098	seq580	290	301	-	GACCCCAAGGCA
MEOX1	10.032	0.932304608	seq580	888	897	-	ACTAATTGCC
LHX2	10.0216	0.931594081	seq580	888	897	-	ACTAATTGCC
FOXI1	10.0053	0.938542174	seq580	154	160	+	GTCAACA
MEOX1	9.99872	0.931619038	seq580	881	890	-	GCCAATTATC
BSX	9.988	0.978687529	seq580	889	896	+	GCAATTAG
Barhl1	9.98305	0.968572522	seq580	888	897	-	ACTAATTGCC
Dlx4	9.97755	0.977074901	seq580	271	278	+	ACAATTAA
PRRX1	9.97203	0.960063369	seq580	882	889	-	CCAATTAT
Dlx3	9.97027	0.983780722	seq580	271	278	+	ACAATTAA
NRL	9.96035	0.915805147	seq580	731	741	-	TCTTTGCTGAT
MEIS1	9.94789	0.991412464	seq580	99	105	+	CTGACAG
Pitx1	9.93519	0.942158595	seq580	203	210	-	TTAATCTC
NKX3-2	9.93181	0.91601082	seq580	18	26	+	CACACTTAG
TFAP2C(var.2)	9.93134	0.907150629	seq580	290	300	-	ACCCCAAGGCA
LHX9	9.93057	0.97316464	seq580	889	896	+	GCAATTAG
LHX9	9.92949	0.973135241	seq580	271	278	+	ACAATTAA
VSX2	9.91681	0.932455956	seq580	882	889	-	CCAATTAT
MAX	9.91268	0.914249561	seq580	797	806	+	TACCACATGC
MAX	9.90917	0.917999113	seq580	798	807	+	ACCACATGCC
Klf4	9.89813	0.904676657	seq580	32	41	+	AAGGTGGGGC

PITX3	9.86552	0.931485714	seq580	203	211	-	GTTAATCTC
BSX	9.85156	0.975681924	seq580	882	889	-	CCAATTAT
Prrx2	9.84969	0.974420675	seq580	882	889	-	CCAATTAT
HIC2	9.84812	0.947873887	seq580	803	811	+	ATGCCAAGT
DLX6	9.84315	0.968395592	seq580	889	896	+	GCAATTAG
SHOX	9.82432	0.968897059	seq580	882	889	+	ATAATTGG
Foxj2	9.77521	0.92377284	seq580	154	161	+	GTCAACAT
NKX6-1	9.76626	0.949077744	seq580	271	278	+	ACAATTAA
PDX1	9.75256	0.959590712	seq580	271	278	+	ACAATTAA
EVX1	9.74441	0.944333434	seq580	881	890	-	GCCAATTATC
KLF5	9.7411	0.927173271	seq580	681	690	-	CTCCCTCCCT
NFIX	9.7312	0.974603158	seq580	885	893	-	ATTGCCAAT
EN1	9.69944	0.952340889	seq580	882	889	-	CCAATTAT
NFIC	9.69742	1.000000005	seq580	249	254	+	TTGGCA
NFIC	9.69742	1.000000005	seq580	804	809	-	TTGGCA
NFIC	9.69742	1.000000005	seq580	886	891	+	TTGGCA
Barhl1	9.69671	0.961026895	seq580	881	890	+	GATAATTGGC
BARX1	9.69546	0.967965537	seq580	882	889	-	CCAATTAT
VSX1	9.69502	0.941454618	seq580	889	896	-	CTAATTGC
Dlx3	9.68754	0.975103888	seq580	889	896	+	GCAATTAG
NKX6-2	9.68748	0.967310546	seq580	271	278	+	ACAATTAA
RAX2	9.6831	0.963552455	seq580	882	889	-	CCAATTAT
Bhlha15	9.68161	0.926819077	seq580	851	858	+	CCAGCTGT
NEUROD2	9.68135	0.922973931	seq580	798	807	+	ACCACATGCC
Gfi1	9.67943	0.91282897	seq580	546	555	-	ACAATCTCTG
Nkx3-1	9.67713	0.903895073	seq580	18	26	+	CACACTTAG
VAX2	9.67675	0.949884842	seq580	889	896	-	CTAATTGC
VSX1	9.67348	0.940849211	seq580	882	889	-	CCAATTAT
PRRX1	9.66782	0.952096705	seq580	889	896	+	GCAATTAG
SP1	9.66275	0.90270913	seq580	684	694	-	CTTCCTCCCTC

RAX2	9.6585	0.962836174	seq580	889	896	+	GCAATTAG
MZF1(var.2)	9.65682	0.926551632	seq580	750	759	+	GGAGGGTGAA
HOXB3	9.6568	0.958699377	seq580	888	897	+	GGCAATTAGT
Hoxd9	9.62999	0.907859879	seq580	310	319	-	ATAATAAAGA
ESX1	9.59289	0.938184584	seq580	270	279	+	GACAATTAAT
LMX1B	9.5765	0.955694502	seq580	271	278	+	ACAATTAA
Pdx1	9.56986	0.999999988	seq580	891	896	-	CTAATT
SHOX	9.55997	0.96037869	seq580	889	896	-	CTAATTGC
LBX2	9.55751	0.93541234	seq580	888	897	+	GGCAATTAGT
BSX	9.53119	0.968624376	seq580	271	278	+	ACAATTAA
Sox17	9.51747	0.930785683	seq580	270	278	-	TTAATTGTC
Lhx8	9.51399	0.956942808	seq580	889	896	-	CTAATTGC
SPIB	9.50433	0.967023633	seq580	239	245	-	ACAGGAA
EVX2	9.4965	0.939430706	seq580	888	897	+	GGCAATTAGT
VSX2	9.48973	0.921634946	seq580	889	896	-	CTAATTGC
TFAP2A	9.47575	0.970106455	seq580	291	299	+	GCCTTGGGG
MIXL1	9.44234	0.950957064	seq580	881	890	-	GCCAATTATC
Prrx2	9.42924	0.960967869	seq580	271	278	+	ACAATTAA
EN1	9.42346	0.946344063	seq580	271	278	+	ACAATTAA
LHX9	9.41394	0.959033068	seq580	882	889	-	CCAATTAT
ISL2	9.41227	0.932368546	seq580	19	26	+	ACACTTAG
GSC2	9.38763	0.919719779	seq580	202	211	-	GTTAATCTCC
RAX2	9.37672	0.954632707	seq580	271	278	+	ACAATTAA
FOXL1	9.37263	0.947012591	seq580	154	160	+	GTCAACA
ISL2	9.36897	0.931241996	seq580	271	278	+	ACAATTAA
TEAD3	9.342	0.9370164	seq580	801	808	+	ACATGCCA
SHOX	9.33228	0.953041619	seq580	271	278	-	TTAATTGT
Prrx2	9.32648	0.957680014	seq580	889	896	+	GCAATTAG
Nkx2-5	9.31719	0.999999994	seq580	272	278	-	TTAATTG
TCF4	9.31716	0.929924828	seq580	850	859	-	AACAGCTGGG

VAX1	9.30547	0.944263138	seq580	889	896	-	CTAATTGC
NOTO	9.29914	0.932175336	seq580	881	890	-	GCCAATTATC
MNX1	9.28393	0.921911113	seq580	881	890	-	GCCAATTATC
FOXP3	9.27913	0.949146185	seq580	541	547	+	GTAAGCA
HOXA2	9.27374	0.940098453	seq580	881	890	-	GCCAATTATC
EMX2	9.27356	0.927089062	seq580	881	890	-	GCCAATTATC
UNCX	9.2673	0.95071075	seq580	271	278	+	ACAATTAA
SOX15	9.25677	0.905947952	seq580	213	222	-	CCTTTGTAAA
ALX3	9.24564	0.917163661	seq580	881	890	-	GCCAATTATC
MNX1	9.23963	0.920895694	seq580	888	897	+	GGCAATTAGT
NFIX	9.2358	0.962940191	seq580	248	256	-	TCTGCCAAT
EVX2	9.23148	0.93371522	seq580	881	890	-	GCCAATTATC
SPI1	9.19841	0.921884202	seq580	707	713	-	AGGAAGC
Nobox	9.19413	0.928472125	seq580	270	277	-	TAATTGTC
KLF5	9.18162	0.920056003	seq580	844	853	+	ATCCCTCCCA
UNCX	9.17031	0.947856233	seq580	882	889	-	CCAATTAT
HOXB2	9.1397	0.948397827	seq580	888	897	+	GGCAATTAGT
FOXH1	9.12875	0.901045	seq580	243	253	-	GCCAATTCACA
Prrx2	9.12437	0.999999981	seq580	273	277	+	AATTA
Prrx2	9.12437	0.999999981	seq580	883	887	-	AATTA
Prrx2	9.12437	0.999999981	seq580	891	895	+	AATTA
MGA	9.11513	0.907978064	seq580	5	12	-	GGGTGCGA
TCF3	9.08927	0.922295677	seq580	850	859	+	CCCAGCTGTT
ZEB1	9.08791	0.993091776	seq580	32	37	-	CACCTT
MZF1	9.08528	0.999999979	seq580	634	639	+	TGGGGA
MZF1	9.08528	0.999999979	seq580	927	932	-	TGGGGA
ESX1	9.0837	0.925094211	seq580	888	897	+	GGCAATTAGT
UNCX	9.06654	0.944801929	seq580	889	896	+	GCAATTAG
Barhl1	9.04684	0.943901191	seq580	270	279	-	ATTAATTGTC
NFATC2	9.04446	0.914608949	seq580	488	494	-	ATTTCCA

VSX1	9.04439	0.923170822	seq580	271	278	-	TTAATTGT
Arid3a	9.01498	0.967648145	seq580	172	177	+	ATCAAA
NKX6-2	9.00718	0.948586543	seq580	882	889	-	CCAATTAT
Nkx2-5	8.99637	0.987083436	seq580	882	888	+	ATAATTG
LBX2	8.99345	0.919911429	seq580	270	279	+	GACAATTAAT
Lhx8	8.9858	0.946965551	seq580	889	896	+	GCAATTAG
PDX1	8.98425	0.9442214	seq580	882	889	-	CCAATTAT
EVX1	8.98176	0.926978504	seq580	888	897	+	GGCAATTAGT
MEIS2	8.97559	0.900114101	seq580	99	106	+	CTGACAGA
FOXD2	8.96347	0.943112013	seq580	154	160	+	GTCAACA
HOXA2	8.96259	0.933063751	seq580	888	897	+	GGCAATTAGT
HOXB3	8.95492	0.942354041	seq580	270	279	+	GACAATTAAT
ZNF354C	8.91578	1.000000021	seq580	828	833	-	ATCCAC
SOX10	8.90979	0.999999997	seq580	216	221	-	CTTTGT
Lhx4	8.90365	0.92913641	seq580	271	278	+	ACAATTAA
LMX1B	8.90264	0.93552574	seq580	312	319	-	ATAATAAA
VENTX	8.89898	0.913889711	seq580	888	896	+	GGCAATTAG
MIXL1	8.89253	0.936648236	seq580	888	897	+	GGCAATTAGT
NFIX	8.81203	0.952963408	seq580	303	311	-	GATGCCAGA
EMX2	8.8039	0.91914656	seq580	270	279	+	GACAATTAAT
OTX1	8.78439	0.930588841	seq580	203	210	-	TTAATCTC
NFATC1	8.78243	0.900180634	seq580	857	866	-	GGTTTCCAAC
HIC2	8.77759	0.924040283	seq580	609	617	-	ATGCCCTGC
SPIB	8.77469	0.942096079	seq580	709	715	-	TCAGGAA
BARHL2	8.76633	0.929780501	seq580	881	890	+	GATAATTGGC
VAX1	8.73368	0.928031839	seq580	271	278	-	TTAATTGT
ZNF354C	8.72314	0.991568145	seq580	122	127	-	CTCCAC
Bhlha15	8.71855	0.90880784	seq580	285	292	-	GCAGATGG
HOXB2	8.71098	0.937260919	seq580	881	890	-	GCCAATTATC
GSX2	8.69924	0.919552895	seq580	270	279	+	GACAATTAAT

SPI1	8.67949	0.904593553	seq580	689	695	+	AGGAAGA
LHX2	8.6736	0.908849162	seq580	888	897	+	GGCAATTAGT
GBX1	8.66743	0.905899116	seq580	270	279	+	GACAATTAAT
NFATC2	8.66	0.900429363	seq580	859	865	-	GTTTCCA
VENTX	8.64723	0.90970875	seq580	270	278	+	GACAATTAA
SPI1	8.63721	0.903184569	seq580	790	796	-	AGGAACT
MEOX2	8.63412	0.907158786	seq580	881	890	-	GCCAATTATC
MIXL1	8.62364	0.929650296	seq580	270	279	+	GACAATTAAT
HOXB3	8.62071	0.934570856	seq580	881	890	-	GCCAATTATC
EN2	8.61562	0.912089353	seq580	270	279	+	GACAATTAAT
EMX1	8.61512	0.905182286	seq580	270	279	-	ATTAATTGTC
TCF4	8.61379	0.919167604	seq580	850	859	+	CCCAGCTGTT
HOXB2	8.58867	0.934083635	seq580	270	279	+	GACAATTAAT
NOTO	8.58018	0.919461169	seq580	888	897	-	ACTAATTGCC
Klf4	8.55639	0.908020276	seq580	746	755	+	CAGAGGAGGG
NKX2-3	8.54685	0.902866675	seq580	18	27	+	CACACTTAGC
VAX2	8.53506	0.919703367	seq580	271	278	-	TTAATTGT
Dlx1	8.53106	0.919839816	seq580	270	279	+	GACAATTAAT
Lhx4	8.51851	0.920278259	seq580	889	896	+	GCAATTAG
THAP1	8.50014	0.927779248	seq580	224	232	+	CTGCCCTTC
VAX1	8.48158	0.920875577	seq580	882	889	-	CCAATTAT
EVX1	8.42809	0.914379155	seq580	881	890	+	GATAATTGGC
NKX6-1	8.42627	0.919964332	seq580	882	889	-	CCAATTAT
MNX1	8.40109	0.901678666	seq580	311	320	-	TATAATAAAG
NFIC	8.39594	0.956408629	seq580	304	309	+	CTGGCA
LMX1B	8.39424	0.920309449	seq580	889	896	+	GCAATTAG
HIC2	8.39114	0.915436507	seq580	604	612	-	CTGCCCAGT
VAX2	8.37256	0.915407705	seq580	882	889	-	CCAATTAT
GSX2	8.33173	0.909386315	seq580	881	890	-	GCCAATTATC
Mafb	8.32307	0.949057655	seq580	75	82	-	GCTGAAGG

Mafb	8.32307	0.949057655	seq580	228	235	-	GCTGAAGG
Arid3a	8.29923	0.939724518	seq580	274	279	+	ATTAAT
Arid3a	8.29923	0.939724518	seq580	274	279	-	ATTAAT
GSX2	8.25795	0.9073452	seq580	888	897	+	GGCAATTAGT
LHX2	8.24381	0.901597171	seq580	270	279	+	GACAATTAAT
Mafb	8.22907	0.94498653	seq580	481	488	+	GCTGACTT
RHOXF1	8.22014	0.96272556	seq580	841	848	+	AAAATCCC
ISL2	8.19874	0.900796286	seq580	882	889	-	CCAATTAT
GSX1	8.19392	0.916087142	seq580	881	890	-	GCCAATTATC
FOS::JUN	8.18522	0.909521262	seq580	506	512	+	TGCCTCA
SPI1	8.18402	0.977897674	seq580	689	694	+	AGGAAG
SPI1	8.18402	0.977897674	seq580	708	713	-	AGGAAG
GATA5	8.17778	0.920753374	seq580	146	153	+	TGATAGGA
EVX2	8.1746	0.910922116	seq580	881	890	+	GATAATTGGC
FOXL1	8.17045	0.924997273	seq580	897	903	+	TTAAACA
BARHL2	8.12383	0.917820278	seq580	209	218	-	TGTAAATGTT
Lhx8	8.12359	0.930679227	seq580	882	889	-	CCAATTAT
EVX2	8.12292	0.909807591	seq580	270	279	+	GACAATTAAT
Pdx1	8.10589	0.939754415	seq580	273	278	-	TTAATT
GATA3	8.09247	0.987597174	seq580	146	151	+	TGATAG
GATA3	8.09247	0.987597174	seq580	729	734	-	TGATAG
KLF5	8.08721	0.906133564	seq580	752	761	-	GCTTCACCCT
Dlx1	8.06522	0.908051117	seq580	888	897	+	GGCAATTAGT
GSX1	8.03549	0.911784593	seq580	888	897	+	GGCAATTAGT
Lhx8	7.99466	0.928243756	seq580	882	889	+	ATAATTGG
NFIC	7.96934	0.942120312	seq580	115	120	+	TTGGCC
NFIC	7.96934	0.942120312	seq580	783	788	-	TTGGCC
GSX1	7.91459	0.908501188	seq580	270	279	+	GACAATTAAT
TCF4	7.89312	0.908145832	seq580	284	293	+	CCCATCTGCC
RHOXF1	7.89119	0.956385175	seq580	203	210	-	TTAATCTC

Barhl1	7.8815	0.913191825	seq580	209	218	-	TGTAAATGTT
GATA3	7.87977	0.902395683	seq580	146	153	+	TGATAGGA
NFIX	7.87632	0.930934521	seq580	114	122	-	CAGGCCAAG
FOXP3	7.86599	0.913591958	seq580	310	316	-	ATAAAGA
BARHL2	7.86553	0.913011811	seq580	896	905	+	GTTAAACAAC
NFIX	7.86241	0.930607071	seq580	781	789	+	GAGGCCAAG
HOXA2	7.84036	0.907691869	seq580	270	279	+	GACAATTAAT
Barhl1	7.83353	0.911927594	seq580	18	27	-	GCTAAGTGTG
TFAP2A	7.82868	0.916358899	seq580	261	269	+	GCCAGAAGG
FOXP3	7.82529	0.912568054	seq580	206	212	+	ATTAACA
HLTF	7.82243	0.955857887	seq580	196	205	-	CTCCTTATGC
LMX1B	7.76186	0.901381923	seq580	882	889	-	CCAATTAT
HIC2	7.74163	0.900976266	seq580	597	605	-	GTGCACAGC
SPI1	7.72714	0.95872444	seq580	166	171	+	GGGAAC
THAP1	7.69406	0.903109267	seq580	604	612	-	CTGCCCAGT
LHX9	7.64716	0.910705622	seq580	464	471	-	GCAATGAG
HLTF	7.64148	0.949480589	seq580	489	498	-	TACCATTTCC
ETS1	7.63289	0.992421538	seq580	689	694	-	CTTCCT
ETS1	7.63289	0.992421538	seq580	708	713	+	CTTCCT
HOXA5	7.63223	0.92167722	seq580	891	898	-	AACTAATT
NKX6-2	7.59797	0.909800602	seq580	889	896	+	GCAATTAG
NFIC	7.58675	0.929305861	seq580	487	492	+	TTGGAA
NFIC	7.58675	0.929305861	seq580	858	863	+	TTGGAA
BARHL2	7.51751	0.906533448	seq580	888	897	-	ACTAATTGCC
FOXD2	7.45128	0.911041566	seq580	523	529	-	GAAAATA
GATA3	7.42236	0.959484907	seq580	549	554	+	AGATTG
TFAP2A	7.41859	0.902976848	seq580	455	463	-	GCCCTGGAG
HLTF	7.40636	0.941193817	seq580	208	217	+	TAACATTTAC
Lhx8	7.39249	0.916869284	seq580	271	278	+	ACAATTAA
NKX2-8	7.37806	0.903953023	seq580	226	234	+	GCCCTTCAG

BARHL2	7.37035	0.903793951	seq580	270	279	-	ATTAATTGTC
FOXD2	7.34323	0.908750013	seq580	909	915	-	CTAAACA
SPI1	7.3324	0.94215831	seq580	791	796	-	AGGAAC
Mafb	7.31731	0.90550177	seq580	729	736	-	GCTGATAG
Mafb	7.31538	0.905417951	seq580	50	57	-	GCTGAAGA
Mafb	7.31148	0.905249281	seq580	507	514	-	GCTGAGGC
HLTF	7.30285	0.937545764	seq580	19	28	+	ACACTTAGCT
NKX6-2	7.26785	0.900714573	seq580	312	319	-	ATAATAAA
FOXC1	7.24921	0.987559919	seq580	61	68	+	GGTGAGTA
FOXD2	7.2346	0.906446122	seq580	211	217	-	GTAAATG
En1	7.22314	0.91350315	seq580	491	501	+	AAATGGTAGTC
YY1	7.21934	0.940561022	seq580	142	147	+	GCCATG
NFIC	7.21893	0.916986192	seq580	260	265	-	CTGGCT
NFIC	7.21893	0.916986192	seq580	478	483	+	CTGGCT
GATA3	7.18943	0.949713117	seq580	880	885	+	AGATAA
NFIX	7.17816	0.914497993	seq580	258	266	+	ATAGCCAGA
MEIS1	7.1429	0.932010773	seq580	176	182	+	AAGACAG
Tcfl5	7.10866	0.909896605	seq580	759	768	+	AGCACGGGCT
Tcfl5	7.10866	0.909896605	seq580	759	768	-	AGCCCGTGCT
YY1	7.02748	0.930762288	seq580	492	497	-	ACCATT
HLTF	7.02072	0.927602727	seq580	429	438	+	CTCCTTTGCT
Pax2	6.94769	0.916823956	seq580	143	150	-	TATCATGG
MAFG::NFE2L1	6.93186	0.918561235	seq580	144	149	+	CATGAT
MAFG::NFE2L1	6.93186	0.918561235	seq580	616	621	-	CATGAT
Gata1	6.92224	0.990063527	seq580	285	290	-	AGATGG
FOXL1	6.90722	0.918071643	seq580	577	584	+	TGTACATA
Lhx8	6.86528	0.906910626	seq580	271	278	-	TTAATTGT
NFIX	6.82877	0.906272438	seq580	477	485	-	TCAGCCAGG
SOX10	6.81243	0.906887448	seq580	592	597	-	CAGTGT
ZNF354C	6.72314	0.904030665	seq580	10	15	+	CCCCAC

ZNF354C	6.72314	0.904030665	seq580	15	20	+	CCCCAC
ZNF354C	6.72314	0.904030665	seq580	35	40	-	CCCCAC
ZNF354C	6.72314	0.904030665	seq580	928	933	+	CCCCAC
NFIX	6.68194	0.902815751	seq580	857	865	-	GTTTCCAAC
GATA2	6.65143	1.000000007	seq580	830	834	+	GGATA
Pax2	6.6393	0.904713916	seq580	615	622	+	CATCATGG
NFIX	6.56387	0.900036011	seq580	486	494	-	ATTTCCAAG
FOXL1	6.55354	0.902042003	seq580	188	195	-	TAAAGATA
FOXC1	6.53049	0.947356876	seq580	579	586	-	CGTATGTA
Gata1	6.50356	0.967284639	seq580	307	312	-	AGATGC
FOXC1	6.44185	0.942398512	seq580	517	524	+	TCTGAGTA
FOXC1	6.44185	0.942398512	seq580	671	678	-	TCTGAGTA
GATA3	6.42296	0.917558655	seq580	187	192	-	AGATAT
GATA3	6.42296	0.917558655	seq580	254	259	+	AGATAT
MEIS1	6.34659	0.91514722	seq580	552	558	-	AAGACAA
ETS1	6.29975	0.930928106	seq580	488	493	-	TTTCCA
ETS1	6.29975	0.930928106	seq580	859	864	-	TTTCCA
Gata1	6.29441	0.955905469	seq580	614	619	-	TGATGC
Gata1	6.24911	0.953440493	seq580	830	835	+	GGATAG
GATA2	6.23202	0.975650738	seq580	188	192	-	AGATA
GATA2	6.23202	0.975650738	seq580	254	258	+	AGATA
GATA2	6.23202	0.975650738	seq580	880	884	+	AGATA
GATA3	6.22367	0.90919803	seq580	204	209	+	AGATTA
GATA3	6.21526	0.908845139	seq580	830	835	+	GGATAG
GATA3	6.12732	0.905155835	seq580	278	283	-	TGATAT
MEIS1	6.0117	0.908055285	seq580	768	774	-	CAGACAA
ETS1	5.97749	0.916063081	seq580	238	243	+	ATTCCT
ETS1	5.97749	0.916063081	seq580	791	796	+	GTTCCT
RHOXF1	5.90668	0.918134224	seq580	879	886	-	ATTATCTC
ETS1	5.89604	0.912306063	seq580	829	834	-	TATCCA

Gata1	5.87797	0.933248074	seq580	819	824	-	CGATGT
MEIS1	5.86076	0.904858957	seq580	441	447	-	GAGACAG
MEIS1	5.86076	0.904858957	seq580	447	453	-	GAGACAG
Gata1	5.85733	0.932124859	seq580	146	151	+	TGATAG
Gata1	5.85733	0.932124859	seq580	729	734	-	TGATAG
GATA2	5.77818	0.949302466	seq580	146	150	+	TGATA
GATA2	5.77818	0.949302466	seq580	279	283	-	TGATA
GATA2	5.77818	0.949302466	seq580	730	734	-	TGATA
Gata1	5.61263	0.91881172	seq580	549	554	+	AGATTG
Gata1	5.57462	0.916743547	seq580	170	175	-	TGATGT
GATA2	5.55889	0.93657158	seq580	286	290	-	AGATG
GATA2	5.55889	0.93657158	seq580	308	312	-	AGATG
GATA2	5.55889	0.93657158	seq580	820	824	-	CGATG
Gata1	5.37659	0.905969296	seq580	714	719	-	GGATTC
Gata1	5.32681	0.903260764	seq580	71	76	-	GGATCG
GATA2	5.10505	0.91022328	seq580	171	175	-	TGATG
GATA2	5.10505	0.91022328	seq580	615	619	-	TGATG
RHOXF1	5.05597	0.90173707	seq580	257	264	+	TATAGCCA
GATA2	5.04698	0.906851967	seq580	72	76	-	GGATC
RHOXF1	5.00826	0.900817475	seq580	713	720	+	TGAATCCT